

A D. melanogaster parkin mutant larval model of
Parkinson's Disease

Amanda Vincent
PhD

University of York

Biology

May
2013

Abstract

Parkinson's Disease (PD) is a neurodegenerative disease, with severely reduced movement in patients. The main effect is the loss of dopaminergic neurons in the central nervous system (CNS). Null mutations of the *parkin* gene are known to cause PD. I found that *Drosophila melanogaster* (*D. melanogaster*) *parkin* null (*dparkin*) mutant larvae show neurophysiological abnormalities, a bradykinesia-like locomotory defect and synaptic overgrowth at the neuromuscular junction (NMJ). Neuronal overgrowth is rescued with either muscle or neuronal expression of wild-type *dparkin* in *dparkin* mutant larvae. The ubiquitous expression of antioxidant enzymes have varying degrees of rescue dependent on their properties and site of action in *dparkin* mutant larvae. Manipulating c-jun-N-terminal kinase (*JNK*) signaling components or *JNK* interacting detoxification enzymes (Glutathione-s-transferase (*GST*) or Thioredoxin reductase 2 (*TRX-R2*) ameliorated all the types of *dparkin* mutant larval phenotypes. Superoxide Dismutase 1 (*Sod1*) expression rescued overgrowth but failed to rescue the neurophysiological defect or the locomotion in *dparkin* mutant larvae. Additionally, genetically manipulating AMP-activated protein Kinase (*AMPK*), which is involved in the energy homeostasis, rescued overgrowth and neurophysiological dysfunction but not the locomotory defects. The pharmacological manipulation with dopaminergic drugs, and classical *AMPK* activators (metformin and 5-Aminoimidazole-4-carboxamide ribonucleotide (AICAR)) or resveratrol failed to rescue *dparkin* larval phenotypes. I conclude that neuronal, rather than muscle, failure is key to the bradykinesia observed in *dparkin* mutant larvae. The main defect is suggested to be the depletion of neuronal energy reserve leading to synaptic dysfunction, rather than oxidative stress. Together these observations suggest oxidative stress could be a downstream consequence of a metabolic dysfunction.

LIST OF CONTENTS

Abstract	
List of Figures	v
List of Tables	viii
Acknowledgment	1
Declaration	2
Chapter 1: Introduction	3
1.1 Overview of Parkinson's Disease	3
1.2 Classical hallmarks of PD	5
1.2.1 PD pathology: Lewy bodies, ubiquitin and α -synuclein	5
1.2.2 Anatomy of the basal ganglia and hypokinetic features of PD	6
1.3 Braak's staging of PD pathogenesis	10
1.4 Models of PD	10
1.4.1 Overview of PD models	10
1.4.2 Neurotoxin-induced models	11
1.4.2.1 1-methyl-4-phenyl-1, 2, 3, 6-tetrahydropyridine (MPTP)	11
1.4.2.2 6-hydroxydopamine (6-ODHA)	12
1.4.2.3 Common findings from toxin models of PD	12
1.4.2.4 Evaluation of toxin models of PD	13
1.4.3 Genetic mutations of PD	13
1.4.3.1 Genetic models shed light of idiopathic PD	15
1.4.3.2 <i>parkin</i> gene	15
1.5 Pathogenesis of PD	19
1.5.1 Oxidative stress and the generation of reactive oxygen species	19
1.5.2 Dopamine induced oxidative stress	23
1.5.3 The Reactive Oxygen Species (ROS) generated from mitochondria	24
1.5.3.1 Mitochondria and its associated functions	28
1.5.3.2 Mitochondrial abnormalities in PD	29
1.5.4 Aggregation induced proteolytic stress and the ubiquitin proteosomal system (UPS)	32
1.6 <i>Parkin</i> models of PD	36

1.6.1 <i>D. melanogaster</i> models of PD	36
1.6.1.2 <i>parkin/ PINK1</i> mitochondrial associated roles	37
1.7 <i>D. melanogaster</i> approaches to model neurodegenerative diseases	41
1.7.1 Introduction to <i>D. melanogaster</i> genes and their conservation to human genes	41
1.7.2 <i>D. melanogaster</i> models of neurodegeneration	42
1.7.3 Genetic approaches using <i>D. melanogaster</i>	42
1.7.4 <i>D. melanogaster</i> genetic toolbox used to model Parkinson's Disease	43
1.7.5 Advantages and disadvantages of <i>D. melanogaster</i> PD models	48
1.7.6 Observations made from <i>D. melanogaster</i> PD models	48
1.7.7 The <i>D. melanogaster</i> life cycle	50
1.7.8 The <i>D. melanogaster</i> nervous system	53
1.7.8.1 The <i>D. melanogaster</i> dopaminergic system	54
1.7.9 Larval locomotion for motor function assays	55
1.7.9.1 Neuronal network contribution to larval locomotion	56
1.7.10 Motoneuron development and connectivity to muscle	57
1.7.10.1 The Neuromuscular junction (NMJ)	58
1.9 Neurotransmission	62
1.9.1 Membrane potential and action potentials	62
1.9.2 Advantages of <i>D. melanogaster</i> NMJ for assessing synaptic function	64
1.10 Rationale for the thesis project	65
1.10.1 Aim and objectives of the thesis	66
Chapter 2: Methods and Materials	68
Overview	68
2.1.1 Fly husbandry and protocols	68
2.1.1 <i>D. melanogaster</i> stocks	68
2.1.2 <i>D. melanogaster</i> diet	72
2.1.3 Fly Pushing	72
2.1.4 Recombination Crossing Scheme	73
2.2 Molecular Biology	75
2.2.1 Genomic DNA extraction	78
2.2.2 Polymerase chain reaction (PCR)	78
2.2.3 DNA agarose gel electrophoresis	78

2.3 Techniques to assess <i>D. melanogaster</i> larval physiology	79
2.3.1 Experimental Solutions	79
2.3.2 Larval Dissection	80
2.3.3 Electrophysiology: Intracellular muscle recordings	80
2.3.4 Behavioral locomotion assay	84
2.4 Anatomy at the larval neuromuscular junction (NMJ)	88
2.4.1 Fixing and immunohistochemistry	88
2.4.2 Confocal images of the NMJ	89
2.4.3 Measuring and quantifying at the NMJ	90
2.6 Statistics	95
2.7 Rationale for drug concentration	95
Chapter 3: <i>dparkin</i> larvae show reduced locomotion, synaptic dysfunction and overgrown synapses	96
3.1 Introduction	96
3.2 Results	99
3.3 Discussion	138
Chapter 4: Investigating the role of oxidative stress and metabolic dysfunction in <i>dparkin</i> mutant larvae	149
4.1 Introduction	149
4.2 Aims	153
4.3 Results	154
4.4 Discussion	185
Chapter 5: Pharmacological manipulation of dopaminergic signaling and AMPK activity	190
5.1 Introduction	191
5.1.1 Role of dopamine	191
5.2 Role of AMPK in the manipulation of ATP synthesis	191
5.3 Aims	195
5.4 Results	196
5.4 Discussion	228
Chapter 6: General Discussion	237
6.1 Summary of main results of my thesis	237
6.2 Main significance of this thesis	237
6.3 Further work investigating the neuronal dysfunction in <i>dparkin</i> larvae	238
6.4 Larval and adult phenotypes	240

6.5 Comparison of pharmacological and genetic approaches	241
6.6 Implication for Parkinson's Disease therapy	241
Abbreviation List	246
References	251

List of Figures

Figure 1.1 The basal ganglia	8
Figure 1.2 Schematic diagram indicating functional domain organization and structural domain boundaries of parkin protein between human and <i>D. melanogaster</i>	17
Figure 1.3 Reactive oxygen species (ROS) and their interaction with reactive nitrogen species (RNS)	21
Figure 1.4 Reactive oxygen species (ROS) are produced during the oxidation of fuels in mitochondria	26
Figure 1.5 The association between familial PD and mitochondrial biology	30
Figure 1.6 Parkin and ubiquitin proteasome system	34
Figure 1.7 <i>parkin</i> -induced mitophagy	39
Figure 1.8 The GAL4-UAS system	46
Figure 1.9 The <i>D. melanogaster</i> life cycle.	51
Figure 1.10 The organization of the neuromuscular junctions (NMJ) of <i>D. melanogaster</i> larvae	59
Figure 2.1 Recombination Crossing Scheme	74
Figure 2.2 PCR of <i>dparkin</i> mutant recombinants	76
Figure 2.3 Recording at the NMJ	82
Figure 2.4 Analysis of larval crawling by ImageJ and MTrack2	86
Figure 2.5 Confocal image of the NMJ anatomy	91
Figure 2.6 Light microscope image of the NMJ	93
Figure 3.1 <i>dparkin</i> mutant larvae show reduced locomotion	100
Figure 3.2 Dopaminergic expression of transgenic <i>dparkin</i> RNAi fails to show dysfunction in larval crawling	102
Figure 3.3 Loss of <i>dparkin</i> -induced overgrowth rescued by neuronal or muscle expression of wild-type <i>dparkin</i>	106
Figure 3.4 Global expression of transgenic <i>dparkin</i> RNAi shows overgrowth phenotype	110
Figure 3.5 <i>dparkin</i> mutant larvae show more positive (depolarized) RMP that is rescued by global, neuronal or muscle expression of wild-type <i>dparkin</i>	114
Figure 3.6 Scatter regression plot show <i>dparkin</i> mutant larvae have depolarized RMPs and smaller EJPs across a range of RMPs	116
Figure 3.7 <i>dparkin</i> mutant larvae show reduced synaptic transmission	118

is not rescued by either global, neuronal or muscle expression of wild-type <i>dparkin</i>	
Figure 3.8 <i>dparkin</i> mutant larvae have smaller miniature excitatory junction potentials	121
Figure 3.9 The distribution of mEJP amplitudes show <i>dparkin</i> mutant larvae have smaller miniature excitatory junction potentials	123
Figure 3.10 Cumulative frequency curve show <i>dparkin</i> mutant larvae have smaller miniature excitatory junction potentials	125
Figure 3.11 <i>dparkin</i> mutant larvae show more positive (depolarized) RMP that is rescued by global, neuronal or muscle expression of wild-type <i>dparkin</i>	129
Figure 3.12 Scatter regression plot show <i>dparkin</i> null mutant larvae have depolarized RMP and reduced synaptic transmission across a range RMP	131
Figure 3.13 <i>dparkin</i> mutant larvae show a reduction in synaptic transmission and with either global, neuronal or muscle of wild-type <i>dparkin</i> expression shows partial rescue of synaptic function	133
Figure 3.14 The difference in RMP between <i>dparkin</i> mutant and wild-type larvae is most pronounced at low external potassium concentrations.	136
Figure 4.1 Cytosolic ROS scavenger, Sod1, rescues overgrowth in <i>dparkin</i> larvae	155
Figure 4.2 ROS scavengers fail to rescue RMP defect in <i>dparkin</i> larvae	159
Figure 4.3 Global AMPK activation fail to rescue locomotory dysfunction in <i>dparkin</i> larvae	162
Figure 4.4 Global expression of AMPK rescues neuronal overgrowth in <i>dparkin</i> larvae	165
Figure 4.5 Global AMPK activation rescues RMP defect in <i>dparkin</i> larvae	168
Figure 4.6 Global GST, and not TRX-R2, expression rescues locomotory dysfunction in <i>dparkin</i> larvae	171
Figure 4.7 Global GST or TRX-R2 expression rescues RMP defect in <i>dparkin</i> larvae	174
Figure 4.8 Global BSKDN, not JUNDN, expression rescues locomotory dysfunction in <i>dparkin</i> larvae	177

Figure 4.9 Global JUNDN expression rescues overgrowth in <i>dparkin</i> larvae	180
Figure 4.10 Global JUNDN and BSKDN expression rescues RMP defect in <i>dparkin</i> larvae	183
Figure 5.1 Dopaminergics fail to rescue locomotory dysfunction in <i>dparkin</i> larvae	197
Figure 5.2 A-F Dopaminergics fail to rescue overgrowth in <i>dparkin</i> larvae	200
Figure 5.3 The AMPK activating drug AICAR fails to rescue locomotory dysfunction in <i>dparkin</i> larvae	205
Figure 5.4 AMPK-activating AICAR, fails to rescue synaptic overgrowth in <i>dparkin</i> larvae	209
Figure 5.5 Metformin fails to rescue locomotory dysfunction in <i>dparkin</i> larvae	213
Figure 5.6 Metformin fails to rescue depolarized RMP defect in <i>dparkin</i> larvae	216
Figure 5.7 Resveratrol fails to rescue locomotory dysfunction in <i>dparkin</i> larvae	219
Figure 5.8 Resveratrol fails to rescue synaptic overgrowth in <i>dparkin</i> larvae	222
Figure 5.9 Resveratrol fails to rescue depolarized RMP defect in <i>dparkin</i> larvae	226
Figure 6.1 Summary of experiments with genetic expression of transgenes	241

List of Tables

2.1 Table of Stocks	68
2.2 Table of antibodies used for NMJ bouton counts	89

Acknowledgment

Firstly, I would like to thank to my supervisor Chris Elliott for his guidance and support throughout the course of my PhD.

I want to also extend my thanks to past and present members of the fly group at York whom have complimented my knowledge and understanding of the field in a variety of ways. I would like to take this opportunity to thank my TAP committee for their advice and members of technology facility at the York's Biology Department for their technical help. Additionally, I am grateful to my funders, BBSRC.

Last and by no means least, I would finally like to thank my amazing family (notably my parents) and friends for their enduring encouragement, interest and support of all my endeavours.

Declaration

I hereby declare that the written work in this thesis is my own work except where stated in the text or figures.

Chapters: 1, 2, 3 and 4 contains images from journals adapted or used with modified text.

Chapter 3 contains figures and text derived from this paper, on which I was first author:

Vincent A., Briggs L., Chatwin G.F.J., Emery E., Tomlins R., Oswald M., Middleton C.A., Evans G.J.O., Sweeney S.T., Elliott C.J.H. Parkin induced defects in neurophysiology and locomotion are generated by metabolic dysfunction and not oxidative stress. *Hum. Mol. Genet.* 2012; 21: 1760-1769.

Chapter 1 : Introduction

1.1 Overview of Parkinson's Disease

Parkinson's Disease (PD), was first described by James Parkinson in 1817, and is the most common movement disorder and the second most common neurodegenerative disease after Alzheimer's Disease (AD). PD affects 1% of the population over 65 years of age increasing to 4-5 % after 85 years of age for males and females (Farrer, 2006). The mean onset of autosomal recessive juvenile parkinsonism (AR-JP), which gives rise to an early onset form of PD that is characterized by levodopa-responsive Parkinsonism, is 23.2 years for males and females (Saito et al., 1998). PD is a degenerative condition affecting the central nervous system (CNS). Clinically, PD is characterized by resting tremor, bradykinesia, rigidity and postural instability these can be accompanied by non-motor symptoms such as autonomic dysfunction, olfactory deficits, sleep impairment, musculoskeletal abnormalities, skin lesions, dementia and neuropsychiatric disorders (Simuni and Sethi, 2008, Meissner et al., 2011). The profound dopamine deficiency is the cardinal biochemical abnormality in PD. This is primarily (but not exclusively) due to the loss of neurons from the *substantia nigra pars compacta*. These are dopaminergic neurons with very long axons that project to the striatum (Dauer and Przedborski, 2003). Preceding the neuropathology associated with the death of neurons in the nigrostriatal pathway, are histological abnormalities often characterized by proteinaceous inclusions called Lewy body (LB) and also gliosis (Przedborski and Goldman, 2004). Since the introduction of L-3,4-dihydroxyphenylalanine (Levodopa or L-DOPA) in 1968 it has remained the most efficacious treatment in PD, despite a significant number of dopaminergic reagents becoming available (including dopamine agonists, dopamine reuptake inhibitors, and Monoamine oxidase B (MAO-B) inhibitors, and surgical alternatives. Together, this provides clinicians with a range of viable

treatment options (Cotzias et al., 1969). Although dopamine replacement therapy alleviates some of the motor symptoms, it has its drawbacks as it becomes less effective over the course of the treatment accompanied by intolerable side effects. Motor complications (termed dyskinesias) are observed in patients who have been taking L-DOPA for a long time. By 5 years, dyskinesias are seen in 50% of patients taking L-DOPA, and by 8 years 80% (Golbe, 1991, Forno, 1996, Fahn, 2000). The risk of developing of young onset PD is associated with a higher incidence of L-DOPA induced dyskinesias (LID) (Kumar, 2005). The risk of developing LID for patients on treatment for at least 5 years who are aged between 40-59 years was 50%, whereas it is 16% for those with an onset of 70 years and over. This suggests that there are age-related dynamics with L-DOPA treatment in PD patients. The nigral degeneration or disease severity is suggested also to be a key risk factor. It is reported, that with the administration of clinical dose of L-DOPA idiopathic PD patients develop LID almost exclusively whereas normal and others with different neurological disorders do not develop LID (Markham, 1971, Chase et al., 1973).

Dopaminergic dysfunction contributes to few of the non-motor symptoms (NMS) (Chaudhuri and Schapira, 2009). Depression, anxiety and apathy are due to dopamine deficiency and are improved with L-DOPA treatment but these could lead to side effects including dopamine dysregulation syndrome, drug induced hallucinations, psychosis, hypomania, addiction to the and impulse control disorders (Voon et al., 2009). Additionally, this dopamine replacement treatment is not completely effective on all NMS. For example, depression occurs in approximately 28% of PD patients in the early stage of the disease (Ravina et al., 2007). Depression is thought to involve more than one pathway with damage to serotonergic (raphe nuclei), dopaminergic (amygdala, cingular cortex, and mesolimbic and mesocortical mesothalamic pathways) and

noradrenergic (locus coeruleus) innervations (Tom and Cummings, 1998, Remy et al., 2005). The majority of NMS are related to non-dopaminergic systems: serotonergic, cholinergic and noradrenergic neurotransmitter transmission (Wolters, 2009). Treatment for depression for PD patients include tricyclic antidepressants, selective serotonin uptake inhibitors and a combination therapy in which medication that acts on several neurotransmitter pathways is given, for example noradrenergic and serotonergic medication (Devos et al., 2008). There is currently no cure or effective treatment to stop the progression or manage all debilitating symptoms of PD and the quest for novel treatments and to find a definitive cure remains a challenge for both basic science and clinical research.

1.2 Classical hallmarks of PD

1.2.1 PD pathology: Lewy bodies, ubiquitin and α -synuclein

The post mortem brain samples from PD patients show Lewy body (LB) pathology, a classical hallmark of PD. These contain ubiquitin and α -synuclein. Ubiquitin is a cytosolic enzyme that plays a key role in protein degradation (Lecker et al., 2006). α -synuclein is a small protein normally located presynaptically *in vivo* and suggested to play an important role in synaptic function (Chandra et al., 2004). The importance of α -synuclein in PD is based on the observation that mutations in the α -synuclein gene lead to early onset PD (Polymeropoulos et al., 1997). α -synuclein induced dopaminergic neuronal loss has been successfully demonstrated in animal models including *D. melanogaster* (Feany and Bender, 2000, Auluck et al., 2002, Park and Lee, 2006) and in mouse (Oliveras-Salva et al., 2013). The mechanism where by this selective loss of dopaminergic neurodegeneration occurs is unclear. The cytotoxic effect of α -synuclein is likely to be due to a gain-of-function (GOF) rather than from a loss-of-function (LOF), consistent with the dominant inheritance pattern of mutations. This is supported

further by animal studies in mouse with the loss of *α-synuclein* that were observed to have minimal effects on their development and function (Abeliovich et al., 2000). *D. melanogaster* models have recapitulated other key anatomical and behavioral features as observed from PD patients including *α-synuclein* and ubiquitin positive LB-like pathology (Feany and Bender, 2000, Auluck et al., 2002) and locomotor dysfunction (Feany and Bender, 2000, Pendleton et al., 2002).

Another cause of the disease is the genomic triplication of the wild-type allele *SNCA*, the gene that encodes the *α-synuclein* protein (Singleton et al., 2003). The measurement of wild-type protein levels indicates the predicted doubling of *α-synuclein* expression in the blood, while in the parts of the cerebral cortex region where LB are found, there is a rise in the levels and deposition of *α-synuclein* (Miller et al., 1999, Miller et al., 2004). Patients with *SNCA* duplication have a brainstem associated PD phenotype whereas the triplication of *SNCA* results in a widespread with LB associated PD pathology (Singleton et al., 2003, Fuchs et al., 2007).

1.2.2 Anatomy of the basal ganglia and hypokinetic features of PD

The classical view of PD is that it is the result of the damage in the basal ganglia. The basal ganglia consist of four nuclei (**Fig 1.1**) that include the following: the striatum (caudate nucleus, putamen and the ventral striatum that includes nucleus accumbens), the globus pallidus, the *substantia nigra* (*pars compacta* and *pars reticulata*) and the subthalamic nucleus. At the anterior part of the striatum it is divided into caudate nucleus and putamen by the internal capsule. The striatum is the main recipient of inputs to the basal ganglia from the cerebral cortex, thalamus, and the brain stem where its neurons project to globus pallidus and *substantia nigra*. Globus pallidus lies medial to the putamen and is divided into two parts, internal and external segments. The

neurons that project from the striatum to the internal globus pallidus segment and to the substantia nigra reticulata use gamma-aminobutyric acid (GABA) as their neurotransmitter. This inhibits neuronal activity. The *Substantia nigra pars compacta* zone is a distinct nucleus that lies dorsal to the reticulata zone. The *pars compacta* zone contains dopaminergic neurons and neuromelanin, a black pigment derived from the oxidized dopamine. Dopaminergic neurons are also found in the ventral tegmental area. The subthalamic nucleus is connected both to the globus pallidus segments and the *substantia nigra*. The glutamatergic cells of the subthalamic nucleus are the only excitatory projection in the basal ganglia.

The dopaminergic nigrostriatal projections from the *Substantia nigra pars compacta* to the striatum are important in the modulation of the direct and indirect pathway. The loss of dopaminergic neurons in the nigrostriatal pathway causes an imbalance in the activation and inhibition of the direct and indirect pathway respectively that leads to the PD associated motor dysfunction. As the effects of the functioning nigrostriatal pathway excites the direct pathway and inhibits the indirect one, the loss of these dopaminergic neuronal input, tips the balance in favour of activity of the indirect pathway and the decreased activity on the direct pathway as dopamine has different actions on the two dopamine receptors (D1 and D2, respectively). These changes lead to increased activity of the internal pallidus segment that results in increased inhibition of the thalamocortical and midbrain tegmental neurons leads to the hypokinetic features of PD.

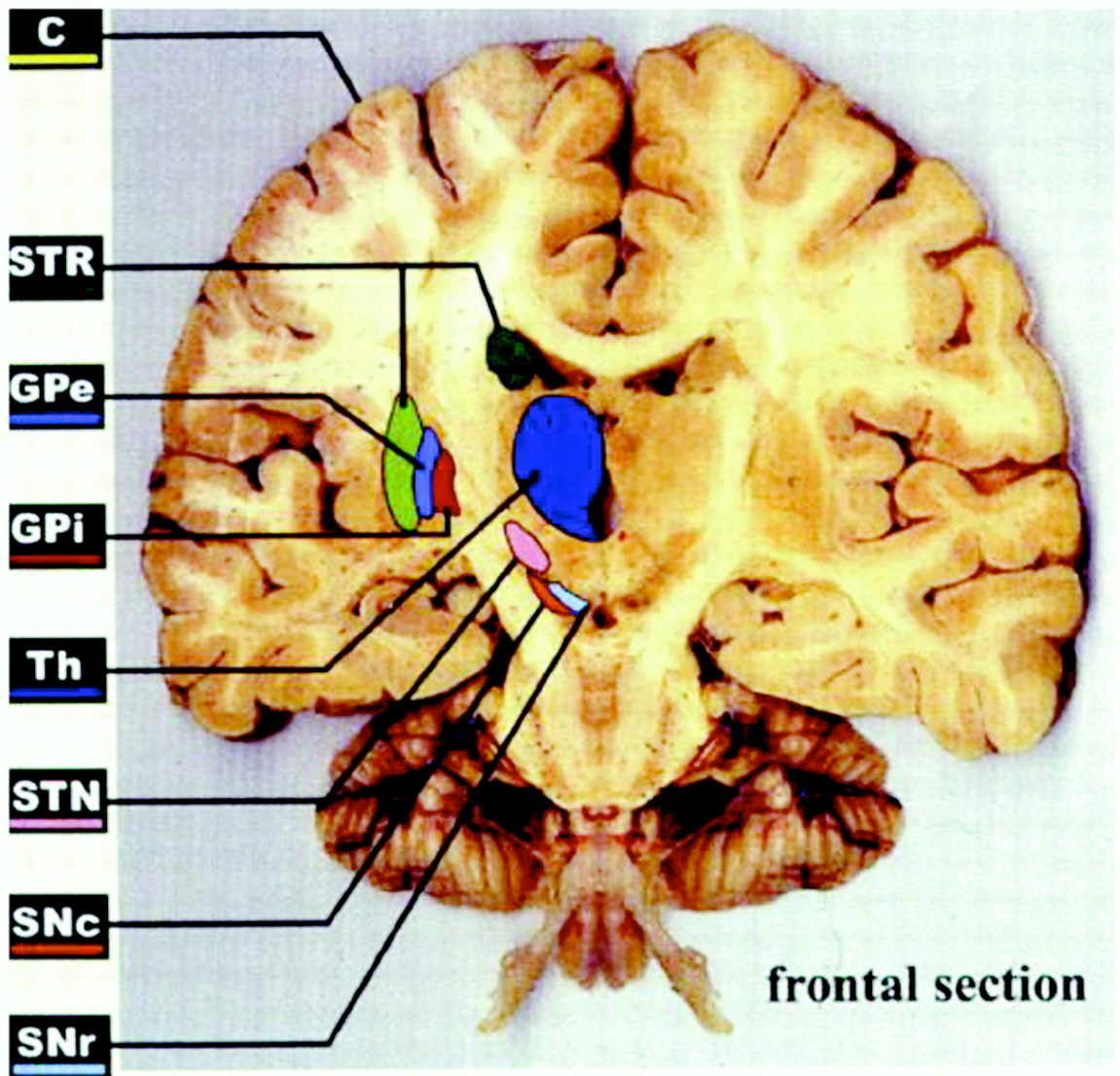


Figure 1.1 The basal ganglia. This region of the brain consists of: the striatum caudate nucleus, putamen and the ventral striatum that includes nucleus accumbens, the globus pallidus, the *substantia nigra* (*pars compacta* (*SNC*) and *pars reticulata*, (*SNr*)) and the subthalamic nucleus (STN). At the anterior part of the striatum (STR) it is divided into caudate nucleus and putamen by the internal capsule. The striatum is the main recipient of inputs to the basal ganglia from the cerebral cortex (C), thalamus (Th), and the brain stem where its neurons project to globus pallidus and *substantia nigra*. The Globus pallidus lies medial to the putamen and is divided into two parts, know as the internal and external segments (GPi and GPe). The GPi segment and SNr neurons release gamma-aminobutyric acid (GABA) as their inhibitory neurotransmitter. The *SNC* zone is a distinct nucleus that lies dorsal to the reticulata zone. The *SNC* zone contains dopaminergic neurons and neuromelanin, a black pigment derived from the oxidized dopamine. Dopaminergic neurons are also found in the ventral tegmental area. The STN is connected both to the globus pallidal segments and the *substantia nigra*.

(No permission required to use this diagram (Obeso et al., 2002)).

1.3 Braak's staging of PD pathogenesis

Braak revolutionized our view of PD, suggesting it was a spreading pathology starting in the neurons of the olfactory and/or digestive system. This was based on observations that some non-motor symptoms preceded the motor symptoms for example, such as the loss of smell (Braak et al., 2003, Braak and Del Tredici, 2008) and frequently constipation (Jost and Schimrigk, 1991, Sakakibara et al., 2001).

In Braak's hypothesis, the earliest stage of PD is called Stage 1, and it is characterized by the abnormal *α-synuclein* immunostaining in only the medulla oblongata or the olfactory bulb. Later (Stage "2"), abnormal *α-synuclein* immunostaining is seen in the caudal raphe nuclei and the locus coeruleus (LC). In Stage 3 and 4 prominent *α-synuclein* immunostaining is in the *substantia nigra pars compacta*. This is associated with clinical Parkinsonism and dopaminergic neuronal loss that spreads into the cortex. Thus Braak's hypothesis proposes that synuclein pathology in the lower brainstem is required for the later appearance of PD. The idea that early stages of PD may start in non-dopaminergic structures of the brain stem or even the in the peripheral autonomic nervous system will continue to influence approaches to early diagnosis of PD, the development of biomarkers and how critically to think about animal models in the future (Burke et al., 2008) and thus reflects PD pathogenesis as a complex multifactorial disease.

1.4 Models of PD

1.4.1 Overview of PD models

Studies on human materials are limited by ethical issues, slow reproductive turnover and by the limited genetic tools available, and thus require us to turn to model systems including the mouse, fly, worm and cell culture to understand etiology, the pathology

and molecular mechanisms of PD. 95% cases of PD are sporadic and are caused by a variety of risk factors including aging (Langston, 2002). However, age is not a risk factor for the early onset form of PD. Other risk factors are genetic susceptibility and environmental association. The association of environmental toxins, herbicides and pesticides with PD (Lees et al., 2009), has led to the development of several toxin-induced models: 1-methyl-4-phenyl-1, 2, 3, 6-tetrahydropyridine (MPTP), 6-hydroxydopamine (6-OHDA), paraquat and rotenone. These have provided insight into the molecular mechanisms underlying the pathogenesis of PD.

1.4.2 Neurotoxin-induced models

An accidental discovery in 1982 showed that the exposure of mitochondrial toxin 1-methyl-4-phenyl-1, 2, 3, 6-tetrahydropyridine (MPTP) resulted in the death of dopaminergic neurons and induced PD-like motor symptoms in humans (Langston and Ballard, 1983, Bové et al., 2005). Rodent and primate models have used the following model to test compounds that induce both reversible (reserpine) and irreversible (MPTP, 6-hydroxydopamine (6-OHDA), paraquat and rotenone) effects that have been able to reproduce PD associated pathology and disease related symptoms. The two “classical” toxin models, 6-OHDA and MPTP that selectively and rapidly destroy catecholaminergic neurons (Bové et al., 2005), will be discussed further below.

1.4.2.1 1-methyl-4-phenyl-1, 2, 3, 6-tetrahydropyridine (MPTP)

As previously discussed above, abnormalities in indirect pathway activation have been studied using microelectrode technology to record activity from brains of monkeys treated with meperidine derivative 1-methyl-4-phenyl-1, 2, 3, 6-tetrahydropyridine (MPTP) and symptoms have been ameliorated with lesions made to the overactive subthalamic nucleus which reduced the excessive excitatory drive onto the internal pallidal segment. The cardinal motor symptoms (akinesia, tremor and rigidity) were

ameliorated with specific lesions to the sensorimotor portion of the subthalamic nucleus or the internal pallidal segment in MPTP-treated monkeys (Porrás et al., 2012).

1.4.2.2 6-hydroxydopamine (6-ODHA)

Systemic administration of 6-ODHA fails to effectively cross the blood brain barrier (BBB) and thus poorly accumulates in the brain parenchyma and does not generate a nigrostriatal lesion, like other toxins (MPTP, rotenone or paraquat). To selectively damage the nigrostriatal dopaminergic pathways, stereotaxic methods have been employed to inject 6-ODHA into the *substantia nigra*, the medial forebrain bundle that is part of the nigrostriatal tract or the striatum. Injections into these three areas of lesions lead to dopaminergic cell death, reduced dopamine levels and gliosis. LB pathology has not been confidently shown in the brains of 6-ODHA infused rats, a major shortcoming of this model (Bové et al., 2005).

6-OHDA shares some structural similarities to the neurotransmitters dopamine and noradrenaline (also known as norepinephrine). 6-OHDA has a high affinity for plasma membrane transporters including dopamine (DAT) and noradrenaline (NET) transporters (Luthman et al., 1989). As a result of this, 6-OHDA enters both dopaminergic and noradrenergic neurons. Once the toxin enters the neurons via the transporters, it becomes a highly reactive molecule. 6-OHDA induces oxidative stress by generating reactive oxygen species (ROS) and quinones (Cohen, 1984) leading to cell death (Jeon et al., 1995).

1.4.2.3 Common findings from toxin models of PD

A common feature of all toxin models-induced models is their ability to recapitulate oxidative stress (OS) and cell death in the dopaminergic neurons as observed in PD patient samples. Research from the neurotoxic models concluded that mitochondrial

dysfunction via complex I or III and OS are key players in the demise of dopaminergic neurons (Abou-Sleiman et al., 2006). Human samples obtained from PD patients have shown the presence of ROS along with compromised function of the mitochondrial respiratory chain component, complex 1 (Schapira et al., 1990, Mizuno et al., 1989).

1.4.2.4 Evaluation of toxin models of PD

Toxin-induced models fall short because of their acute nature: one or two injections, given over a short period of time, are enough to lead to rapid or immediate onset of symptoms. This limits their usefulness as a model of the slowly progressive PD observed in humans. The failures in clinical trials, after observing positive effects in these mouse models suggested the mechanisms underlying the pharmacological models of PD were different from those occurring in PD patients (Linazasoro, 2004, Meissner et al., 2011, Guo, 2012). There may be compensatory mechanisms that could occur during the course of PD in patients, whereas in these acute toxin models there is little chance of this taking place. Another difference is that, a large proportion of PD occurs in the elderly, whereas the majority of the pathology in these toxin models occurs in the early stages of rodent toxin models because of the cost and inconvenience of housing them for an extended period of time. Other factors which may explain the difference between PD drug trials and rodent experiments are differences in physiology, behaviour and gene expression.

1.4.3 Genetic mutations of PD

Although PD was initially believed to be idiopathic in nature (being of an unknown origin), the discovery of α -synuclein mutations as a cause of PD (Polymeropoulos et al., 1997) led to a revolution in understanding (Hardy et al., 2009, Martin et al., 2011). However genetic mutations are rare and account for approximately 10-15% of all PD cases (Dauer and Przedborski, 2003, Houlden and Singleton, 2012). Nonetheless, the

development of genetic animal models of PD has revolutionized our understanding of the cellular mechanism underlying PD.

Some PD-related mutations are associated with autosomal dominant forms of the disease. These include the amino acid substitutions in α -synuclein protein produced from the *SNCA* gene (*PARK1*). The A53T and A30P missense mutations in the α -synuclein gene were discovered in a large Italian-American Greek and German kindred respectively (Polymeropoulos et al., 1997, Spillantini et al., 1997, Krüger et al., 1998). Triplication of *SNCA* is linked to a second form of inherited PD (called *PARK4*) where increased dosage of the wild-type α -synuclein gene results in autosomal dominant PD (Singleton et al., 2003). Other autosomal dominant forms include mutations in Leucine rich-repeat kinase 2 (*LRRK2*, *PARK8*) (Paisán-Ruiz et al., 2004, Zimprich et al., 2004), vacuolar protein sorting 35 (*VPS35*, *PARK17*) (Vilariño-Güell et al., 2011, Chartier-Harlin et al., 2011, Zimprich et al., 2011) and eukaryotic translation initiation factor 4 gamma-1 (*EIF4G1*, *PARK18*) (Chartier-Harlin et al., 2011).

Other forms of PD are recessive: genes that are associated with these forms of PD include *parkin* (*PARK2*) (Kitada et al., 1998), *DJ-1* (*PARK7*) (Bonifati et al., 2003), and phosphatase and tensin homolog (PTEN)-induced putative kinase-1 (*PINK1*, *PARK6*) (Valente et al., 2004b). Additionally, a mutation in *ATP132A2* (*PARK9*) that encodes a lysosomal ATPase has also been linked to an atypical form of autosomal recessive PD (Ramirez et al., 2006). Other mutations have also been shown in *FGF20*, *GIGYF2*, ubiquitin carboxy-terminal hydrolase-L1 (*UCH-L1*, *PARK5*) and High Temperature Requirement A2 (*HtrA2/ Omi*, *PARK13*) (Strauss et al., 2005) Heterozygous mutations in *GBA* gene encoding glucocerebrosidase is linked to Gaucher's disease has also been linked to typical PD with LB pathology (Clark et al., 2007). Supporting this, genome-

wide association studies have shown a handful of polymorphic variants, mostly genes already identified from familial PD (Peeraully and Tan, 2012).

1.4.3.1 Genetic models shed light of idiopathic PD

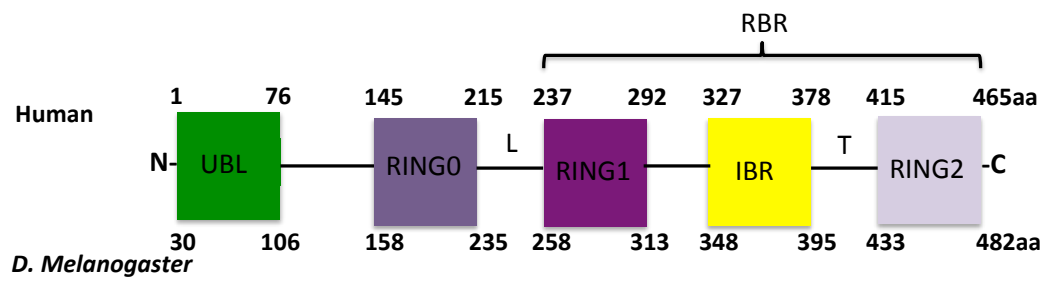
The epidemiological studies and the discovery of genes from the rare familial forms of PD have revealed cellular dysfunction implicated in the formation and/or progression of both familial and sporadic PD that include abnormal protein aggregation, oxidative stress and mitochondrial dysfunction. Inherited PD is often indistinguishable in terms of nature and severity from the sporadic form (Savitt et al., 2006, Hardy et al., 2009, Martin et al., 2011). This allows us to speculate that the basic molecular signals are also likely to be similar in both genetic and sporadic form. PD-related genes are used to study *in vivo* function of the disease causing mutations altered in patients to generate reliable animal model of PD. This has encouraged the engineering of genetic models.

The thesis aims to look into the neuronal dysfunction caused by mutations in *parkin* gene in *D. melanogaster* and there will be more of a focus on the impact of the mutations in *parkin* which cause early onset PD.

1.4.3.2 *parkin* gene

The *parkin* gene accounts for the majority of the autosomal recessive juvenile Parkinsonism (ARJP) cases, with over 100 pathogenic mutations having been reported (Exner et al., 2012). In 1998, the *parkin* gene was identified as a cause of early onset ARJP (Kitada et al., 1998). The *parkin* gene in humans encodes a polypeptide chain with 465 length amino acid chain containing a ubiquitin-like (UBL) domain at the N-terminus and an RBR (RING-between-RING) domain close to the C-terminus. The in-between RING (IBR) domain sits in the middle of the two RING fingers that make up the RBR region that coordinates the six zinc ions. Additionally, another RING finger

domain has also been identified between the UBL and the RBR regions that are thought to assist in the binding of zinc ions (Hristova et al., 2009). Studies have shown that *parkin* functions as an *E3* ubiquitin protein ligase (Shimura et al., 2000). A single *Drosophila* orthologue of mammalian *parkin*, CG10523, has been identified. It has a protein sequence of 482 amino acids (Greene et al., 2003, Pesah et al., 2004) and shows an overall similarity of 59% with its human homologue. The orthologue contains all of the characteristic canonical motifs of human Parkin, including a ubiquitin-like domain, two RING finger domains, and an in-between RING fingers domain (**Fig 1.2**).



UBL NH2-terminal ubiquitin-like domain
RING(0-2) Really interesting new gene finger domain
IBR In-between ring domain
L Linker
T Tether
RBR RING-between-RING

Figure 1.2 Schematic diagram indicating functional domain organization and structural domain boundaries of parkin protein between human and *D. melanogaster*. Domain structure of parkin protein showing the C-terminal RING1, IBR and RING2 domains found in all RBR E3 ligase proteins. The ubiquitin-like (Ubl) and RING0 domains are specific to the *parkin* E3 ligase. Residue numbering is shown for both the human (top) and *D. melanogaster* (*bottom*) *parkin* sequences.

(Modified from (Spratt et al., 2013))

1.5 Pathogenesis of PD

Animal models have given great insight to the etiology, pathology and molecular mechanisms of PD (Dawson et al., 2010), but the complete disease process has yet to be determined. Over several decades, a variety of animal models have been developed based on toxins or genetic manipulations. Research from animal models has provided clues into the disease pathogenesis and cellular dysfunction: the role of oxidative stress, mitochondrial abnormalities, aggregation-induced toxicity and/ or impairment of the proteosomal/ lysosomal degradation pathways (Dawson et al., 2010, Corti et al., 2011, Martin et al., 2011, Shulman et al., 2011). These will be reviewed below.

1.5.1 Oxidative stress and the generation of reactive oxygen species

The mechanisms that result in the loss of dopaminergic cells have been debated for decades. The brain in particular, is susceptible to oxidative damage as a result of its high metabolic rate and its relatively reduced renewing capacity compared to other organs. Approximately 20% of the molecular oxygen and a quarter of the glucose consumed by the human body are used for cerebral functions, even though the brain only represents only 2% of the total body mass. The maintenance and restoration of ionic gradients altered by signaling processes results in high brain energy requirements (Attwell and Laughlin, 2001, Alle et al., 2009). Among the signaling processes, synaptic potentials, rather than action potentials, appear to represent by far the main energetic cost related to maintenance of excitability (Alle et al., 2009).

Oxidative stress (OS) is defined as the imbalance between the production of reactive oxygen species (ROS) and the capacity of antioxidant defense mechanisms to scavenge these ROS, leading to an increase in free radicals. Severe OS can cause cell damage and death by several mechanisms (Halliwell, 1992). The balance of ROS production and antioxidant capacity has been shown to be compromised in many neurodegenerative

conditions like PD, AD (Alzheimer's Disease) and Amyotrophic lateral sclerosis (ALS).

There are several markers of ROS damage reported within specific brain regions (**Fig 1.3**), which eventually undergo neurodegeneration. These include 4-Hydroxynonenal (4-HNE) and malondialdehyde (MDA) that are markers of lipid peroxidation, and protein nitration that is a marker of protein oxidation, both of which have been reported to be present in all the above conditions. This however does not prove these are involved in the neurodegenerative process. Nigral dopaminergic neurons may be susceptible to OS as a result of dopamine metabolism which give rise to toxic species (Maker et al., 1981, Jenner, 2003).

Figure 1.3 Reactive oxygen species (ROS) and their interaction with reactive nitrogen species (RNS). ROS include the free radical group possessing highly reactive unpaired electrons such as superoxide ($O_2^{\cdot-}$) and hydroxyl (OH^{\cdot}) radicals; and the second types of molecular species are hydrogen peroxide (H_2O_2) and peroxynitrite ($ONOO^{\cdot-}$). $O_2^{\cdot-}$ is broken down to H_2O_2 by superoxide dismutases (SOD). H_2O_2 is broken down by catalase (CAT), glutathione peroxidase (GPX) and peroxiredoxins (PRX) to water (H_2O). Additionally H_2O_2 can also be reduced to the OH^{\cdot} radical via the Fenton reaction in the presence of reduced transition metals such as iron (Fe^{2+}) that can be further reduced to superoxide $O_2^{\cdot-}$. $O_2^{\cdot-}$ is able to also react with a reactive nitrogen species (RNS) called nitric oxide (NO^{\cdot}) radicals to produce another RNS, $ONOO^{\cdot-}$. NO^{\cdot} is formed from the conversion of conversion of arginine to citrulline by nitric oxide synthase (NOS).

Diagram based on (Bogaerts et al., 2008)

1.5.2 Dopamine induced oxidative stress

Dopamine is a neurotransmitter and itself has been widely held responsible for the induction of oxidative stress and impairment of mitochondrial function. This is due to the oxidization of cytosolic dopamine and its metabolites leading to the generation of highly ROS that oxidize lipids and other compounds (Berman and Hastings, 1999, Gluck et al., 2002, Greenamyre and Hastings, 2004, Sulzer, 2007, Naoi et al., 2009).

Reduced sequestration of dopamine into synaptic vesicles has been proposed as a vulnerability factor of dopamine neurons. This is because at neutral or more alkaline pH dopamine undergoes auto-oxidation, but inside the synaptic vesicle the pH is lower and dopamine is unable to auto-oxidize (Obeso et al., 2010). Dopamine storage dysfunction can be caused by *α-synuclein* protofibrils, oxidative stress and neurotoxins such as methamphetamine (Caudle et al., 2008). A direct consequence of storage dysfunction is elevated dopamine in the cytosolic compartment resulting in the generation of reactive metabolites via two distinct pathways. Dopamine in the cytoplasmic compartment is metabolized by monoamine oxidase (MAO) located on the outer surface of the mitochondria or by auto-oxidation to generate harmful byproducts such as ROS, and subsequent neuromelanin formation. Oxidation of dopamine by MAO or aldehyde dehydrogenase results in the generation of hydrogen peroxide (H₂O₂) and dihydroxyphenylacetic acid (DOPAC). The generation of ROS from dopamine metabolism can inhibit complex I of the electron transport chain (Suzuki et al., 1992, Glinka and Youdim, 1995) and complex I activity has been found to be decreased in nigral tissues from PD patients' brains (Reichmann and Janetzky, 2000). There is reason to question the “excess cytosolic dopamine leads to PD” hypothesis as L-DOPA administration ameliorates motor dysfunction by replacing lost dopamine and shows no accelerating effect on the disease progression of these patients (Fahn and Group, 2005).

This suggests that dopamine does not accelerate oxidative stress induced- PD pathogenesis.

Additionally, there is regional variability in the loss of dopamine containing cells in PD where there are certain regions that show no sign of pathology (Damier et al., 1999). On the other hand a study has shown calcium entry through L-type channels stimulates dopamine metabolism in dopaminergic neurons thereby increasing the cytosolic concentrations to a toxic range with L-DOPA addition (Mosharov et al., 2009). Pro-oxidants produced from dopamine metabolism such as H_2O_2 , aldehydes and quinones could also react with other components that could result in cell loss. It should be noted non-dopaminergic cell death also occurs in PD, thereby arguing dopamine itself is unlikely to be the cause.

1.5.3 The Reactive Oxygen Species (ROS) generated from mitochondria

Oxidative damage has been shown to extend its effect to other cellular components such as lipid, proteins, RNA and DNA in the substantia nigra of patients with PD (Zhang et al., 1999), where the source of oxidative stress was shown to originate from the mitochondria. ROS are of two types: first the free radical group. These possess highly reactive unpaired electrons such as superoxide ($O_2^{\cdot-}$), nitric oxide (NO^{\cdot}) and hydroxyl (OH^{\cdot}) radicals. The second type are composed of molecular species including hydrogen peroxide (H_2O_2) and peroxynitrite ($ONOO^{\cdot}$). $O_2^{\cdot-}$ is broken down to H_2O_2 by superoxide dismutase (SOD). H_2O_2 is broken down by catalase (CAT), glutathione peroxidase (GPX) and peroxiredoxins (PRX) to water (H_2O). Additionally H_2O_2 can also be reduced to OH^{\cdot} radical via the Fenton reaction in the presence of reduced transition metals such as iron (Fe^{2+}) that can be re-reduced to superoxide $O_2^{\cdot-}$. $O_2^{\cdot-}$ is able to also react with NO^{\cdot} radicals to produce $ONOO^{\cdot}$. NO^{\cdot} is formed from the conversion of conversion of arginine to citrulline by nitric oxide synthase (NOS)

(Bogaerts et al., 2008).

Mitochondria generate ATP coupled with the production of superoxide ($O_2^{\cdot-}$) and ROS. 1–2% of oxygen consumed during physiological respiration is converted into $O_2^{\cdot-}$ when electrons prematurely leak from the electron transport chain (ETC) and are aberrantly transferred to molecular oxygen (O_2). The mitochondrial ETC, responsible for carrying out oxidative phosphorylation, is composed of five multi-subunit protein complexes, coenzyme Q (CoQ) and cytochrome c (Cyt c). Leakage of superoxides ($O_2^{\cdot-}$) occurs at complex I, II or III. $O_2^{\cdot-}$ from complex I and II is released into the matrix, whereas $O_2^{\cdot-}$ from complex III can be produced on either side of the inner membrane. $O_2^{\cdot-}$ can then cross the outer mitochondria membrane (OMM) via a voltage-dependent anion-selective channel (*VDAC*). Additionally, $O_2^{\cdot-}$ can be converted into H_2O_2 in the matrix by superoxide dismutase 2 (*Sod2*) or in the intermembrane space by *Sod1*. In the cytosol, superoxide is converted by *Sod1* into H_2O_2 , which is further detoxified by the peroxisomal enzyme catalase. H_2O_2 can then freely cross mitochondrial membranes and can be further detoxified by additional antioxidant enzymes including peroxiredoxins (*PRX*) and glutathione peroxidase (*GPX*) (Veal et al., 2007) (**Fig 1.4**).

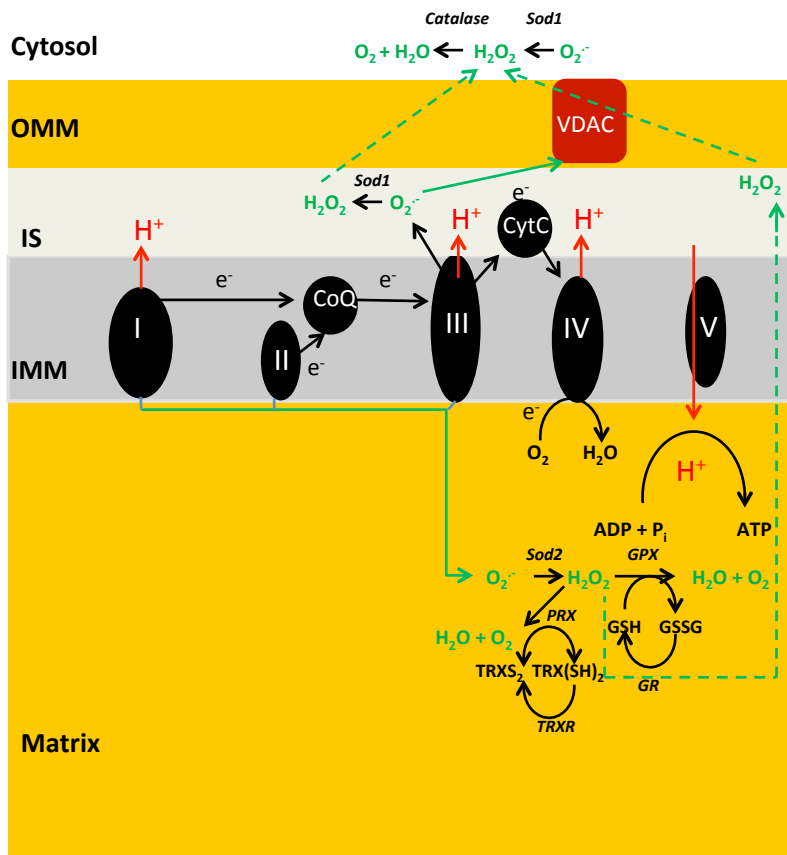


Figure 1.4 Reactive oxygen species (ROS) are produced during the oxidation of fuels in mitochondria. There are multiple sites of ROS production in the mitochondrion and ROS are kept within tolerable limits by a range of antioxidant systems, including glutathione and thioredoxin systems. The mitochondrial electron transport chain (ETC) is responsible for carrying out oxidative phosphorylation. Leakage of superoxides ($O_2^{\cdot-}$) occurs at complex I, II or III. $O_2^{\cdot-}$ from complex I and II is released into the matrix, whereas $O_2^{\cdot-}$ from complex III can be produced on either side of the inner membrane. $O_2^{\cdot-}$ can then cross the outer mitochondria membrane (OMM) via a voltage-dependent anion-selective channel (VDAC). Additionally, $O_2^{\cdot-}$ can be converted into H_2O_2 in the matrix by superoxide dismutase 2 (*Sod2*) or in the intermembrane space by *Sod1*. In the cytosol, superoxide is converted by *Sod1* into H_2O_2 , which is further detoxified by the peroxisomal enzyme catalase. H_2O_2 can then freely cross mitochondrial membranes and can be further detoxified by additional antioxidant enzymes including peroxiredoxins (*PRX*) and glutathione peroxidase (*GPX*). Mitochondrial ROS emission levels are not simply scaled to fuel oxidation rate, but are affected by fuel type and by mitochondrial membrane potential. Glutathione (GSH) not only quenches ROS but also covalently modifies proteins to affect their function or protect proteins from oxidative damage. The fly does not have a glutathione reductase, and the reduction of glutathione disulphide (GSSG) is undertaken by the fly thioredoxin system (Kanzok et al., 2001).

During the cellular oxidation of fuels, electrons are used to power the proton pumps of the mitochondrial electron transport chain (ETC) and ultimately drive ATP synthesis and the reduction of molecular oxygen to water. During these oxidative processes, some electrons can ‘spin off’ during fuel oxidation and electron transport to univalently reduce O₂, forming reactive oxygen species (ROS). In excess, ROS can be detrimental; however, at low concentrations oxyradicals are essential signaling molecules. Mitochondria thus use a battery of systems to finely control types and levels of ROS, including antioxidants. Several antioxidant systems depend on glutathione.

1.5.3.1 Mitochondria and its associated functions

Mitochondria are the “powerhouses of the cell” and they are responsible for the production of cellular energy, in the form of adenosine triphosphate (ATP), from the breakdown of carbohydrates and fatty acids, which are then converted to ATP by the process of oxidative phosphorylation in the inner mitochondrial membrane. The initial stages of glucose metabolism, glycolysis, occurs in the cytosol where glucose is converted into pyruvate. Pyruvate is transported into the mitochondria where pyruvate is converted in the process of being oxidized into Acetyl-Co enzyme A (Acetyl CoA) which is broken down to carbon dioxide in the citric acid cycle. The enzymes of the citric acid cycle is located in the matrix of the mitochondria and play a central part in the breakdown of both carbohydrates and fatty acids.

Mitochondria are also involved in other functions including biosynthesis of amino acids and steroids, beta-oxidation of fatty acids, homeostatic levels of cytosolic calcium concentration, buffering of calcium fluctuations and production and modulation of ROS. Mitochondria also play a central role in apoptosis. Taken together, the energy demands of neurons and their poor regenerative capacity, suggests mitochondrial

dysfunction could lead to poor neuronal survival.

The importance of mitochondrial function has been highlighted throughout a variety of neurodegenerative diseases, including PD (Henchcliffe and Beal, 2008, Exner et al., 2012). Toxins that affect mitochondria cause PD phenotypes (Przedborski et al., 2004). One of the first links between PD and mitochondria came in the early 1980s, when it was discovered the neurotoxin MPTP that caused a form of Parkinsonian syndrome after being metabolized into MPP⁺ is taken up into dopaminergic neurons by dopamine transporter, vesicular monoamine transporter 2 (*VMAT2*), accumulates in the mitochondria and inhibits mitochondrial respiration (Langston and Ballard, 1983, Nicklas et al., 1985). Human post-mortem brain samples show substantial decrease in mitochondrial complex I (NADH ubiquinone oxidoreductase) activity in *substantia nigra* of PD patients (Mann et al., 1994), which appears to be a result of oxidative damage to complex I (Keeney et al., 2006). Mitochondrial DNA (mDNA) is vulnerable as they are close to the sites of superoxide generation and high levels of superoxide production are a possible cause of the increased number of somatic DNA mutations observed in dopaminergic neurons in the substantia nigra of PD patients (Soong et al., 1992). Mutations in mDNA impact on electron chain function (Bender et al., 2006) and as a consequence cause disruption to the bioenergetics of *substantia nigra* neurons. 13 proteins associated with the respiratory chain are encoded by the mitochondrial genome, 7 of which are involved in complex I formation (Schapira, 2008).

1.5.3.2 Mitochondrial abnormalities in PD

Several of the genes found to be associated with PD are mitochondrially-linked proteins (Abou-Sleiman et al., 2006, Exner et al., 2012) (**Fig 1.5**). These include *parkin*, *PTEN-induced kinase 1 (PINK1)*, *DJI*, and *α-synuclein*.

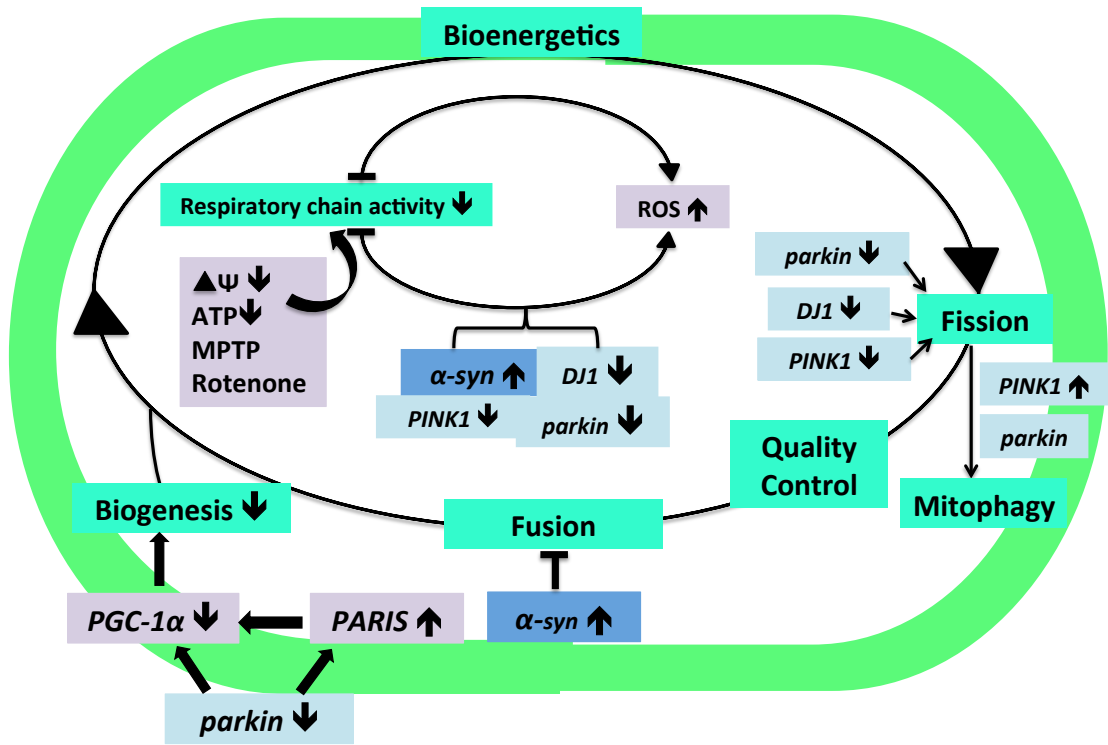


Figure 1.5 The association between familial PD and mitochondrial biology. The involvement of autosomal recessive PD proteins (pale blue) or autosomal dominant PD proteins (dark blue) in mitochondrial processes, have been represented in the diagram. This includes their life cycle, bioenergetic capacity, quality control, dynamics, and subcellular distribution.

Adapted from (Exner et al., 2012)

The level of the characteristic muscle and germline defects seen in *D. melanogaster parkin* mutants are not observed to equally manifest in PD patients or mammalian mouse models. Mitochondrial abnormalities on the other hand are far more common in patients with early onset as well as sporadic PD. These organelle-associated defects are conserved in all model organisms and in humans with *parkin* mutations (Müftüoglu et al., 2004, Mortiboys et al., 2008, Palacino et al., 2004)

Additionally, conditional knockout mice, disruptions to the gene for mitochondrial transcription factor A (*Tfam*) in dopaminergic neurons, lead to reduced copy number of mtDNA and inefficient respiratory chain function leading the adult onset and progressive decline of motor dysfunction with LB pathology and nerve death (Ekstrand et al., 2007). Dawson and colleagues recently showed a *parkin* interacting substrate, *PARIS*, to suppress peroxisome proliferator-activated receptor γ co-activator (*PGC-1 α*) expression induced mitochondrial biogenesis (Shin et al., 2011). When *parkin* is absent this elevates the activity of *PARIS* leading to suppression of *PGC-1 α* and causing dopaminergic cell loss (Shin et al., 2011). This implicates mitochondrial stress as an important factor in dopaminergic neuron survival, which could be due to the fact that dopaminergic neurons with their large arbors are metabolically very active than compared to other neurons. The increased metabolic demands may make dopaminergic neurons more vulnerable to mitochondrial dysfunction and cell death.

1.5.4 Aggregation induced proteolytic stress and the ubiquitin proteosomal system (UPS)

In addition to impairments of the respiratory chain component, complex 1, and oxidative stress there is also evidence of aberrant activity of the ubiquitin proteosomal system (UPS) leading to proteolytic stress that may be involved in the demise of

dopaminergic neurons (Chung et al., 2001, McNaught et al., 2003). Two PD-related genes (*parkin* and *UCH-L1*) are involved in the UPS, supporting this notion. *parkin* is an E3 ubiquitin ligase that confers substrate specificity via the process of ubiquitination with the aid of E1 ubiquitin-activating enzyme and E2 ubiquitin-conjugating enzyme, thereby targeting damaged polyubiquitinated proteins to the UPS once recognized by the 26S proteasome (**Fig 1.6**) (Pickart, 2001). The over 30 or so putative *parkin* substrates have been identified including modified glycosylated form α -synuclein (Shimura et al., 2001), including PARIS (Shin et al., 2011). The overexpression some of these substrates has been shown to exert cytotoxicity and the overexpression of *parkin* protects against substrate toxicity (Dong et al., 2003, Ren et al., 2003, Staropoli et al., 2003). *parkin* has been described as a multifaceted neuroprotective agent (Feany and Pallanck, 2003).

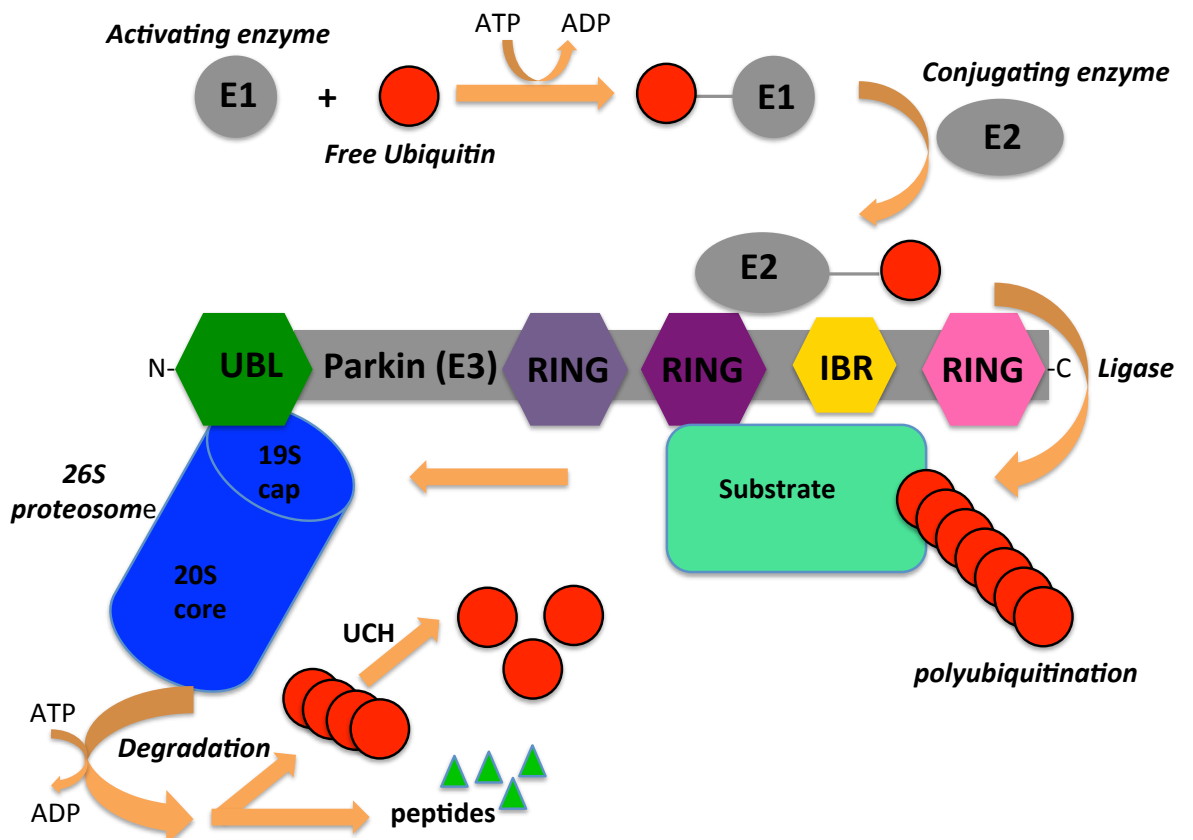


Figure 1.6 Parkin and ubiquitin proteasome system. A series of reactions are mediated by the enzymes of the UPS which ubiquitinate substrates and subsequently degrade them. Parkin binds to E2 enzymes and a number of substrates through its C-terminal RING-box domain and promotes ubiquitination of the substrates. Polyubiquitinated substrates are transported to the 26S proteasome, which is thought to bind to the ubiquitin-like domain of Parkin, and are rapidly degraded. This an energy-dependent protein degradation system in which proteins covalently modified with polyubiquitin chains are recognized and degraded by 26S proteasome. Ubiquitination is a sequential enzymatic reaction carried out by three enzymes, E1 (ubiquitin activating enzyme), E2 (ubiquitin conjugating enzyme) and E3 (ubiquitin ligase). E3 specifically recognizes the protein fated to be degraded and promotes its ubiquitination in concert with E2. Human Parkin has an E3 ubiquitin ligase activity (Shimura et al., 2001), a function that requires an intact RING finger and studies in *D. melanogaster* have shown similar mutations in this domain and others that compromise ubiquitin ligase activity (Cha et al., 2005).

1.6 *Parkin* models of PD

1.6.1 *D. melanogaster* models of PD

In *D. melanogaster*, *dparkin* is highly expressed in the central nervous system (CNS) and in the testis (Horowitz et al., 2001, Bae et al., 2003, Chintapalli et al., 2007). Adult flies with the loss of function of *dparkin* are semi-viable with reduced life span and locomotion (Greene et al., 2003, Pesah et al., 2004). Additionally, there are reports of dopamine-specific neuronal loss in *dparkin* mutant flies (Greene et al., 2003, Cha et al., 2005, Whitworth et al., 2005, Sang et al., 2007, Wang et al., 2007), but one group failed to show this age-dependent dopaminergic specific loss (Pesah et al., 2004). Irrespective of the loss of dopaminergic neurons, *dparkin* mutants have reduced staining in their CNS for tyrosine hydroxylase (*TH*), a key enzyme in the synthesis of dopamine (Greene et al., 2003, Cha et al., 2005, Whitworth et al., 2005, Wang et al., 2007). There is widespread apoptotic degeneration of adult flight muscles that correlates with the motor dysfunction as observed from geotaxis climbing assays of *dparkin* mutant flies (Greene et al., 2003). The locomotory defects observed in *parkin* mutant flies have been mainly shown to be due to muscle abnormalities rather than a neuronal failure (or more specifically to dopaminergic death) (Pesah et al., 2004). Additional defects include sterility in both male and female (Greene et al., 2003, Ottone et al., 2011). Male sterility is a result of late defects in spermatid formation in the germline (Greene et al., 2003).

A key observation from *dparkin* mutant flies was the presence of droopy wings and associated loss of thoracic muscles (Greene et al., 2003). The thoracic muscles showed mitochondrial abnormalities (Greene et al., 2003) suggesting oxidative stress most likely occur in flies with *dparkin* mutations. Firstly, longevity was reduced when flies were fed with a free radical generator agent, paraquat (Pesah et al., 2004). Secondly, a

loss of function allele of Glutathione S-transferase (*GST*) was identified as an enhancer of *dparkin*²⁵ (null) mutant phenotype from a genomic screen (Pesah et al., 2004). *GST*1 is an antioxidant and the flies without both the *dparkin* and *GST* genes show progressive loss of dopaminergic neurons and oxidative stress (Whitworth et al., 2005). Thirdly, *D. melanogaster parkin* is a negative regulator of the c-Jun N-terminal kinase (*JNK*) pathway suggesting its involvement in oxidative stress mediated signaling cascade (Cha et al., 2005). Finally, the lifespan of *dparkin* mutant flies was extended by enhancing antioxidant pathways (Saini et al., 2010). All of the above has shown that oxidative stress is as important in *dparkin* mutant fly models as in human PD. *dparkin* mutants are not only restricted to mitochondrial stress but also to proteosomal and endoplasmic reticulum stress. Mitochondrial dysfunction could explain the reduction in ATP in energetic tissues, like the muscle for instance, that results in the eventual degeneration (and also may affect some dopaminergic neurons) leading to motor dysfunction. The mitochondrial-associated defects in the form of their morphology, integrity and function observed in *dparkin* mutants has been shown to be ameliorated by up-regulating alternate modes of energy production via *AMPK* activity (Kim et al., 2012).

As noted above, most *dparkin* phenotypes in flies were not neuronal. Apart from one group that specifically stated that third instar *dparkin* mutant larvae have normal neuromuscular junction physiology, (Pesah et al., 2004) no other groups have reported whether or not they had investigated the any of the larval stages of *dparkin* mutant fly models.

1.6.1.2 *parkin*/ *PINK1* mitochondrial associated roles

Both *parkin* and *PINK1* have been shown to interact (Kim et al., 2008, Xiong et al.,

2009), showing they are both involved in a common pathway to preserve mitochondrial integrity. Mutations in *PINK1* gene, that encodes for serine threonine kinase, are also responsible for a proportion of early onset autosomal recessive PD (Valente et al., 2004a). This enzyme possesses a kinase domain, with an additional mitochondrial-targeting signal (Clark et al., 2006). *PINK1* is rich in the heads as well as the testes of adult flies, similar to that of *parkin* expression (Park et al., 2006, Park and Lee, 2006). *PINK1* mutants show very similar phenotypes to *parkin* mutants including reduced longevity, motor defects, mitochondrial abnormalities, male sterility and apoptotic muscle degeneration (Wang et al., 2006, Yang et al., 2006). *PINK1* mutants show a decline in mitochondrial numbers from dopaminergic neurons with increasing age. *PINK1-parkin* double mutants show similar phenotypes as individual mutants. *PINK1* mutant phenotypes are rescued by wild-type expression of *parkin*, whereas *PINK1* expression failed to rescue *parkin* phenotypes, thereby implicating *PINK1* action upstream of *parkin* in the *PINK1-parkin* pathway. This pathway is vital for the survival of the dopaminergic neuronal loss in *PINK1* mutants, as this selective neuronal loss is rescued with wild-type *parkin* expression (Clark et al., 2006, Park et al., 2006, Vos et al., 2012).

PINK1/parkin regulate mitochondrial integrity (Greene et al., 2003, Pesah et al., 2004, Guo, 2012, Vos et al., 2012). Cultured cells show that *PINK1* and *parkin* regulate mitophagy in *D. melanogaster*. This is supported by mammalian work and suggests the exciting possibility that failure of mitophagy, a quality control process, underlies the pathogenesis of *PINK1/ parkin* pathway (**Fig 1.7**).

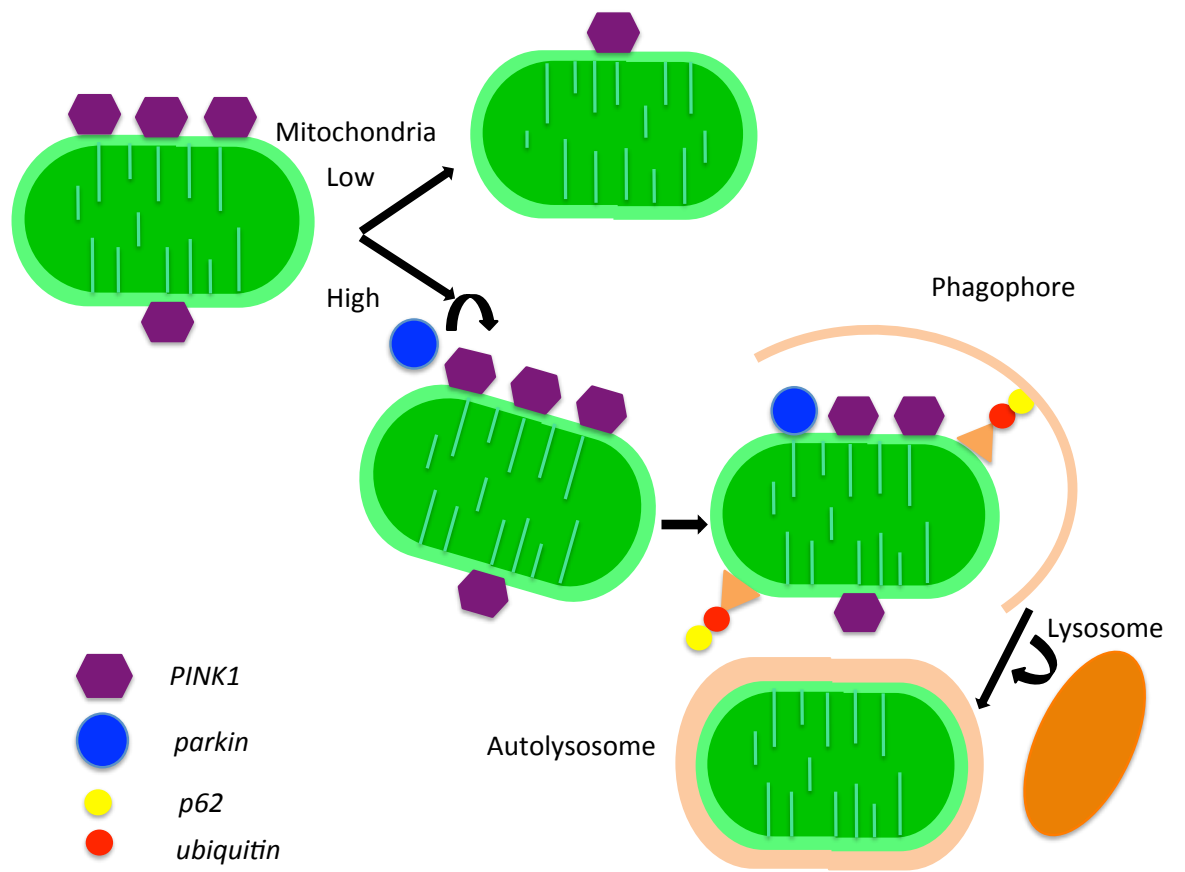


Figure 1.7 *parkin*-induced mitophagy. Under normal physiological conditions that maintain mitochondrial homeostasis: *PINK1* recruits *parkin* to the mitochondria, where these two proteins interact to eliminate abnormal mitochondria through mitophagy. Alterations in mitochondrial membrane potential ($\Delta\Psi_m$; a key indicator of mitochondrial physiology and cell viability) initiates the *PINK1-parkin* cascade of events leading to mitophagy. High mitochondrial membrane potential causes *PINK1* to be imported into mitochondria, then to be proteolytically processed and rapidly degraded (to have low endogenous levels of *PINK1*) under basal conditions. In the instance of low mitochondrial membrane potential, *PINK1* accumulates on the mitochondrial surface that signals to *parkin* to translocate to the mitochondria. *parkin* ubiquitinates mitochondrial proteins at the outer membrane, causes the recruitment of adaptor proteins (e.g. p62), which link ubiquitinated cargo to the autophagic machinery. Dysfunctional mitochondria are engulfed by phagophores, which matures into autophagosomes and fuse with lysosomes to autolysosomes, which eventually degrade their content.

Adapted from (Castillo-Quan, 2011).

dparkin (as well as *PINK1*) mutant phenotypes were rescued with the expression of pro-fission genes and decreasing expression of genes that promote mitochondrial fusion (Deng et al., 2008, Park et al., 2009, Poole et al., 2008, Yang et al., 2008). Reduction in gene copy number of dynamin-related protein 1 (*drp1*), a pro-fission gene, in a *PINK1* mutant background caused lethality (Deng et al., 2008, Poole et al., 2008). Thus, suggesting mitochondrial fission is promoted by both *PINK1* and *parkin*. The difference in the phenotypes of *drp1* mutants compared to that of *PINK1* or *parkin* mutant suggests that *PINK1/parkin* pathway aid to regulate mitochondrial fission machinery. Parkin is recruited to dysfunctional (depolarized) mitochondria involved in the organelle specific turnover of mitochondria termed mitophagy (Narendra et al., 2009).

1.7 D. melanogaster approaches to model neurodegenerative diseases

1.7.1 Introduction to D. melanogaster genes and their conservation to human genes

D. melanogaster, the common fruit-fly, has over 100 years' worth of research and has been extensively used for investigating basic questions concerning biological processes (Bellen et al., 2010). The completion of the *D. melanogaster* and human genome sequences revealed *D. melanogaster* and humans have many genes they share in common. Although *D. melanogaster* possesses a compact genome, approximately 1/30 of the human genome, approximately two thirds of the known human genes have a counterpart in *D. melanogaster* (666 of 911 genes in *D. melanogaster*) (Reiter et al., 2001), while 77% of human disease related genes are conserved in the fly (Rubin, 2000, Bier, 2005). Additionally, there is a considerable degree of conservation of metabolic and signaling pathways at a cellular level, and more strikingly the molecular mechanisms for complex behaviors such as circadian rhythm, learning and memory, sleep and aggression (Hall, 2003, Mershin et al., 2004, Greenspan et al., 2001, Bellen et al., 2010). *D. melanogaster* has been widely used to research a variety of biological

processes including cell death, cell proliferation, growth and migration. This remarkable organism is useful in our understanding of disease mechanisms through the identification of novel targets for potential therapeutic approaches towards human diseases (Auluck et al., 2005, Tain et al., 2009).

1.7.2 *D. melanogaster* models of neurodegeneration

The studies on neurodegenerative diseases using *D. melanogaster* models have mostly focused on Huntington disease (HD) (Ravikumar et al., 2004), Parkinson's disease (PD) (Pendleton et al., 2002) and Alzheimer's disease (AD) (Torroja et al., 1999), involving the misexpression of the relevant mutant human genes for huntingtin, α -synuclein and $A\beta_{1-42}$, respectively (Bilen and Bonini, 2005). *Drosophila* was shown to be an excellent model system for neurodegenerative disease (Hirth, 2010). *D. melanogaster* have short life cycles with 10 days generation time and 60-80 day life span allowing age related experiments to be completed within short periods of time. Therefore they are cheap to maintain compared to mammalian models (Guo, 2012). The fully sequenced and annotated *D. melanogaster* genome (Adams et al., 2000), along with the tools available for homology search algorithms, has aided the identification of several candidate *D. melanogaster*-disease homologues. Four of the five well-studied PD-related genes have fly homologues, these include single homologues for *Dardarin/ LRRK2*, *parkin*, *PINK1* and two closely related homologues for *DJ-1*. α -synuclein was the first gene associated with PD and the first PD-associated gene to be studied in *D. melanogaster*, although with no orthologue in the fly.

1.7.3 Genetic approaches using *D. melanogaster*

Reverse genetic approaches have been useful in the generation of loss-of-function (LOF) and gain-of-function (GOF) phenotypes that may successfully recapitulate symptoms of certain diseases. LOF phenotypes can be produced by inducing mutations

that lower or abolish the activity of gene of interest, e.g. by EMS mutation or by excision of P-elements. Alternatively, directed expression of an RNAi interfering transgene can be used to achieve subtle LOF phenotypes in, for example, specific types of neurons. A GOF phenotype can be generated through the directed expression of a dominant gene of interest. This could be used to increase the expression of the gene to abnormally high level, in those tissues where it is normally expressed. Alternatively, it may be expressed in tissues where it is not normally expressed. These techniques are facilitated by the *D. melanogaster* stock centers (e.g. Bloomington, Kyoto), which make stocks readily available and the many worldwide research laboratories which generously share reagents (fly lines, antibodies etc.).

1.7.4 *D. melanogaster* genetic toolbox used to model Parkinson's Disease

An array of sophisticated molecular genetic tools have been developed by the *D. melanogaster* community which has made the common fruit fly a remarkable organism to work with (Adams and Sekelsky, 2002; Johnston, 2002; Venken and Bellen, 2005). Genetic tools to achieve temporally controlled, tissue specific expression *in vivo* began with fusion of a promoter and a structural gene, for example, the *ninaE* promoter and the Rh2 opsin (Zuker et al., 1988). In this technique, the gene to be expressed was inserted next to the promoter, so that a new construct had to be generated for each gene to be expressed. This limited flexibility was overcome in the GAL4-UAS bipartite transcription activation system (Brand and Perrimon, 1993). In the GAL4-UAS system (**Fig 1.8**), two fly lines are deployed: in one stock, a promoter (or other genomic enhancer) is used to drive expression of GAL4 protein, which has no effect on the fly genome. The second transgenic fly line holds the gene of interest, under the control of Upstream Activating Sequence (UAS) to which GAL4 binds. In this stock, since there

is no GAL4 protein, there is no binding to the UAS and hence no expression of the gene of interest. When these two fly lines are crossed, the progeny contain both GAL4-UAS components, the expressed GAL4 binds to the UAS site, and this activates transcription of the gene of interest in a controlled fashion. The construction of many UAS stocks allows the directed production of a wide range of proteins, all with the same pattern of tissue expression. Equally, the production of many GAL4 lines, each with a different tissue specific pattern, enables comparison of the effects of the protein in a known place. The types of neuron in which a particular promoter drives expression may be identified by expressing a reporter (e.g. *lacZ* or GFP) which can be easily visualised

To generate GAL4 lines in *D. melanogaster*, enhancer trapping is often used. The principle of the GAL4 enhancer trap technique is the insertion of the GAL4 gene into a P-element. The P-element contains a weak promoter, which will respond to enhancers from the surrounding region of the genome. When these bind to the weak promoter in the genome, they activate GAL4 production (Bellen, 1999). The P-elements are transposable elements that insert randomly into the genome. Transposable elements are discrete pieces of DNA that are mobile, but the P-elements used in enhancer traps do not have transposase coding regions, which makes them stable insertions into the genome. P-elements used in enhancer trapping commonly also include a marker (e.g. *mini-white*⁺ eye colour gene) and sometimes *lacZ* or GFP as a reporter. The inclusion of the eye colour gene allows the investigator to trace the presence of the P-element during genetic crosses. By mobilising the P-elements and tracking lethality and expression patterns, new GAL4 lines are readily established (Duffy, 2002).

The immense flexibility of the enhancer trap and GAL4/UAS system has rapidly advanced the fly as a model of disease as it allows the expression of human disease-

related genes during the course of development and/or adulthood. The GAL4-UAS system has been very useful in the generation of models of PD, where pathological wild-type and mutant proteins (for example α -synuclein) have been specifically expressed in the fly brain in order to investigate effects on dopaminergic neurons (Feany and Bender, 2000).

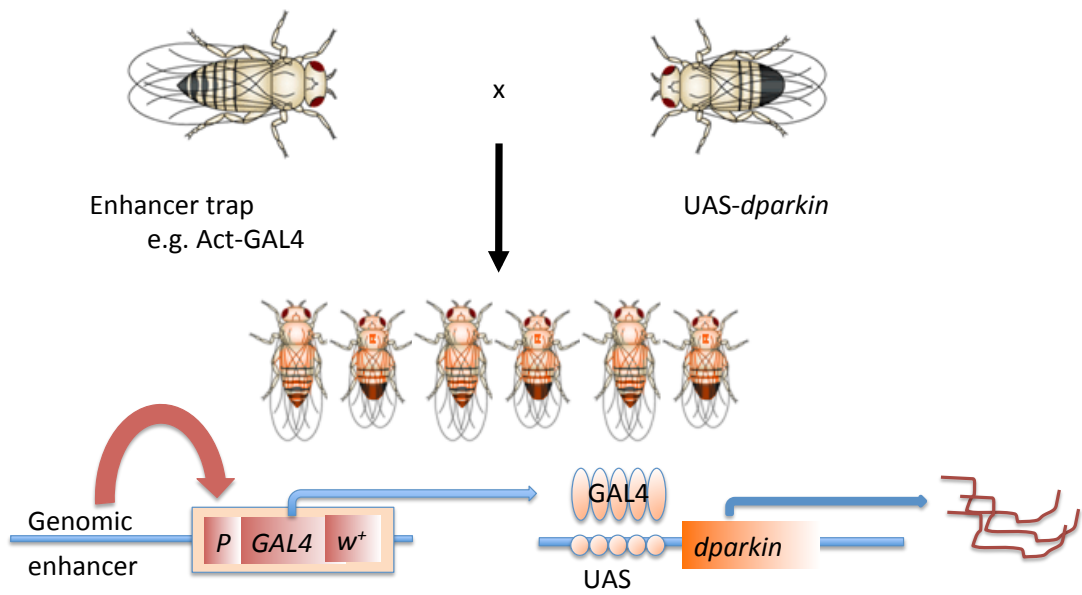


Figure 1.8 The GAL4-UAS system. The bipartite expression system that is composed of two separate parental fly lines, the responder (UAS) and the driver (GAL4).

1.7.5 Advantages and disadvantages of *D. melanogaster* PD models

Although many experimental advantages accrue from the lifespan and genetics of flies, the mouse does have some advantages. For disease-related gene homologs, the mouse has a higher degree of conservation to humans than the fly (Waterston et al., 2002). Additionally, having inbred mouse strains with the same genetic background and rapidly developing genetic tools may be able to induce a broad spectrum of phenotypic manifestations associated with PD. A few mouse models have shown mild perturbation of dopamine transmission in nigrostriatal circuits with behavioral defects (Fernagut and Chesselet, 2004) and some *α-synuclein* transgenic mice models show *α-synuclein*-induced aggregation accompanied with neuronal degeneration (Anwar et al., 2011).

Disappointingly, the majority of the genetic mice models fail to show all features of PD and many show no dopaminergic degeneration from *substantia nigra* (Fernagut and Chesselet, 2004, Von Coelln et al., 2004, Kitada et al., 2009, Gispert et al., 2009), whereas very few only show mild dopaminergic degeneration (Ramonet et al., 2011, Shin et al., 2011). The lack of dopaminergic cell death in mice, have been attributed to adaptive changes during the course of development over the life span of the mice. However there has been recent success in the development of mouse models recapitulating key aspects of PD, for example Dawson and co-workers used a conditional knockout mouse, to model the loss of *parkin* function. This model showed a progressive degeneration of dopaminergic neurons (Shin et al., 2011).

1.7.6 Observations made from *D. melanogaster* PD models

Flies have shown to be better at replicating the disease phenotypes as seen in humans, with specific dopaminergic degeneration and also presence of LB-like aggregates in fly

neurons. Manipulating the expression of PD-associated genes in the dopaminergic neurons in flies has been shown to lead to dopaminergic degeneration. For example Feany and Bender (2000) used transgenic flies to aberrantly express high levels of wild-type human *α-synuclein* in dopaminergic cells and this caused the death of some dopaminergic neurons of the adult fly. Similar results were also obtained from the expression of A53T or A30P (which are PD-related mutations) forms of the *α-synuclein* gene, in the fly nervous system (Feany and Bender, 2000). More importantly, the serotonergic neuronal population and the gross brain morphology in the *α-synuclein*-expressing flies were not altered, suggesting that toxicity caused by *α-synuclein* is specific to dopamine containing neurons in the CNS. Although, there is evidence to suggest *α-synuclein* toxicity is not restricted to the dopamine neurons as the expression of *α-synuclein* in the fly eye induced retinal degeneration (Feany and Bender, 2000).

The adult fly brain contains clusters of dopaminergic neurons (Nässel and Elekes, 1992). These dopaminergic neurons have been shown to degenerate when flies are fed with a complex 1 inhibitor, rotenone (Coulom and Birman, 2004). Rotenone has also shown to cause the degeneration of dopaminergic neurons in mammals (Sherer et al., 2003, Bové et al., 2005). Together these provide evidence that the toxin rotenone induces similar effects on the dopaminergic neurons in two different animal models, suggesting the existence of a common conserved mechanism of rotenone between mammals and flies.

Although some *D. melanogaster* PD models show dopaminergic cell death (Feany and Bender, 2000, Whitworth et al., 2005, Trinh et al., 2008), it is not common to all. PD models show much more than just dopaminergic cell death including non-dopaminergic neuronal dysfunction, locomotory deficits, reduced life span, abnormal wing posture,

aggregate formation, abnormal mitochondrial morphology and organization and energetic tissue degeneration.

1.7.7 The *D. melanogaster* life cycle

Through a series of larval moults, the larva grows approximately 100-fold in size until it crawls out of the food as a third instar larva and selects a site for pupation. When the fly undergoes metamorphosis, the majority of the larval tissues including muscles degenerate and adult tissues develop from imaginal discs and histoblasts. The larval nervous system is not lysed, although further development occurs. Other tissue including the Malpighian tubules (excretory structures), fat bodies and gonads remain.

During pupal development, which lasts 3-4 days, the axons of the motoneurons innervating the degenerating muscles of the larva retract and renew their connections with newly regenerated adult muscles. At the end of the metamorphosis phase, an adult fly ecloses from the pupal case (**Fig 1.9**).

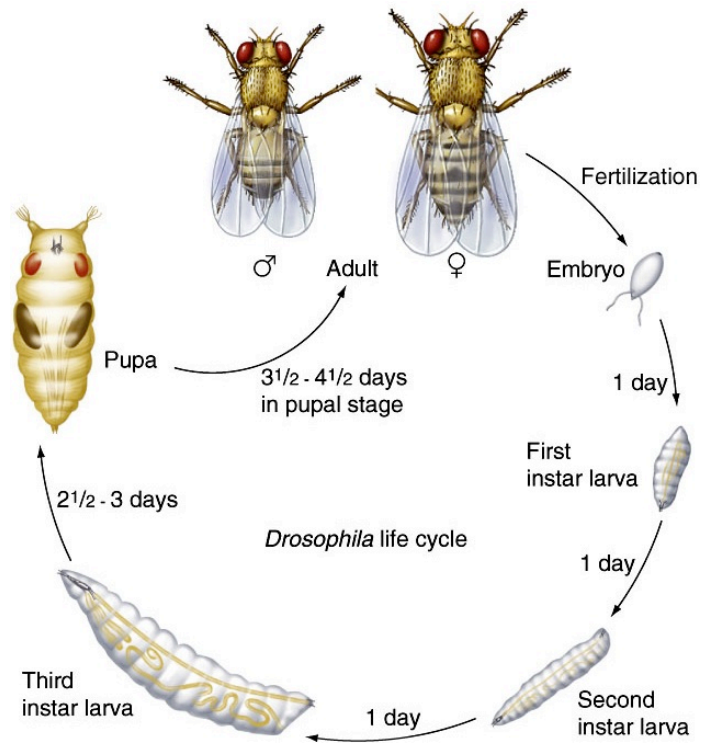


Figure 1.9 The *D. melanogaster* life cycle. The embryo develops and gives rise to a first instar larva, subsequent growth leads to the second and third instar larvae. The transitions between larval instars are moults. The process that converts a third instar larva to a pupa is termed pupariation. Emergence of the adult from the pupal case is termed eclosion.

Derived from Hartwell, Genetics: From genes to genomes, McGraw-Hill (Hartwell et al., 2010).

1.7.8 The *D. melanogaster* nervous system

The developmental period from the time of the unfertilized egg to reach a fully functional larval nervous system (or to the first instar larval stage crawling around the food) takes less than 24 hours. The larval CNS comprises the two lobes and the ventral nerve cord (VNC) where the motor neurons descend their neuronal axons to innervate muscle cells forming synapses at the level of neuromuscular junction (NMJ). The larval CNS contains approximately 125,000 neurons (whereas the fully developed more complex fly brain has 250,000 neurons). This is a million fold less than an average human brain, but with a similar complexity of neuronal variety (Venken et al., 2011). Flies use the same neurotransmitters (glutamate, GABA and acetylcholine), as mammals, share biogenic amines (e.g. dopamine and serotonin) and also possess a variety of neuro-modulatory peptides. However, flies, unlike vertebrates, use glutamate as an excitatory neurotransmitter at the neuromuscular junction (NMJ) and acetylcholine in most sensory and central synapses. Another difference between the fly and vertebrate nervous system is the ratio of neurons to glia, in flies this is 1:10 whereas in vertebrates it is 10:1 (Venken et al., 2011). This may be because glia surround the bundles or fascicles of neurons, rather than individual neurons in flies. However, a number of glial types exist in flies (Venken et al., 2011).

D. melanogaster neuronal cell bodies are located in a cortical rind encapsulating the brain neuropile and made up of axons, dendrites and synapses. The majority of synapses make contacts with multiple postsynaptic targets often forming diads, triads or tetrads. On average, there are far fewer fly synapses per neuron compared to vertebrate synapse (Venken et al., 2011). A variety of sensory nerves are embedded in the body wall muscles and feedback to the ventral nerve cord occurs through these nerves.

The larval CNS gives rise to segmental nerves (SN), which innervate the body wall sense organs and muscles, with each muscle being consistently innervated in the same way from larva to another, with a recognizable pattern of synaptic boutons (Budnik et al., 1990, Cattaert and Birman, 2001, Barclay et al., 2002).

1.7.8.1 The *D. melanogaster* dopaminergic system

The biosynthesis of the neurotransmitter, dopamine, is conserved between *D. melanogaster* and humans. Dopamine is synthesized in the cytoplasm from its precursor, tyrosine, with two enzymatic steps. Firstly, tyrosine is broken down by tyrosine hydroxylase (TH) to produce L-3,4-Dihydroxyphenylalanine (LEVODOPA or L-DOPA), and then subsequent decarboxylation occurs by the aromatic L-amino acid decarboxylase (AAAD) to produce dopamine. Dopamine does not cross the blood brain barrier (BBB) whereas L-DOPA and AAAD can. Gene products involved in dopamine homeostasis have the potential to hold neuroprotective properties, as dopamine itself is suggested to possess neurotoxic effects (Miller et al., 1999).

The excess dopamine from extracellular spaces is taken up via the plasma membrane dopamine transporters (*DAT*) (Nass and Blakely, 2003, Ritz et al., 2009). Additionally, dopamine packaging into synaptic vesicles via the vesicular monoamine transporter (*VMAT*) removes excess dopamine. *VMATs* are required by all aminergic cells to transport the dopamine synthesized in the cytoplasm to be taken up into the lumen of the synaptic vesicles (Chaudhry et al., 1998). Dopamine is stored in high millimolar concentration in synaptic vesicles (SV) by the vesicular monoamine transporter, where it is kept in a stable form (Staal et al., 2004). Mammals possess two *VMAT* genes (*VMAT1* and *VMAT2*). In mammals, the neural isoform *VMAT2*, is responsible for the

storage of dopamine, serotonin, and noradrenaline in all central aminergic neurons whereas the *VMAT1* gene is expressed at the periphery and in neuroendocrine cells (Liu and Edwards, 1997, Erickson and Varoqui, 2000, Eiden et al., 2004). *D. melanogaster* contains a single *VMAT* ortholog (*dVMAT*) that is expressed in all dopaminergic, serotonergic, and octopaminergic cells in both larvae and adults (Greer et al., 2005, Chang et al., 2006).

Dopamine is an essential neuromodulator in the mammalian CNS that is involved in attention, movement control, motivation and cognition (Riemensperger et al., 2011). The dopaminergic system is involved in locomotor control in humans as well as in *D. melanogaster* (Yellman et al., 1997, Lima and Miesenböck, 2005), although complete understanding of the underlying circuits that govern locomotion are still unknown. Approximately 70 dopaminergic neurons have been described in the CNS of the fly third instar larva (Budnik et al., 1986). Dense dopaminergic projections almost completely cover the entire neuropil of the *D. melanogaster* larval CNS. The adult fly brain contains additional dopaminergic neurons, in 15 clusters (Budnik and White, 1988, Nässel and Elekes, 1992, Mao and Davis, 2009), some projecting to higher brain centres including the central complex and the mushroom bodies (Tanaka et al., 2008, Mao and Davis, 2009).

1.7.9 Larval locomotion for motor function assays

Although the *D. melanogaster* brain has a far smaller population of neurons compared to a mammal, the fly still exhibits a large number of behaviors. A promising start has been made on understanding the motor circuits involved in escape behavior, larval crawling and flight, but much of the detail remain to be fully defined (Crisp et al., 2008, Fotowat et al., 2009). The simpler larval nervous system controls a number of

stereotyped behaviors including locomotion, and so provides a platform to make an excellent model system to study nervous system related disorders.

The *D melanogaster* larva poses a range of motions including peristalsis, bending, turning and feeding: peristaltic movement has been extensively studied (Heckscher et al., 2012). The larva has 10 segments: three thoracic segments (T1-T3) and seven abdominal segments (A1-A7) with specialized structures at the anterior and posterior ends (Keshishian et al., 1996). There are approximately 60 muscles in a segment under the epithelium.

The larva propels forward via contraction from the posterior segments to anterior segments leading to forward peristaltic locomotion. During peristalsis, the muscle contraction travels in approximately 1 second from the posterior to anterior. When the peristaltic wave reaches the anterior segment, the head is moved forward and then attached on the crawling surface with mouth hooks. The next cycle resumes when the peristaltic wave is initiated in the posterior end: cycles may be separated by brief pauses, during which head swinging and turning occurs. For the consecutive waves of peristalsis to follow, motor neurons in each segment have to be sequentially activated throughout the body axis in a highly regulated fashion.

1.7.9.1 Neuronal network contribution to larval locomotion

Electrophysiological manipulations allow the recordings of regular rhythmic bursts of motor neuronal activity that concurrently occur with locomotive waves to be monitored (Fox et al., 2006). Rhythmic motor behaviors like crawling involve specialized circuits, central pattern generators (CPGs), to contribute to the patterned discharges in motor

neurons via their peripheral axons to muscles (Johnston and Levine, 1996, Marder and Bucher, 2001). The activities of motor neurons that innervate the body wall muscles have been used as a measure of output from the CPG (Fox et al., 2006). Both the CPG, the neural network involved in the timing of the motor discharge, and the sensory feedback control the rhythmic movements. This concept has been applied to the neuronal networks involved in larval locomotion although the identity of CPGs responsible is presently unknown. However, there is some evidence that patterned motor outputs can be generated in the absence of sensory outputs by central circuits alone (Fox et al., 2006, Hughes and Thomas, 2007). When sensory feedback is compromised, change in peristalsis pattern is observed. This shows that neural circuits including the motor neurons, sensory feedback and interneurons in the CPG, participate in the regulation of coordinated pattern of peristaltic locomotion.

1.7.10 Motoneuron development and connectivity to muscle

D. melanogaster neurons and glia in the embryonic CNS are derived from progenitor cells called neuroblasts, which undergo asymmetric cell divisions to generate a diversity of cell types (Goodman and Doe, 1993). A population of approximately 400 neurons, including an estimated 38 motor neurons, are generated from 30 distinct neuroblasts within each half-segment (also known as hemisegment) of the embryonic ventral nerve cord (VNC) (Schmid et al., 1999). Abdominal hemisegments in the embryo have 30 highly stereotyped body wall muscles, each of which is innervated by one or more of the 38 different motor neurons (Landgraf et al., 1997).

Several transcription factors have been identified as crucial in regulating the process by which motor neurons choose their peripheral branch to later form contact with the muscle, and form the neuromuscular junction (NMJ) (Landgraf and Thor, 2006b,

Landgraf and Thor, 2006a). These include Even-skipped (Eve), Nkx6, Hb9, LIM, Lim3 and POU (Landgraf et al., 1999, Thor et al., 1999, Broihier and Skeath, 2002, Certel and Thor, 2004). The vertebrate orthologues of these transcription factors have similar functions and molecular mechanisms in motor neuron specification. This shows that there is conservation between fly and higher organisms in synapse formation (Thor and Thomas, 2002). Molecules that participate in axon guidance and regulate branch selection have also been discovered these include Toll which inhibits motor innervation when expressed in muscles; and Netrin B, which is a secreted protein from the netrin family, that is expressed in certain muscles including muscle 6 and 7 (Ruiz-Cañada and Budnik, 2006).

The connectivity of motor neurons to muscles determines the intricate pattern of motor output. Approximately 38 motor neurons in the ventral nerve cord descend their axons via one of the six branches of the peripheral nerves that include the intersegmental nerves (ISN, ISNb and ISNd), segmental nerves (SNa and SNc), and a transverse nerve (TN) (Keshishian et al., 1996, Landgraf and Thor, 2006a). Internal muscles in the dorsal, ventro-lateral and ventral domains are innervated by ISN, ISNb and ISNd respectively. Both SNa and SNc motor neurons innervate external muscles in the lateral and ventral domains respectively.

1.7.10.1 The Neuromuscular junction (NMJ)

The synaptic connection between the postsynaptic muscle and the presynaptic motor neuron is often interchangeably termed a synapse or a NMJ (**Fig 1.10**). Both embryonic and larval nervous systems, with particular emphasis on NMJ, have allowed us to understand the basic mechanisms of nervous system development and function.

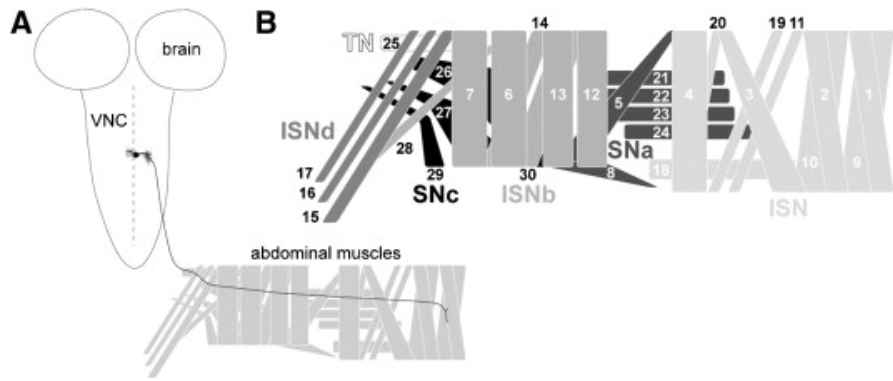


Figure 1.10 The organisation of the neuromuscular junctions (NMJ) of *D. melanogaster* larvae. Movement of the larva is produced by peristaltic waves of contraction of the body wall musculature. The rhythmic contractions of the body wall segments are coordinated by the central pattern generator (CPG). The motor neurons that drive locomotion are located in the dorsal region of the ventral ganglion. (A) The brain and ventral nerve cord (VNC) of the larval CNS. (B) The stereotyped organization of the peripheral body wall muscles. In each abdominal hemisegment, motor axons from the six main nerve branches (ISN, ISNb, ISNd, SNa, SNc, and TN) innervate the 30 muscles.

Reproduced from (Kim et al., 2009) with permission.

Mammals and arthropods have shown that during the course of their NMJ development, dramatic changes in morphology take place both pre and post-synaptically (Gorczyca et al., 1993). An increase in *D. melanogaster* larval muscle size occurs during the course of development to late larval stage, to accommodate this change, to retain synaptic efficacy, the NMJ expands, making forming new branches and synaptic boutons (Schuster et al., 1996, Zito et al., 1999, Ruiz-Cañada and Budnik, 2006). Thus, this makes the NMJ an excellent model synapse to study synaptic growth and plasticity (Ruiz-Cañada and Budnik, 2006, Collins and DiAntonio, 2007). Another important characteristic of these synapses is their ability to homeostatically regulate synaptic activity for example, by increasing neurotransmitter release or altering their receptivity to pre-synaptic signals in order to retain the consistent physiological levels of postsynaptic potentials, in the instance of muscle expansion (Davis, 2006).

The patterned neuromuscular connection is developed by the end of embryogenesis and this pattern remains throughout larval life with small changes in soma position, axon projection and dendrite morphology (Hoang and Chiba, 2001). The molecular mechanisms that regulate synapse formation and function are inherently similar between vertebrates and *D. melanogaster* (Keshishian et al., 1996, Featherstone and Broadie, 2000). Key molecules and processes that are regulate NMJ development, for example TGF β /BMP and Wnt/Wg pathways, endocytic machinery, autophagy, and electrical excitability, have been uncovered (Budnik et al., 1990, Keshishian et al., 1996, Featherstone and Broadie, 2000, Marqués, 2005, Dickman et al., 2006, Collins and DiAntonio, 2007, Shen and Ganetzky, 2009). The synaptic growth is achieved typically by a synaptic bouton budding from a parent bouton at the end of the nerve branch, where it extends from the parent bouton and becomes an individual mature

bouton itself thereafter (Zito et al., 1999). The NMJ typically consists of branched chains of varicosities called synaptic boutons (often described as ‘pearls on a string’) that arise (or ‘sprout’) from the motor neurons and are embedded by an elaborate membranous compartment formed by the muscle. The larval NMJ terminals, synaptic boutons, are classified into larger type I endings, smaller type II endings and minor type III endings. Type I are subdivided into type-I small (Is) and type-I big (Ib) (Atwood et al., 1993) (please refer to methods). Motor neurons with terminals type-Ib have bigger boutons with low threshold firing project onto single muscles, whereas type-Is motor neurons have smaller boutons with a high threshold innervate groups of muscles (Choi et al., 2004, Schaefer et al., 2010)

Individual boutons possess multiple release sites, termed active zones, where synaptic vesicles dock and later fuse. In front of each active zone there are postsynaptic glutamate receptors clustered ready to sense the release of glutamate, the transmitter (Marrus et al., 2004). Each bouton contains roughly ten active zones and each motor neuron can form around 500 such synapses onto an individual muscle cell.

1.9 Neurotransmission

1.9.1 Membrane potential and action potentials

The precise electrophysiological understanding of nerve and muscle emerged from the discovery of electricity itself. Techniques were devised by a number of European scientists including Luigi Galvani, Emil Du Bois-Reymond, Carlo Matteucci and Hermann von Helmholtz (Brazier, 1979). These electrophysiologists showed through the application of electrical stimulus to the nerve and the muscles, that the flow of the electricity along the nerve fibres was the cause of movements generated from such commands from the brain to the muscle.

Electrophysiological studies of electrical activity of nerves revealed that the conduction of information along the length of the axon was mediated via the active generation of electrical potential known as the action potential (AP). The squid giant axon is an excellent preparation to study the AP as its diameter (0.5 mm) made it amenable to intracellular recording. Alan Hodgkin and Andrew Huxley demonstrated that axons at rest are electrically polarized thus having a resting membrane potential (RMP) that was negative, ~ -60 mV inside compared to the outside (Hodgkin, 1939, Hodgkin and Huxley, 1945). The RMP is maintained by the sodium-potassium pumps, which extrude 3 sodium ions outwards and 2 potassium inwards, at the cost of ATP hydrolysis. When an AP is generated, the polarization seen at rest is abolished (consequently the cells became depolarized) and shifted toward and beyond 0 mV. At rest all of the sodium permeable voltage gated ion channels are closed. When a stimulus reaches the threshold (~ -55 mV) this causes the initiation of an AP, where the voltage gated sodium channels open allowing the sodium ions to enter the cells. All voltage gated sodium channels open to allow more sodium into the cell until it reaches its equilibrium potential. Thereafter, repolarization occurs and as it becomes slightly more negative in comparison to the RMP. This period of increased polarization is known as the after-hyperpolarization (also known as the undershoot). The AP generation in all types of neurons and muscle cells follows the same principles of those described in the giant squid by Hodgkin and Huxley (HODGKIN and HUXLEY, 1952, Squire et al., 2003). Flies and mammals have sodium channels that propagate action potentials, additionally the potassium and calcium channels that regulate the membrane potential are from the same families (Venken et al., 2011).

1.9.2 Advantages of *D. melanogaster* NMJ for assessing synaptic function

The release of neurotransmitters at the fly NMJ is similar to the chemical transmission at the vertebrate synapses. However the neurotransmitter released at the fly NMJ is glutamate whereas acetylcholine is released from vertebrate motor neurons. The fly NMJ mimics a central synapse. The neurotransmitter is packaged into synaptic vesicles and then releases glutamate into the synaptic cleft upon exocytosis. Miniature excitatory junctional postsynaptic potentials (mEJPs) also known as “minis” occur when single vesicles fuse spontaneously giving rise to individual ‘quantal’ events.

The *D. melanogaster* NMJ is an accessible model synapse for the studying all aspects of synaptic development, function and plasticity. The NMJ has played a significant role in understanding neurotransmitter release. The molecules involved in synaptic transmission are also conserved between *D. melanogaster* and vertebrates. For example, acetylcholine and glutamate are neurotransmitters in both groups, and calcium, syntaxin and synaptobrevin are always involved in vesicle release (Richmond and Broadie, 2002, Broadie and Richmond, 2002). The function of proteins involved in synaptic transmission has been explored using biochemistry and genetics in flies (Broadie, 1995, Broadie et al., 1995, Schulze et al., 1995). Studies now shed light on the nature of exocytotic event, distinctions between exocytotic pathways in neurons and the mechanisms regulating synaptic strength. The mechanism of neurotransmitter release is important in the context of the development of synaptic function and how synaptic activity can shape development.

The third instar larval preparations are well suited for electrophysiological manipulations as they possess large muscle fibers that are relatively easy to access and impale. Additionally, it is possible to draw the segmental nerves from the ventral nerve

cord into a stimulating pipette, so that the neuromuscular junction activity can be controlled precisely. In comparison, the first instar larvae are a little more challenging to work with, but this earlier stage allows recordings of strains with lethal mutations. From embryonic to third instar, quantal events along with evoked (stimulated) postsynaptic responses can be observed and resolved from noise signals (Ruiz-Cañada and Budnik, 2006). Jan and Jan's (1976) electrophysiological studies demonstrated the multiple motoneurons innervate individual body wall hemi-segment (Jan and Jan, 1976). The stereotypical arrangement of fly NMJ synapses shows comparability and little variation from animal to animal (Keshishian et al., 1996). A physiological saline based on the composition of larval hemolymph, HL3 (Stewart et al., 1994), preserves synaptic transmission as well as muscular function, synaptic integrity and offers extended period in which recordings can be undertaken. The majority of the recordings are undertaken in the third instar larva or an earlier stage, once an incision is made along the dorsal midline, commonly on muscle 6 and 7 due to their accessibility and the large size (Li et al., 2002). These muscles are innervated by two different types (Ib and Is terminals) of motor neuron contributing to the generation of the postsynaptic response, Excitatory Junctional Potentials (EJPs) (Atwood et al., 1993, Hoang and Chiba, 2001, Lnenicka and Keshishian, 2000).

1.10. Rationale for the thesis project

PD is characterized by motor dysfunction accompanied with selective loss of dopamine producing cells. The *parkin* gene, as previously mentioned, encodes a highly conserved E3 ubiquitin ligase involved in the UPS degradation pathway. LOF mutations in *parkin* gene are a common cause early onset autosomal recessive juvenile Parkinsonism (ARJP), with an average age of onset of 32 years old. Previous *D. melanogaster parkin* (*dparkin*) models confidently describe non-neuronal phenotypes, for example, apoptotic

muscle degeneration, defects in spermatogenesis and droopy wings. Adult fly models of *dparkin* knockouts have shown promising phenotypes (including mitochondrial abnormalities, locomotory defects and dopaminergic loss) that have been related to human forms of PD. Some studies (not all) have shown dopaminergic degeneration in specific clusters. At the start of the investigation, there were no known reports of investigations into the *dparkin* larva except for one group that found normal NMJ morphology and physiology (Pesah et al., 2004). The characteristic neuronal death associated with PD suggested that it was important to examine neuronal (rather than muscle) phenotypes. Finally, working with the larva, a juvenile stage in the fly, offered the opportunity to test for early phenotypes at the start of the (neuro) degenerative process.

1.10.1 Aim and objectives of the thesis

The aim of the project was uncover neuronal dysfunction in *parkin* larvae.

Objectives:

1. What are the neurophysiological or anatomical dysfunctions observed in the juvenile *parkin* larvae?
 - a. Is their synaptic function altered?
 - b. Do they show a motor dysfunction at the level of behavior?
 - c. Do they show abnormal synapse morphology?
 - d. Is there a metabolic dysfunction?

2. What role does oxidative stress play in *parkin* larval dysfunction?
 - a. What is the impact of ubiquitous expression of 'pure' antioxidant transgenes?
 - b. What is the impact of ubiquitous expression of multi-action antioxidant transgenes?
 - c. Are oxidative stress-induced signals up-regulated?

- d. What effect does manipulating energy homeostatic mechanism have?
3. What are the benefits of pharmacological manipulation of AMPK or dopamine synthesis?
 - a. What does activation of *AMPK* have on larval phenotypes?
 - b. *parkin* larvae show reduced crawling, is this a indicator of a loss of dopamine signaling?

Chapter 2: Methods and Materials

2.1 Overview

D. melanogaster is one of the most genetically tractable model organisms. This chapter describes the genetic techniques employed in this project. It also describes the ways in which the behavioural, electrophysiological and anatomical changes in *dparkin* mutant larvae were measured.

2.1 Fly husbandry and protocols

2.1.1 *D. melanogaster* stocks

dparkin (*parkin*²⁵/*TM6B* and *parkin*^{Z3678}/*TM6B*) mutant *D. melanogaster* lines were kind gifts from Dr Alex Whitworth (University of Sheffield). *D. melanogaster* stocks for this project were originally purchased from Bloomington Stock Centre (Indiana; <http://flystocks.bio.indiana.edu/>), already present in the lab or created by Dr Sean Sweeney. All the stocks used for this research are outlined in table below.

Stocks obtained from external sources were quarantined for at least two generations. These stocks were transferred twice a week to fresh food to be confident they were free of mites. Mites feed on the eggs and prevent breeding. Thereafter, the flies were maintained either at 25°C or 18°C. Stocks were transferred into fresh food as required, as the *D. melanogaster* life cycle takes 10-11 days at 25°C and twice as long at 18°C.

2.1 Table of Stocks

STOCKS	STOCK SPECIFIC INFORMATION	SOURCE	REFERENCE
Control Stocks			
<i>w</i> ¹¹¹⁸	White-eyed mutant Loss of function (referred to as <i>w</i> in the	Gift of John Sparrow, (University of York, (UoY))	

	text and w- in legends)		
<i>Canton S</i>	Wild-type Red eyes	Gift of John Sparrow, UoY	
<i>CS/w⁻</i>	Cross between our <i>Canton S</i> and <i>w¹¹¹⁸</i> stocks		
Balancer Stocks			
<i>CyO-GFP/If; TM6b/MKRS</i>	Second and Third chromosome balancers	Gift of Sean Sweeney, UoY	
<i>TM3/TM6b</i>	Third balancer chromosome	Gift of Sean Sweeney, UoY	
GAL4 Stocks			
<i>elav^{3E1}-GAL4/ TM6b</i>	Embryonic lethal abnormal vision; Third chromosome; Pan-neuronal driver	Bloomington Stock Centre	
<i>G14-GAL4/ CyO-GFP</i>	Second chromosome; Muscle driver	Akinao Nose (Tokyo)	(Shishido et al., 1998)
<i>TH-GAL4</i>	Tyrosine hydroxylase driver; Third chromosome; Dopaminergic neuron driver	Friggi-Grelin	(Friggi-Grelin et al., 2003)
<i>Act5c-GAL4/ CyO-GFP</i>	Second chromosome; Ubiquitous driver	Bloomington Stock Centre	

STOCKS	STOCK SPECIFIC INFORMATION	SOURCE	REFERENCE
UAS Stocks			
UAS- <i>fos</i> ^{DN}	Second chromosome; Reduces expression of FOS	Bloomington Stock Centre	(Sanyal et al., 2002)
UAS- <i>jun</i> ^{DN}	Second chromosome; Reduces expression of JUN	Sean Sweeney, UoY	(Eresh et al., 1997)
UAS- <i>BSK</i> ^{(K53R)DN}	Third chromosome; Lack of kinase activity	Sean Sweeney, UoY	(Weber et al., 2000)
UAS- <i>AMPK-α</i> ^{T184D}	Third chromosome; Phosphomimetic, activated version of AMPK	Jay Brennan	(Swick et al., 2013)
UAS- <i>Sod1</i>	Second chromosome; Wild-type Superoxide dismutase 1 (Cytoplasmic)	Sean Sweeney, UoY	(Milton et al., 2011)
UAS- <i>Sod2</i>	Second chromosome; Wild-type Superoxide dismutase 2 (Mitochondrial)	Sean Sweeney, UoY	(Milton et al., 2011)
UAS- <i>Cat</i>	Second chromosome; Wild-type catalase	Fanis Missirlis, Queen Mary's London (QML)	(Missirlis et al., 2001)
UAS- <i>TRX-R2</i>	Third chromosome; Wild-type (mitochondrial) Thioredoxin reductase	Fanis Missirlis, QML	(Tsuda et al., 2010)
UAS- <i>gst-S1</i>	Third chromosome; Wild-type glutathione-s-transferase Sigma-1	Alex Whitworth, University of Sheffield (UoS)	(Whitworth et al., 2005)
UAS- <i>parkin</i> ^{C2}	Second chromosome; Wild-type <i>Drosophila parkin</i>	Alex Whitworth, UoS	(Whitworth et al., 2005)

STOCKS	STOCK SPECIFIC INFORMATION	SOURCE	REFERENCE
Mutant Stocks			
<i>parkin</i> ²⁵ <i>/TM6b</i>	Third chromosome; <i>parkin</i> (null) mutant induced by p-element excision of the full first three exons and half of exon 4. Complete loss of protein.	Alex Whitworth, UoS	(Greene et al., 2003)
<i>parkin</i> ^{Z3678} <i>/TM6b</i>	Third chromosome; <i>parkin</i> (hypomorph) mutant; an ethyl methanesulfonate (EMS)- induced missense point mutation (stop codon). Some protein produced.	Alex Whitworth, UoS	(Whitworth et al., 2005)
<i>nubian/</i> <i>CyO</i>	Second chromosome; Phosphoglycerate kinase mutant	Troy Littlejohn	(Wang et al., 2004)
RNAi Stocks			
<i>dparkin</i> RNAi	Third chromosome; RNAi knockdown of <i>parkin</i> transcript	Bingwei Lu, (Stanford University, USA)	(Yang et al., 2003)

2.1.2 *D. melanogaster* diet

Experimental crosses were reared at 25°C and parental flies were transferred into fresh fly media every 3-4 days to prevent overcrowding of larvae, mixing of generations or death of parental flies by sticking onto the surface of churned media. All stocks and few experiments, detailed later, were raised on standard yeast-sugar-agar media. The Technology Facility (TF) at the University of York produced autoclaved standard media based on Carpenter's recipe (Carpenter, 1950). All the following components were mixed in a large conical flask: yeast, 25 g/l sucrose, 3.75 g/l agar, 0.125 g/l calcium chloride, 0.125 g/l ferrous sulphate, 0.125 g/l manganese chloride and 0.125 g/l sodium chloride, and 2g/l potassium-sodium tartrate. After autoclaving and cooling anti-fungal agents were added to the medium: 0.0015 g/l Bavistine and 0.2 g/l p-hydroxybenzoic acid methyl ester (Nipagin). ~8 ml of medium was pipetted into each 25 cm³ vial which was topped with a cotton wool bung (ensuring air circulation but no escape of flies).

'Instant media' Formula 4-24 (Carolina Biological Supplies) was prepared for drug experiments. This proprietary mixture is a trade secret formula. The media was prepared by using equal volume of water (in which drugs or vehicle had been dissolved) and instant media flakes along with a pinch of yeast granules for each vial. This instant media was also used to overcome problems of reliability and viability of *dparkin* mutant lines, because (when they were grown on yeast-sugar-agar media) mould and/or slime sometimes developed.

Fly food was prepared freshly every week as required and extra trays were stored at 18°C before use.

2.1.3 Fly Pushing

A dissection microscope (Zeiss Stemi 2000 Dissection Microscope) was used to distinguish between the sexes, to look for virgin traits and to identify phenotypic

markers. Flies from vials were transferred onto a porous pad connected via tubing leading to an outlet valve on the CO₂ gas cylinder (Dutscher Scientific, UK) allowing gas to seep through and anaesthetize the flies.

The primary method of collection of virgin females involves tipping out all flies from the vial in the morning and collecting females within 8 h after the time of emptying the vial, as flies do not mate for up to 8 hours after eclosion. Secondly, flies that had eclosed during the night and early morning can be identified on this basis. Freshly eclosed female flies (less than 2 h old) were identified by their light body color and dark meconium in the gut, or by their unexpanded wings. Females that could be potential virgins were collected separately, dated and left for a week to check their virginity status by ensuring any eggs laid by them remained unhatched.

2.1.4 Recombination crossing scheme

Recombination was employed when a mutation of the recessive third chromosome gene *parkin* was required along with a third chromosome UAS transgene, for example *parkin*²⁵ and UAS-*AMPK*. The scheme for this is shown in (**Fig 2.1**). First, *w*⁻; *parkin*²⁵/*TM6b* flies were crossed with UAS-*AMPK* flies and virgin females were selected from the progeny. The virgin females were chosen because recombination only occurs in female in *D. melanogaster*. These females were individually crossed with a *w*⁺; *TM3*/*TM6b* male. As the *parkin*²⁵ and UAS-genes are both marked with *w*⁺, potential recombinants have darker orange eyes.

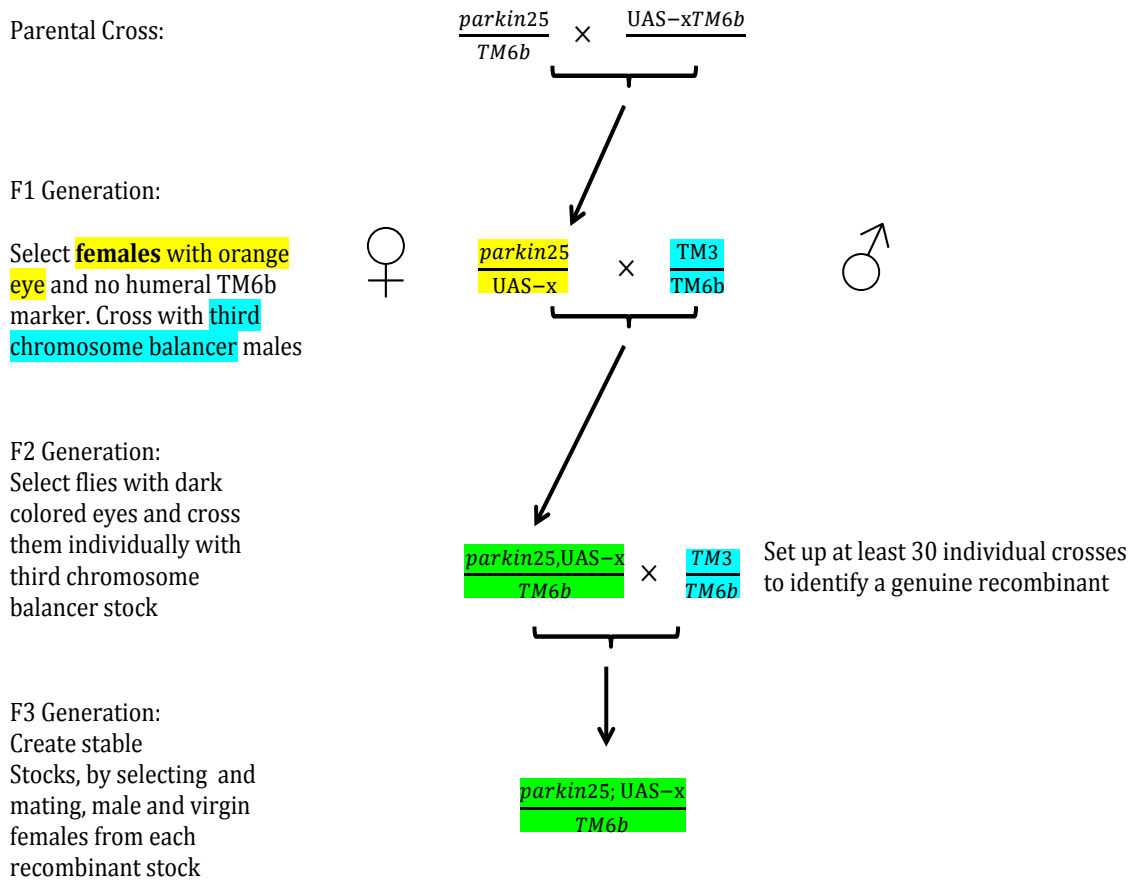


Figure 2.1 Recombination Crossing Scheme

The progeny of this cross was scanned for males or virgin females with dark eyes. 30-40 flies were individually mated with $w^{\bar{}};TM3/TM6b$ flies. The offspring of each pair carrying a TM6b chromosome 3 (identified by the tubby (*Tb*) marker) were used to generate stocks of potential recombinants. To confirm recombination, a single fly from each stock was later screened via polymerase chain reaction (PCR) for the *parkin* null mutation (see section 2.3). Other third chromosome UAS stocks included: UAS-*AMPK*, UAS-*BSK-DN*, UAS-*TRX-R2* and UAS-*GST*.

2.2 Molecular Biology

Screening for *dparkin* null mutation was performed via polymerase chain reaction (PCR) to identify potential recombined mutant stocks (Fig 2.2).

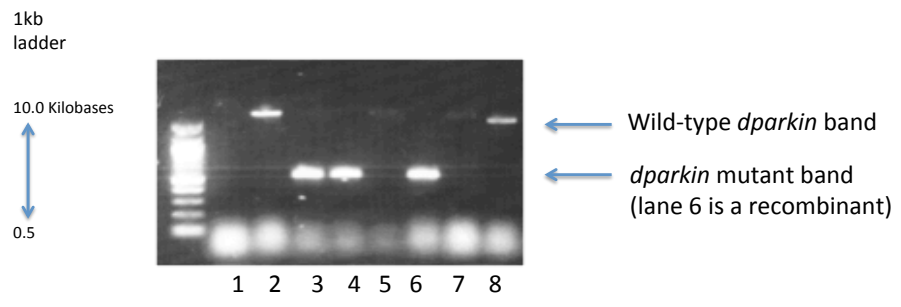


Figure 2.2 PCR of *dparkin* mutant recombinants. Wild-type (CS/w^+) larvae and *dparkin* (p^{25}/p^{25}) larvae were used as controls against the possible *dparkin* mutant recombinants. The PCR products were run in parallel with a 1kb ladder. The sample in Lane 1 was not successfully extracted. Lane 2 shows a successful extraction from a CS/w^+ larva. Lanes 3 and 4 show successful extraction of two *dparkin* larvae. Lanes 5-8 are from larvae that were possible recombinations of *dparkin* with UAS-*GST*; recombination was not successful in samples 5, 7 and 8. However, Lane 6 shows a *dparkin* (p^{25}/p^{25}) larvae recombinant with UAS-*GST* transgene.

2.2.1 Genomic DNA extraction

A single fly together with 50 μ l of DNA extraction buffer (10 mM Tris pH 8.2, 1mM EDTA, 25 mM NaCl) and with fresh 200 μ g/ml proteinase K, was used to rupture and release the DNA by repeated squishing motion using the end of a pipette tip. Then, the homogenized mixture was incubated at 37°C for 30 minutes and then at 85°C for 10 minutes where the proteinase K is deactivated. The mixture was centrifuged at 13,000 for one minute to form a pellet, where 2-3 μ l of the supernatant was used as a template PCR reaction thereafter.

2.2.2 Polymerase chain reaction (PCR)

2X PCR mastermix (Promega, UK) was used to make up a 20 μ l reaction volume containing 0.5 μ M of each primer and 2-3 μ l of homogenized fly DNA template to amplify the genomic DNA. Primers were designed using Primer3 software and synthesized by Eurogentec (UK). The melting temperature (T_m) was calculated using Net Primer. The annealing temperature was set 5°C lower than the lowest melting point temperature of all primer pairs used. The elongation time for a fragment was determined based on the fact that 1kb of DNA is produced per minute by *Taq* polymerase.

Standard PCR cycling were as follows: initial denaturation was at 94°C for 10 minutes, followed by another denaturation step of 94°C for 30 seconds, then annealing step at T_m (explained above) for 60 seconds, followed by 72°C for initial elongations step (1kb for 1 minute), followed by final elongation cycles at 72°C for 5 minutes. Reaction mixtures were set to cool to 4°C.

2.2.3 DNA agarose gel electrophoresis

DNA products from the PCR were analysed by agarose gel electrophoresis made from agarose and 1x TAE buffer (Tris-Acetate and 0.05M EDTA). 0.7 % or 1.4 % agarose gels were made depending on the product size being large (>1kb) or small (<1kb)

respectively. 0.1% SYBR Safe (Invitrogen, UK) was added to the heated and dissolved agarose, to visualize the PCR products later. 10 μ l of PCR product was mixed with loading dye (Bromophenol Blue, 10% glycerol) at a time and loaded into individual wells of the solidified agarose gel placed in a tank filled with 1x TAE buffer. A 1 kb or 100kb DNA ladder (NEB, Ipswich or Promega depending on the % agarose gel), was also loaded to determine the size of the PCR products. The gel was run for approximately 45 minutes at 90 volts. The gel was placed on a safe imager 2.0 Blue Light Transilluminator (Life technologies), to visualize the PCR products and the ladder, and an image taken (**Fig 2.2**).

2.3 Techniques to assess *D. melanogaster* larval physiology

2.3.1 Experimental Solutions

Phosphate Buffer Solution 1x (PBS) was composed of 10 mM PBS: 137 mM NaCl; 2.7 mM KCl; 10 mM Na₂HPO₄ and 2 mM KH₂PO₄. Modified 'haemolymph-like buffer 'HL3' solution was made with sodium chloride, 70 mM; potassium chloride, 5 mM; calcium chloride, 1mM; sodium hydrogen carbonate, 10 mM; BES (N, N-bis(2-hydroxyethyl)-2-aminoethanesulphonic acid), 5 mM; trehalose, 5mM; sucrose, 115 mM; pH 7.5. This solution was used previously at York (Hill & Elliott, unpubl.) in assays of octopaminergic modulation, and was found to give stable resting membrane potentials. It is based on the original composition detailed by Stewart *et al.* (1994), but omits magnesium chloride (Stewart et al., 1994). This modified HL3 solution was used to dissect the wandering third instar larvae in all the electrophysiological experiments (see section 2.4.2).

2.3.2 Larval Dissection

Third instar wandering larvae, found on the sides of food vials that have crawled out of the food, were picked using sharp forceps and placed on a Sylgard petri plate (Silicone

elastomer kit, Dow Corning) immersed in either PBS or modified Haemolymph-like buffer 'HL3 solution'. The larva was pinned down at both anterior and posterior ends using dissection minuten pins (Austerlitz Insect Pins 0.1mm diameter, Fine Science Tools, Heidelberg, Germany). An incision was made using sharp BowSpring scissors (Fine Science Tools, Heidelberg, Germany) at the two ends close to each pin. From the posterior dorsal, the scissors were used to cut open the larva along the dorsal midline, up to the anterior end. All internal organs including trachea, gut, fat bodies and salivary glands were removed cautiously using a plastic Pasteur pipette. The body cavity was washed in fresh PBS or HL3. The larval body wall was fully exposed by pinning out the four corners.

2.3.3 Electrophysiology: Intracellular muscle recordings

All preparations used for recording resting membrane potential (RMP), basal level synaptic activity (excitatory junctional potentials, EJPs) (**Fig 2.3**) and spontaneous minis (mEJPs) were dissected in a 21-22°C room where the rig was set up for the intracellular recordings and the dissected preparations were used within 5-10 minutes from the start of pinning them down. As temperature affects glutamate receptor kinetics and EJP amplitudes, the room was checked for fluctuations of temperature from 21-22°C and the HL3 solution was left in the room to acclimatize to room temperature before use.

Sharp micropipettes were pulled using 1mm diameter borosilicate glass with a resistance of 10-20Mohms from a puller (Flaming Brown micropipette puller model P-97, Stutter Instrument Co) and filled with 3 M potassium acetate.

RMP recordings were taken from muscles 6, 7, 13, or 12 using a sharp electrode from abdominal A2-A6 segments. When recording basal synaptic transmission, the larval

brain was left in place, so that the motor neurons still synapsed onto the body wall muscles and frequent spontaneous EJPs could be recorded. Spontaneous EJPs were recorded from muscles 6 and 7 of the A3 segment (**Fig 2.3**). All EJPs from a range RMPs were recorded to disk and later replayed to determine the mean amplitude. The RMP was also noted from the overlaid EJP trace.

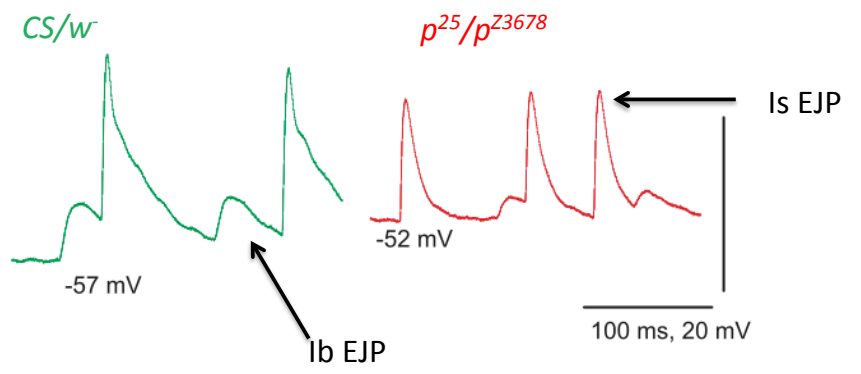


Figure 2.3 Recording at the NMJ. Spontaneous EJPs were recorded from muscles 6 and 7 of the A3 segment from wild type (*CS/w⁻*) and *dparkin* (*p²⁵p^{z3678}*) larvae. At the larval NMJ, the Type I synaptic boutons are subdivided into type-I small (Is) and type-I big (Ib) (Atwood et al., 1993). Motor neurons with terminals type-Ib have bigger boutons with low threshold firing, project onto single muscles and produce small EJPs (arrows), whereas type-Is motor neurons have smaller boutons with a high threshold and innervate groups of muscles, producing large EJPs (arrows).

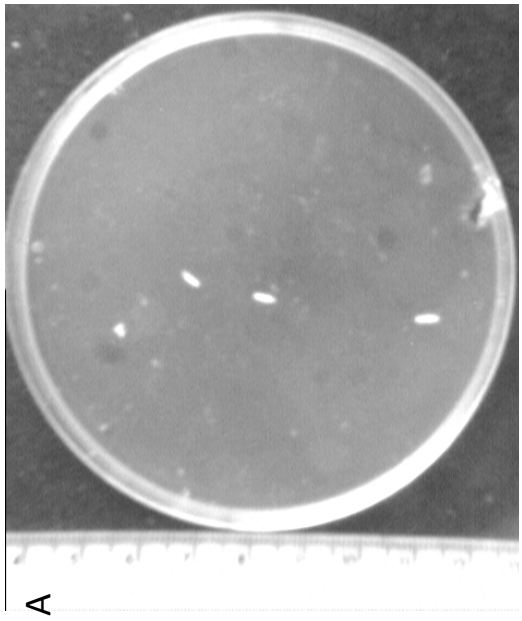
For mEJPs the brain was removed during dissection. All mEJPs were recorded from muscle 6 or 7 of the A3 segments only. Only mEJPs that had a RMP around -60mV were used for analysis. Recordings lasted up for 2 minutes and the first 50 mEJP amplitudes were calculated manually. mEJPs were represented on a cumulative frequency chart.

All data files were recorded using *DASYLab* software (DasyLab v9, Measurement Computing). The RMP, EJPs or mEJPs were measured using *DASYView* (Version 2.1.1, customised software, C. Elliott, University of York). A scatter graph was constructed, plotting the EJP values against the RMP at which they had been recorded. The line of best fit (regression or trend line) was calculated for the *dparkin* mutants using their EJP/RMP points. The residual plot was constructed by calculating the mean distance of all individual points from the *dparkin* mutant line for all the different genotypes.

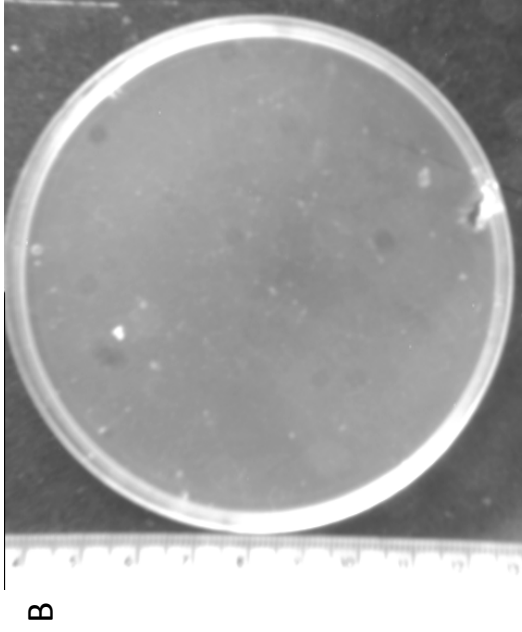
2.3.4 Behavioral locomotion assay

Larval crawling was determined as follows: larvae were dipped and washed in HL3 solution in the 25°C room where the apparatus was set up. A camera and computer software VirtualDub (Hill, 2008) (**Fig 2.4**) was used to record larval tracks on a 1% agar plate (0.01 g/ml agar in water). The AVI video file containing the recording of larval crawling across an agar petri dish was opened using the ImageJ analysis program (Schneider et al., 2012). The average background image was calculated using the median z projection algorithm across the entire file (Image/ Stacks/ Z project). The image showing only the larvae against a dark grey frame was produced by subtracting the background image from their individual frame (Process/ Image calculator- subtract the original from median image). In the Mtrack2 plugin, a minimum object size of 5 pixels was selected to eliminate speckles. The other default settings (maximum object

size (999999), maximum velocity (10) and minimum track length (2)) were used. All the option boxes (Save results file, Display path length, Show labels, Show positions & Show path) were ticked. This produced the larval tracks and the individual x - y coordinates throughout the 2 minutes recording. The x - y coordinates were saved to disk in an Excel format file, and an Excel template used to calculate the distance travelled in 2 minutes by each larva. The number of pixels occupied by a 20 mm bar on the ruler was used to determine the distance represented by each pixel. In daily use, this procedure was automated using the tools at (<http://biolpc22.york.ac.uk/drosophila/larvae/>) giving an output of the median speed of each larva (**Fig 2.4**).



A



B



C



D

Figure 2.4 Analysis of larval crawling by ImageJ and MTrack2. **A** An AVI file recording the motion of wild-type larvae across the agar plate is opened in the ImageJ analysis program. **B** ImageJ is used to calculate the median intensity across the entire file of 120 frames, giving a background image. **C** The image sequence showing just the larvae that is produced by subtracting the background image from each of the individual frames. **D** MTrack2 is used to locate the center of each larva in each frame. It generates a sequence of frames showing the calculated x - y coordinates for each larva (for example, in the illustration shown, for position 1, $x=304$, $y=170$). These positions are then saved in an Excel format file by the MTrack2 software.

2.4 Anatomy at the larval neuromuscular junction (NMJ)

2.4.1 Fixing and immunohistochemistry

PBS was completely removed from the freshly dissected larval preparation and replaced with a solution of 3.7% formaldehyde in PBS for 7mins at room temperature (RT). The pins were taken off the preparation and the preparation was transferred to an Eppendorf tube containing PBS-T (PBS with 0.1% (v/v) Triton X-100) at RT to rinse off any remaining fixative and placed on a rocker, followed by another 3 washes in PBS-T left on the rocker for 10 mins incubation each at RT. Primary antibodies (see **Table 2.2**) were added at their desired concentrations (1/200 or 1/1000) and left to incubate overnight at 4°C on a rocker. To remove excess primary antibody, 3x 10 mins washes with PBS-T at RT were carried out before adding the secondary antibody (see **Table 2.2**) for 2 hrs on the rocker at RT. The final 3 washes with PBS-T for 10 mins at RT were undertaken to remove any excess secondary antibody. To reduce air bubbles, the preparations were transferred into fresh Eppendorf tubes containing 70% (v/v) glycerol/PBS and left for 2 h standing upright at RT or 4°C overnight until they sank to the bottom of the tubes. Larval preparations were taken and mounted onto microscope slides with a drop of Vectashield (Vector Laboratories) and a 22mm x 22mm coverslip was placed directly on top. Nail varnish was used to seal the edges of the preparation with Vectashield and the slide was stored in the dark (slide box).

2.2 Table of antibodies used for NMJ bouton counts

Antibody/ stains	Raised host species	Dilution factor	Source
Anti-Horseradish-peroxidase-Cy3 (HRP-Cy3) Neuronal Tissue	Goat	1:200	(Middleton et al., 2006)
Anti-synaptotagmin (Anti-SYT) Synaptic Boutons	Rabbit	1:1000	(Sweeney and Davis, 2002)
FITC secondary	Goat	1:200	Jackson Laboratories, USA

2.4.2 Confocal images of the NMJ

NMJ images were taken using a laser scanning confocal microscope (Zeiss LSM 510 meta Axiovert 200M). The following objectives were used: 10x, 20x and 63x oil immersion. The 63x objective was used to take a z-stack image of the NMJ.

2.4.3 Measuring and quantifying at the NMJ

Bouton count quantification was undertaken where individual spherical structures stained with anti-synaptotagmin at the NMJ at the A3 segment from NMJ 6/7 were counted using a Leica DMLA fluorescence microscope using a 40x objective and FITC filter (**Fig 2.5**). Muscle surface area (MSA) measurement was found by taking an image with a 10x objective using bright field of the A3 muscle (**Fig 2.6**) which had also been used to count the number of boutons. ImageJ was used to analyse the resulting images. The length and width of the muscle was measured in pixels and this was converted into μm . An image was taken of a 1mm graticule with 100 divisions using the 10x objective used to take the muscle images. The markings of the graticule permits the calculation of pixel to μm ratio.

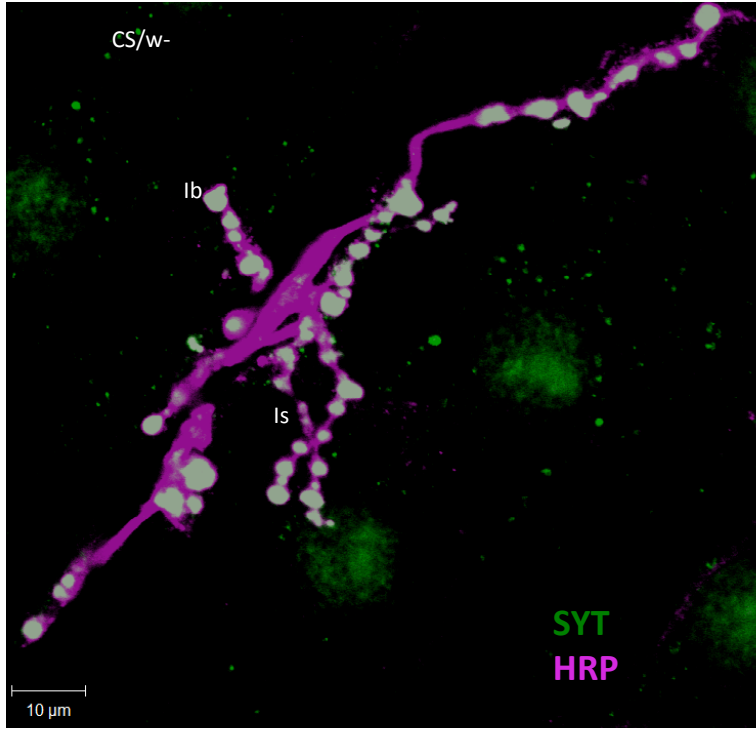


Figure 2.5 Confocal image of the NMJ anatomy. *D. melanogaster* wild-type (*CS/w⁺*) third instar larval NMJ stained with horseradish peroxidase (HRP, purple) and synaptotagmin (SYT, green). HRP stains neuronal membrane and SYT is a synaptic bouton marker, both of which are used together to determine the raw bouton count.

To provide a fair comparison of larvae of different sizes, a normalized bouton count was calculated as follows: for each neuromuscular junction, the actual “raw” bouton count (**Fig 2.5**) was divided by the corresponding individual MSA (**Fig 2.6**). To compare different genotypes, or the effects of drug treatment, the mean raw bouton count/MSA for each genotype or treatment was calculated. The mean was then expressed as a percentage of the normalized average of control (normally the wild-type or drug-free) larvae.

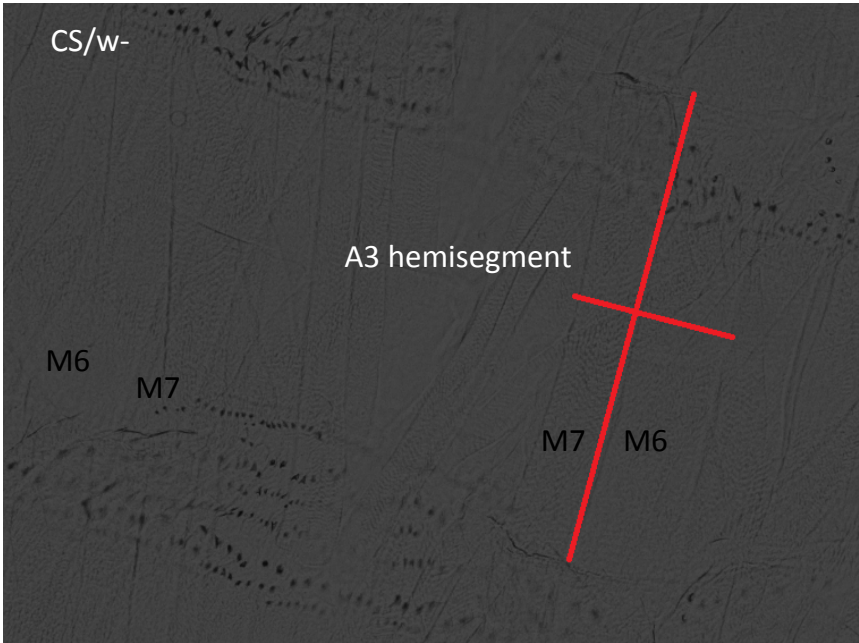


Figure 2.6 Light microscope image of the NMJ. *D. melanogaster* wild-type (*CS/w⁺*) third instar larval NMJ muscle 6/7 is indicated on the diagram by a cross. The surface area of this region was measured to normalize bouton count.

2.5 Statistics

Here we report the results of Tukey post hoc tests. While these are not as conservative as the Bonferroni tests, the Tukey tests provide an accurate indication of the significance level. Kolmogorov–Smirnov test statistics was used to calculate the probability for the cumulative frequency histogram plot. In the figures, * → $P < 0.05$; ** → $P < 0.01$; *** → $P \leq 0.001$.

2.6 Rationale for drug concentration

Preliminary unpublished data from student projects suggested that L-DOPA at 3 μM concentration was successful in experiments recording behavioral phenotypes in *D. melanogaster* adults. Metformin and AICAR started with 3 μM concentrations. Additionally, other higher concentrations (50 μM) were used for AICAR and these were starting points for Resveratrol experiments. A 200 μM concentration of Resveratrol used based on studies by Partridge's group for adult flies (Slack et al., 2012).

Chapter 3: *dparkin* mutant larvae show reduced locomotion, synaptic dysfunction and overgrown synapses

3.1 Introduction

D. melanogaster is a good model system to model PD, which has been reviewed in Chapter 1. Since PD is characterized by motor dysfunction, it was logical to test whether the *dparkin* mutant larvae showed signs of a motor defect. Larval locomotion has been studied using a number of crawling assays (Fox et al., 2006, Steinert et al., 2012), for example showing reduced velocity when octopamine or tyramine levels were manipulated (Hill, 2008, Selcho et al., 2012). The method developed in York by Hill (2008) will be used to measure the overall velocity. The velocity index used for the experiments in this thesis will be the overall distance covered by the larva in a period of 2 minutes. Crawling assays were used to test for locomotory dysfunction in all *dparkin* mutant larvae, as this is characteristic of the human disease.

Morphological and electrophysiological analysis from larval synapses will test for abnormal anatomy and physiology to complement the behavioral analysis. The electrophysiological (*in vivo*) recordings will be taken from larval longitudinal body wall muscles 6, 7, 12 and 13, as these have been well characterized and studied extensively (Atwood et al., 1993). This will allow the comparison of the resting (spontaneous not stimulated) synaptic function between mutants and control.

A key experiment is to assess the extent of overgrown synapses in the *dparkin* larva, as overgrown synapses are indicative of oxidative stress in a range of neurodegenerative and chemically-induced *D. melanogaster* models (Milton et al., 2011). Therefore, we investigated whether there was neuronal overgrowth in *dparkin* mutant larvae that might be caused by oxidative stress. Mitochondrial-associated defects are observed in humans with *parkin* mutations and this is conserved in all model organisms (Müftüoğlu et al.,

2004, Mortiboys et al., 2008, Palacino et al., 2004).

To investigate the effect of loss of *dparkin*, we deployed 2 well-characterized mutations. Like other mutations in the *PARKIN* gene, these result in a loss of function, (rather than a gain of function as seen with other PD genes such as *α-synuclein* (Eriksen et al., 2003)). *parkin*²⁵ flies were generated by P-element induced excision, in which the first three exons of the *dparkin* gene have been deleted along with half of exon 4. *parkin*²⁵ is a null with complete loss of parkin protein (Greene et al., 2003). *parkin*^{Z3678} is EMS induced point (missense) mutation (stop codon, Whitworth, personal communication). It is a hypomorph with reduced protein production. A transheterozygote (*parkin*²⁵/*parkin*^{Z3678}) mutant combination was normally used to avoid artifacts due to second site mutations, but additionally there will be comparisons of transheterozygote mutant data with the homozygous *parkin*²⁵ null mutants in this chapter.

The GAL4-UAS system was used to rescue the mutant phenotypes in a tissue specific manner, expressing wild-type *dparkin* in a mutant background. For ubiquitous expression of *dparkin*, the *Actin5c*-GAL4 driver was used, and the *G14*-GAL4 enhancer trap line was used to express *dparkin* in all somatic muscles and salivary glands (Aberle et al., 2002). Embryonic lethal abnormal vision (*elav*^{3E1}-GAL4) enhancer trap (Davis et al., 1997) was used to express *dparkin* pan-neuronally. This will test whether the presynaptic or postsynaptic loss of *dparkin* is responsible for the respective mutant phenotypes.

A second approach to manipulate *dparkin* levels was used. In this RNAi targeted at *dparkin* was expressed to knock down parkin protein in all tissues, or in a tissue specific manner (e.g. in muscle, neurons, or specifically in the dopaminergic neurons). Bingwei

Lu's lab developed an *in vivo D. melanogaster* RNAi model with *dparkin*-mediated neurotoxicity and showed targeted expression of *dparkin* dsRNA in fly dopaminergic and serotonergic neurons in which the expression of GAL4 is under the control of the DOPA decarboxylase gene promoter (*Ddc*-GAL4) (Li et al., 2000) that did not result in neuronal loss. However, targeted overexpression of human Pael-R protein, another *parkin* substrate, resulted in the reduction of TH-positive dopaminergic neurons. The co-expression of *dparkin* dsRNA and Pael-R protein exacerbated the Pael-R phenotype age dependent selective loss of *D. melanogaster* dopaminergic neurons whereas the co-expression of Pael-R with human *parkin* resulted in the degradation of Pael-R and prevented the degeneration phenotype (Yang et al., 2003). The knock down of *dparkin* by RNAi under a *heat shock (hs)*-GAL4 was confirmed with RT-PCR analysis that showed the *dparkin* mRNA transcript levels was undetectable (Yang et al., 2003).

3.2. Results

***dparkin* larvae crawl more slowly**

Motor dysfunction is a classical feature in PD patients. The crawling assay for *D. melanogaster* larvae was used to assess motor dysfunction. This was done by placing larvae on the surface of an agar plate and tracking the full path travelled over the course of 2 minutes. The crawling assay showed that, with a global loss of *dparkin*, the tracks were, on average, 26% shorter. As velocity is distance/time, this corresponds to a 26% reduction in velocity ($p < 0.007$) in *dparkin* (p^{25}/p^{Z3678}) transheterozygote mutant larvae (0.57mm/s) compared to their wild-type (*CS/w*) controls (0.73mm/s), (**Fig. 3.1**).

Dopaminergic neurons are metabolically active neurons having extensive arbors and many synapses, and so are prone to oxidative insults and energy depletion. To test the role of *dparkin* on dopaminergic integrity and function, the tyrosine hydroxylase (*TH*)-GAL4 driver was chosen to induce knock down of *dparkin* specifically in dopaminergic cells by RNAi silencing using *dparkin* RNAi (Yang et al., 2003). *TH*-GAL4 expression studies are known to target most of the dopaminergic neurons in the central nervous system (CNS) with the exception of protocerebral anterior medial (PAM) cluster (Friggi-Grelin et al., 2003, Botella et al., 2008). Expressing *dparkin* RNAi with the *TH*-GAL4 did not affect the speed of crawling (0.71mm/s, $p = 0.975$) compared to their wild-type (0.73mm/s, *CS/w*) controls. The *TH*-GAL4 (*TH/CS*) control showed no significant difference to wild-type (*CS/w*) controls (**Fig. 3.2**).

Fig 3.1

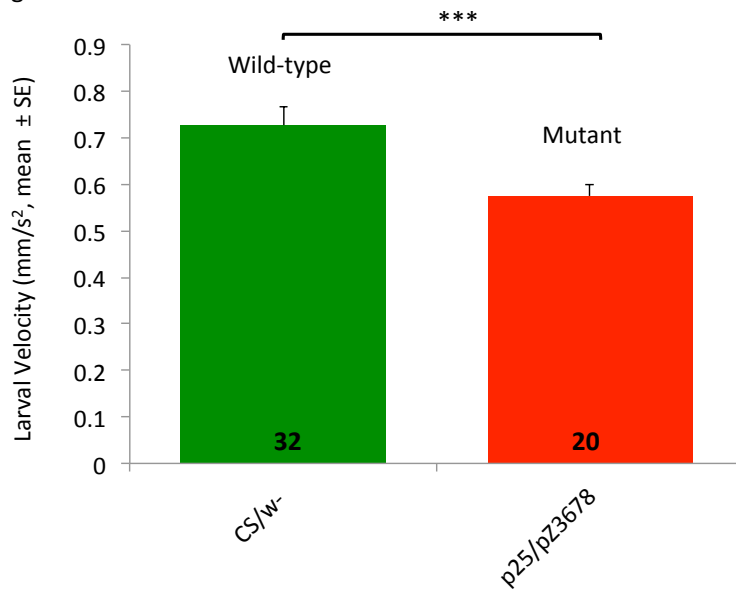


Figure 3.1 *dparkin* mutant larvae show reduced locomotion

dparkin (p^{25}/p^{Z3678}) transheterozygote mutant larvae show reduced velocity compared to wild-type control (CS/w^+) larvae ($p = 0.007$).

Fig 3.2

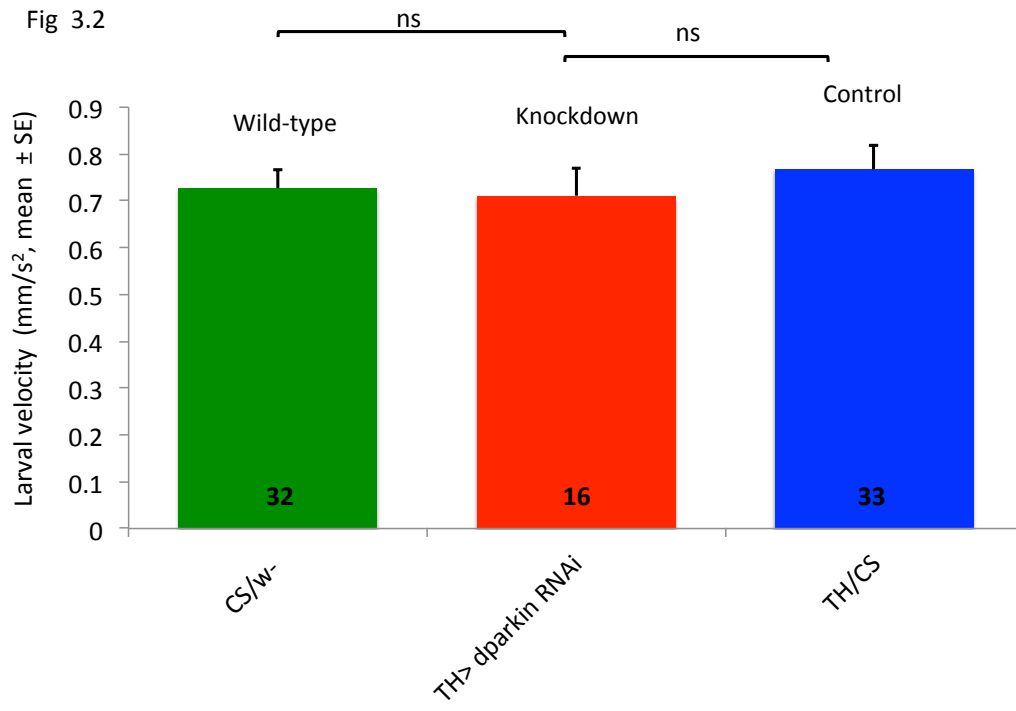


Figure 3.2 Dopaminergic expression of transgenic *dparkin* RNAi fails to show dysfunction in larval crawling

The *dparkin* RNAi line was crossed with the *tyrosine hydroxylase* driver (*TH*-GAL4), to induce the loss of *dparkin* specifically in dopaminergic neurons. Such *TH*>*dparkin* RNAi larvae showed no difference in crawling speed compared to wild-type (*CS/w*⁻) larvae ($p = 0.975$). The GAL4 control larvae (*TH/CS*) showed no difference in crawling to wild-type larvae ($p = 0.810$) or the knockdown ($p = 0.752$). *TH/CS* was used as a control to see whether the insertion of the GAL4 had any effect in a wild-type (*CS*) background.

***dparkin* mutant larvae show neuronal overgrowth at the neuromuscular junction**

With the findings of motor impairment in our *dparkin* (p^{25}/p^{Z3567}) transheterozygote mutant line, we next checked for morphological abnormalities. The neuromuscular junction (NMJ) of *dparkin* (p^{25}/p^{Z3567}) mutant larvae was shown to be 82% overgrown ($p = 0.001$, Fig. 3.3A) compared to their wild-type (CS/w^+) controls. The overgrowth is a result of an increase in neuronal growth (24%, $p = 0.001$, Fig. 3.3B) and a reduction (29%, $p = 0.001$, Fig. 3.3C) in muscle surface area (MSA) compared to wild-type (CS/w^+) synapses. The neuronal (*elav*^{3E1}-GAL4) or muscle (*G14*-GAL4) expression of wild-type *dparkin* in the *dparkin* (p^{25}/p^{Z3567}) mutant background rescued the normalized overgrowth to 5% and 10% below wild-type (CS/w^+) levels respectively (Fig. 3.3). The neuronal or muscle expression of wild-type *dparkin* in a *dparkin* (p^{25}/p^{Z3678}) mutant background also decreased raw bouton number (B, $p < 0.001$ and $p < 0.001$ respectively) and increased muscle surface area (C, $p = 0.05$ and $p < 0.001$ respectively), when compared to *dparkin* (p^{25}/p^{Z3678}) mutant larvae. There is no difference in overgrowth (normalized bouton count, raw bouton count or muscle surface area) between the neuronal (*elav*^{3E1} > *dparkin*; p^{25}/p^{Z3678}) or muscle (*G14* > *dparkin*; p^{25}/p^{Z3678}) rescue in a mutant background compared to wild-type control (CS/w^+) larvae (A, $p = 0.984$ and $p = 0.842$; B, $p = 0.326$ and $p = 0.914$; C, $p = 0.538$ and $p = 0.823$ neuronal or muscle respectively).

To support this data, we used a second technique, expressing *dparkin* RNAi by the ubiquitous *Act5c*-GAL4 driver. This resulted in an increased overgrowth (49%, $p = 0.008$, Fig. 3.4A) compared their wild-type (CS/w^+) control. The *dparkin* transheterozygote mutants showed overgrowth at approximately twice the level of that of global knockdown of *dparkin* RNAi (Fig. 3.4A). The global knockdown of *dparkin* RNAi shows an increase in raw bouton number ($p = 0.008$, Fig. 3.4B) and a decrease in

muscle surface area (MSA) ($p < 0.001$, **Fig. 3.4C**), when compared to wild-type (CS/w^+) larvae. There is no significant difference between the actin control ($Act5c/CS$) and the wild-type (CS/w^+) control (normalized, raw bouton count and MSA; $p = 0.918$, $p = 0.121$ and $p = 0.683$ respectively; **Fig. 3.4A-C**).

Fig 3.3 A

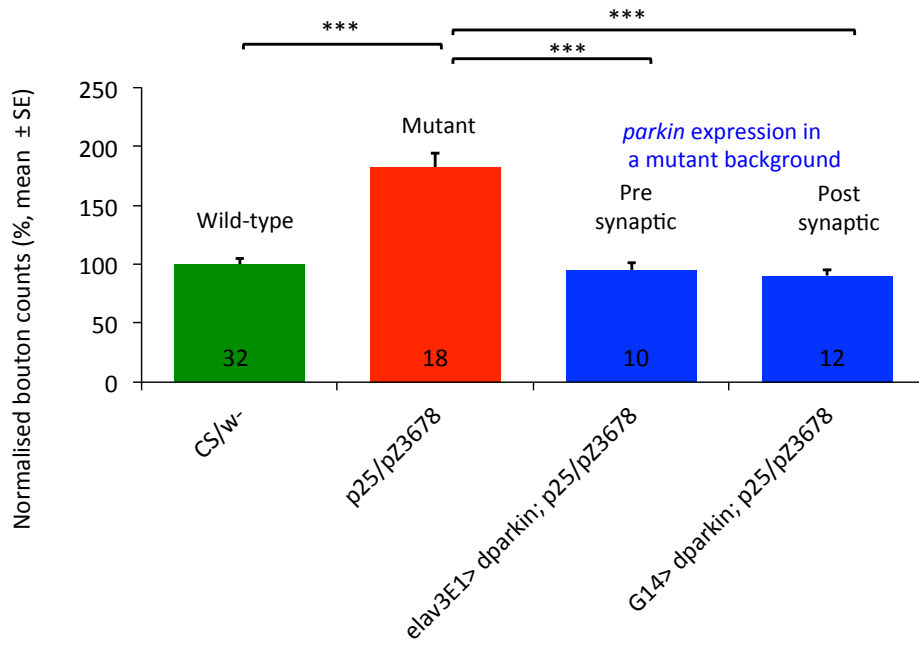


Fig 3.3 B

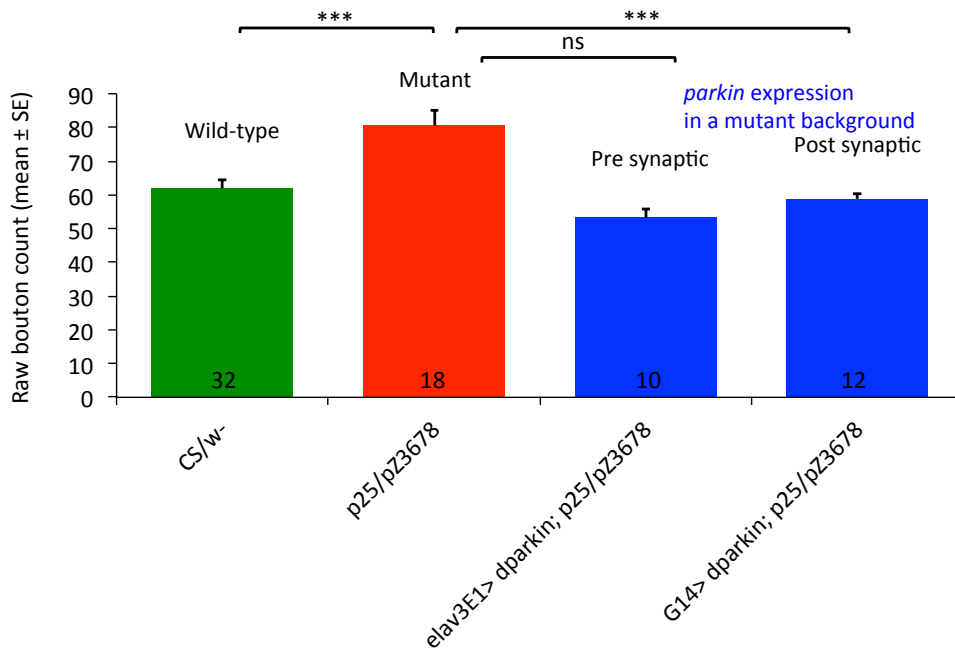


Fig 3.3 C

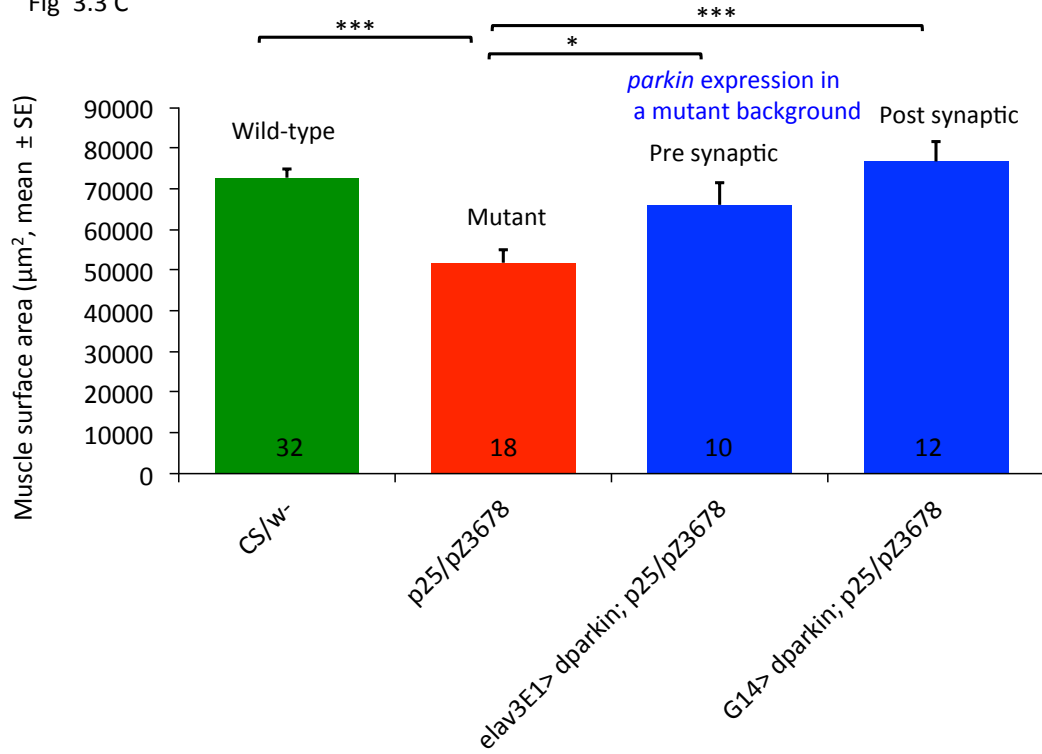


Figure 3.3 Loss of *dparkin*-induced overgrowth rescued by neuronal or muscle expression of wild-type *dparkin*

A-C *dparkin* (p^{25}/p^{Z3678}) mutant larval neuromuscular junctions show an increase in normalized bouton overgrowth (**A**, $p < 0.001$), an increase in raw bouton number (**B**, $p < 0.001$) and a decrease in muscle surface area (**C**, $p < 0.001$), when compared to wild-type (CS/w^+) larvae. The neuronal or muscle expression of wild-type *dparkin* in a *dparkin* (p^{25}/p^{Z3678}) mutant background also decreased raw bouton number (**B**, $p < 0.001$ and $p < 0.001$ respectively) and increased muscle surface area (**C**, $p = 0.05$ and $p < 0.001$ respectively), when compared to *dparkin* (p^{25}/p^{Z3678}) mutant larvae. There is no difference in overgrowth (normalized bouton count, raw bouton count or muscle surface area) between the neuronal ($elav^{3E1} > dparkin; p^{25}/p^{Z3678}$) or muscle ($G14 > dparkin; p^{25}/p^{Z3678}$) rescue in a mutant background compared to wild-type control (CS/w^+ larvae (**A**, $p = 0.984$ and $p = 0.842$; **B**, $p = 0.326$ and $p = 0.914$; **C**, $p = 0.538$ and $p = 0.823$ neuronal or muscle respectively).

Fig 3.4 A

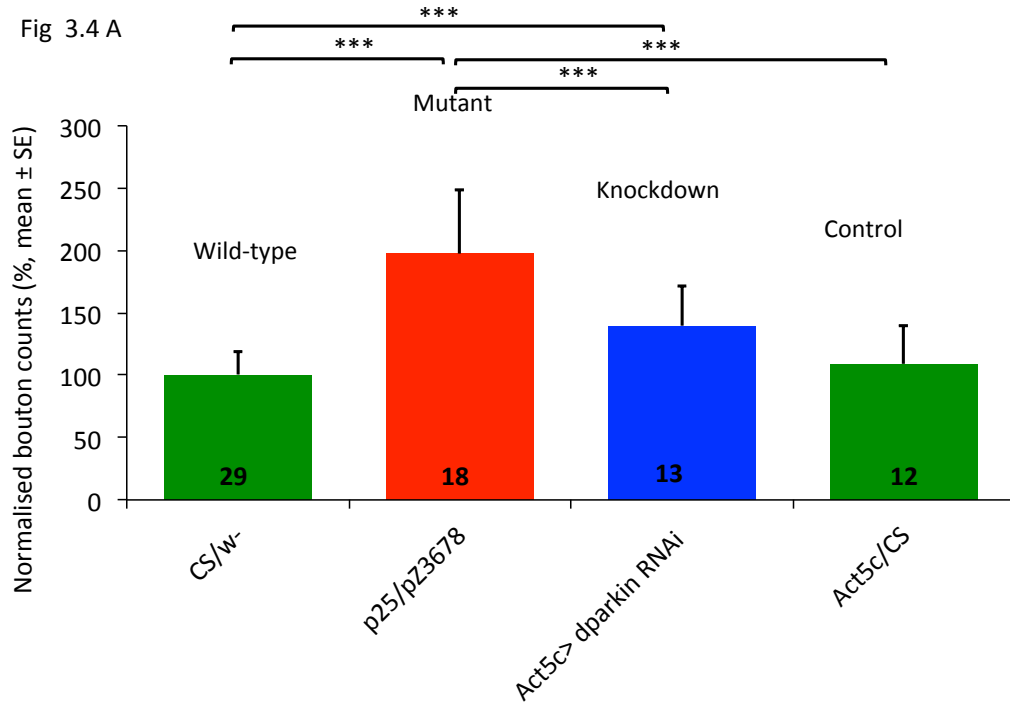


Fig 3.4 B

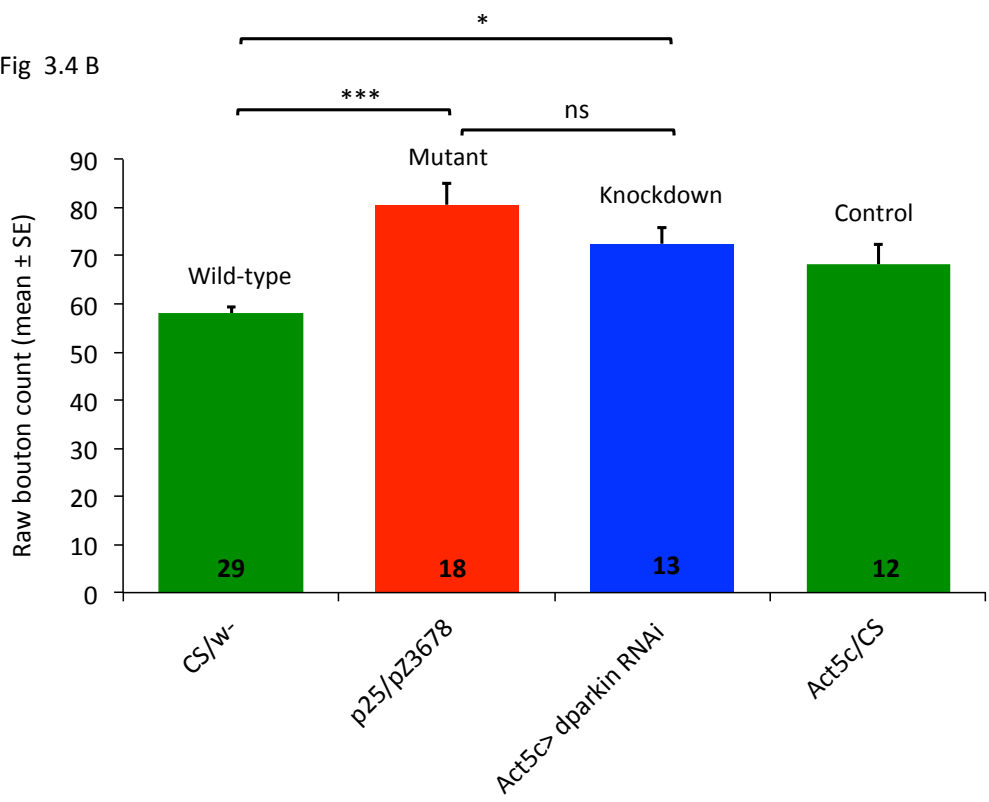


Fig 3.4 C

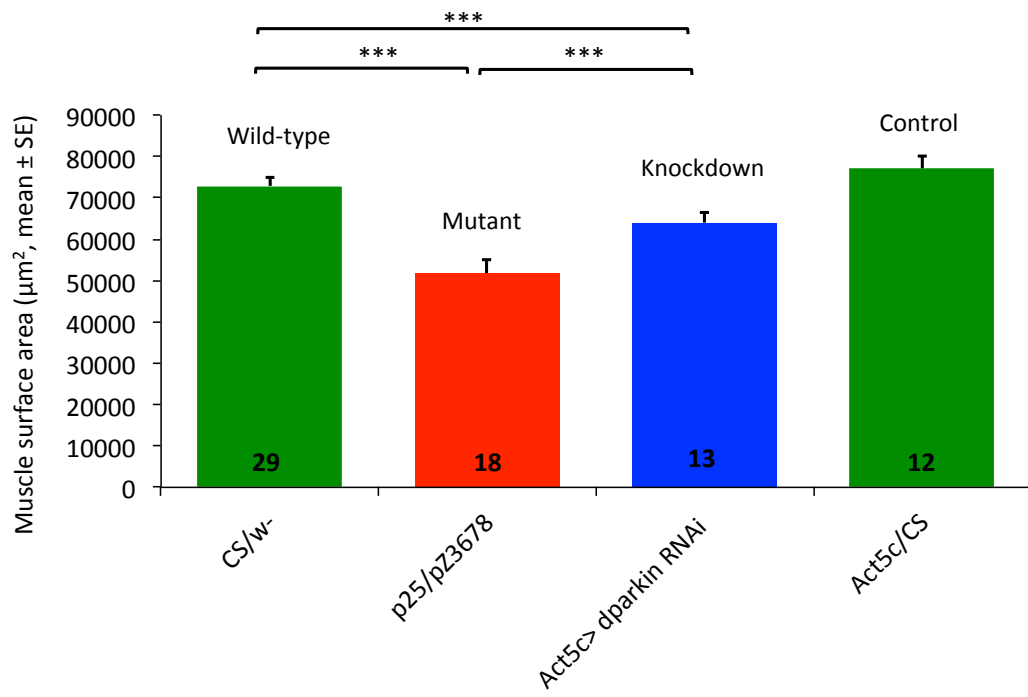


Figure 3.4 Global expression of transgenic *dparkin* RNAi shows an enhanced overgrowth phenotype.

A-C The global expression of the *dparkin* transgenic RNAi shows an increase in normalized bouton overgrowth (**A**, $p = 0.008$), an increase in raw bouton number (**B**, $p = 0.008$) and a decrease in muscle surface area (**C**, $p < 0.001$), when compared to wild-type (*CS/w⁺*) larvae.

***dparkin* mutant larvae have depolarized resting membrane potentials**

The larval neuromuscular junction (NMJ) is a glutamatergic synapse that models a central synapse of mammals as it uses glutamate as its transmitter in the NMJ synapse. The intracellular recordings from the longitudinal body wall muscles 6 and 7 of *dparkin* (p^{25}/p^{Z3678}) transheterozygote mutant larvae commonly show depolarized resting membrane potentials (RMPs, N= 34), (**Fig. 3.5**). This is confirmed by the mean data: *dparkin* (p^{25}/p^{Z3678}) mutant larvae show more positive (depolarized) RMPs compared to wild-type (CS/w^+) larvae (mean difference 12 mV, $p < 0.001$, **Fig. 3.5**). Global (*Act5c-GAL4*) or neuronal (*elav^{31E}*) expression of wild-type *dparkin* in a *dparkin* (p^{25}/p^{Z3678}) transheterozygote mutant background failed to rescue the RMP defects ($p = 0.734$ and $p = 0.504$ respectively, **Fig. 3.5**). On the other hand, muscle (*G14-GAL4*) expression of wild-type *dparkin* rescued the mutant RMP phenotype ($p = 0.017$, **Fig. 3.5**). *dparkin* mutant larvae have smaller EJPs (**Fig. 3.6**).

In preparations in which the brain and nerves are left intact, intracellular recordings from larval muscles frequently show spontaneous excitatory junctional potentials (EJPs). In recordings from *dparkin* transheterozygote larvae, the EJPs appear smaller (**Fig. 3.6**). To examine this in detail we focused on the Is EJPs, finding that the mean size of the *dparkin* (p^{25}/p^{Z3678}) mutant larvae was 14% of the wild-type (CS/w^+) controls.

The size of the EJPs is affected by transmitter binding to the postsynaptic glutamate receptors, but also by the muscle RMP. As the RMP becomes more depolarized, and moves towards the reversal potential (-1mV, (Jan and Jan, 1976)) (Jan and Jan, 1976) the EJP will decrease; conversely as the RMP becomes more negative, the EJP will increase. As the RMPs of *dparkin* (p^{25}/p^{Z3678}) transheterozygote mutant larvae were more depolarized compared to wild-type (CS/w^+) controls, the synaptic potentials might

be smaller just because of this difference in membrane potential. To explore this, the size of the Is EJP was plotted against the RMP (**Fig. 3.6**). It appears that the data points from the *dparkin* (p^{25}/p^{Z3678}) mutant larvae tend to lie below those from the wild-type (CS/w^+) controls. To confirm this, the best-fit regression lines were drawn for both genotypes, using data points in which the RMP was between -40 and -75 mV data to construct the line (**Fig. 3.7**). The lower regression line for *dparkin* (p^{25}/p^{Z3678}) mutant larvae confirmed that their spontaneous EJPs appear smaller than those from wild-type (CS/w^+) controls at the corresponding RMP (**Fig. 3.7**). To confirm this statistically, I measured the vertical distance between each data point and the *dparkin* (p^{25}/p^{Z3678}) mutant larvae regression line (the residual). For each genotype, I calculated the mean and standard error of the residual, and plotted this (**Fig. 3.7**). I tested the null hypothesis, that if each genotype had the same size EJP as the *dparkin*, the mean deviation from the *dparkin* regression line should be zero. For the wild-type (CS/w^+) data, the t-test confirmed that the wild-type larvae have a larger EJP than the *dparkin* (p^{25}/p^{Z3678}) mutant larvae ($p < 0.001$, **Fig. 3.7**). On this analysis, which allows for the effect of RMP, the average synaptic potentials of *dparkin* larvae were estimated to be 7mV smaller than the wild-type (CS/w^+) controls. In the same way, we examined the effect of expressing wild-type *dparkin* globally (*Act5c*-GAL4), neuronally (*elav^{3E1}*-GAL4) or in muscle (*G14*-GAL4) in a *dparkin* (p^{25}/p^{Z3678}) transheterozygote background. In each case this rescued the synaptic transmission defect compared to *dparkin* (p^{25}/p^{Z3678}) mutant larvae ($p = 0.001$, $p < 0.001$ and $p = 0.033$ respectively).

Fig 3.5

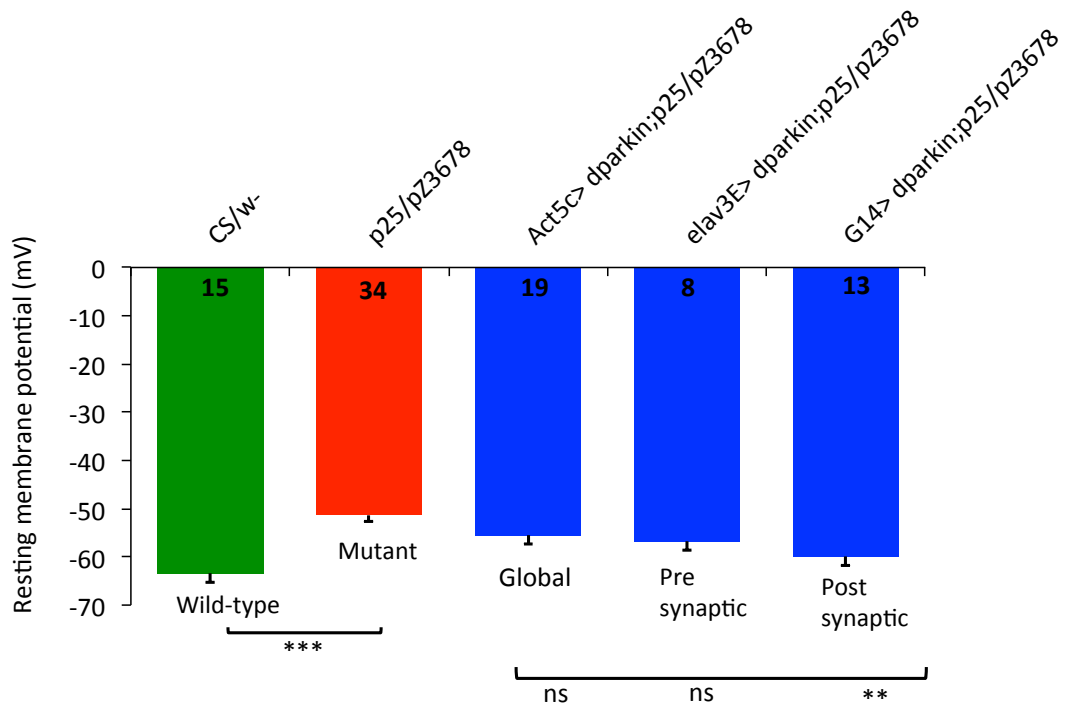


Figure 3.5 *dparkin* mutant larvae show more positive (depolarized) RMP that is rescued by global, neuronal or muscle expression of wild-type *dparkin*

dparkin (p^{25}/p^{Z3678}) mutant larvae show more positive (depolarized) RMP (resting membrane potential) compared to wild-type (CS/w^+) larvae ($p < 0.001$). Global (*Act5c-GAL4*) or neuronal (*elav^{3E}-GAL4*) expression of wild-type *dparkin* in a *dparkin* (p^{25}/p^{Z3678}) mutant transheterozygote background failed to rescue the RMP defects ($p = 0.734$ and $p = 0.504$ respectively) compared to *dparkin* (p^{25}/p^{25}) mutant larvae, whereas the muscle (*G14-GAL4*) expression of wild-type *dparkin* rescued the mutant RMP phenotype ($p = 0.017$). These recordings were taken from muscle 6/7.

Fig 3.6

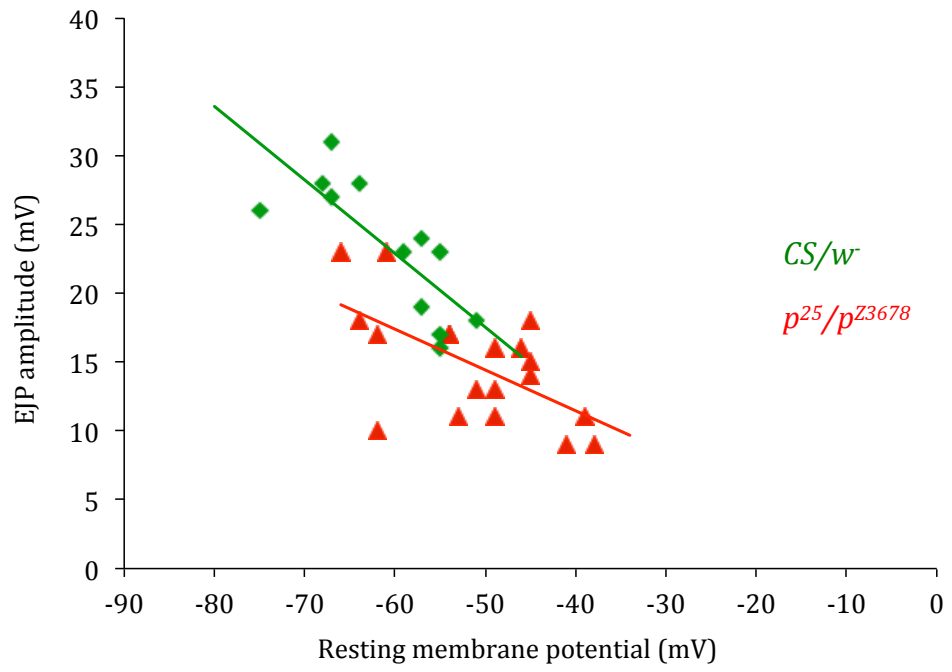


Figure 3.6 Scatter regression plot show *dparkin* mutant larvae have depolarized RMPs and smaller EJPs across a range of RMPs.

dparkin (p^{25}/p^{Z3678}) mutant larvae show more positive (depolarized) RMP compared to wild-type (CS/w^+) larvae. The *dparkin* larval EJPs were on average smaller compared to their wild-type controls across a range of RMPs. The solid lines are the linear regression across *dparkin* and wild-type larvae. These recordings were taken from 6/7 muscles (n = 12, CS/w^+ and n = 18, p^{25}/p^{Z3678}).

Fig 3.7

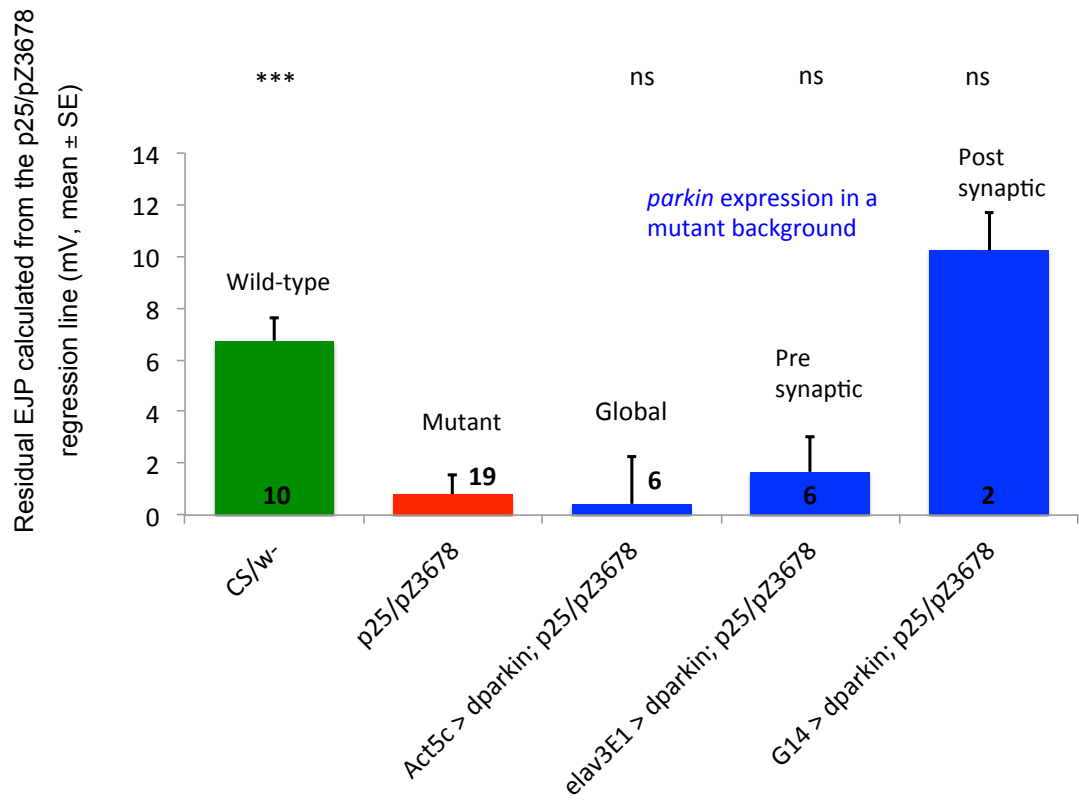


Figure 3.7 *dparkin* mutant larvae show reduced synaptic transmission is not rescued by either global, neuronal or muscle expression of wild-type *dparkin*

For each observation, the difference between the recorded EJP and the value expected from the p^{25}/p^{Z3678} regression line was determined. This shows that the *dparkin* (p^{25}/p^{Z3678}) larvae have reduced synaptic transmission compared to wild-type (CS/w^+) control larvae ($p < 0.001$). Global (*Act5c*-GAL4), neuronal (*elav^{3E}*-GAL4) or muscle (*G14*-GAL4) expression of wild-type *dparkin* on a *dparkin* (p^{25}/p^{Z3678}) mutant transheterozygote background failed to rescue the synaptic transmission defect ($p = 0.829$, $p < 0.093$ and $p = 0.283$ respectively) compared to *dparkin* (p^{25}/p^{Z3678}) mutant larvae.

***dparkin* mutant larvae have smaller mEJP amplitudes**

Synaptic EJPs are the result of release of many transmitter vesicles. In recordings from larval muscles, in which their innervation had been severed, miniature excitatory junctional potentials (mEJPs) were recorded (**Fig. 3.8**). The mEJPs correspond with spontaneous single vesicle release (Fatt and Katz, 1952, Dudel and Orkand, 1960, Usherwood, 1963). For these experiments mEJPs were recorded in a number of preparations. However, since the size of the mEJP is affected by membrane potential, we analyzed only a few preparations from *dparkin* (p^{25}/p^{Z3678}) and wild-type ($CS/w^{\bar{}}$) larvae in which the RMPs were similar in both genotypes (range -60 mV to -67 mV). The distribution of mEJP amplitudes in the *dparkin* (p^{25}/p^{Z3678}) and wild-type ($CS/w^{\bar{}}$) larvae were plotted (**Fig. 3.9**). The mean and mode of the *dparkin* (p^{25}/p^{Z3678}) mEJPs mutant larvae were 0.7 mV and 0.5 mV, 40% and 16% smaller than of wild-type ($CS/w^{\bar{}}$) control mEJPs (**Fig 3.9**). The cumulative frequency graph shows there are many smaller mEJPs in *dparkin* (p^{25}/p^{Z3678}) mutant larvae than in wild-type ($CS/w^{\bar{}}$) controls (**Fig. 3.9**).

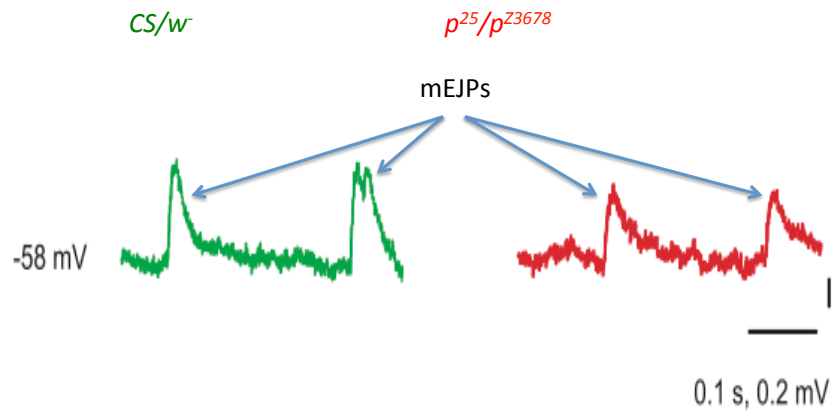


Figure 3.8 *dparkin* mutant larvae have smaller miniature excitatory junction potentials.

Miniature excitatory junction potentials (mEJPs) are smaller in *dparkin* larvae (p^{25}/p^{Z3678}) compared to wild-type (CS/w^+) controls, as shown in this sample recording.

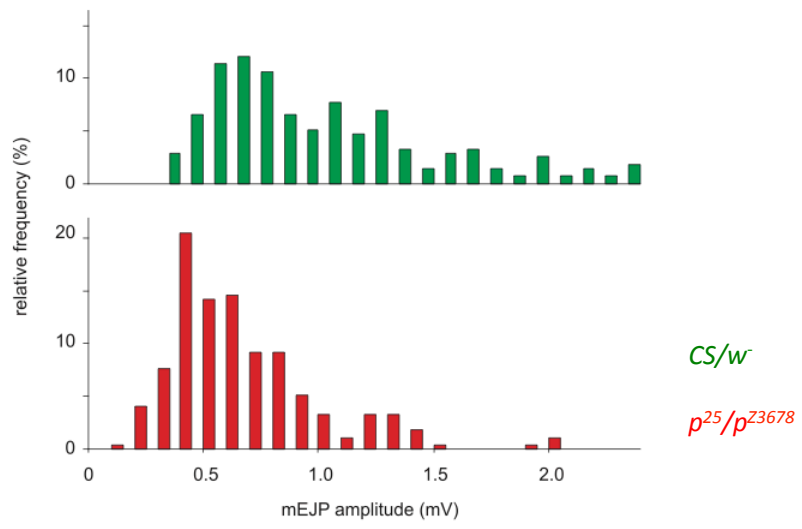


Figure 3.9 The distribution of mEJP amplitudes show *dparkin* mutant larvae have smaller miniature excitatory junction potentials.

Miniature excitatory junction potentials (mEJPs) are smaller in *dparkin* larvae (p^{25}/p^{Z3678}) compared to wild-type (CS/w^+) controls. The distribution of mEJP amplitudes in the *dparkin* (p^{25}/p^{Z3678}) and wild-type (CS/w^+) larvae are plotted. The mean and mode of the *dparkin* (p^{25}/p^{Z3678}) mEJPs mutant larvae were 0.7 mV and 0.5 mV, 40% and 16% smaller than that of wild-type (CS/w^+) control mEJPs.

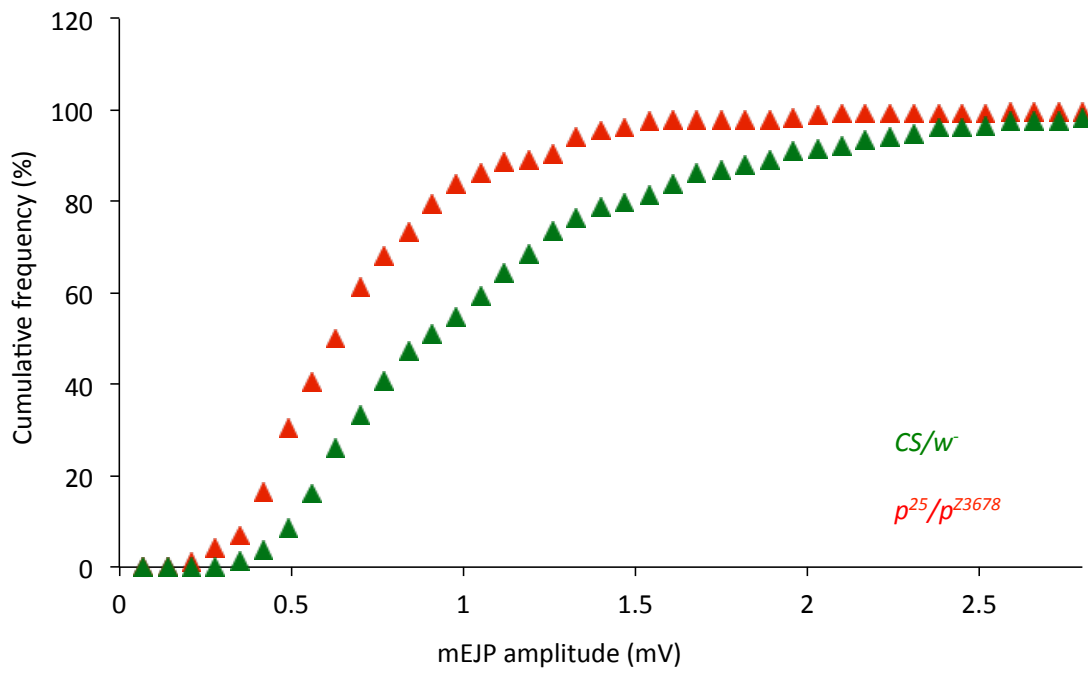


Figure 3.10 Cumulative frequency curve show *dparkin* mutant larvae have smaller miniature excitatory junction potentials.

Cumulative frequency curves show the median mEJP amplitude from *dparkin* larvae (p^{25}/p^{Z3678}) is smaller than that from wild-type larvae (*CS/w*), (Kolmogorov–Smirnov test statistic = 3.5, $P < 0.001$). Additionally, the lower and upper quartiles of the distribution of mEJPs of *dparkin* larvae are lower than those of wild-type controls.

***dparkin* null mutant larvae show electrophysiological deficits**

The last sections have shown that *dparkin* transheterozygote larvae have major electrophysiological deficits, in both RMP and synaptic transmission. In the next section we test if these defects are also seen in another *dparkin* mutant, the homozygote *dparkin*²⁵ (*p*²⁵/*p*²⁵). In these larvae, no *dparkin* protein is synthesized (Greene et al., 2003, Whitworth et al., 2005, Tain et al., 2009).

Intracellular recordings from larval muscles 6 and 7 of *dparkin* (*p*²⁵/*p*²⁵) null mutant show the RMPs are 11 mV ($p < 0.001$) more positive compared to wild-type (*CS/w*⁻) controls (**Fig. 3.11A**). The global (*Actin5*-GAL4) driver or the pan-neuronal (*elav*^{3E1}-GAL4) driver or the *G14*-GAL4 driver (which expresses in all muscles), was used to express wild-type *dparkin* in the *dparkin* (*p*²⁵/*p*²⁵) mutant background. In each case, the RMP deficit was rescued ($p = 0.009$, $p < 0.001$ and $p < 0.001$, respectively, **Fig. 3.11A**).

These observations were extended by testing a second pair of muscles in the *dparkin* (*p*²⁵/*p*²⁵) null mutant, muscles 12/13, which run parallel to muscle 6 and 7 and are also innervated by type Is motoneuron terminals. These muscles were also 9 and 10 mV more depolarized compared to those of wild-type (*CS/w*⁻) controls (**Fig. 3.11B**). Global (*Act5c*-GAL4), neuronal (*elav*^{3E}-GAL4) or muscle (*G14*-GAL4) expression of wild-type *dparkin* on a *dparkin* (*p*²⁵/*p*²⁵) mutant background failed to rescue the RMP defects ($p = 0.170$, $p = 0.329$ and $p = 0.906$, respectively) compared to *dparkin* (*p*²⁵/*p*²⁵) null larvae. *dparkin* transheterozygote (*p*²⁵/*p*^{Z3678}) larvae show no difference in RMP compared to *dparkin* null (*p*²⁵/*p*²⁵) larvae ($p = 0.396$). Wild-type control larvae (*CS* and *CS/w*⁻) show no differences in RMP ($p = 0.590$) (**Fig. 3.11B**).

In a more extensive experiment, both the *dparkin* null (*p*²⁵/*p*²⁵) and transheterozygote (*p*²⁵/*p*^{Z3678}) larvae were also tested. As two mutant strains were used, two wild-types (*CS*

and *CS/w⁻*) were used. The *dparkin* null recordings of spontaneous EJPs in muscles 6 and 7 showed reduced EJPs. As with the transheterozygote experiment, a scatter graph was plotted of the size of the EJP against RMP (**Fig. 3.12**). Using the data from *dparkin* (p^{25}/p^{25}) mutant and wild-type (*CS* and *CS/w⁻*) controls, lines of best fit were drawn to calculate the residual between EJP and regression line calculated (**Fig. 3.12**). *dparkin* (p^{25}/p^{25}) mutants showed reduced synaptic transmission compared to their wild-type controls (*CS* and *CS/w⁻*, $p = 0.004$ and $p = 0.007$ respectively, **Fig. 3.13**). When wild-type *dparkin* was expressed either in a global (*Actin5-GAL4*), pan-neuronal (*elav^{3E1}-GAL4*) or the *G14-GAL4* tissue dependent manner in a *dparkin* (p^{25}/p^{25}) mutant background, the EJP was increased ($p = 0.010$, $p = 0.024$ and $p = 0.001$ respectively, **Fig. 3.13A**). Muscle 13 and 12 recordings also showed that *dparkin* (p^{25}/p^{25}) mutant larvae have a reduction in synaptic transmission compared to wild-type (*CS*, $p = 0.007$) control larvae, but not with the wild-type outcross (*CS/w⁻*, $p = 0.703$, **Fig. 3.13B**) larvae. Similar data was seen with muscle 6 and 7. The RMP of *dparkin* (p^{25}/p^{25}) mutant larvae are not significantly different from *dparkin* (p^{25}/p^{Z3678}) mutant larvae ($p = 0.296$). Global (*Act5c-GAL4*) or muscle (*G14-GAL4*) expression of wild-type *dparkin* on a *dparkin* (p^{25}/p^{25}) homozygous mutant background showed an increase in synaptic transmission ($p = 0.001$ and $p = 0.002$, respectively) whereas neuronal (*elav^{3E}-GAL4*) expression of wild-type *dparkin* showed no difference ($p = 0.199$) compared to *dparkin* (p^{25}/p^{25}) mutant larvae (**Fig 3.13B**).

Fig 3.11A

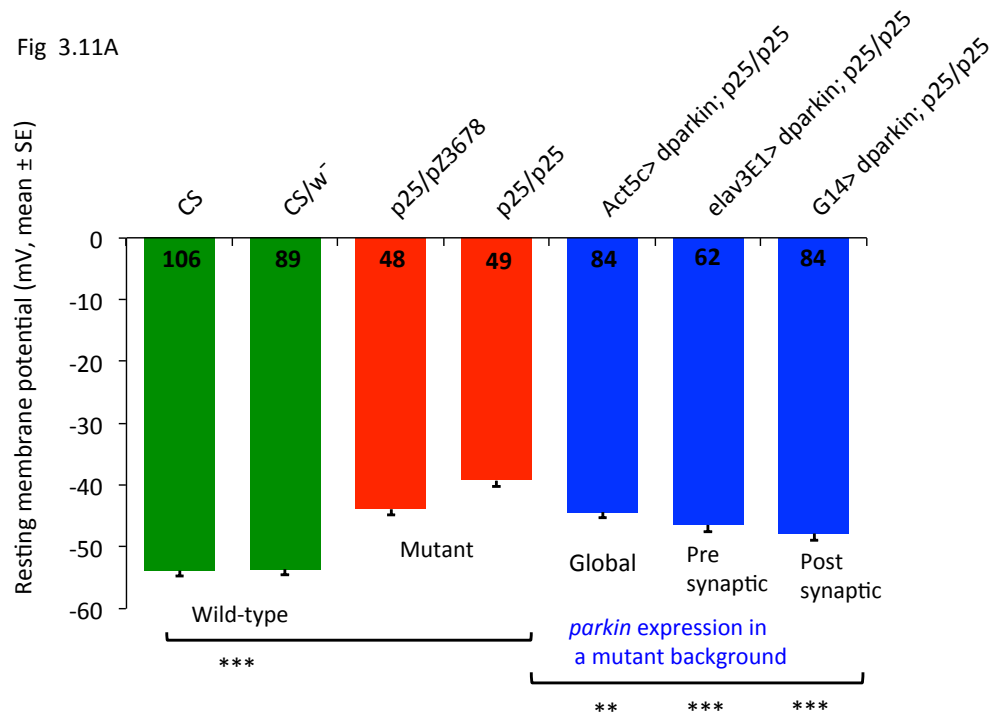


Figure 3.11 *dparkin* mutant larvae show more positive (depolarized) RMP that is rescued by global, neuronal or muscle expression of wild-type *dparkin*

A Muscle 6 and 7 intracellular recordings revealed *dparkin* (p^{25}/p^{Z3678} or p^{25}/p^{25}) mutant larvae show more positive (depolarized) RMP (resting membrane potential) compared to wild-type (*CS* or *CS/w⁻*) larvae ($p < 0.001$). Global (*Act5c-GAL4*), neuronal (*elav^{3E}-GAL4*) or muscle (*G14-GAL4*) expression of wild-type *dparkin* on a *dparkin* (p^{25}/p^{25}) mutant background rescued the RMP defects ($p = 0.009$, $p < 0.001$ and $p < 0.001$ respectively) compared to *dparkin* (p^{25}/p^{25}) mutant larvae. *dparkin* transheterozygote (p^{25}/p^{Z3678}) larvae show no difference in RMP compared to *dparkin* null (p^{25}/p^{25}) larvae ($p = 0.087$). Wild-type control larvae (*CS* and *CS/w⁻*) show no differences in RMP ($p = 1.0$). **B** Recordings from muscle 12 and 13 show that *dparkin* (p^{25}/p^{Z3678} or p^{25}/p^{25}) mutant larvae show more depolarized RMP compared to wild-type (*CS* or *CS/w⁻*) larvae ($p < 0.001$ and $p = 0.001$, respectively). Global (*Act5c-GAL4*), neuronal (*elav^{3E}-GAL4*) or muscle (*G14-GAL4*) expression of wild-type *dparkin* on a *dparkin* (p^{25}/p^{25}) mutant background failed to rescue the RMP defects ($p = 0.170$, $p = 0.329$ and $p = 0.906$, respectively) compared to *dparkin* (p^{25}/p^{25}) mutant larvae. *dparkin* transheterozygote (p^{25}/p^{Z3678}) larvae show no difference in RMP compared to *dparkin* null (p^{25}/p^{25}) larvae ($p = 0.396$). Wild-type control larvae (*CS* and *CS/w⁻*) show no differences in RMP ($p = 0.590$).

Fig 3.12B

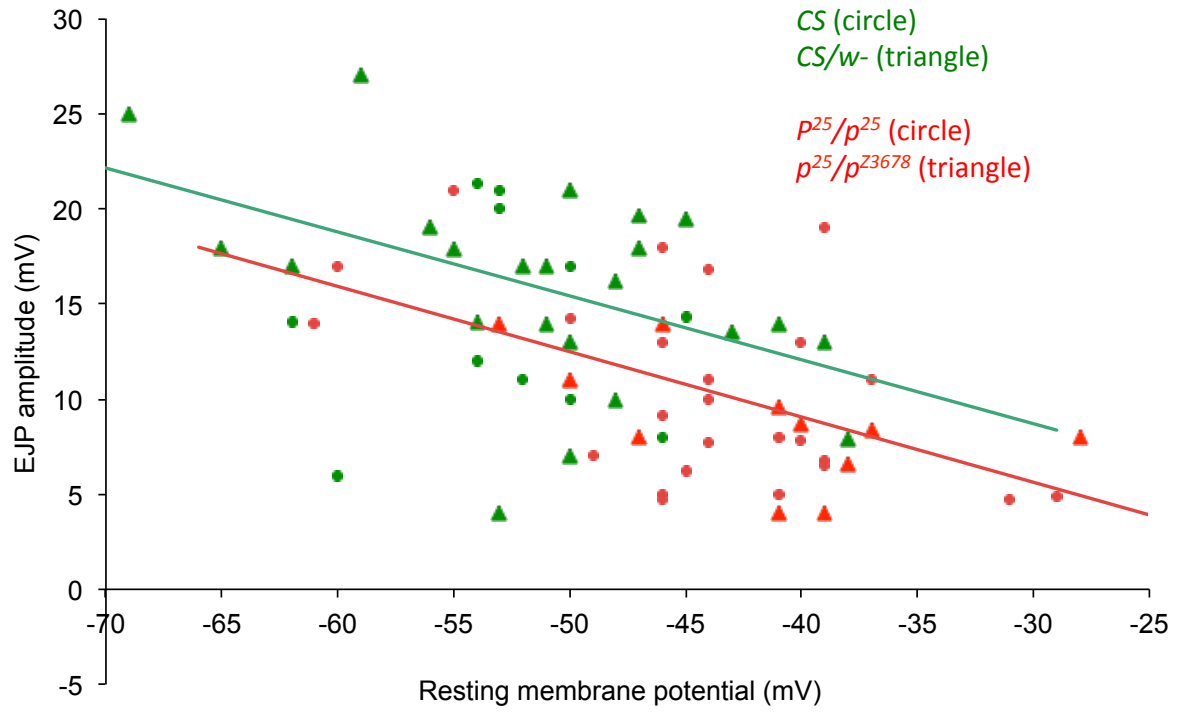


Figure 3.12 Scatter regression plot show *dparkin* null mutant larvae have depolarized RMP and reduced synaptic transmission across a range RMP.

dparkin (p^{25}/p^{Z3678} or p^{25}/p^{25} , in red) mutant larvae show more positive (depolarized) RMP compared to wild-type (*CS* or *CS/w⁻*, in green) larvae. The *dparkin* larval EJPs were on average smaller compared to their wild-type controls across a range of RMPs recorded from either muscles 6 and 7, or 12 and 13 (**Fig. 3.12 A** and **B** respectively). The solid lines are the linear regressions across *dparkin* and wild-type larvae.

Fig 3.13B

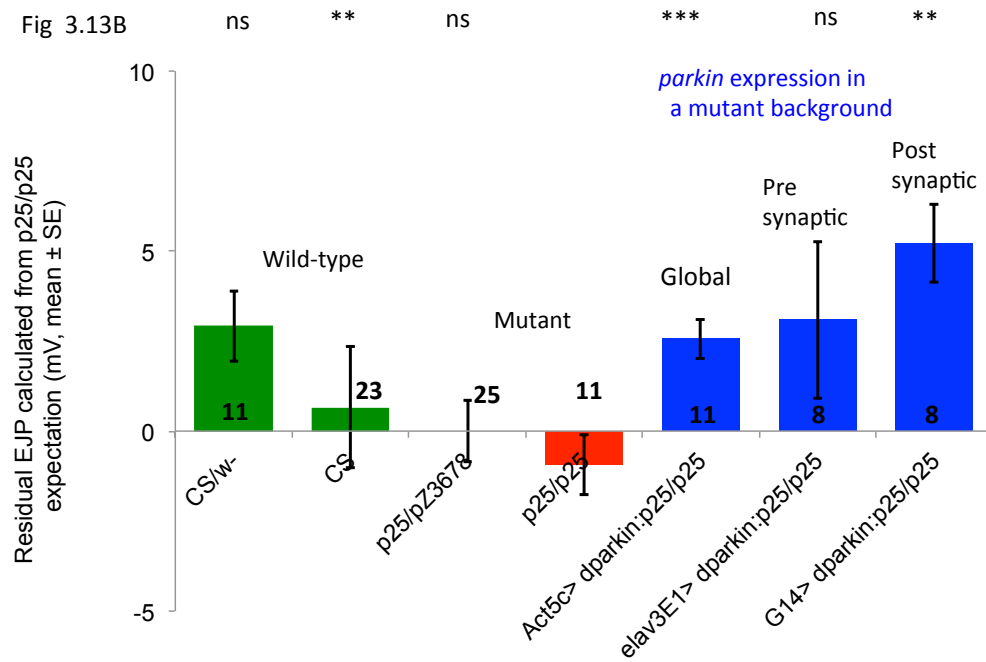


Fig 3.13A

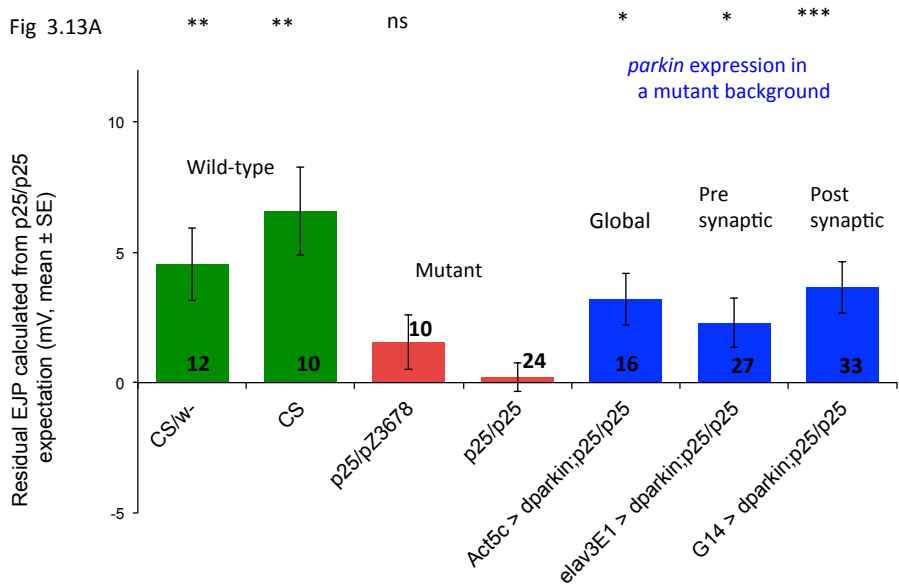


Figure 3.13 *dparkin* mutant larvae show a reduction in synaptic transmission and with either global, neuronal or muscle of wild-type *dparkin* expression shows partial rescue of synaptic

A *dparkin* (p^{25}/p^{25}) mutant larvae show a reduction in synaptic transmission in muscle 6 and 7 compared to wild-type (*CS/w⁻* or *CS*) control larvae ($p = 0.007$ and $p = 0.004$, respectively). *dparkin* (p^{25}/p^{25}) mutant larvae are not significantly different from *dparkin* (p^{25}/p^{Z3678}) mutant larvae ($p = 0.964$). Global (*Act5c*-GAL4), neuronal (*elav^{3E}*-GAL4) or muscle (*G14*-GAL4) expression of wild-type *dparkin* on a *dparkin* (p^{25}/p^{25}) homozygous mutant background showed an increase in synaptic transmission ($p = 0.010$, $p = 0.024$ and $p = 0.001$, respectively) compared to *dparkin* (p^{25}/p^{25}) mutant larvae. **B** Recordings from muscle 12 and 13 show *dparkin* (p^{25}/p^{25}) mutant larvae show a reduction in synaptic transmission compared to wild-type (*CS*, $p = 0.007$) control larvae but not with the other wild-type (*CS/w⁻*, $p = 0.703$) larvae. *dparkin* (p^{25}/p^{25}) mutant larvae are not significantly different from *dparkin* (p^{25}/p^{Z3678}) mutant larvae ($p = 0.296$). Global (*Act5c*-GAL4) or muscle (*G14*-GAL4) expression of wild-type *dparkin* on a *dparkin* (p^{25}/p^{25}) homozygous mutant background showed an increase in synaptic transmission ($p = 0.001$ and $p = 0.002$, respectively) whereas neuronal (*elav^{3E}*-GAL4) expression of wild-type *dparkin* showed no difference ($p = 0.199$) compared to *dparkin* (p^{25}/p^{25}) mutant larvae. Bold numbers indicate the number of larvae used in each genotype.

***dparkin* mutant larvae show pronounced difference in RMP at low external potassium concentrations**

Altering the external potassium concentration in the 1mM calcium-containing HL3 solution that bathes the preparation caused a more positive shift in both wild-type (*CS/w⁻*) and *dparkin* (*p²⁵/p^{Z3678}*) mutant and RMP as the potassium concentration increased. When the Nernst equation line was plotted for potassium, the higher concentration points of both the wild-type and *dparkin* mutant larvae was consistent with the Nernst line whereas the lower concentration showed a deviation from the line. The deviation from the line suggests that different ions could result in the depolarization of RMP when there is lower a concentration of external potassium (Cl^- and Na^+ ions). The changing of extracellular potassium ion concentration caused changes in RMP in both wild-type controls and *dparkin* transheterozygote mutant larvae. *dparkin* mutants show a more depolarized RMP throughout the different concentration of potassium compared to their wild-type controls (Fig 3.14).

Fig 3.14

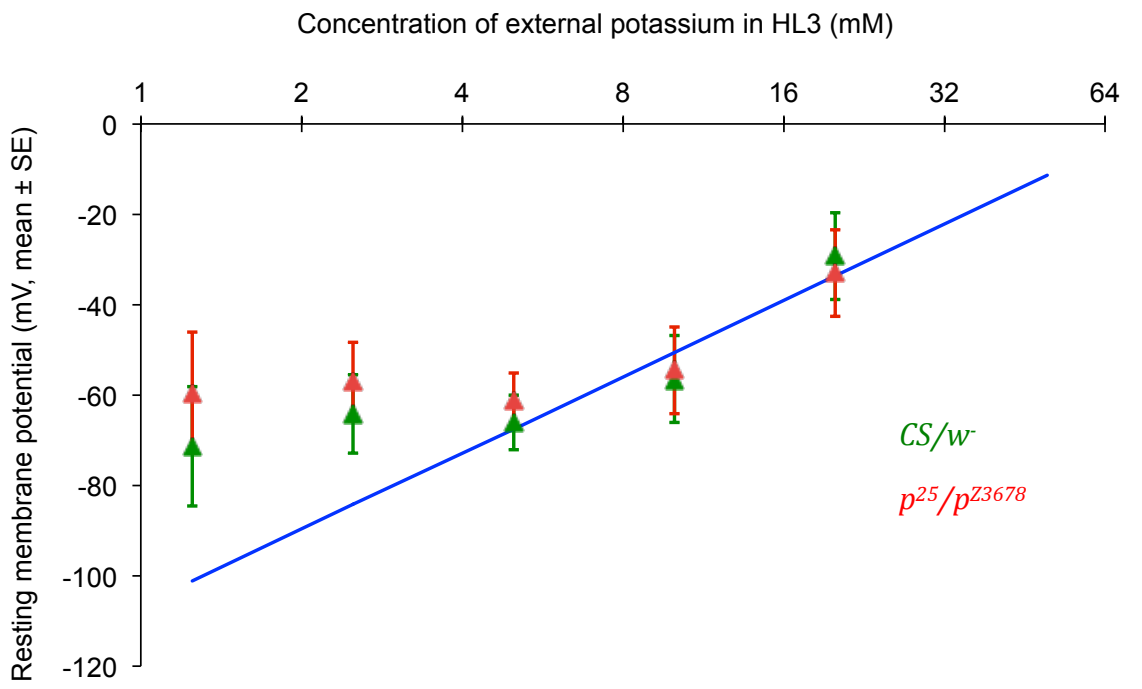


Figure 3.14 The difference in RMP between *dparkin* mutant and wild-type larvae is most pronounced at low external potassium concentrations.

At higher potassium concentrations, above 4 mM, the RMP of both *dparkin* (p^{25}/p^{Z3678}) and wild-type (CS/w^-) muscles were close together and followed the line calculated for the Nernst equation. At lower potassium concentrations the RMP of both genotypes is consistently above the line. At the lowest concentration, the difference between the *dparkin* and wild-type larvae is marked, with the *dparkin* larvae being more positive than the wild-type.

3.3 Discussion

The key findings in this chapter are that *dparkin* mutant larvae show slower locomotion, overgrown synapses, a reduction in synaptic transmission (both spontaneous EJPs and mEJPs) and a more positive (depolarized) resting membrane potential (RMP), especially at lower extracellular potassium concentrations. These phenotypes are principally due to the neural impact of *dparkin*. Trans-synaptic signalling plays a key role in the phenotype.

Crawling speed is reduced in *dparkin* transheterozygote mutant larvae

dparkin transheterozygote mutant larvae show reduced velocity in the crawling assay used to measure motor performance. The homozygotes (p^{25}/p^{25} null) also crawl more slowly (Vincent et al., 2012). Adult *dparkin* mutants also demonstrate reduced locomotion in adult negative geotaxis assays (Greene et al., 2003, Whitworth et al., 2005). In these assays, locomotion could have been reduced by changes in sensitivity to mechanical stimuli or to changes in locomotory ability. Our assays, monitoring spontaneous crawling, provide a more specific demonstration of the loss of *dparkin*-induced locomotory failure.

Crawling speed rescued with the neuronal wild-type *dparkin* expression in *dparkin* transheterozygote mutant larvae

Since the crawling phenotype was observed in the *dparkin* transheterozygote mutant larvae, it is likely that the phenotype was due to *dparkin* loss rather than a second site mutation. The reduced crawling phenotype was rescued by global expression of wild-type *dparkin* in a *dparkin* mutant background (Vincent et al., 2012). More importantly, the neuronal expression of wild-type *dparkin* also rescued, unlike muscle expression of wild-type *dparkin* in a mutant background (Vincent et al., 2012). This shows the reduced crawling speed was a result of *dparkin* loss in neurons rather than from the

muscles. Additionally, *dparkin* null mutant larvae show reduced number of contractions as observed from the larval extensometer or ‘bendy-beam’ assay (Vincent et al., 2012), along with a bradykinesia-like phenotype (reminiscent of PD patients). Both phenotypes may lead to an overall reduction in crawling speeds in *dparkin* transheterozygote mutant larvae. Neuronal expression of wild-type *dparkin* in nerve rescues this defect whereas muscle expression does not (Vincent et al., 2012). From this it was concluded that the behavioral (crawling) defect arises from the loss of *dparkin* in neurons and not the muscles.

Are dopaminergic neurons key to the crawling defect?

Our paper hypothesized that reduced dopaminergic function is key to the reduced crawling seen in *dparkin* mutants (Vincent et al., 2012). To test this hypothesis of dopaminergic dysfunction, *dparkin* was knocked down by using the *tyrosine hydroxylase* (*TH-GAL4*) driver with the *dparkin dsRNAi* generated by Yang *et al.* (2003). There was no difference in crawling speed compared to wild-type controls. This result suggests dopaminergic *dparkin* is not absolutely essential for locomotory dysfunction. On the other hand, disruption to aminergic neurotransmission has been reported to have an impact on crawling behavior as seen by *D. melanogaster* vesicular aminergic transporter (*DVMAT*) mutants that exhibit a distinct slow crawling phenotype, thereby suggesting disruption to the aminergic system may be the reason behind the larval bradykinesia phenotype seen in our *dparkin* mutant larvae.

However, we do not know how effective the *TH > RNAi* transgenes were at reducing the level of PARKIN protein, as this was not measured in these experiments. Expression of *dparkin dsRNAi* with our *Act5c-GAL4* provided a marked overgrowth phenotype at the neuromuscular junction. Further, expression of this *dsRNAi* using a ubiquitous *heat-shock-GAL4* driver showed both a reduction in mRNA levels (by PCR)

and an interaction with the *Pael-R* transgene. However, there was no net loss of dopaminergic neurons. My experiments indicate a synaptic role for *dparkin* in the overgrowth phenotype and so the wild-type *dparkin* from the surrounding cells could have provided a neuroprotective effect and thus not induce the *dparkin* transheterozygote mutant larvae crawling phenotype. I conclude that further experiments are needed to confirm if *dparkin* knockdown is effectively achieved in the dopaminergic neurons by the *TH-GAL4*.

Synaptic overgrowth phenotype in *dparkin* mutants

As neuronal loss of *dparkin* was shown to cause locomotory dysfunction I assessed the integrity of both the neuronal architecture involved in carrying signals required for movement by the postsynaptic cell (the muscle). *dparkin* transheterozygote mutants show overgrown synapses brought about with increased raw bouton count and decreased muscle surface area. Additionally, I assessed whether the neuronal or muscle loss was important for the overgrowth phenotype. Morphological analysis of *dparkin* mutant larval neuromuscular junction (NMJ) showed that either muscle or neuronal expression of wild-type *dparkin* is sufficient to reduce the overgrowth phenotype back down to wild-type control levels. This was achieved by either a decrease in raw bouton number alone or with an additional increase in muscle surface area with either (neuronal or muscle respectively) GAL4 driver induced expression of wild-type *dparkin* in a *dparkin* transheterozygote background. This suggests that unlike the crawling where only the neuronal expression of wild-type *dparkin* rescued the speed of *dparkin* mutants, the overgrowth phenotype is rescued by either the muscle or neuronal expression of wild-type *dparkin* and suggests it is sufficient to cause an overgrowth with either muscle or neuronal loss of *dparkin*. This is a non-cell autonomous effect where the tissue specific expression of wild-type *dparkin* (for instance in muscles) is

able to affect other tissues with the mutation (and reduce neuronal growth), as opposed to the tissue in which the wild-type *dparkin* is only being expressed. Global knockdown of *dparkin* showed approximately 50% of the overgrowth observed in that of *dparkin* transheterozygote mutant larval NMJs affecting both the raw bouton number and muscle surface area. This shows wild-type *dparkin* expression regulates overgrowth through a cell-cell signalling mechanism between neurons and muscle cells.

Studies in *D. melanogaster* studies have identified a number of signalling pathways between postsynaptic targets and presynaptic terminals. These are important in synapse formation, growth and plasticity and survival of the presynaptic neuron. Retrograde signals include Transforming growth factor beta (TGF- β) and reactive oxygen species (ROS). TGF-beta signalling is necessary for normal NMJ associated synaptic growth (Aberle et al., 2002, Marqués, 2005) while enhanced TGF-beta signalling is linked to presynaptic overgrowth the *spinster* (*spin*) mutant, (Sweeney and Davis, 2002). Induction of autophagy has been shown to cause overgrowth (Shen and Ganetzky, 2009). *spin* and other anti-oxidant compromised mutants are also shown to induce growth in response to the generation of ROS (Milton et al., 2011). Another mutant with an overgrowth phenotype is *highwire* (*hiw*), where the *hiw* mutation leads to 200% expansion of NMJ (DiAntonio et al., 2001). The *highwire* gene encodes an *E3 ubiquitin ligase* which that is expressed at the periaxial zone (Wan et al., 2000). *Hiw* induced overgrowth is suppressed via mutations in *wallenda* a MAP kinase kinase kinase or by mutations that reduce c-jun N-terminal kinase (*JNK*) and *fos* activity. *JNK* or *fos* are required for the *hiw* mutant-induced overgrowth. Signalling by these molecules may account for the non- autonomous rescue that is seen when *parkin* is expressed in the muscle.

There are other mutants in the literature that have altered bouton number but with no

effect on neurotransmission. One of these is another PD-related gene, *hLRRK2*, where the pathogenic mutation *G2019S* has NMJ overgrowth (Lee et al., 2010).

Other signalling pathways act in the opposite, anterograde manner. Davis demonstrated in his model that amount of growth factor regulated synaptic growth. It was also postulated in the paper, inhibitory growth and growth promoting signals exist, that balance the growth of synaptic terminals. The main conclusion from Davis paper was alteration to endosomal/lysosomal function, whether it may be pre- or post-synaptic, can cause misregulation of intercellular signalling systems.

This may be the case with *dparkin* mutant larvae as either neuronal or muscle expression of wild-type *dparkin* in a mutant background was sufficient to completely rescue the overgrowth.

Synaptic transmission is reduced in *dparkin* transheterozygote mutants

dparkin transheterozygote larvae show reduced synaptic transmission, even after allowing for the change in RMP. Additionally, *dparkin* transheterozygote mutants show reduced spontaneous single vesicular release. The mEJPs are smaller in *dparkin* transheterozygote mutants than in wild-type controls. The EJPs and mEJPs are mediated by glutamate receptors with reversal potentials estimated between 0 and 1.7 mV (Jan and Jan, 1976, Macleod and Zinsmaier, 2006, Macleod et al., 2006). The reduced size of EJP observed in *dparkin* mutants is likely to be due to reduced size of mEJPs. This leads us to conclude that there is reduced neurotransmitter that is actively recycled into the synaptic vesicles in an ATP-dependent manner. Alternatively, it may also be as a result of the release mechanism failing, as the pre-synaptic motor terminals may be (like the muscles) more depolarized.

***dparkin* expression partially rescues the synaptic signalling defect**

At muscle 6/7, the global, neuronal or muscle expression of wild-type *dparkin* failed to rescue synaptic defects with wild-type *dparkin* expression using any of the above drivers in the *dparkin* transheterozygote mutants. However, at muscle 12/13, global or muscle expression of wild-type *dparkin* partially restored the synaptic transmission defect in *dparkin* null mutants. The global, neuronal or muscle expression of wild-type *dparkin* rescued synaptic defects with wild-type *dparkin* expression using any of the above drivers in the *dparkin* null mutants. Difficulties in collecting enough data due to the variability in food quality from tray to tray limited the sample size. The results may also be more difficult to interpret due to possible differences in genetic background. Nonetheless, overall, I cautiously conclude that *dparkin* global, neuronal and muscle rescue of EJP is likely to be effective with a larger population.

Sang and colleagues showed a decrease in neuronal activity observed from *parkin* mutant adult fly brains (as a result of expression of human mutant *parkin* using *Ddc-GAL4*) compared to their controls, as monitored by the measure of fluorescence intensity from genetically encoded calcium indicators (G-CaMP) (Sang et al., 2007, Wang et al., 2003). The expression of wild-type human *parkin* (*hparkin*) using the *Ddc-GAL4* driver showed no difference in the signal intensity compared to their wild-type controls, suggesting neuronal activity is not compromised with the overexpression of *hparkin* in aminergic cells in the fly (Sang et al., 2007). As with *dparkin* mutant larvae, another PD-related gene, *LRRK2*, has shown perturbed synaptic transmission in a *dLRRK* *in vivo* model where there is reduced neurotransmitter release in the *dLRRK* knockout (Lee et al., 2010).

***dparkin* mutant show depolarized RMP**

RMP were more depolarized from the muscles 6/7 of both transheterozygote and the

null larvae and also this trend were as shown in another set of adjacent muscles/ 12/13. This suggests that all muscles are affected, rather than just the most frequently selected muscles. The resting membrane potential of *D. melanogaster* larval muscles changes with varied extracellular calcium concentrations in physiological studies (Jan and Jan, 1976, Jan et al., 1977, Mackler et al., 2002). These effects are similar between HL-3 and standard saline A (SSA) saline although there are fundamental differences between the two salines' compositions (Krans et al., 2010). RMP in wild-type larvae in other studies have shown voltage data of < -55 mV (Macleod et al., 2006). Calcium-dependent depolarization was noted in *D. melanogaster* by Jan and Jan (1976) in their early studies. Elevated potassium in HL3 was shown to have similar effect as the hemolymph concentration of Mg^{2+} that is the same concentration as the HL3 formulae. We had omitted Mg^{2+} from HL3 throughout the course of all electrophysiological experiments as it has deleterious effect on stable membrane potential (Hoyle, 1953, Stewart et al., 1994). Additionally, HL3 contains 20 mM concentration of Mg^{2+} , and it has been suggested that high Mg^{2+} would abolish neural activity in many crustaceans (Takeuchi and Takeuchi, 1963). Feng *et al.* (2004) recently adapted the HL3 with a reduced- Mg^{2+} version called HL3.1 (with a concentration of 4 mM Mg^{2+}), which restores some attenuated electrophysiological phenomena in the larva (Feng et al., 2004). Here we note that the difference in RMP was largest at low external potassium concentrations. This suggests other ions (most likely Na^+ , Ca^{2+} , Cl^-) also make a contribution to the RMP.

It must also be noted the rare depolarized RMP phenotype accompanied by synaptic dysfunction reported in this *parkin* model may have been detected here and not in other *parkin* models as a result of differences in the electrophysiological approach. Firstly, it was important to report on spontaneous recording rather than stimulated EJPs. It must

be noted with electrophysiological recordings such as postsynaptic responses there is a chance there may be damage to the preparation, improper adjustment of the stimulating voltage, a result of high-frequency stimulating voltage or a mutant phenotype. All of which may cause one of the two axons being stimulated and thus cause a decrease in EJP amplitude. Secondly, the modified HL3 omitted magnesium chloride from the original recipe of HL3 solution (Stewart et al., 1994). This could have possibly affected the production of ATP (Ko et al., 1999) and so disrupted the RMP. Thirdly, a voltage clamp was not used to clamp the resting membrane potential to a set voltage. This means the residual plot had to be used. Working in high calcium saline with large EJP amplitudes helps to observe a clear distinction in amplitude reduction and failure of one of the axons to contribute to the EJP. In the case when one of the two is intermittently activated, the EJP amplitudes will fluctuate dependent on axons that have signaled. The failure of an action potential to spread throughout all the terminal branches of the axons onto the postsynaptic muscle also affects EJP amplitude. Since M6/7 and M12/13 are each innervated by two motoneurons this provides extra ambiguity. This could have been avoided by working with a muscle receiving input from only one motoneuron, for example muscle 5 (Hoang and Chiba, 2001). Such recordings would be more straightforward to interpret.

***dparkin* rescues the RMP phenotype**

Electrophysiological data from muscle recordings showed the muscle expression of wild-type *dparkin* rescued the RMP in the transheterozygote background from muscle 6 and 7 recordings, whereas the global, neuronal or muscle expression only partially rescue the RMP defect in *dparkin* null mutants. In muscles 12 and 13 of *dparkin* null larvae the RMP was also more depolarized compared to wild-type controls. In these muscles, the wild-type expression of *dparkin* globally, neuronally or in muscles failed

to show any rescue. This could be a result of the reduced count of muscle recordings for the muscle 12 and 13 data set compared to the muscle 6 and 7 for the *dparkin* null mutant larvae. The muscle recordings presented here from muscle 6 / 7 or 12 / 13 were from two complete data sets, each from one food batch to limit variability. The *dparkin* transheterozygote mutant data from muscle 6 / 7 had overall fewer data points compared to *dparkin* null mutant larvae but these were all undertaken in one day.

Metabolic Dysfunction in parkin larvae is key to RMP depolarization and synaptic dysfunction

Few *D. melanogaster* mutants show a depolarized RMP, but one which does is *nubian* (Wang et al., 2004). This is a mutation in phosphoglycerate kinase (*PGK*). This enzyme is key in the terminal stage of glycolysis that leads to the production of ATP, one of the two ATP steps before oxidative phosphorylation. This glycolytic mutant shows severe depletion of ATP, leading to the failure to maintain a more negative RMP. *dparkin* null mutant larvae have 30% less oxygen consumption compared to wild-type larvae with ATP levels that were 14% of controls (Vincent et al., 2012). These both suggest aerobic respiration and mitochondrial production of ATP have been compromised. Recently, adult *dparkin* null mutant flies were reported to recover from their motor deficits after being fed with Vitamin K2. This compound targeted the respiratory chain and increased ATP generation (Vos et al., 2012). The depolarized RMP in *dparkin* mutant larvae is also suggested to be a result of metabolic dysfunction (a depletion of ATP stores to facilitate the ATP dependent pumps). RMP are maintained by the selective permeability of ions (potassium, sodium and chloride) and by the sodium-potassium (Na^+/K^+ -ATPase) electrogenic pump that is ATP dependent.

The *D. melanogaster* sodium pump only becomes functional as an α - β heterodimer (Lingrel and Kuntzweiler, 1994, Lingrel et al., 1994a, Lingrel et al., 1994b). The fly,

Na⁺/K⁺-ATPase α subunit is encoded by a single gene (Lebovitz *et al.*, 1989), and but two β subunit genes (*Nervana 1* and 2) code for three different β isoforms, which are expressed in a tissue specific manner (Sun and Salvaterra, 1995). During fictive crawling (when the peristaltic rhythm is recorded from the isolated CNS) each burst of action potentials are followed a brief period of hyperpolarisation. This is essential for restoration of neural activity (Pulver and Griffith, 2010). During the hyperpolarisation, ions are transported via ATP-dependent pumps to restore ionic balance. If the RMP is compromised, pumping deficits arising from ATP depletion could result in a much slower restoration of ionic balance, and thus causing a reduction in CPG activity. This would slow the initiation of subsequent contraction.

Metabolic dysfunction has been observed in PD patients. Neuronal samples cannot be readily obtained from human patients. Therefore skin biopsies were used to obtain fibroblasts to determine the metabolic status of tissue with a loss of *parkin*. Fibroblasts, which are known to make skin, were obtained from patients with mutations in *parkin*. These show metabolic failure with reduced complex I mediated ATP production (Mortiboys *et al.*, 2008), similar to the ATP depletion observed in *parkin* larvae (Vincent *et al.*, 2012).

Locomotory deficits accompanied by synaptic dysfunction

dparkin mutant flies have previously focused on describing adult phenotypes, with a single study reporting no larval phenotypes observed in *dparkin* null mutant (Pesah *et al.*, 2004). My thesis is the first to report larval phenotypes at the level of behavior, physiology and anatomy caused by mutations in this early-onset gene. The homozygous *dparkin* null mutants and the transheterozygote hypomorph mutants we raise on our standard food in our laboratory conditions often fail to survive beyond

pupal stage. However, in other laboratories they seem to emerge into adults and have an average life span of 28 - 50 days (Greene et al., 2003, Whitworth et al., 2005, Tain et al., 2009). This difference could arise from their diet, as our food contains 0.125 g/l manganese chloride: manganese is known to reduce the viability of *parkin* mammalian cell lines (Roth et al., 2012, Higashi et al., 2004) and is associated with the risk of developing Parkinson's disease (Roth, 2014). Furthermore, low levels of other minerals may impact the survival of *dparkin* mutants since PARKIN interacts with Metal-Responsive Transcription Factor (MTF-1) (Saini et al., 2011).

Summary of key findings:

- * *dparkin* mutant larvae have synaptic dysfunction, locomotory defect and overgrown synapses at the NMJ

- * Expression of wild-type *dparkin* rescues synaptic potentials

- * Expression of *dparkin* rescue muscle RMP

- * *dparkin* mutant larvae have depolarized muscle RMP, as a global mutant thus suggesting the neurons too could be depolarized

- * Synaptic overgrowth is rescued with either muscle or neuronal *dparkin* expression

Chapter 4: Investigating the role of oxidative stress and metabolic dysfunction in *dparkin* mutant larvae

4.1 Introduction

Chapter 3 established that *dparkin* mutant larvae show reduced locomotion, overgrown synapses, a reduction in synaptic transmission and depolarized resting membrane potentials. This was also reported by Vincent et al., (2012). Global overexpression of scavengers of reactive oxygen species (ROS), acting in either cytoplasmic or mitochondrial compartments, reverted the synaptic overgrowth normally seen in the *dparkin* null background (Vincent et al., 2012). Further, the transcriptional profile clearly shows the up-regulation of oxidative stress response elements, while mutations in these oxidative response elements enhance *dparkin* mutant phenotypes (Greene et al., 2005). All this supports the oxidative stress hypothesis of the *dparkin* phenotype. Oxidative stress is also a key driver of synaptic overgrowth in other fly systems (Milton et al., 2011). This suggested that oxidative stress was a key component of the *dparkin* synaptic overgrowth phenotype.

However, ROS scavengers did not revert the reduced locomotion, synaptic or resting membrane potential (RMP) physiology in the *dparkin* null larvae. This is contradictory to other studies, in the case of adult flies, where eliminating oxidative stress rescued all *dparkin* mutant phenotypes (Umeda-Kameyama et al., 2007, Underwood et al., 2010, Whitworth et al., 2005).

These observations suggest we should explore the impact of oxidative stress in more detail. I therefore used the same (or related) transgenes as previously used in adults. These transgenes were for glutathione-S-transferase S1 (*GST* or *GST-S1*) and a mitochondrial enzyme thioredoxin reductase (Umeda-Kameyama et al., 2007, Whitworth et al., 2005). These systems are important in the brain where catalase

activity is very low. Both the thiol-reducing systems via thioredoxin or glutathione with glutathione peroxidase activity break down hydrogen peroxide to water and oxygen thus reducing oxidative damage.

Studies have shown Complex I activity is redox-dependent and thiol-regulated (Sriram et al., 1998, Annepu and Ravindranath, 2000). PD pathogenesis has shown to consistently be associated to reactive oxygen and nitrogen species generation (Bové et al., 2005, Li and Holbrook, 2003, Przedborski and Ischiropoulos, 2005) and this may be the reason, at least in part, why complex I is inhibited. Thus, depletion of glutathione (*GSH*), an antioxidant and redox modulator, may be one of the early events leading to the inhibition of complex I activity and loss of mitochondrial function (Chinta et al., 2006, Jha et al., 2000). This is relevant as *dparkin* larvae show reduced oxygen consumption suggesting mitochondrial abnormalities (Vincent et al., 2012).

Thioredoxin has been found in the submicromolar range to protect neuronal cell lines from toxin-induced oxidative stress, which normally would lead to apoptosis (Andoh et al., 2002). The reduced forms of *thioredoxin* suppressed hydroxyl radicals, and the inhibition of *thioredoxin reductase* abolished the protective effects (Andoh et al., 2002). Reduced thioredoxin not only binds to and inhibits *ASK-1* (Saitoh et al., 1998), it also enhances DNA binding to transcription factors including *nuclear factor-kB* and *API*. Thioredoxin system has a variety of actions that are neuroprotective due to suppression of hydroxyl radical damage, lipid peroxidation, caspase activation, cytochrome c release and apoptosis (Andoh et al., 2002, Andoh et al., 2003, Svensson and Larsson, 2007). *D. melanogaster* do not have glutathione reductase, but have thioredoxin reductase in which is part of the thioredoxin system, and which causes the glutathione disulphide (GSSG) reduction reaction (Kanzok et al., 2001).

Glutathione-S-transferases are a set of enzymes that aid in the detoxification process as they promote the conjugation of glutathione to a variety of electrophilic substrates. Findings from Whitworth's group suggested altered *GST-SI* activity influenced *dparkin* mutant phenotypes: for example, increased *GST-SI* activity rescued the dopaminergic neuronal loss seen in *dparkin* mutant adult brains. Additionally, a member of the *GST* family, Glutathione-S-transferase Omega 1 (*GST-O1*), rescues both degeneration of neuronal and muscle phenotypes of *dparkin* mutants including increased ATP production (Kim et al., 2012).

dparkin has also been suggested to negatively regulate c-jun-N-terminal kinase (*JNK*) signaling (Cha et al., 2005) and oxidative stress activates *JNK/AP-1* signaling pathway, thereby promoting overgrowth in *D. melanogaster* oxidative stress induced mutant larvae (Milton et al., 2011). Vincent *et al.* (2012) proposed that the oxidative stress-induced overgrowth seen in *dparkin* mutants was a result of increased *JNK/AP-1* signaling (Milton et al., 2011, Vincent et al., 2012). Therefore the relationship of *JNK* activation and oxidative stress in *dparkin* mutant larvae was investigated.

AMPK is activated in response to oxidative stress, hypoxia, high ATP consumption and low nutrient availability. This is regulated by elevated levels of adenosine monophosphate (AMP), adenosine diphosphate (ADP) or Ca^{2+} (Hardie, 2007, Hardie, 2011, Hardie et al., 2011). *AMPK* activation is regulated by high concentrations of ATP, therefore the system is responsive to rises in AMP: ATP ratio rather than AMP alone.

AMPK is a heterotrimeric complex that includes the following subunits: a catalytic alpha (α), regulatory gamma (δ) that bind AMP and a scaffolding beta (β) subunit. *AMPK* activity is increased upon phosphorylation of the Thr172 residue of the catalytic α -subunit by an upstream kinase, Ca^{2+} calmodulin kinase kinase (*CaMKK*) or liver

kinase B1 (*LKB1*) transforming growth factor beta activated kinase 1 (*TGFβ1*) (Shaw et al., 2004, Peng et al., 2010).

AMPK activation has been shown to increase mitochondrial biogenesis via the expression of peroxisome proliferator-activated receptor- γ co-activator (*PGC*)-*1 α (Jäger et al., 2007). *AMPK* has many other targets including autophagy initiator *ATG1* and phosphofructokinase-2 (*PFK-2*), and results in activation of autophagy and glycolysis respectively. These targets are relevant to *dparkin* mutant larvae as they show energy perturbation and oxidative stress. AMPK activation targets include autophagy gene, *ATG1* (Egan et al., 2011, Kim et al., 2011). *dparkin* is also involved in mitophagy (Narendra et al., 2008, Narendra et al., 2009).*

As well as responding to oxidative stress, AMPK is a key sensor of cell autonomous energetic changes. This is important as there is an ATP deficit in *dparkin* mutants larvae (Vincent et al., 2012). I wish to investigate alternative modes of energy production via altering the expression of *AMPK* by expressing a constitutively active *AMPK*^{T184D}- α form. This *AMPK*^{T184D}- α construct is generated from a transgenic line, in which the *Thr184* is replaced by an aspartate, which mimics the activating phosphorylation of this site by *LKB1* (Lizcano et al., 2004). It has been shown to rescue *LKB1* mutants from energetic stress (Mirouse et al., 2007).

The use of PD-toxin induced mouse models have shown *AMPK* function is increased and additionally this activity is inhibited with, the *AMPK* inhibitor, compound C leading to cell death (Choi et al., 2010). More recently in *dparkin* and *dLRRK2* have been shown to interact with *AMPK* in adults both genetically and pharmacologically (Ng et al., 2012).

4.2 Aims

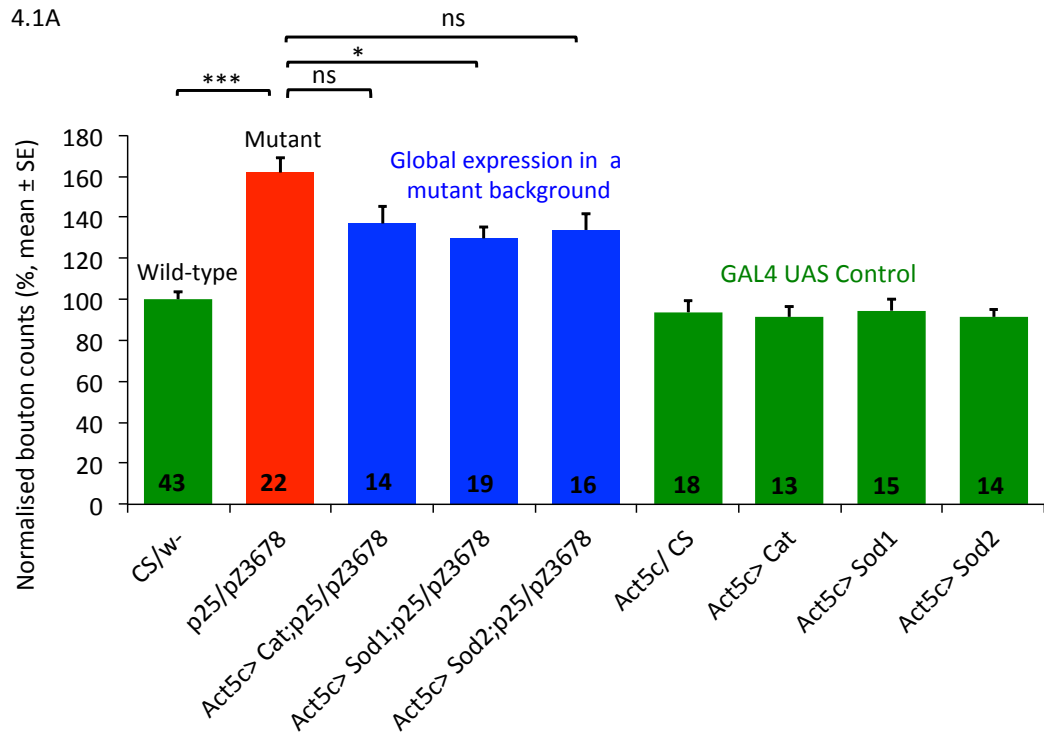
My aim in this chapter was to evaluate the role of oxidative stress on *dparkin* larvae. The experimental approach was to rescue *dparkin* larval phenotypes with transgenes known to play a role in oxidative stress in adult flies. The objectives were to test the effects of the transgenes on neuromuscular junction overgrowth, larval locomotion and resting membrane potential.

4.3 Results

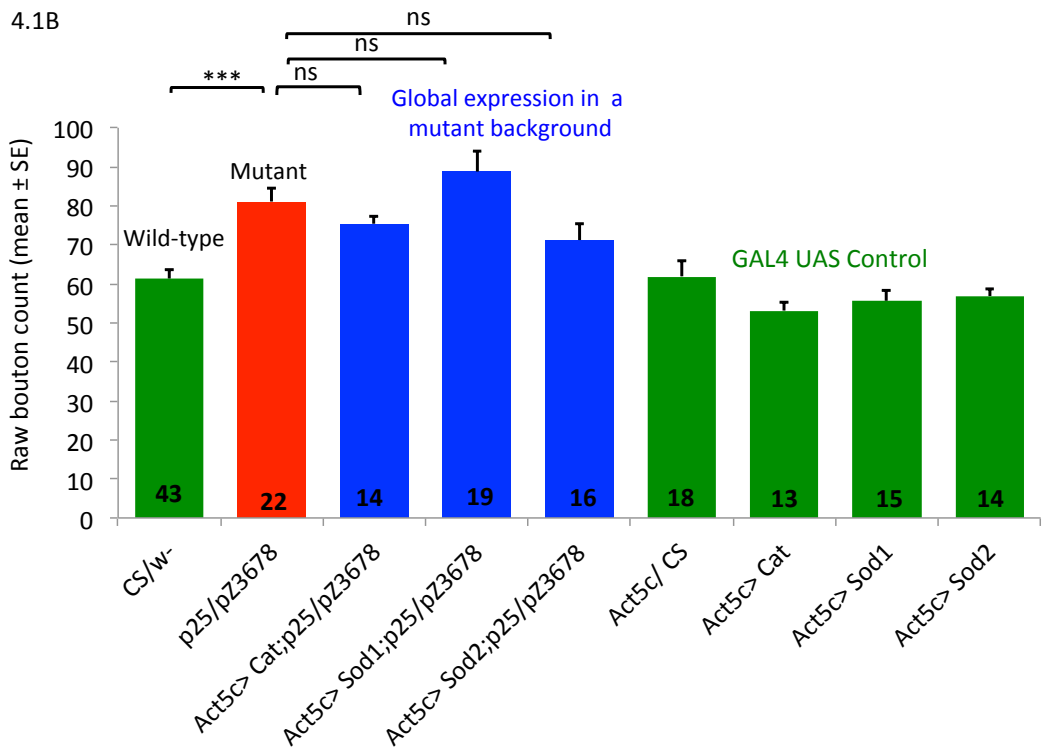
Cytosolic *Sod1* ROS scavenger rescues overgrowth

To investigate the possible mechanisms underlying the neuronal overgrowth phenotype induced by the global loss of *dparkin* as shown in chapter 1, I determined whether the global expression of antioxidants Superoxide Dismutase 1 (*Sod1*), *Sod2* or *Catalase* (*Cat*) would lead to the prevention of the overgrowth phenotypes in *dparkin* (p^{25}/p^{Z3678}) mutant larvae. *Sod1* is an antioxidant enzyme present in the cytosol, nucleus, peroxisomes and mitochondrial intermembrane space of eukaryotic cells. *Sod2* is expressed in the mitochondrial membrane whereas *Cat* is expressed in the cytosol. Global expression of Superoxide Dismutase 1 (*Sod1*) in a *dparkin* (p^{25}/p^{Z3678}) transheterozygote mutant background shows 22 % reduction in overgrowth from normalized bouton counts ($p = 0.016$), whereas *Sod2* and *Cat* did not show an effect, when compared to *dparkin* (p^{25}/p^{Z3678}) mutant controls (**Fig. 4.1A**). Global expression of *Sod1*, *Sod2* or *Cat* all failed to affect raw bouton number (**Fig. 4.1B**), whereas the muscle surface area was only increased 31% by *Sod1* ($p = 0.001$) but not by either the expression with *Sod2* or *Cat* (**Fig. 4.1C**). As reported in chapter 3, there is overgrowth (60 %) in *dparkin* (p^{25}/p^{Z3678}) larval neuromuscular junctions ($p < 0.001$, $p < 0.001$ and $p = 0.036$, respectively) compared to wild-type (*CS/w⁺*) larvae (**Fig. 4.1A**). There are no differences between the GAL4/UAS control NMJ growth (normalized bouton count, raw bouton number or muscle surface area) compared to wild-type (*CS/w⁺*) larvae (**Fig. 4.1**).

4.1A



4.1B



4.1C

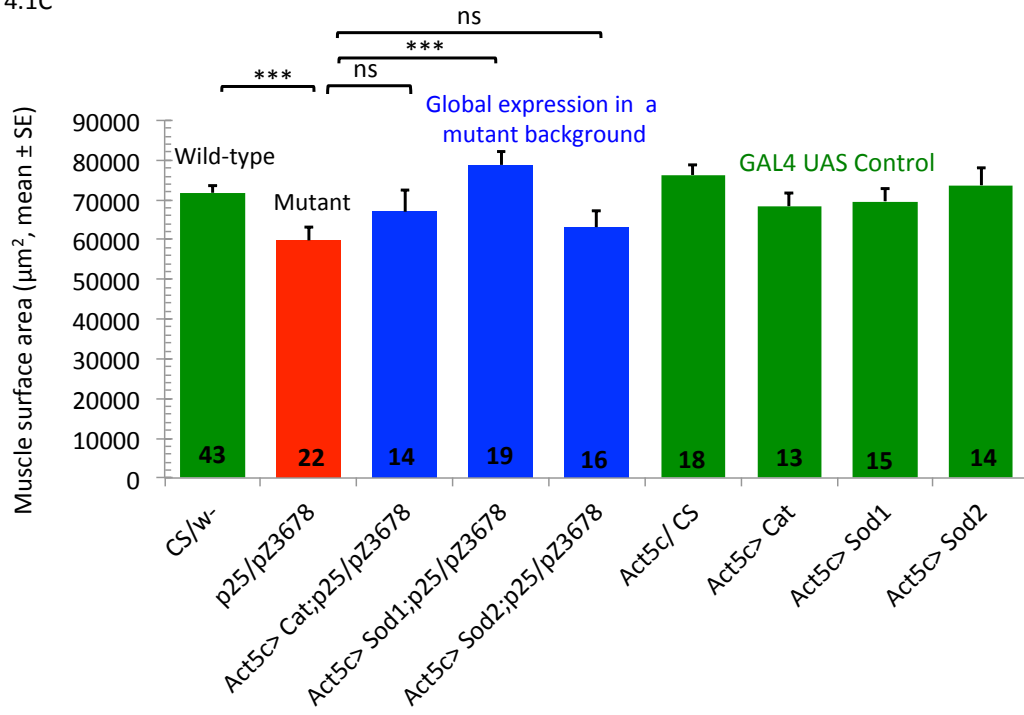


Figure 4.1 Cytosolic ROS scavenger, *Sod1*, rescues overgrowth in *dparkin* larvae.

A-C Global expression of Superoxide Dismutase 1 (*Sod1*) in a *dparkin* (p^{25}/p^{Z3678}) transheterozygote mutant background shows a 22% reduction in overgrowth from normalized bouton counts (**A**, $p = 0.016$), whereas Catalase (*Cat*) (**A**, $p = 0.239$) and Superoxide Dismutase 2 (*Sod2*) (**A**, $p = 0.084$) did not show an effect, when compared to mutant controls. Global expression of *Sod1*, *Sod2* or *Cat* all failed to affect raw bouton number (**B**, $p = 0.742$, $p = 0.538$ and $p = 0.970$ respectively), whereas the muscle surface area was only by 31% increased by *Sod1* (**C**, $p = 0.001$) and not by either *Sod2* or *Cat* (**C**, $p = 0.998$ and $p = 0.853$ respectively). As reported in chapter 3, there is an overgrowth of 60% in *dparkin* (p^{25}/p^{Z3678}) larval neuromuscular junctions (**A**, **B** and **C**, $p = 0.001$) compared to wild-type (*CS/w⁻*) larvae. There are no differences in NMJ growth (normalized bouton count, raw bouton number or muscle surface area) between the GAL4/UAS control (*Act5c/CS*, *Act5c > Sod1*, *Act5c > Sod1* and *Act5c > Cat*) and wild-type (*CS/w⁻*) larvae.

ROS scavengers fail to rescue RMP

To further investigate the involvement of oxidative stress as a mechanism involved in other mutant phenotypes, we globally expressed *Sod1*, *Sod2* or *Cat* in a *dparkin* (p^{25}/p^{Z3678}) transheterozygote mutant background and measured the RMP and found no differences in RMP compared to *dparkin* (p^{25}/p^{Z3678}) larvae. *dparkin* (p^{25}/p^{Z3678}) larvae show 13% more positive (depolarized) RMP compared to wild-type (CS/w^+) larvae ($p < 0.001$). There are no differences between any of the controls (*Act5c/CS*, *Act5c > Sod1*, *Act5c > Sod1* and *Act5c > Cat*) RMP compared to wild-type (CS/w^+) larvae (**Fig. 4.2**).

4.2

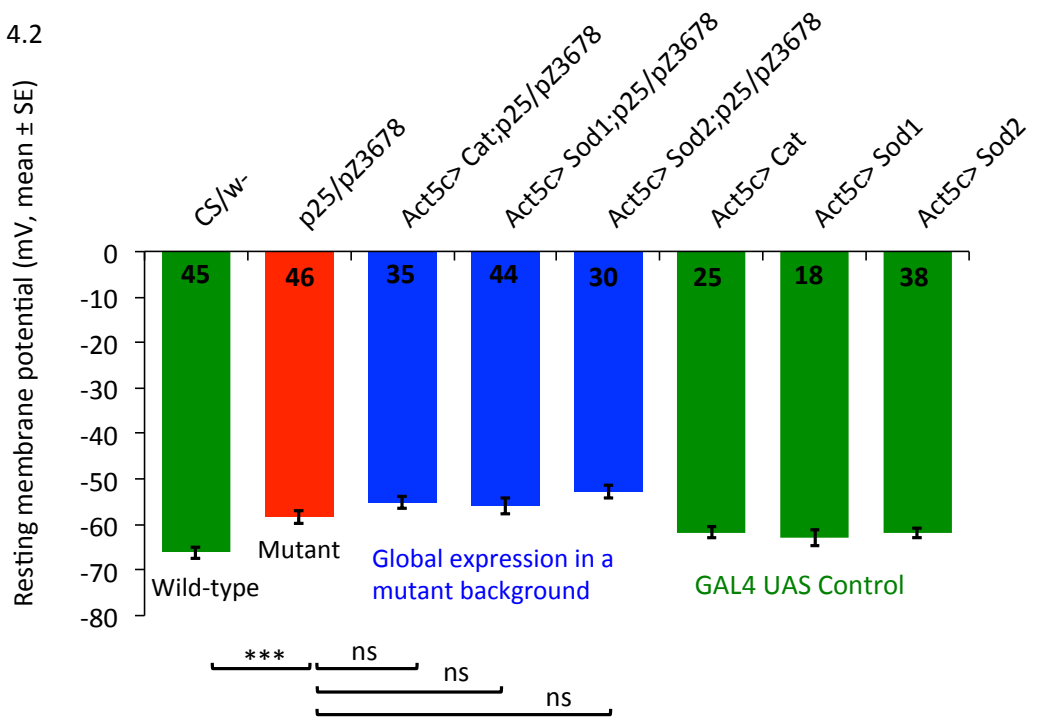


Figure 4.2 ROS scavengers fail to rescue RMP defect in *dparkin* larvae.

Global expression of ROS scavengers (*Sod1*, *Sod2* or *Cat*) in a *dparkin* (p^{25}/p^{Z3678}) transheterozygote mutant background showed no difference in RMP ($p = 0.923$, $p = 0.123$ and $p = 0.752$ respectively) compared to mutant (p^{25}/p^{Z3678}) larvae. As previously reported in chapter 3, *dparkin* (p^{25}/p^{Z3678}) larvae show 13% more positive (depolarized) RMP compared to wild-type (*CS/w⁺*) larvae ($p < 0.001$). There are no differences between any of the GAL4/UAS control (*Act5c/CS*, *Act5c > Sod1*, *Act5c > Sod1* and *Act5c > Cat*) RMP compared to wild-type (*CS/w⁺*) larvae ($p = 0.902$, $p = 0.913$, $p = 0.319$ and $p = 0.482$, respectively).

***AMPK* activation fail to rescue locomotory dysfunction**

When ATP is consumed there is a rise in AMP levels. This change requires activation of ATP synthesis, and a key mediator of the response is AMPK. *dparkin* (p^{25}/p^{Z3678}) larvae show reduced ATP levels (Vincent et al., 2012). To determine whether *AMPK* activation mechanism is sufficient to revert the locomotory phenotype, we globally expressed *constitutively active AMPK-a^{T184D}* (*AMPK*) in a *dparkin* (p^{25}/p^{Z3678}) transheterozygote mutant background and found no differences in average velocity compared to *dparkin* (p^{25}/p^{Z3678}) larvae. As previously reported in chapter 3, *dparkin* (p^{25}/p^{Z3678}) larvae have reduced speed compared to wild-type control (*CS/w*) larvae that was not rescued by global expression of *AMPK* in the mutant background (**Fig. 4.3**).

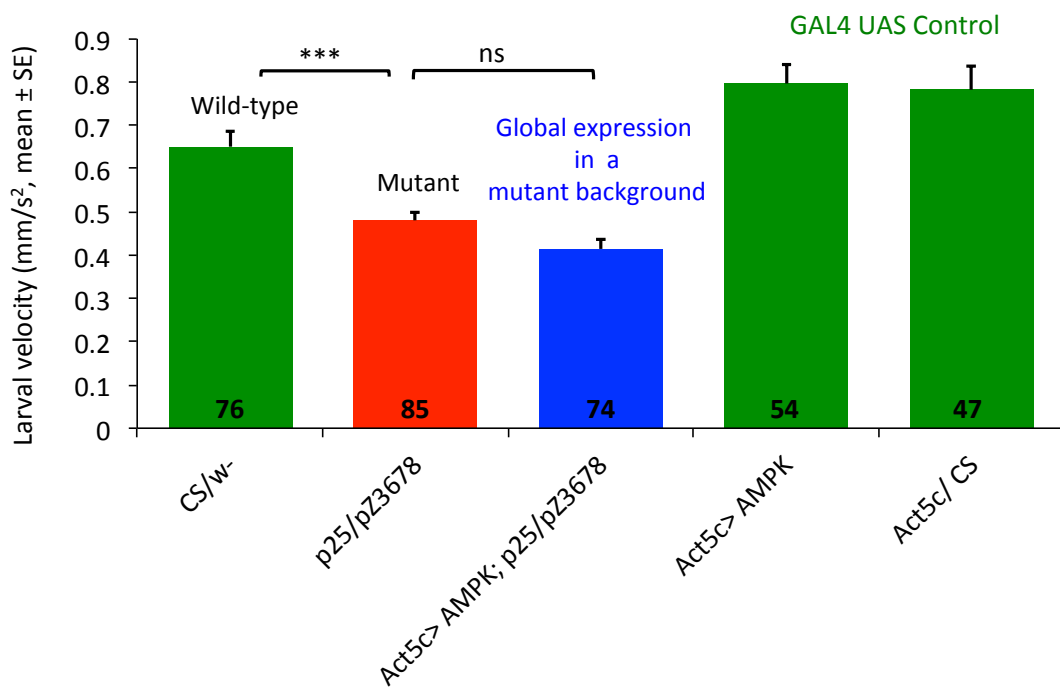


Figure 4.3 Global *AMPK* activation fail to rescue locomotory dysfunction in *dparkin* larvae.

Global expression of constitutively active *AMPK- α^{T184D}* (*AMPK*) in a *dparkin* (p^{25}/p^{Z3678}) transheterozygote mutant background shows no differences in average velocity compared to *dparkin* (p^{25}/p^{Z3678}) larvae ($p = 0.512$). *dparkin* (p^{25}/p^{Z3678}) larvae have 25% reduced speed compared to wild-type control (*CS/w⁻*) larvae ($p < 0.001$) that was not rescued by global expression of *AMPK* in the mutant background ($p = 1.0$).

***AMPK* activation rescues overgrowth**

To determine whether *AMPK* activation independent antioxidant mechanism is sufficient to revert the mutant overgrowth we used the global expression of *constitutively active AMPK- α^{T184D}* (*AMPK*) in a *dparkin* (p^{25}/p^{Z3678}) transheterozygote mutant background shows a 32% reduction in overgrowth from normalized bouton counts compared to mutant controls ($p < 0.001$). As reported in chapter 3, there is an overgrowth at the *dparkin* (p^{25}/p^{Z3678}) larval NMJ ($p > 0.001$) compared to wild-type (*CS/w⁻*) larvae. There are no differences between the GAL4 control NMJ normalized growth, compared to wild-type (*CS/w⁻*) larvae (**Fig. 4.4**).

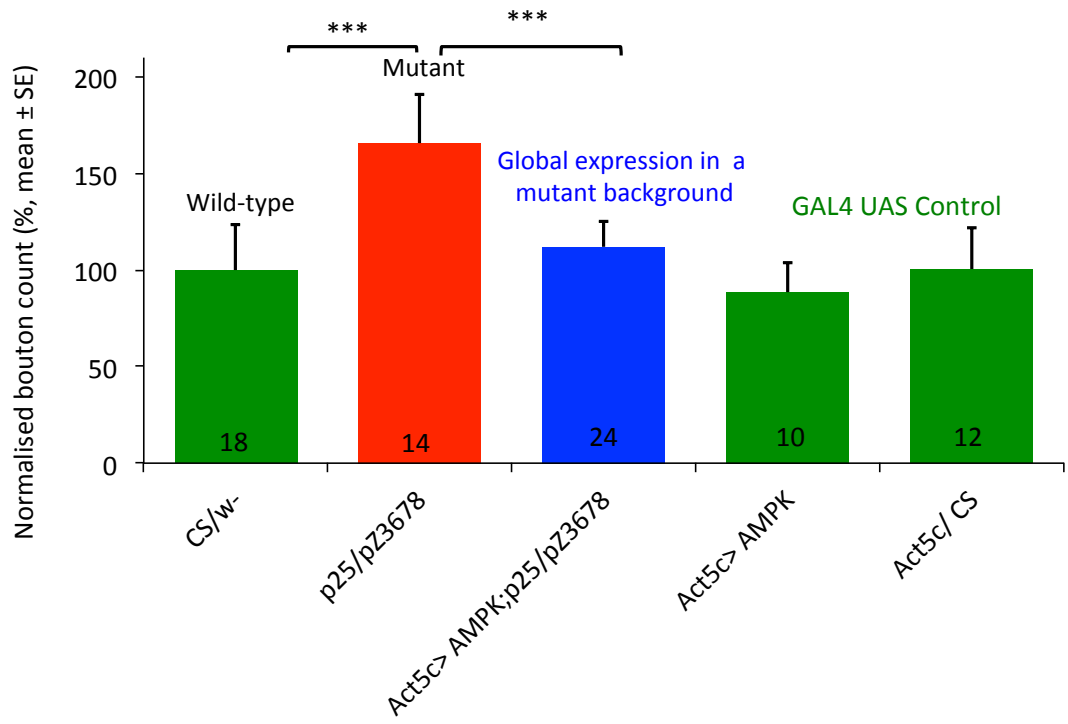


Figure 4.4 Global expression of *AMPK* rescues neuronal overgrowth in *dparkin* larvae.

Global expression of *constitutively active AMPK- α^{T184D}* (*AMPK*) in a *dparkin* (p^{25}/p^{Z3678}) transheterozygote mutant background shows a 32% reduction in overgrowth from normalized bouton counts compared to mutant controls ($p < 0.001$). There is a 60% overgrowth in *dparkin* (p^{25}/p^{Z3678}) larval neuromuscular junctions ($p > 0.001$) compared to wild-type (CS/w^+) larvae. There are no differences between the GAL4 controls (*Act5c* > *AMPK*, *Act5c/CS*) and wild-type (CS/w^+) larvae ($p = 1.0$).

AMPK activation rescues RMP defect

Global expression of *constitutively active AMPK- α^{T184D}* (AMPK) in a *dparkin* (p^{25}/p^{Z3678}) transheterozygote mutant background shows a 7% more negative RMP ($p = 0.012$) compared to the *dparkin* (p^{25}/p^{Z3678}) larvae. The mean difference is 4mV. As previously reported in chapter 3, *dparkin* (p^{25}/p^{Z3678}) larvae again show a more positive (depolarized) RMP compared to wild-type (CS/w^+) larvae ($p < 0.001$). There are no differences between the GAL4 or UAS controls (*Act5c/CS* and *AMPK/CS*) RMP or the rescue compared to wild-type (CS/w^+) larvae ($p = 0.908$ and $p = 0.911$ respectively). The GAL4 control also has a 30% more negative RMP compared to *dparkin* (p^{25}/p^{Z3678}) larvae ($p < 0.001$). There is no difference in RMP between the UAS control and wild-type (CS/w^+) muscles (**Fig. 4.5**).

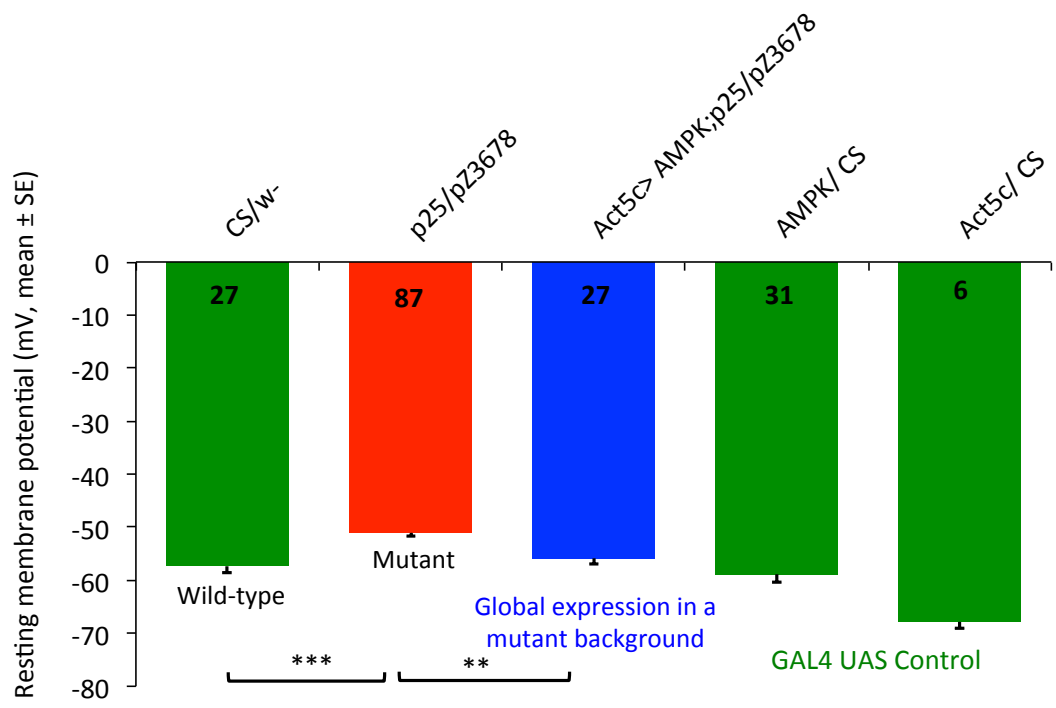


Figure 4.5 Global *AMPK* activation rescues RMP defect in *dparkin* larvae.

Global expression of constitutively active *AMPK- α^{T184D}* (*AMPK*) in a *parkin* (p^{25}/p^{Z3678}) transheterozygote mutant background shows a 7% more negative RMP ($p = 0.012$) compared to the *dparkin* (p^{25}/p^{Z3678}) larvae. *dparkin* (p^{25}/p^{Z3678}) larvae show more positive (depolarized) RMP compared to wild-type (*CS/w⁻*) larvae ($p < 0.001$). There are no differences between the UAS control (*Act5c/CS* and *AMPK/CS*) RMP or the rescue compared to wild-type (*CS/w⁻*) larvae ($p = 0.908$ and $p = 0.911$ respectively). The GAL4 control is different compared to *dparkin* (p^{25}/p^{Z3678}) larvae ($p < 0.001$).

***GST*, and not *TRX-R2*, expression rescues locomotory dysfunction**

Global expression of *GST* expression in a *dparkin* (p^{25}/p^{Z3678}) transheterozygote mutant background shows a 28% increase in the average velocity ($p = 0.001$), whereas global *TRX-R2* expression in the mutant background did not show any differences in velocity compared to *dparkin* (p^{25}/p^{Z3678}) larvae. As previously reported in chapter 3, *dparkin* (p^{25}/p^{Z3678}) larvae have reduced speed compared to wild-type control (*CS/w*) larvae ($p < 0.001$). There are no differences between the GAL4/UAS control speeds compared to wild-type (*CS/w*) larvae for Act5c > *GST* or Act5c > *TRX-R2* (Fig 4.6).

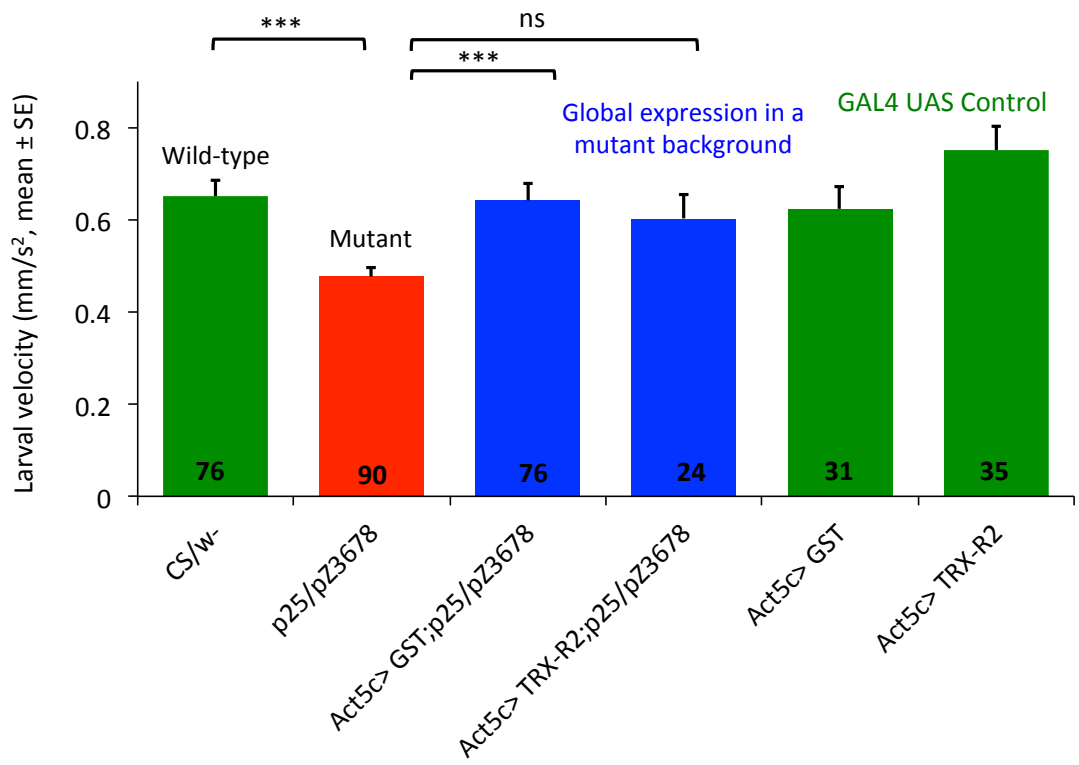


Figure 4.6 Global *GST*, and not *TRX-R2*, expression rescues locomotory dysfunction in *dparkin* larvae.

Global expression of *GST* expression in a *dparkin* (p^{25}/p^{Z3678}) transheterozygote mutant background shows a 28% increase in the average velocity, whereas global *TRX-R2* expression in the mutant background did not show any differences in velocity compared to *dparkin* (p^{25}/p^{Z3678}) larvae ($p = 0.001$ and $p = 0.329$, respectively). *dparkin* (p^{25}/p^{Z3678}) larvae have a reduced speed compared to wild-type control (*CS/w*) larvae ($p < 0.001$). There are no differences between the GAL4 UAS control (*Act5c* > *GST* or *Act5c* > *TRX-R2*) speeds compared to wild-type (*CS/w*) larvae ($p = 0.995$ and $p = 0.469$ respectively).

***GST* or *TRX-R2* expression rescues RMP defect in *parkin* larvae**

Global expression of either *GST* or *TRX-R2* in a *dparkin* (p^{25}/p^{Z3678}) transheterozygote mutant background shows a 20 % and 29% more negative RMP ($p = 0.001$ and $p < 0.001$ respectively) compared to mutant (p^{25}/p^{Z3678}) larvae. As previously reported in chapter 3, *dparkin* (p^{25}/p^{Z3678}) larvae show more positive (depolarized) RMP compared to wild-type (*CS/w*) larvae ($p < 0.001$). There are no differences between the GAL4/UAS control RMP, Act5c > *GST* or Act5c > *TRX-R2* compared to wild-type (*CS/w*) larvae (**Fig. 4.7**).

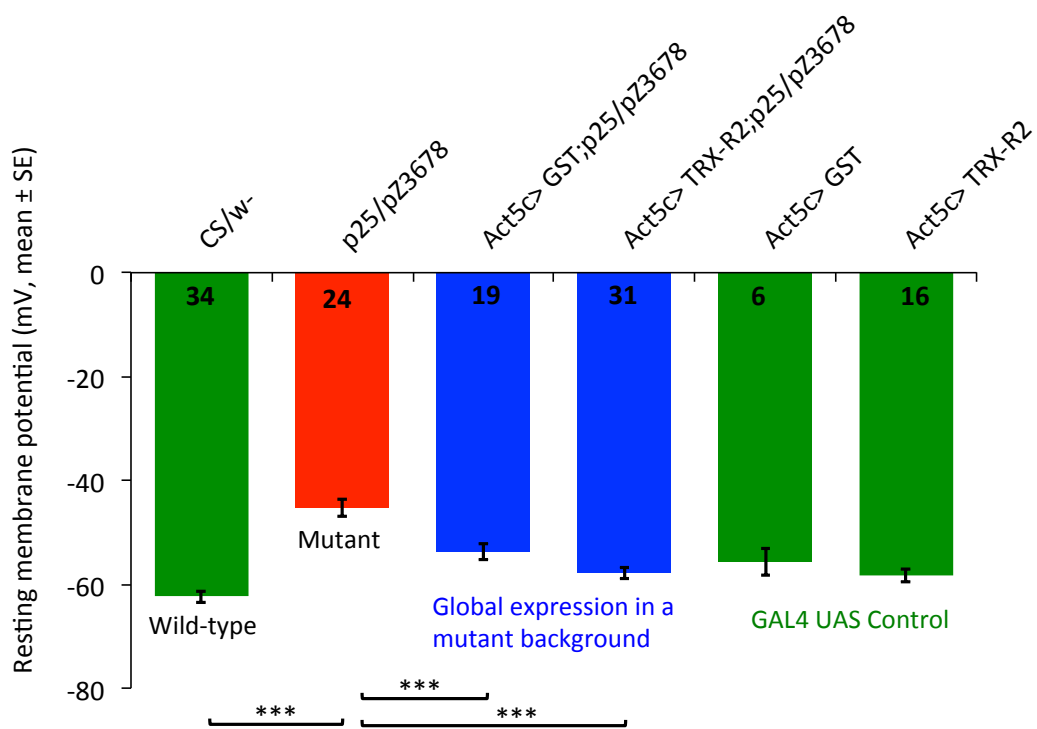


Figure 4.7 Global *GST* or *TRX-R2* expression rescues RMP defect in *dparkin* larvae.

Global expression of either *GST* or *TRX-R2* in a *dparkin* (p^{25}/p^{Z3678}) transheterozygote mutant background shows a 20% and 29% more negative RMP ($p = 0.001$ and $p < 0.001$ respectively) compared to mutant (p^{25}/p^{Z3678}) larvae. As previously reported in chapter 3, *dparkin* (p^{25}/p^{Z3678}) larvae show more positive (depolarized) RMP compared to wild-type (*CS/w*) larvae ($p < 0.001$). There are no differences between the GAL4 UAS control (*Act5c* > *GST* or *Act5c* > *TRX-R2*) RMP compared to wild-type (*CS/w*) larvae ($p = 0.191$ and $p = 0.396$, respectively).

***BSK^{DN}*, not *JUN^{DN}*, expression rescues locomotory dysfunction in *parkin* larvae**

Global expression of *BSK^{DN}* expression in a *dparkin* (*p²⁵/p^{Z3678}*) transheterozygote mutant background shows a 20 % increase in the average velocity ($p = 0.018$), whereas global *JUN^{DN}* expression in the mutant background did not show any differences in velocity compared to *dparkin* (*p²⁵/p^{Z3678}*) larvae (**Fig. 4.8**).

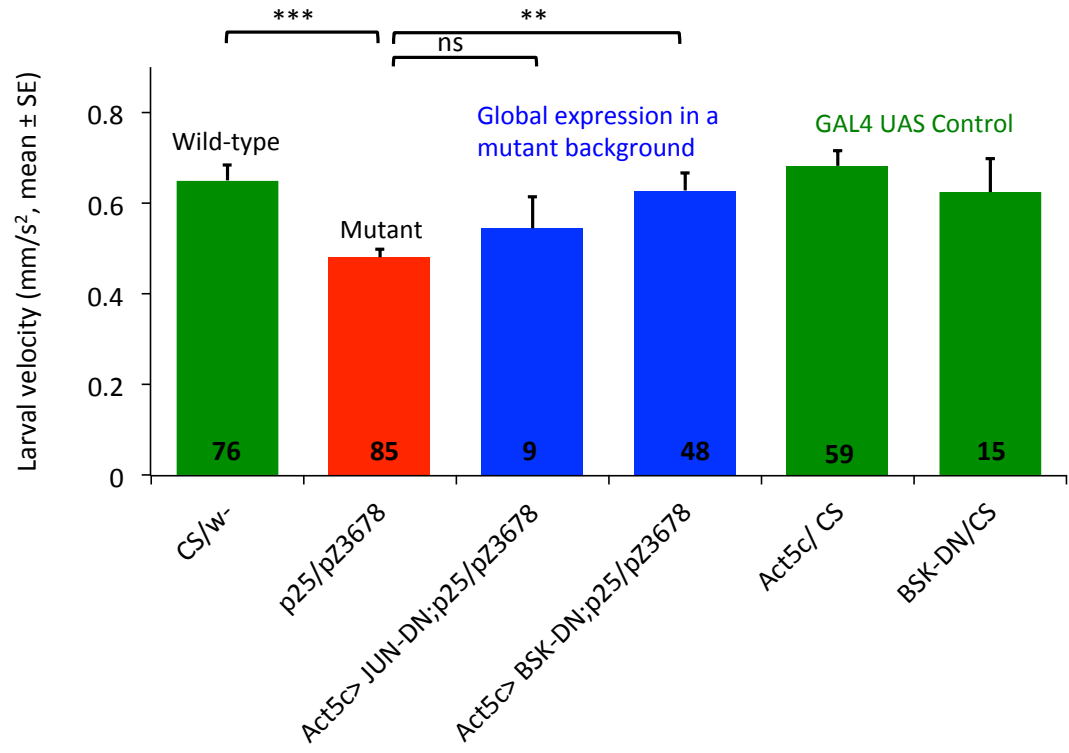


Figure 4.8 Global BSK^{DN} , not JUN^{DN} , expression rescues locomotory dysfunction in *dparkin* larvae.

Global expression of BSK^{DN} expression in a *dparkin* (p^{25}/p^{Z3678}) transheterozygote mutant background shows a 20% increase in the average velocity ($p = 0.018$), whereas global JUN^{DN} expression in the mutant background did not show any differences in velocity ($p = 0.472$) compared to *dparkin* (p^{25}/p^{Z3678}) larvae. As previously reported in chapter 3, *parkin* (p^{25}/p^{Z3678}) larvae have reduced speed compared to wild-type control (CS/w^+) larvae ($p < 0.001$).

***JUN^{DN}* expression rescues overgrowth**

Global expression of *JUN^{DN}* in a *dparkin* (*p²⁵/p^{Z3678}*) transheterozygote mutant background shows a 54% reduction in overgrowth from normalized bouton counts compared to mutant controls ($p < 0.001$). As reported in chapter 3, there is an overgrowth in *dparkin* (*p²⁵/p^{Z3678}*) larval neuromuscular junctions ($p > 0.001$) compared to wild-type (*CS/w⁺*) larvae. There are no differences between the GAL4 control or the *JUN^{DN}* rescue, NMJ normalized growth, compared to wild-type (*CS/w⁺*) larvae (**Fig. 4.9**).

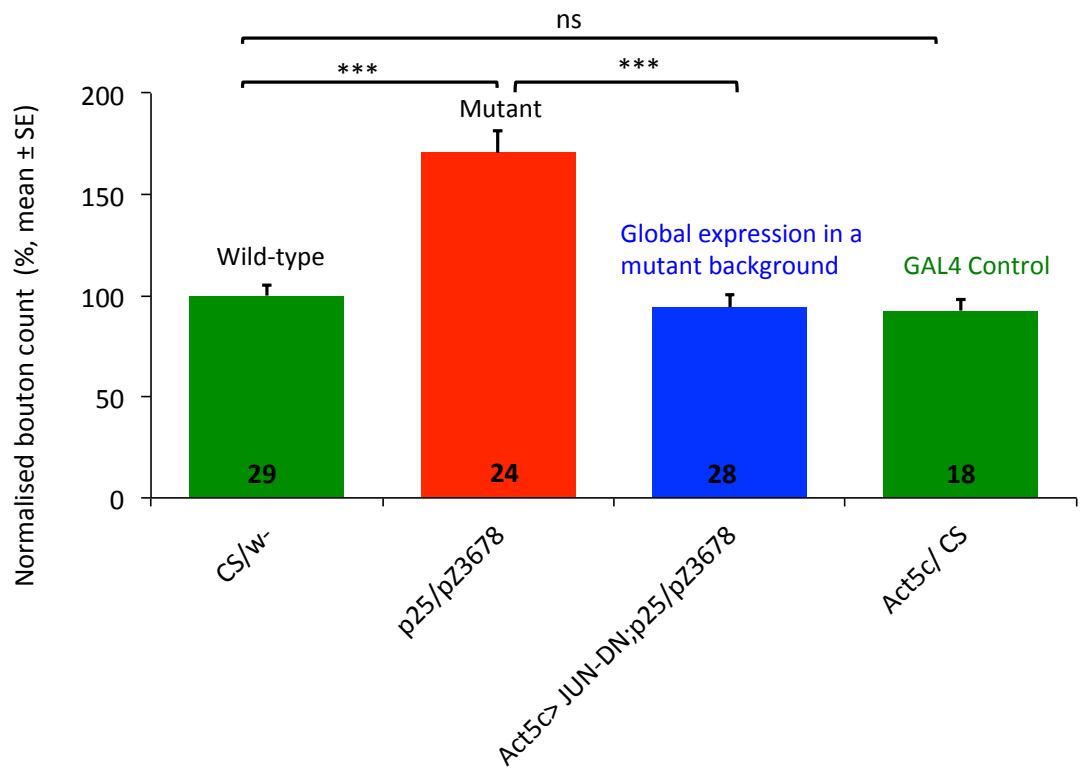


Figure 4.9 Global JUN^{DN} expression rescues overgrowth in *dparkin* larvae.

Global expression of JUN^{DN} in a *dparkin* (p^{25}/p^{Z3678}) transheterozygote mutant background shows a 54% reduction in overgrowth from normalized bouton counts compared to mutant controls ($p < 0.001$). As reported in chapter 3, there is an overgrowth in *dparkin* (p^{25}/p^{Z3678}) larval neuromuscular junctions ($p > 0.001$) compared to wild-type (CS/w^+) larvae. There are no differences between the GAL4 control (*Act5c/CS*, $p = 0.896$) NMJ normalized growth, compared to wild-type (CS/w^+) larvae.

***JUN^{DN}* and *BSK^{DN}* expression rescues RMP defect**

Global expression of or either *JUN^{DN}* or *BSK^{DN}* in a *dparkin* (*p²⁵/p^{Z3678}*) transheterozygote mutant background shows a (%) more negative RMP ($p < 0.001$ and $p < 0.001$ respectively) compared to mutant (*p²⁵/p^{Z3678}*) larvae. As previously reported in chapter 3, *dparkin* (*p²⁵/p^{Z3678}*) larvae show more positive (depolarized) RMP compared to wild-type (*CS/w⁻*) larvae ($p < 0.001$). There are no differences between the GAL4 control RMP or either of the rescues (*JUN^{DN}* or *BSK^{DN}*) compared to wild-type (*CS/w⁻*) larvae (**Fig. 4.10**).

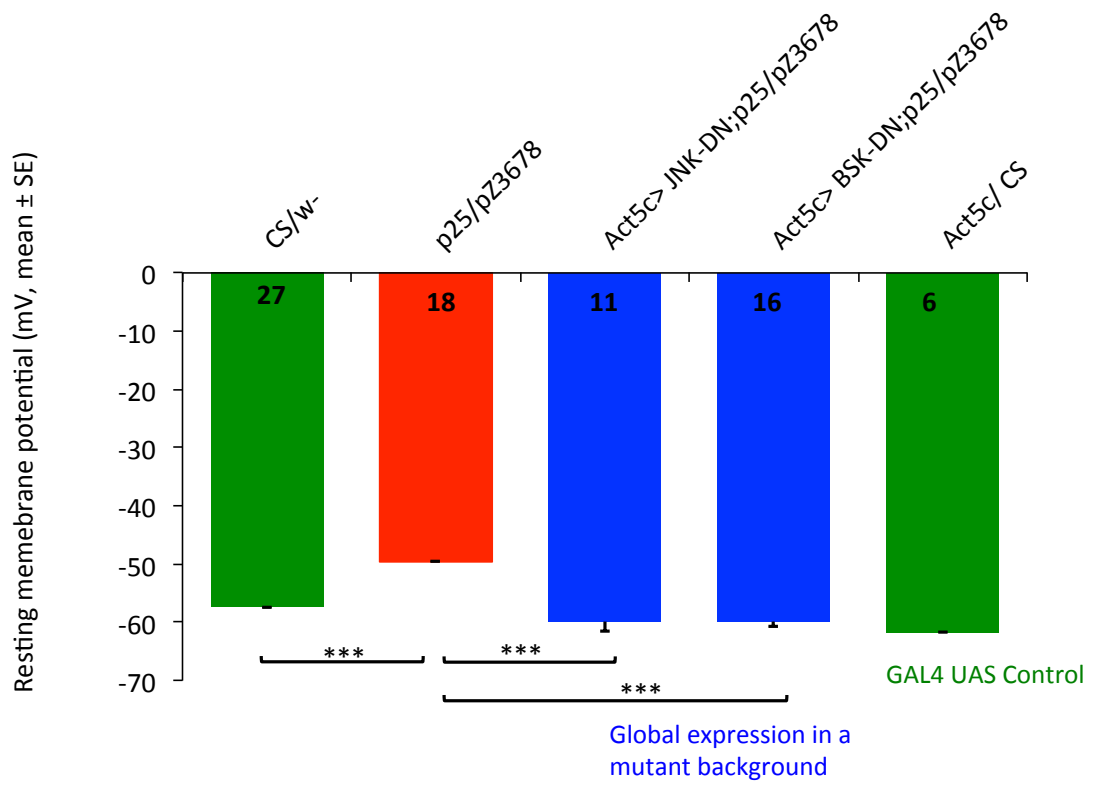


Figure 4.10 Global JUN^{DN} and BSK^{DN} expression rescues RMP defect in *dparkin* larvae.

Global expression of or either JUN^{DN} or BSK^{DN} in a *dparkin* (p^{25}/p^{Z3678}) transheterozygote mutant background shows a more negative RMP ($p < 0.001$ and $p < 0.001$ respectively) compared to mutant (p^{25}/p^{Z3678}) larvae. As previously reported in chapter 3, *dparkin* (p^{25}/p^{Z3678}) larvae show more positive (depolarized) RMP compared to wild-type (CS/w^+) larvae ($p < 0.001$). There are no differences between the RMP of the wild-type (CS/w^+) larvae, the GAL4 control ($Act5c/CS$, $p = 0.413$) and the rescues (JUN^{DN} or BSK^{DN} , $p = 0.701$ and $p = 0.629$ respectively).

4.4 Discussion

Globally expressing the ROS scavengers *Sod1*, *Sod2* or *Cat* fails to rescue RMP. Ubiquitous expression of *Sod1* partially rescues overgrowth, whereas expression of *Sod2* or *Cat* fails to show a significant rescue. *GST* rescued both RMP and locomotion whereas *TRX-R2* only rescued RMP. Inhibiting *D. melanogaster* *JNK* globally via *BSK^{DN}* rescues RMP and locomotion. On the other hand, inhibiting *JUN* via *JUN^{DN}* globally rescues only overgrowth and RMP but fails to rescue locomotion. Expressing the *AMPK* catalytically active subunit globally, rescues overgrowth and RMP but fails to rescue locomotion.

***Sod1* expression rescued overgrowth but failed to rescue RMP in *dparkin* larvae.**

Of the ROS scavengers tested, only the expression of *Sod1* rescued the synaptic overgrowth seen in the *dparkin* knockout. The synaptic growth depends on both the number of boutons and the muscle surface area. The expression of *Sod1* showed rescue of the overgrowth through the increase in muscle surface area, but not by changes in the raw bouton count. The differences in rescue between *Sod1* and the other two ROS scavengers (*Cat* and *Sod2*) might be explained by differences in their location: *SOD1* is predominantly cytoplasmic with some expression in the inner mitochondrial membrane while *Sod2* is expressed in the mitochondrial matrix and *Cat*, located in the peroxysomes in the cytoplasm. Another, less likely explanation is the difference in function: both forms of *Sod* aid the break down of superoxide radicals to oxygen and hydrogen peroxide, while *Cat* accelerates the breakdown of hydrogen peroxide, into water and oxygen.

An increase in *Sod* levels alone might increase the hydrogen peroxide levels in the cell. This might lead to a problem if the physiological levels of *Cat* are insufficient to keep

up with the levels of hydrogen peroxide. Mitochondrial hydrogen peroxide levels seem to exceed that of antioxidant defence. The right balance of antioxidants to break hydrogen peroxide down to maintain physiological levels of reactive oxygen species (ROS) are absent in *dparkin* larvae (Whitworth et al., 2005, Vincent et al., 2012). This suggests there is increase sensitivity to mitochondrial insult with hydrogen peroxide compared to the cytosolic insult in *dparkin* mutant. A dual expression of *Sod* and *Cat* together on the other hand could generate better rescues of other phenotypes. Expression of both *Sod1* and *Cat* together has been shown to increase lifespan of *D. melanogaster* (Orr and Sohal, 1994). However, another study did not find a significant increase in lifespan in *D. melanogaster* (Sun et al., 2004). Globally expressing either *Cat*, *Sod1* or *Sod2* was shown to rescue the synaptic overgrowth in a *dparkin* null background (Vincent et al., 2012), but in my data from the transheterozygote background, there was no change with locomotion and RMP in *dparkin* larvae.

Thioredoxin reductase, *TRX-R2*, expression rescues RMP but fails to rescue locomotion in *dparkin* larvae

The electrophysiological readout, the RMP of muscle, was rescued in the *dparkin* larvae with the global expression of *TRX-R2*. The *Act5c*-GAL4 transgene in a wild-type (*CS*) background showed no significant difference in RMP compared to wild-type controls (*CS/w*).

Adult flies expressing wild-type thioredoxin in a *dparkin* toxicity-induced model had increased locomotor activity and no degeneration of dopaminergic neurons compared to aged matched controls. Additionally, it was found that neuronal function and anatomy were restored as a result of thioredoxin's chaperone activity rather than its antioxidant function (Umeda-Kameyama et al., 2007). The global expression of *thioredoxin reductase (TRX-R2)* in *dparkin* larvae, failed to rescue the locomotion. This could be as

a result of different GAL4 transgenes used to drive expression (*elav* as opposed to the *Act5c* used here) and/or due to different mutant backgrounds. The tissues in which the transgene is expressed may have different degree of impact on larval locomotion (CNS v global).

Glutathione-S-transferase, *GST*, expression rescues both RMP and locomotion

Glutathione-S-transferases participate in the detoxification process and have been shown to prevent dopaminergic neuronal loss in *dparkin* mutants in a range of models of PD (Whitworth et al., 2005, Trinh et al., 2008, Kim et al., 2012). *GST* ameliorates viability, locomotory deficits and dopaminergic cell death in *dparkin* adults. The expression of *GST* in muscle partially rescues climbing defects, and the expression in dopaminergic neurons prevents the death of these neurons in *dparkin* adults (Whitworth et al., 2005). In *dparkin* larvae the global expression of *GST* rescues locomotion close to wild-type speed, whereas *dparkin* adults shows only partial rescue of the climbing defect. The differences in the level of behavioral rescue could arise from the different GAL4 drivers used. The adult study used a muscle specific driver: the reasoning being that the deficit seemed to be in the muscle, *GST* would be best expressed in adult flight muscle. However, some expression was seen in the adult head (Clayton et al., 1998). In our study, we used a global GAL4 driver that provided a complete rescue of the behavioral phenotype possibly due to both muscle and neuronal effects of *GST* expression. Future studies following this may test for neuronal expression of *GST* in *dparkin* larvae to dissect the importance for a more complete rescue of behavior.

The same effective rescue is seen in the RMP data. The RMP was also rescued with global expression of *GST* suggesting the importance of *GST* expression in *dparkin* larvae to ameliorate muscle phenotype close to wild-type RMP voltage. These results show neuronal and muscle phenotypes of *dparkin* larvae are rescued with varying

degrees. It would be interesting to observe how neuronal versus muscle expression of *GST* impacts the rescue levels of *dparkin* larval phenotypes. The expression levels may be quantified by Western Blots of larval brain versus the muscle with the *GST* expression using the neuronal and global GAL4 drivers.

***JUN-DN* expression rescued overgrowth and RMP but failed to rescue locomotion whereas *BSK-DN* expression rescued RMP and locomotion.**

Similar to the *GST* and *TRX-R2*, *c-jun* dominant negative (*JUN^{DN}*) globally expressed rescued overgrowth and RMP, unlike *Cat* or either of the *Sods*. On the other hand, *D. melanogaster JNK*, basket dominant negative (*BSK^{DN}*) rescues RMP and locomotion. *JNK* signaling has been shown to be up-regulated in dopaminergic neurons of *dparkin* mutants (Cha et al., 2005). *dparkin* has been shown to suppress *JNK* signaling by reducing *BSK* transcription (Hwang et al., 2010). Inhibiting *BSK^{DN}*, globally rescues overgrowth, RMP and locomotion. On the other hand, inhibiting *JUN-DN* globally rescues only overgrowth and RMP but fails to rescue locomotion. *dparkin* has been shown to be a repressor of *JNK* signalling via *BSK* and our *dparkin* loss of function mutants show rescue of oxidative stress, neurophysiological and behavioural phenotypes with inhibition of basket function. This suggests *JNK* signalling is activated in *dparkin* larvae, like in adult dopaminergic neurons in *dparkin* flies (Cha et al., 2005). It is likely that *dparkin* has a role in inhibiting *BSK* and thus inhibiting downstream phosphorylation targets such as the transcription factor *c-jun*, *GST* and *TRX-R2*, are detoxification genes also shown to be involved in oxidative stress mediated signaling via inhibition of *JNK* or *ASK-1* respectively. *GST* or *BSK^{DN}* when globally expressed rescued both locomotion, unlike *Cat* or either of the *Sods* or *AMPK*. Data suggests that inhibiting *JNK* activity (*BSK^{DN}*) may likely attenuate *JNK*-associated apoptosis-induced degeneration in *dparkin* mutants.

***AMPK* expression rescues overgrowth and RMP but fails to rescue locomotion in *dparkin* larvae**

Genetic activation of *AMPK* by expressing constitutively active *AMPK* in dopaminergic neurons and in muscles of *dparkin* flies rescued abnormal upright wing posture, climbing and mitochondrial pathology seen in adults (Ng et al., 2012). Unlike in the adults, global expression of *AMPK* in *dparkin* larvae fails to rescue the locomotion phenotype. Similar to the rescue of mitochondrial phenotype in adults, in *dparkin* larvae upregulating *AMPK* rescues the muscle RMP phenotype by restoring a more negative voltage (nearly to the wild-type RMP level). This suggests there is an increase in the availability of ATP and so a reduction in energetic stress. Additionally, synaptic overgrowth was also rescued in *dparkin* larvae by increased *AMPK* activity, possibly through its action on the suppression of oxidative stress or on autophagy. The overgrowth rescues could be explained as a result of mitophagy induction, as *AMPK* is known to phosphorylate *ATG1* (Hardie, 2011), leading to activation of the processes that remove damaged mitochondria from the cell. This alleviates the oxidative stress burden caused from damaged mitochondria.

Finally, it should be noted that *AMPK* has been found to interact with both *dparkin*- and *dLRRK2*-related models of Parkinsonism, thus implicating these three genes in a common pathway in PD pathogenesis (Ng et al., 2012).

Summary of key findings:

- * The neurophysiological and locomotory defects results from the metabolic dysfunction rather than oxidative stress in *dparkin* larvae.
- * The *AMPK*-related regulatory effects of metabolic homeostasis are important for restoring muscle-associated deficits (opposed to neuronal) in *dparkin* larvae.

- * Oxidative stress is a downstream consequence of metabolic dysfunction.

- * Oxidative stress-induced signaling plays a role in *dparkin* larval phenotypes. Targeting *JNK* signaling components or *JNK*-interacting (detoxification) enzymes alleviate both neuronal and muscle-related *dparkin* larval phenotype.

Chapter 5: Pharmacological manipulation of dopaminergic signalling and AMPK activity

5.1 Introduction

In chapter 3, I demonstrated that the *dparkin* larvae showed reduced locomotion, defects in neural signalling and overgrowth. This raised the question of whether these phenotypes could be rescued pharmacologically.

5.1.1 Role of dopamine

Dopamine is a biogenic amine. In *D. melanogaster*, dopamine plays a role in insect neural networks controlling locomotor activity and stereotypical behaviors (Yellman et al., 1997, Friggi-Grelin et al., 2003, Lima and Miesenböck, 2005). As noted earlier in the Introduction (Chapter 1) the main therapy for PD patients is L-DOPA. Administering L-DOPA to adult *dparkin* flies resulted in partial restoration of impaired locomotion suggesting reduced dopamine levels in their brain is partially responsible for their locomotory dysfunction (Cha et al., 2005). To address whether the crawling defect is a result of reduced dopamine signaling, L-DOPA, and a control D-DOPA, was used to replace lost dopamine signaling in the brain to potentially rescue the crawling defects observed in our *dparkin* mutant larvae.

5.2 Role of AMPK in the manipulation of ATP synthesis

As described in chapter 3 *parkin* larvae show depolarized resting membrane potential (RMP), defects in synaptic transmission and reduced crawling. This suggested a metabolic deficit. Since the RMP is highly dependent on ATP production due to the requirements of the sodium potassium-ATPase (Na^+/K^+ -ATPase) to maintain the electrochemical gradients of Na^+ and K^+ ions that are necessary for normal resting potentials and ion flow across the membrane (Attwell and Laughlin, 2001, Niven and Laughlin, 2008, Howarth et al., 2012), the metabolism of the p^{25}/p^{25} larvae was

examined. These had reduced oxygen consumption, higher sensitivity to metabolic poisons, low ATP levels and increased lactate (Vincent et al., 2012). This suggested a switch from aerobic respiration to glycolysis to keep up with the ATP demand (Vincent et al., 2012). Additionally, *dparkin* larvae exhibit oxidative stress induced overgrowth possibly as a result of increased energy demands (as previously described in chapter 3 and Vincent et al., (2012)).

AMP-activated protein kinase (*AMPK*) is a metabolic sensor of intracellular energy metabolism, acting through a combination of homeostatic mechanisms including autophagy and protein degradation at the cellular, organ and whole body level (Steinberg and Kemp, 2009). The background to this enzyme has been introduced in Chapter 4.

5-aminoimidazole-4-carboxamide ribonucleoside (AICAR) is a pharmacological activator of 5'-AMP-activated protein kinase (*AMPK*). In the cell, AICAR is metabolized to AICAR monophosphate (ZMP) (Sabina et al., 1985), which mimics the effects of AMP on *AMPK*. This causes its activation while the cellular levels of AMP, ADP and ATP remain unaffected (Corton et al., 1995, Hardie et al., 2003).

A characteristic feature in Type 2 diabetic patients is their diminished activity of 5'-AMP-activated protein kinase (*AMPK*) compared to healthy individuals. Metformin (1,1-dimethylbiguanide), from the family of biguanides, is a potent antihyperglycemic agent commonly used to treat type-2 diabetes (T2D) to at least to 120 million people worldwide (Adler et al., 2009, Nathan et al., 2009). Despite the introduction of metformin clinically in the 1950s the exact mechanism of action has not been fully uncovered. Clinical trials undertaken in recent years have shown extensive benefits of metformin beyond the treatment of T2D, and have highlighted therapeutic value in other

conductions including diabetic nephropathy, cardiovascular diseases, polycystic ovarian syndrome and cancer. This drug acutely decreases hepatic glucose production via mild and transient inhibition of the respiratory chain component, complex 1. As a result of decrease in hepatic energy levels, this causes the activation of *AMPK* (Zhou et al., 2001).

Another way to affect *AMPK* is by using a polyphenol, e.g. resveratrol. Dietary intake of polyphenols is thought to be sufficient to achieve nutritional benefits. At this level, they may activate one or more pathways (Schroeter et al., 2007, Vauzour et al., 2007, Schroeter et al., 2001, Mandel et al., 2008). In neurons, activation of hormetic pathways leads to the synthesis of cytoprotective proteins including neurotrophic factors, protein chaperone, antioxidant and Phase II enzymes and apoptotic proteins (Mattson, 2006, Mattson and Magnus, 2006, Calabrese, 2008). Polyphenols are characterized by their multiple hydroxyl groups on aromatic rings. They are divided into two groups: flavonoid and non-flavonoid, which are determined by the number of phenol rings and the ways in which the rings interact. Resveratrol possesses a 1,2-diarylethenes structure based on the C₆-C₂-C₆ backbone and classed as the main stilbene in the non-flavanoid group (Vauzour, 2012). This polyphenolic compound is a naturally occurring phytochemical present in over 70 plant species including grapes, berries and peanuts (Das and Maulik, 2006).

Resveratrol (3, 4, 5-trihydroxystilbene), rich in red wine, has been suggested in a variety of studies to show positive effects on health including in cancer, aging stress, cardiovascular and in neurological diseases (Howitz et al., 2003, Baur and Sinclair, 2006, Valenzano and Cellerino, 2006, Goswami and Das, 2009).

Resveratrol affects multiple proteins and pathways (Baur et al., 2006, Baur and Sinclair, 2006, Fröjdö et al., 2008, Pacholec et al., 2010, Park et al., 2012). In the nervous system a protective pathway involving the transcription factor NF-E2-related factor-2 (Nrf2) that has been known to be activated. During basal conditions Nrf2 interacts with a cytosolic repressor protein Keap1 (Kelch ECH associating protein) and prevents Nrf2-mediated gene expression. In oxidative stress conditions, Nrf2 is released from Keap1 and then it translocates to the nucleus (Itoh et al., 1999a, Itoh et al., 1999b). Nrf2 is involved in the upregulation of genes implicated in the regulation of the cellular redox status and the protection of the cell from oxidative insult, when it binds to the antioxidant-responsive element (ARE) and it activates ARE-dependent transcription of phase II and antioxidant defense enzymes, for example glutathione-S-transferase (GST), glutathione peroxidase (GPx), and heme oxygenase-1 (HO-1) (Nguyen et al., 2003). Resveratrol was observed to protect H₂O₂-mediated oxidative stress in vitro (Chen et al., 2005) and to attenuate cerebral ischemic injury in rat (Ren et al., 2011) via the activation of Nrf2 and the upregulation of HO-1.

The mechanism by which resveratrol acts is still controversial: Park *et al.* (2012) have recently shown that SIRT1 is indeed activated indirectly by down stream signalling cascade involving cyclic AMP, Epac1 (a cAMP effector protein) and AMPK by resveratrol in a response to phosphodiesterase enzyme inhibition, its direct target (Park et al., 2012).

SIRT1 has many cellular substrates such as the tumor suppressor p53, the transcription factor NF- κ B, the forkhead box class O (FoxO) family of transcription factors, the peroxisome proliferator-activated receptor (PPAR)- γ , the PPAR- γ coactivator 1 α (PGC-1 α), and endothelial nitric oxide synthase (eNOS) (Michan and Sinclair, 2007).

Using pharmacological activation of AMPK directly and indirectly by using AICAR, Metformin or Resveratrol was fed to *dparkin* mutants, as an aim to rescue their metabolic deficits (including ATP deficiency and increase in compensatory anaerobic metabolism, glycolysis) (Vincent et al., 2012) arising from mitochondrial abnormalities in *dparkin* mutant flies. The RMP defects in *dparkin* mutants are suggested to be associated with metabolic deficits in these mutants (Vincent et al., 2012), which are similar to the ATP deficient RMP defects described in an glycolytic mutant *nubian* (Wang et al., 2004).

5.2 Aims

The aim of this chapter is to address whether the crawling, RMP and synaptic overgrowth phenotypes observed in *dparkin* mutant larvae can be relieved pharmacologically. Dopaminergics (L-DOPA and D-DOPA) will be used to observe whether the effects the dopamine induced loss of signaling is the cause of *dparkin* larval bradykinesia-like phenotype.

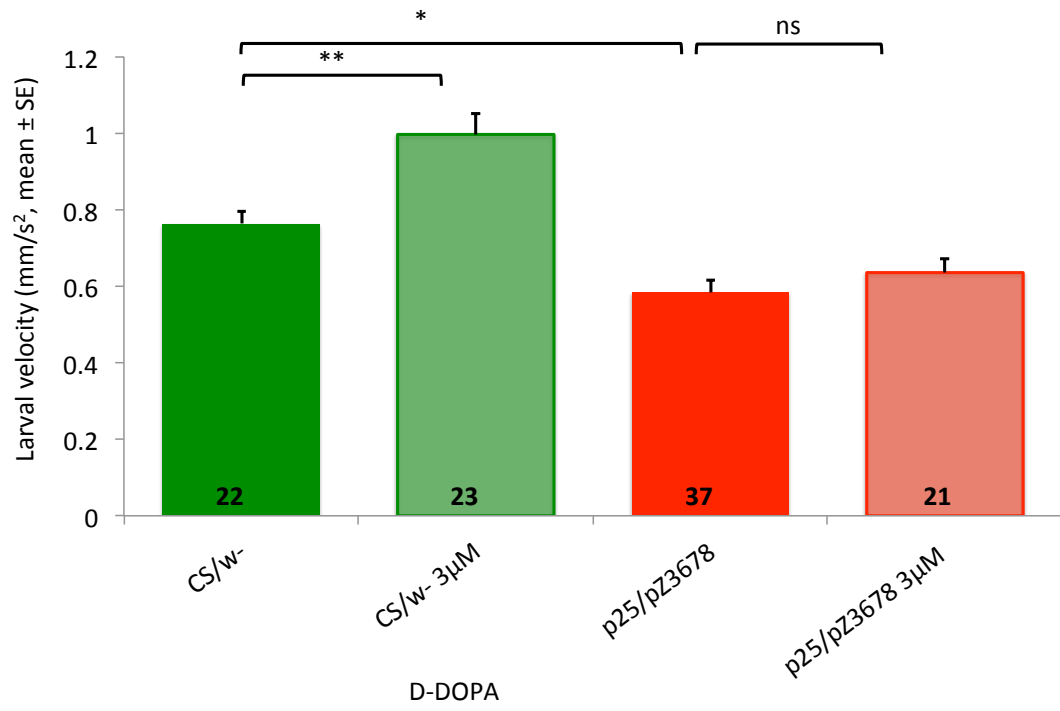
Secondly, to observe the impact on locomotion, RMP and neuronal overgrowth and other phenotypes in *dparkin* larvae with an increase in AMPK activity, I will use pharmacological agents that target AMPK directly (AICAR) or indirectly (Resveratrol and Metformin).

5.3 Results

Dopaminergics fail to rescue crawling defect

To address whether the crawling defect described in chapter 3 in *dparkin* mutants were a result of reduced dopamine signaling, I fed the larvae with either L- or D-DOPA with a final concentration of 3 μ M in food. D-DOPA did not rescue crawling defect in *dparkin* mutant larvae (p^{25}/p^{Z3678}) larvae. D-DOPA increases by 32% the crawling speed of wild-type (*CS/w⁻*) larvae (**A**, $p = 0.004$). (As described before, chapter 3), *dparkin* (p^{25}/p^{Z3678}) larvae crawl with a reduced speed compared to wild-type (*CS/w⁻*) larvae (**A**, $p = 0.009$) (**Fig 5.1A**). 3 μ M L-DOPA has no effect on the crawling velocity of either wild-type larvae (*CS/w⁻*) or the *parkin* larvae (p^{25}/p^{Z3678}) (**Fig 5.1B**).

5.1A



5.1B

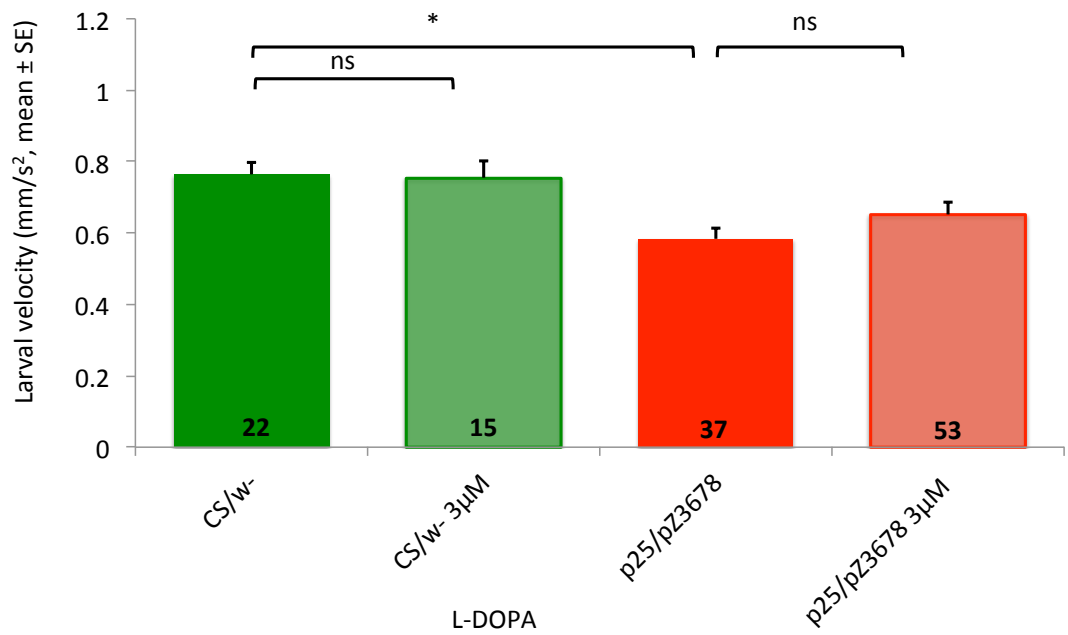


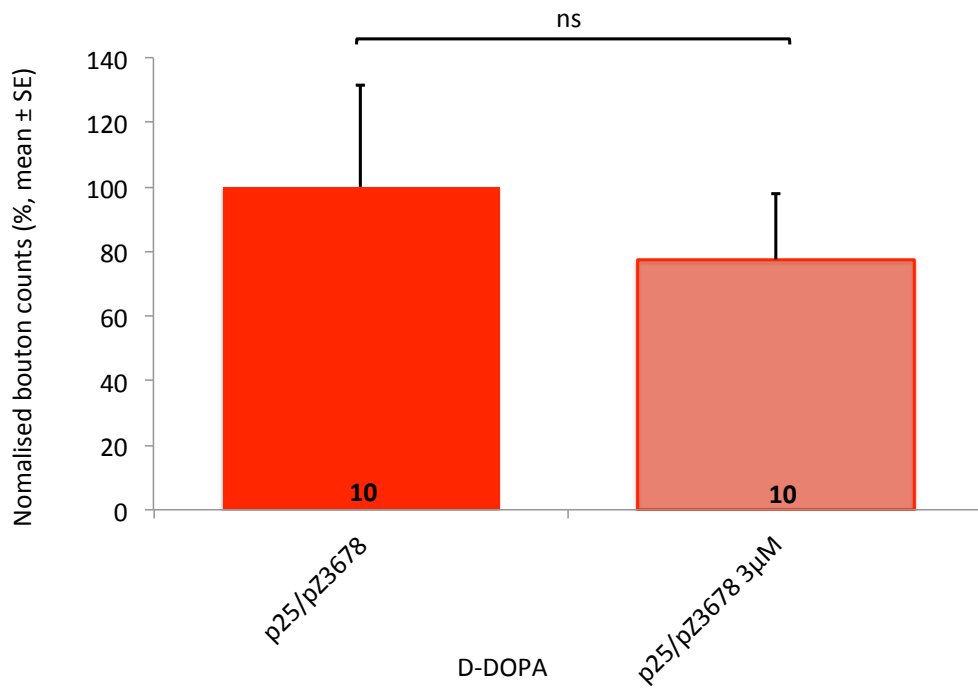
Figure 5.1 Dopaminergics fail to rescue locomotory dysfunction in *dparkin* larvae.

A D-DOPA (3 μ M) does not affect the crawling speed of *dparkin* (p^{25}/p^{Z3678}) larvae ($p = 0.564$). D-DOPA increases the crawling speed of wild-type (CS/w^+) larvae ($p = 0.004$). (As described before, chapter 3), *dparkin* (p^{25}/p^{Z3678}) larvae crawl with a reduced speed compared to wild-type (CS/w^+) larvae ($p = 0.009$). **B** L-DOPA has no effect on the crawling velocity of either wild-type larvae (CS/w^+ , $p = 1$) or the *dparkin* larvae (p^{25}/p^{Z3678} , $p = 0.272$).

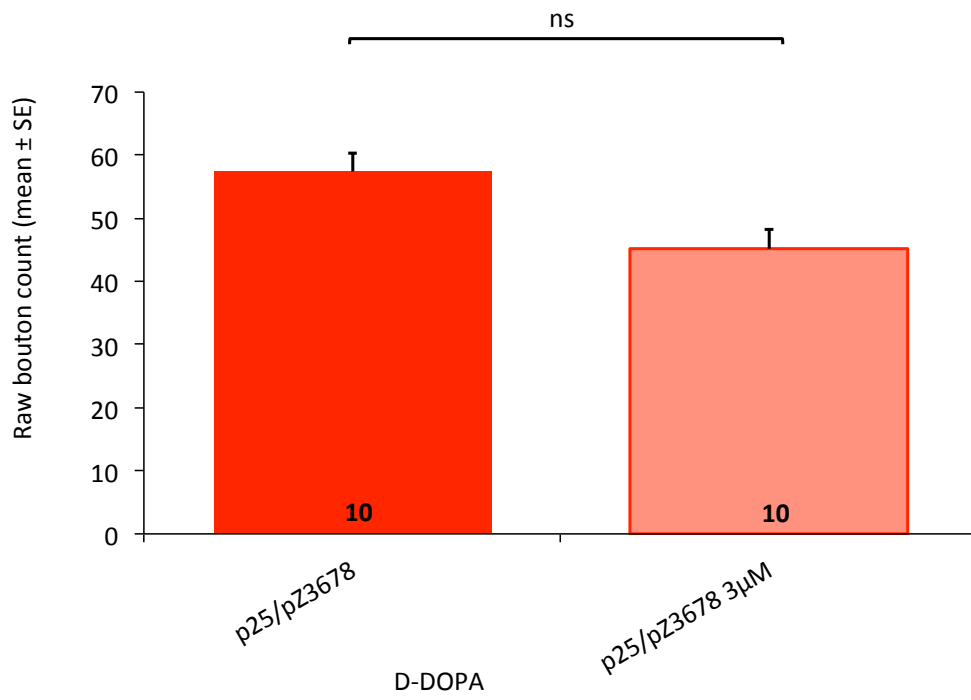
Dopaminergics fail to rescue overgrowth

To test whether dopamine causes further oxidative stress induced by dopamine neuronal overgrowth, dopaminergics were dissolved in the instant food (final concentration $3\mu\text{M}$) throughout the larval stage. D-DOPA in instant food did not affect *dparkin* overgrowth compared to their mutant controls (p^{25}/p^{Z3678}). L-DOPA treatment did not affect *dparkin* overgrowth compared to mutant controls (p^{25}/p^{Z3678}) (**Fig 5.2A-F**).

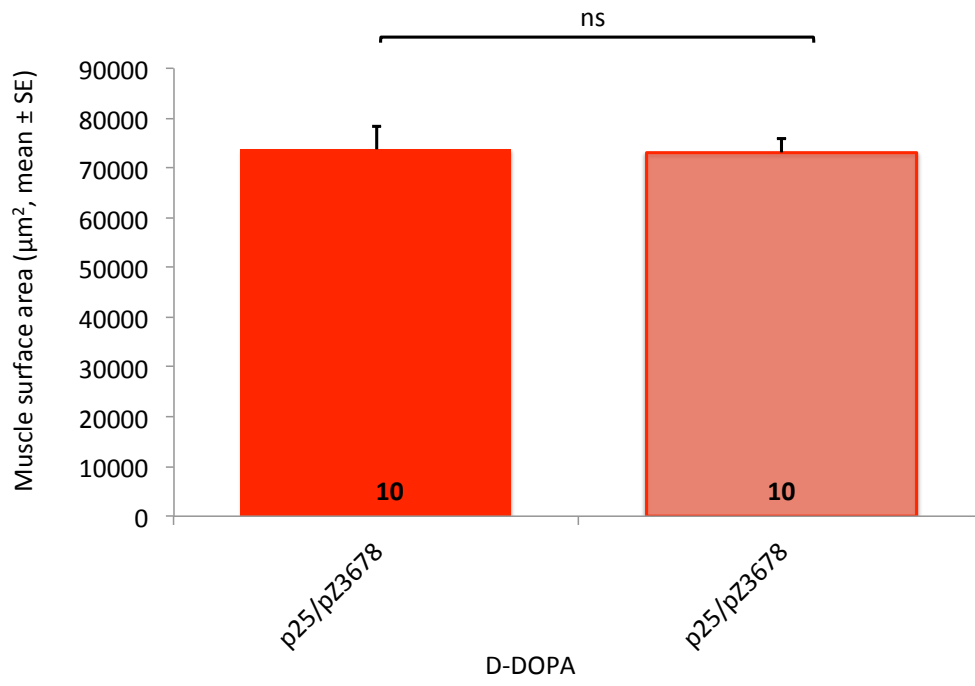
5.2A



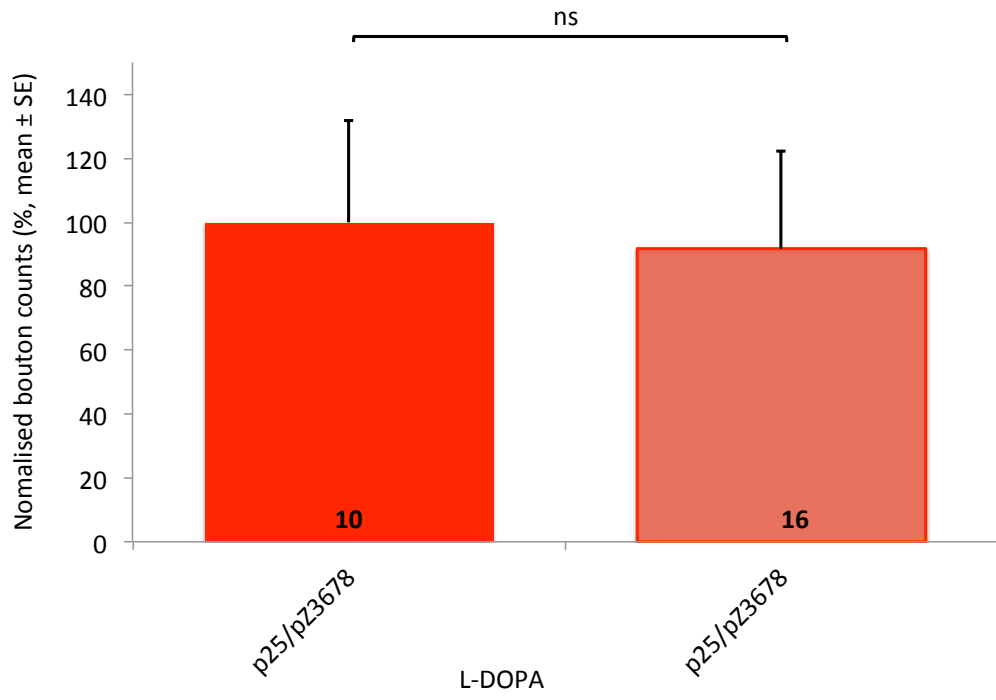
5.2B



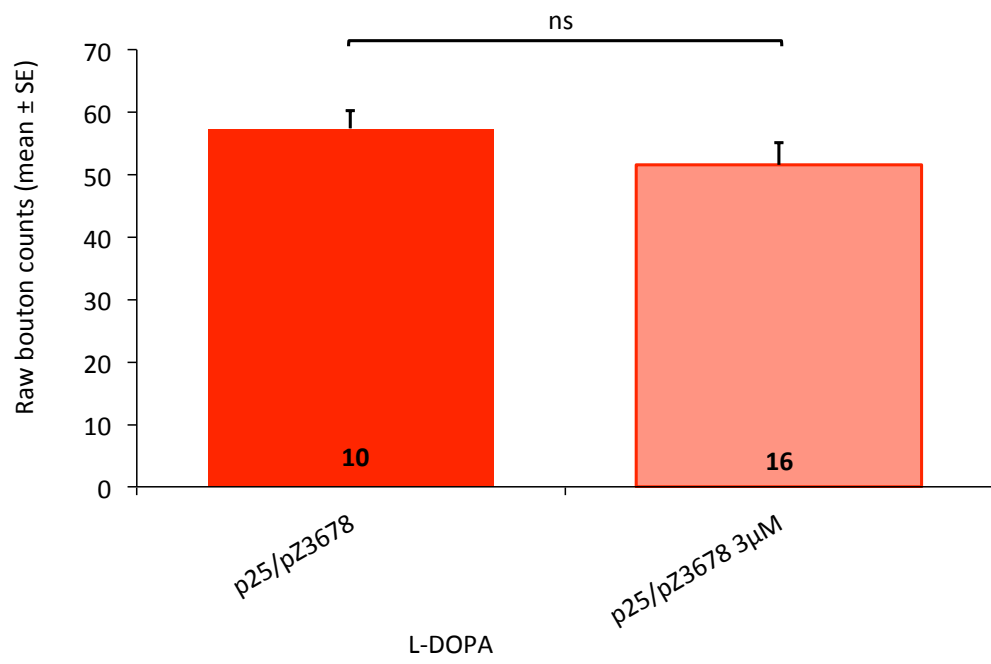
5.2C



5.2D



5.2E



5.2F

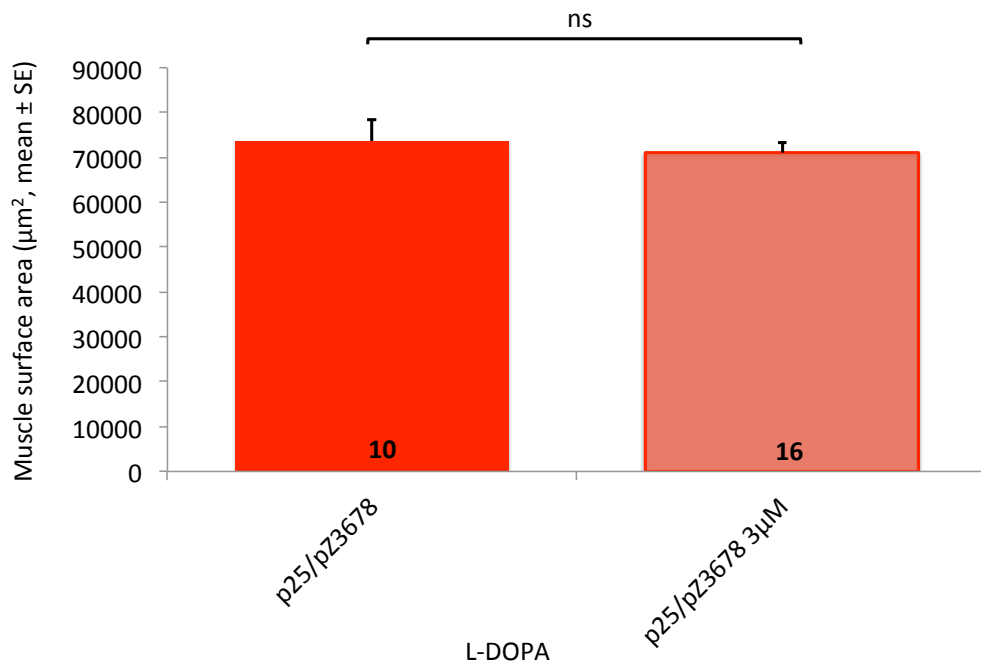


Figure 5. 2 A-F Dopaminergics fail to rescue overgrowth in *dparkin* larvae.

A-C D-DOPA (3 μM) does not affect the normalized bouton counts of *dparkin* (p^{25}/p^{Z3678}) larvae raised on instant food (**A**, $p = 0.107$) or the raw bouton number or muscle surface area (μm^2) compared to their mutant controls (**B**, $p = 0.062$ and **C**, $p = 1$) respectively). **D-F** L-DOPA (3 μM) also does not affect the normalized bouton counts of *dparkin* (p^{25}/p^{Z3678}) larvae raised on instant food (**D**, $p = 0.676$). There was also no difference in raw bouton number or muscle surface area compared to their mutant controls (**E**, $p = 0.433$ and **F**, $p = 0.989$, respectively).

AICAR, an AMPK activating drug, fails to rescue crawling

dparkin (p^{25}/p^{Z3678}) larvae raised on instant food mixed with 2.5 μ M to 50 μ M AICAR at different concentrations have the similar average crawling speed as *parkin* (p^{25}/p^{Z3678}) larvae with no AICAR (with the vehicle, 50 μ M PBS, added to the instant food). Furthermore, the AICAR concentration does not affect the velocity of wild-type (CS/w^+) larvae. As shown in chapter 3, *dparkin* (p^{25}/p^{Z3678}) larvae crawl slowly on average compared to wild-type (CS/w^+) larvae ($p < 0.001$). Wild-type (CS/w^+) larvae crawl 35% faster than *dparkin* (p^{25}/p^{Z3678}) larvae at each AICAR concentration tested ($P < 0.001$) (Fig 5.3).

5.3

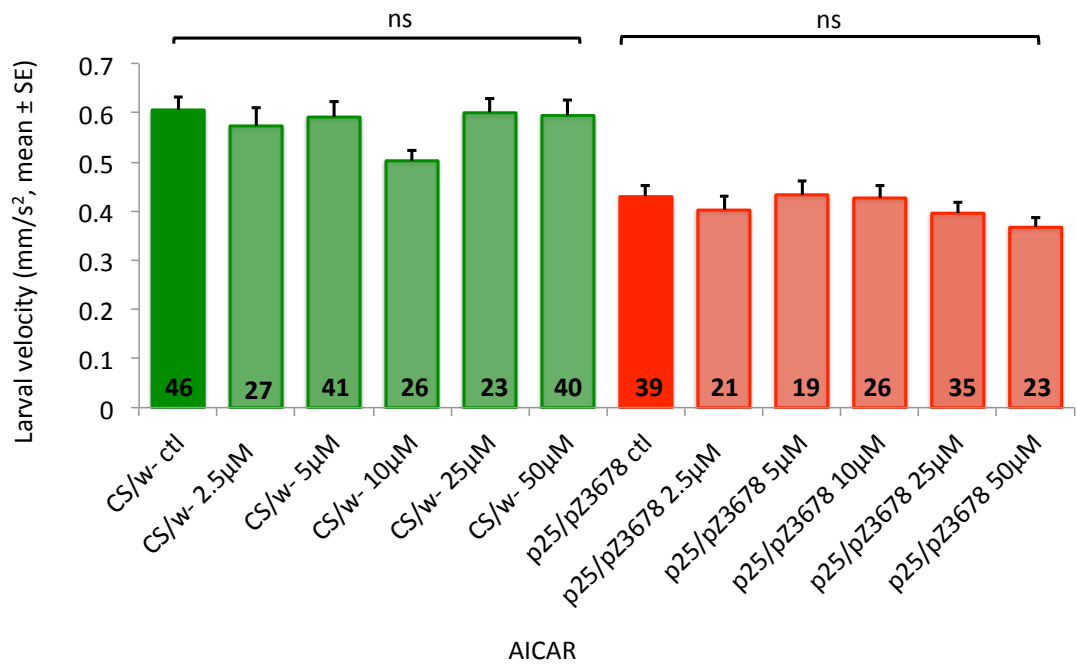


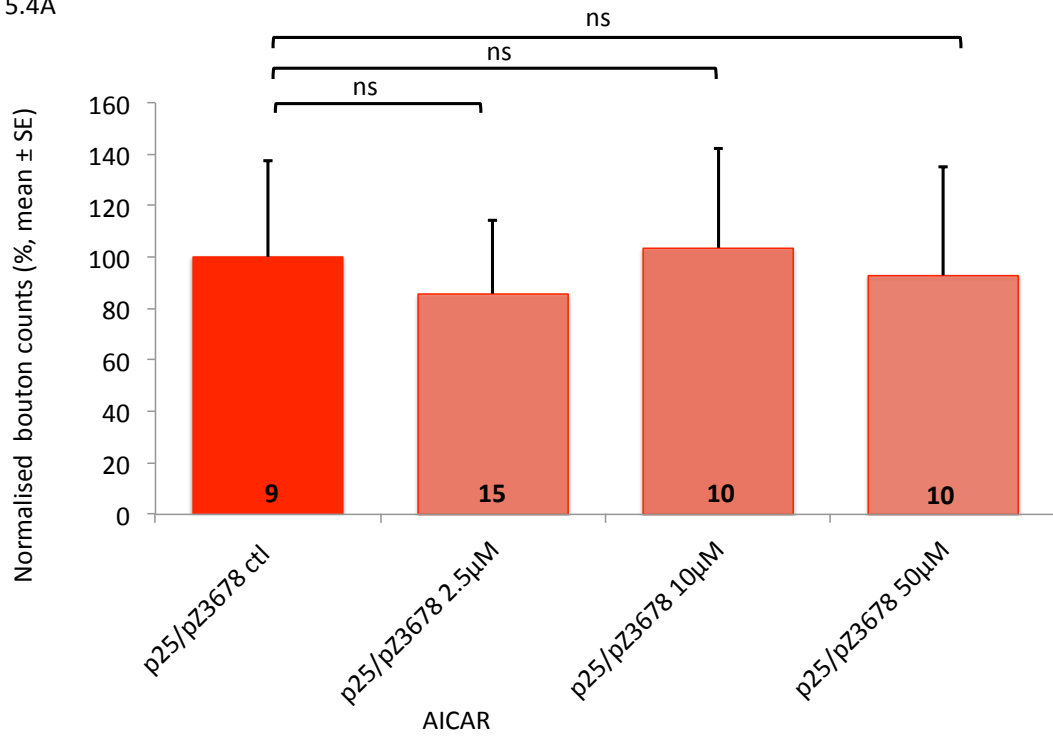
Figure 5.3 The AMPK activating drug AICAR fails to rescue locomotory dysfunction in *dparkin* larvae.

dparkin (p^{25}/p^{Z3678}) larvae raised on instant food mixed with AICAR (2.5, 5, 10, 25 or 50 μM dissolved in PBS) have the same average crawling speed as *dparkin* (p^{25}/p^{Z3678}) larvae with no AICAR (with only 50 μM PBS), ($p = 1$). Again the AICAR concentration does not affect the velocity of wild-type (CS/w^+) larvae, ($p = 1$). As shown in chapter 3, *dparkin* (p^{25}/p^{Z3678}) larvae crawl slowly on average compared to wild-type (CS/w^+) larvae ($p < 0.001$). Wild-type (CS/w^+) larvae crawl faster than *parkin* (p^{25}/p^{Z3678}) larvae at each AICAR concentration tested ($p < 0.001$).

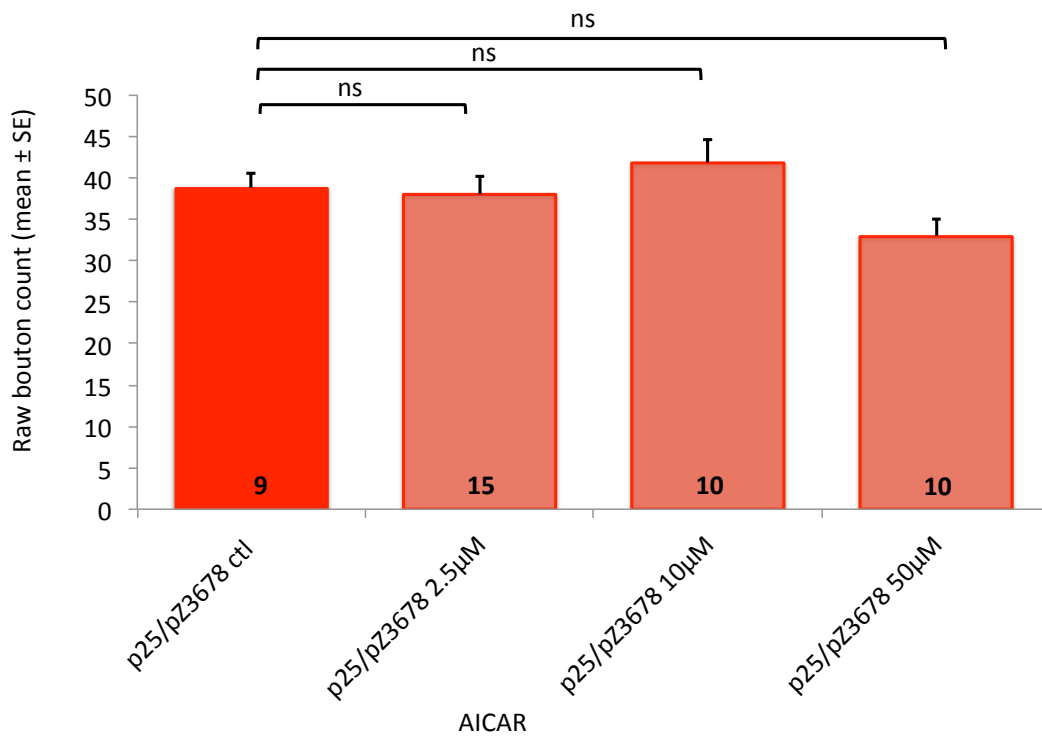
AICAR, the AMPK-activating drug, fails to rescue synaptic overgrowth

dparkin (p^{25}/p^{Z3678}) larvae raised on instant food with a range of concentrations of AICAR (2.5, 10 or 50 μ M, dissolved in PBS) had the same synaptic overgrowth as the *dparkin* larvae raised on the vehicle control (**Fig 5.4**).

5.4A



5.4B



5.4C

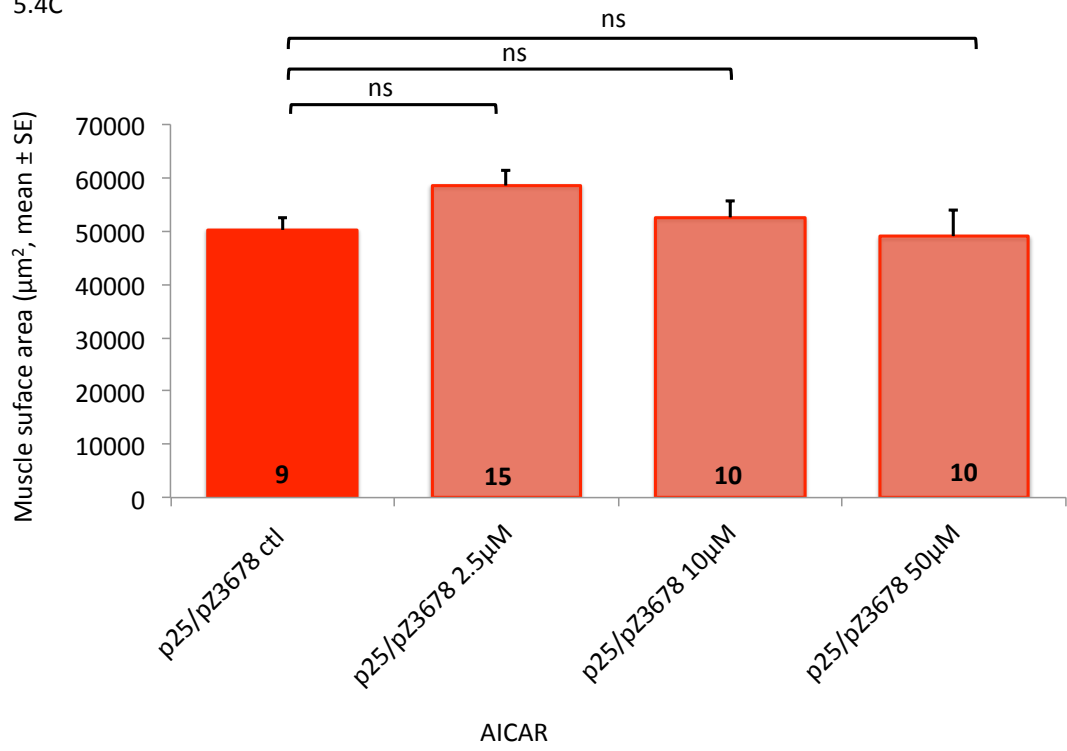


Figure 5.4 AMPK-activating AICAR, fails to rescue synaptic overgrowth in *dparkin* larvae.

A There is no difference in normalised bouton count in *dparkin* (p^{25}/p^{Z3678}) larvae raised on instant food with a range of concentrations of AICAR (2.5, 10 or 50 μM , dissolved in PBS) compared with *dparkin* controls without AICAR (with only 50 μM PBS), ($p = 0.669$, $p = 0.995$ and $p = 0.952$ respectively). **B-C** *dparkin* (p^{25}/p^{Z3678}) larvae raised on AICAR showed no difference in raw bouton number ($p = 0.995$, $p = 0.823$ and $p = 0.348$ respectively) or muscle surface area ($p = 0.319$, $p = 0.968$ and $p = 0.996$ respectively), across a range of concentrations compared to *dparkin* controls without AICAR.

Metformin fails to rescue crawling

Metformin used at a final concentration of 3 μM or 6 μM does not affect the speed at which *dparkin* (p^{25}/p^{Z3678}) larvae crawl, nor does it affect the speed of wild-type larvae (CS/w^+). As previously reported in chapter 3, *dparkin* (p^{25}/p^{Z3678}) larvae crawl 20% more slowly than wild-type (CS/w^+) larvae ($p = 0.006$) (**Fig 5.5**).

5.5

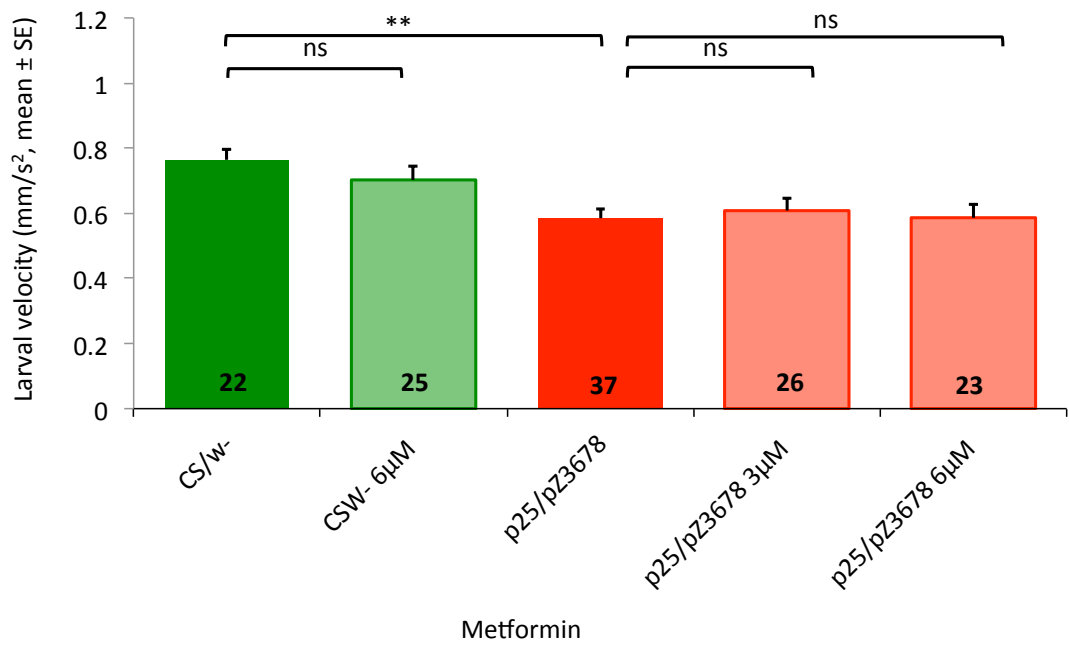


Figure 5.5 Metformin fails to rescue locomotory dysfunction in *dparkin* larvae.

Metformin (6 μM or 3 μM) does not affect the speed at which *parkin* (p^{25}/p^{Z3678}) larvae crawl ($p = 1.0$ or $p = 0.987$, respectively), nor does it affect the speed of wild-type larvae (CS/w^+ , 6 μM , $p = 0.798$). As previously reported in chapter 3, *dparkin* (p^{25}/p^{Z3678}) larvae crawl more slowly than wild-type (CS/w^+) larvae ($p = 0.006$). *dparkin* (p^{25}/p^{Z3678}) larvae raised on instant food mixed with metformin (3 μM or 6 μM) results in no overall change in velocity compared to mutant larvae without the drug (with only 6 μM water), ($p = 1.0$). The wild-type larvae raised on instant food mixed with 6 μM metformin (dissolved in water) has no effect on overall crawling speed compared with wild-type (CS/w^+) controls without metformin (with only 6 μM water), ($p = 1.0$).

Metformin fails to rescue depolarized RMP defect

Metformin does not affect the RMP of *dparkin* larvae raised on instant food mixed with 3 μM of metformin ($p = 0.969$). *dparkin* (p^{25}/p^{Z3678}) larvae show more positive (depolarized) RMP compared to wild-type (*CS/w⁻*) larvae ($p < 0.001$), as previously described in chapter 3 (**Fig 5.6**).

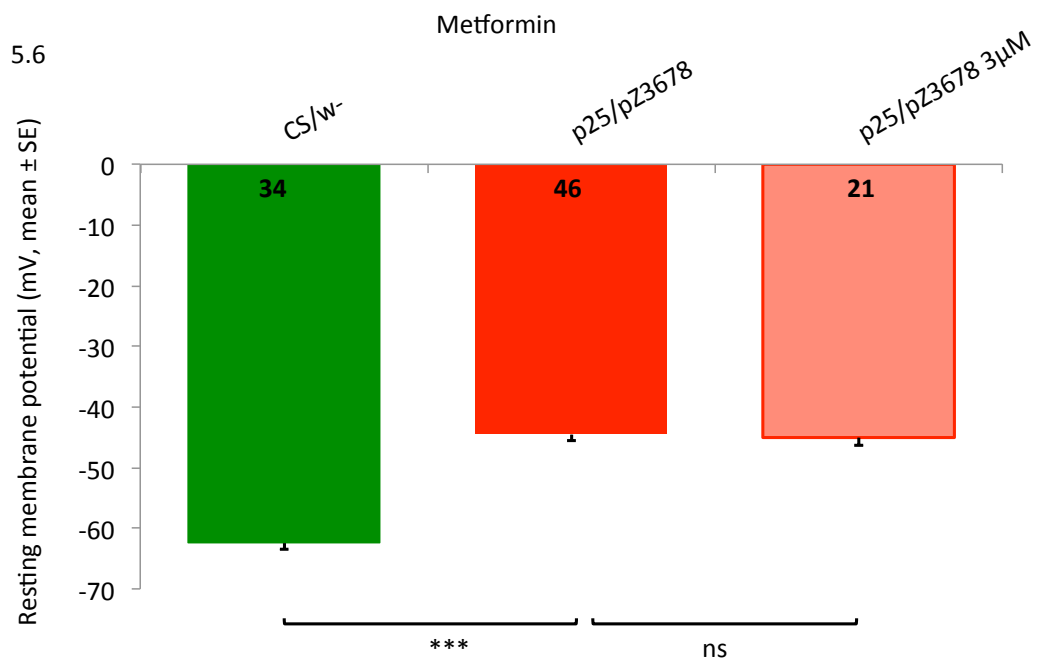


Figure 5.6 Metformin fails to rescue depolarized RMP defect in *dparkin* larvae.

Metformin does not affect the RMP of *dparkin* larvae raised on instant food mixed with 3 μ M of metformin ($p = 0.969$). *dparkin* (p^{25}/p^{Z3678}) larvae show 29% more positive (depolarized) RMP compared to wild-type (CS/w^+) larvae ($p < 0.001$), as previously described in Chapter 3.

Resveratrol fails to rescue locomotory dysfunction

Resveratrol does not affect the mean crawling speed of either wild-type (*CS/w⁻*) or *dparkin* (p^{25}/p^{Z3678}) larvae. As previously reported in chapter 3, *dparkin* (p^{25}/p^{Z3678}) larvae crawl with a reduced speed compared to wild-type (*CS/w⁻*) larvae ($p < 0.001$) (**Fig 5.7**).

5.7

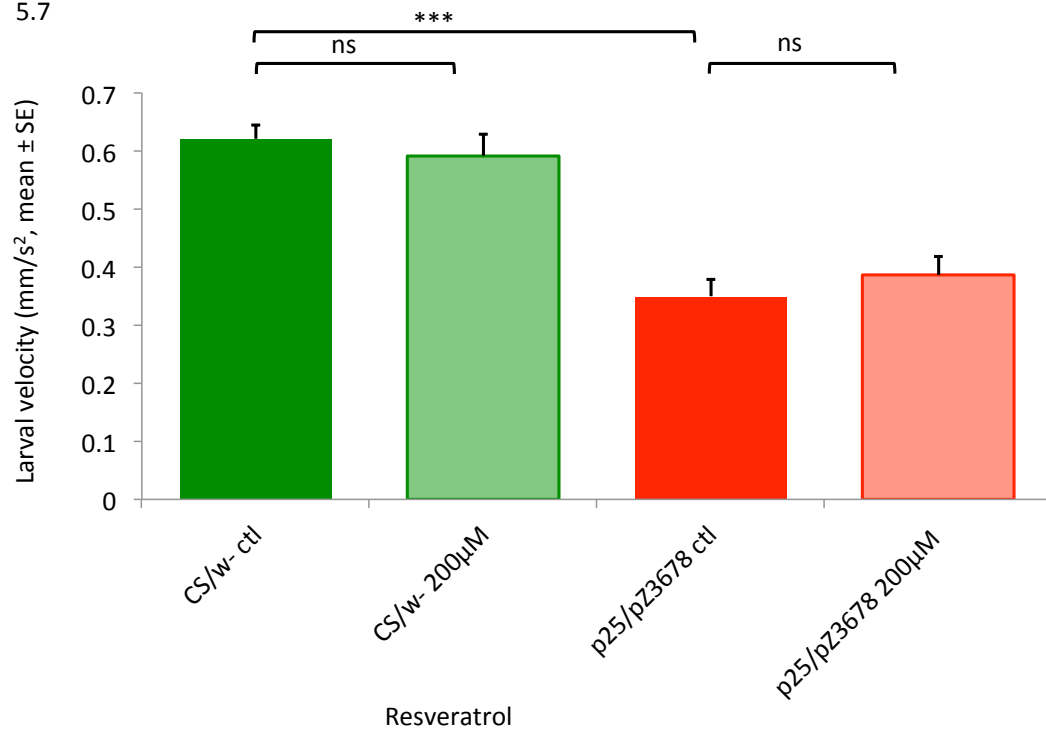
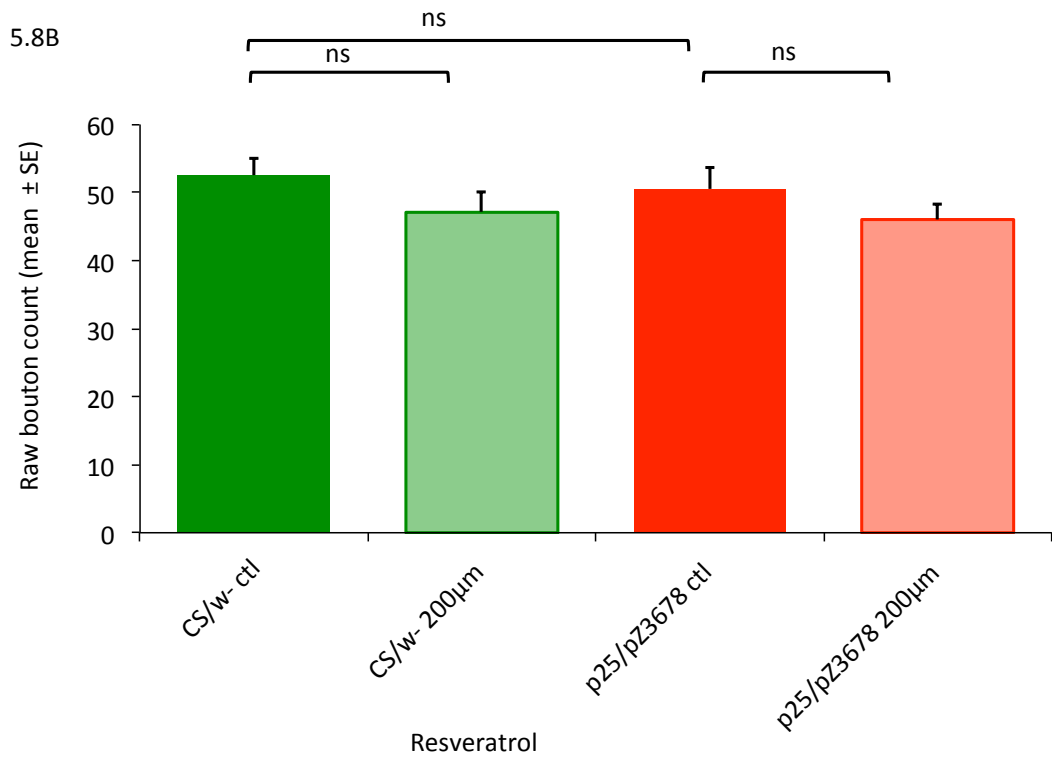
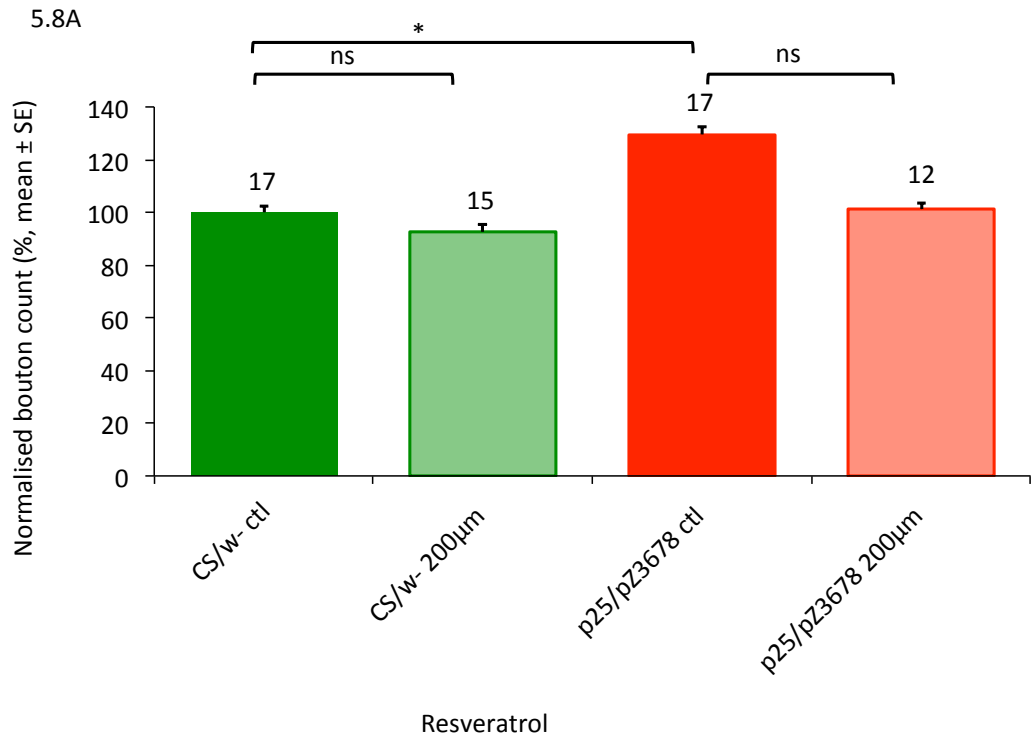


Figure 5.7 Resveratrol fails to rescue locomotory dysfunction in *dparkin* larvae.

Resveratrol (200 μ M) does not affect the mean crawling speed of either wild-type (*CS/w⁻*) or *dparkin* (*p²⁵/p^{Z3678}*) larvae ($p = 0.923$ and $p = 0.819$). As previously reported in chapter 3, *dparkin* (*p²⁵/p^{Z3678}*) larvae crawl with a reduced speed compared to wild-type (*CS/w⁻*) larvae ($p < 0.001$). All data are from flies raised on instant food containing 200 μ M ethanol.

Resveratrol fails to rescue synaptic overgrowth in *parkin* larvae.

dparkin (p^{25}/p^{Z3678}) larvae raised on instant food with Resveratrol (200 μ M dissolved in ethanol) did not rescue *dparkin* (p^{25}/p^{Z3678}) overgrowth (**Fig 5.8**). There is no significant difference between the wild-type raised in 200 μ M Resveratrol compared to their wild-type control raised in vehicle. The vehicle controls, *dparkin* (p^{25}/p^{Z3678}) and wild-type larvae, show a similar increase in synaptic growth ($p = 0.023$) as the larvae raised on solely instant food (Chapter 3).



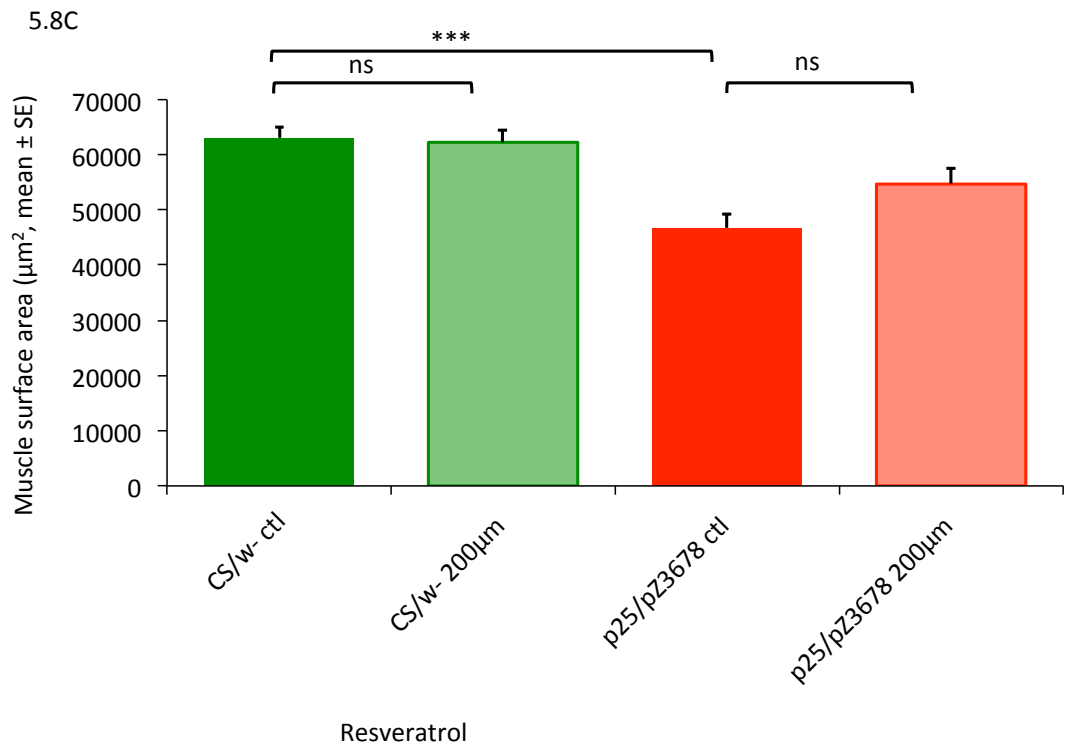


Figure 5.8 Resveratrol fails to rescue synaptic overgrowth in *dparkin* larvae.

A There is no difference in normalised bouton count in *dparkin* (p^{25}/p^{Z3678}) larvae raised on instant food with Resveratrol (200 μ M dissolved in ethanol) compared with *dparkin* (p^{25}/p^{Z3678}) controls without Resveratrol (only with 200 μ M ethanol), ($p = 0.061$). There is no significant difference between the wild-type raised in 200 μ M Resveratrol compared to their wild-type control raised in only 200 μ M ethanol ($p = 0.890$). **B-C** *dparkin* (p^{25}/p^{Z3678}) larvae raised on Resveratrol showed no difference in raw bouton number ($p = 0.710$) or muscle surface area ($p = 0.125$), compared to *dparkin* (p^{25}/p^{Z3678}) controls without Resveratrol. *dparkin* (p^{25}/p^{Z3678}) control larvae (with only ethanol) have overgrown synapses when normalised and compared to wild-type control (with only ethanol) larvae ($p = 0.023$).

Resveratrol fails to rescue depolarized RMP defect

Resveratrol does not affect the RMP of *dparkin* larvae. *dparkin* (p^{25}/p^{Z3678}) larvae show 36% more positive (depolarized) RMP compared to wild-type (CS/w^+) larvae ($p < 0.001$), as previously described in chapter 3. The wild-type (CS/w^+) larvae raised in 200 μ M Resveratrol (dissolved in ethanol) were 10 % depolarized compared to wild-type (CS/w^+) control (ethanol vehicle only) larvae ($p = 0.003$) (**Fig 5.9**).

5.9

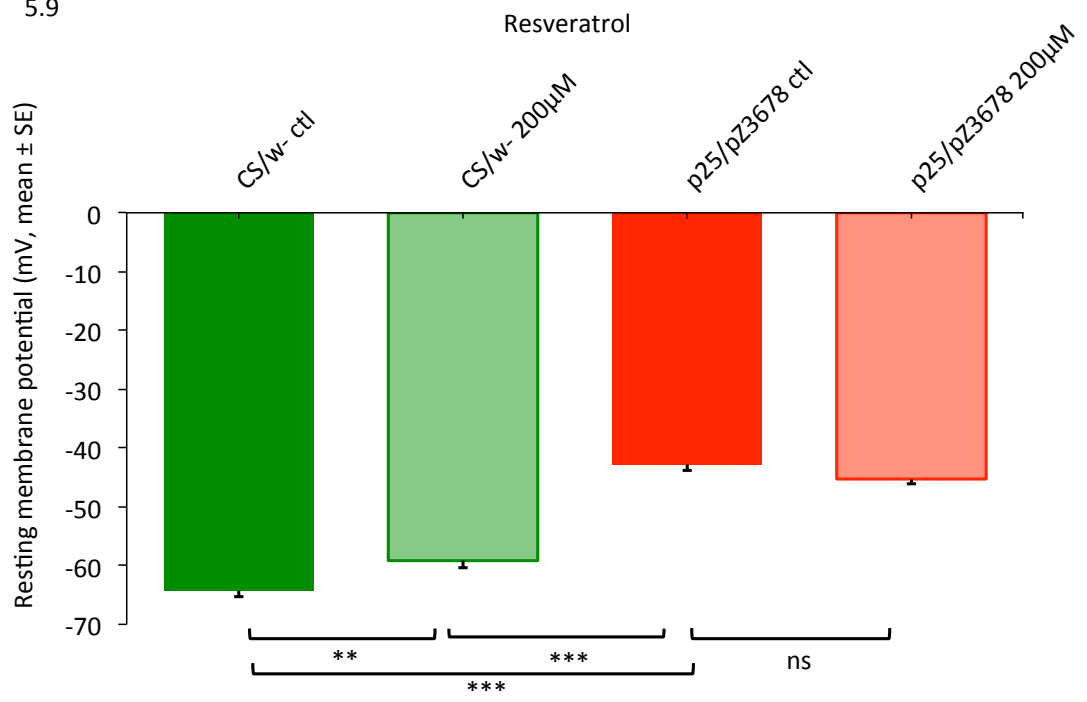


Figure 5.9 Resveratrol fails to rescue depolarized RMP defect in *dparkin* larvae.

The RMP of *dparkin* larvae raised on instant food mixed with 200 μ M of Resveratrol is the same as that of larvae raised on instant food alone ($p = 0.338$). *dparkin* (p^{25}/p^{Z3678}) larvae show more positive (depolarized) RMP compared to wild-type (*CS/w⁻*) larvae ($p < 0.001$), as previously described in chapter 3. The wild-type (*CS/w⁻*) larvae raised in 200 μ M Resveratrol (dissolved in ethanol) were more depolarized compared to wild-type (*CS/w⁻*) control (in 200 μ M ethanol only) larvae ($p = 0.003$).

5.4 Discussion

The main findings of this chapter can be summarized as follows: both L-DOPA and the inactive stereoisomer control, D-DOPA, failed to rescue *dparkin* locomotory defect or the overgrowth. AICAR failed to rescue locomotory defects or the overgrowth in *dparkin* larvae. Metformin had no impact on crawling or RMP of *dparkin* larvae. Resveratrol failed to rescue locomotory or the overgrowth or the RMP defects in *dparkin* larvae.

Dopaminergics failed to rescue crawling or the overgrowth

Locomotor activity in both vertebrates and invertebrates relies on signaling from the brain dopaminergic system (Beninger, 1983, Giros et al., 1996, Yellman et al., 1997, Riemensperger et al., 2011). Studies have reported behavioral impairment that is accompanied by a gradual loss of dopaminergic neurons or tyrosine hydroxylase (*TH*) immunoreactivity in selective cell clusters of the brain (Feany and Bender, 2000, Auluck et al., 2005, Trinh et al., 2008). These studies highlight how brain dopamine plays an important role in the locomotor control in *D. melanogaster*. However, dopaminergics failed to rescue *dparkin* induced crawling or overgrowth defects in the larvae. L-DOPA is a substrate of the terminal step of dopamine synthesis. D-DOPA is an inactive stereoisomer (Cha et al., 2005). In adult flies, the *dparkin* induced locomotor defect was partially rescued by 1mM L-DOPA administration for a period of 10 days after emergence (Cha et al., 2005). This was a concentration approximately 300 times the one I used, and the duration of L-DOPA application was much longer. There are other reasons for the lack of effect seen by either L-DOPA or D-DOPA. The 3 μ M final concentration of the drug made in instant food may have been reduced before reaching the larvae. There are two reasons for this: firstly, the breakdown of these drugs may

start in the food (e.g. by yeast or light). Secondly, L-DOPA may be metabolized in the gut of the larvae and may not reach the neural tissue. Gut metabolism of L-DOPA is extensive in the human (Granerus et al., 1973) and so the inhibitor of peripheral metabolism, Carbidopa, is commonly administered along with L-DOPA (e.g. 1:10 Carbidopa-Levodopa). Additionally, the intake of food by larvae can also vary and may fail to reach the optimum concentration in the larval neuronal tissues. Experiments cited in the literature use adult flies, which feed less than larvae (Cha et al., 2005).

My experiments are in contrast to those with the dominant mutations (*parkin*^{Q311X} and *parkin*^{T240R}). In these flies, knockdown of *dVMAT* increased cytosolic dopamine, along with the vulnerability of dopamine neurons (Sang et al., 2007). By contrast, increasing *dVMAT* expression in *dparkin* mutants partially rescues pupal lethality and dopaminergic degeneration most likely by reducing cytosolic dopamine. We commonly observe pupal lethality with only a few *dparkin* flies reaching eclosion where they die shortly.

A weak base compound, methamphetamine, is known to cause damage to both dopaminergic and serotonergic nerve endings. The dopamine released from the synaptic vesicle resulted in the cytosolic oxidization induced dopaminergic injury as a result of methamphetamine exposure. Superoxides and hydroxyl radicals are generated by auto-oxidation from cytosolic dopamine after methamphetamine exposure. The spontaneous oxidation of the catechol ring of dopamine, this generates reactive oxygen species (ROS) including superoxide and reactive electron-deficient quinones (Sulzer and Zecca, 2000). Superoxide is converted by superoxide dismutase to hydrogen peroxide. Superoxide reacts with nitric oxide radicals to generate peroxynitrate of reactive nitrogen species (RNS) (Sulzer and Zecca, 2000, Sulzer, 2007). Transition metals are abundant in dopaminergic neurons and hydrogen peroxide can react with these, in

particular with iron, to forms hydroxyl radicals (Hastings, 1995). The reactive quinones have the potential to react with cellular nucleophiles for example reduced sulfhydryl group on a small peptide and also protein cysteinyl residues. Protein thiols are targets and their structures are covalently modified by dopamine quinones. Protein modification and the resulting inactivation of their function may be detrimental to cell survival and may cause the degenerative process observed in PD patients (Stokes et al., 1999).

As noted in the Introduction (Chapter 1), Braak suggested PD did not start in the dopaminergic neurons, and that the early stages of the disease developed in the neurons of the olfactory and/or digestive system. Since our *dparkin* mutation is effective in all neurons, and L-DOPA administration does not seem to rescue the effects, it is possible that many of the effects of *dparkin* are mediated by non-dopaminergic neurons. Thus this larval model of an early stage form of PD, is (in this manner) reminiscent of the spreading pathology of the human disease.

AICAR fails to rescue locomotion and the overgrowth defect

AICAR failed to rescue crawling and the overgrowth. *AMPK* activation with the larval administration of AICAR treatment failed to rescue either the locomotion or the overgrowth defects. This may be due to the low concentrations of ZMP-induced activation of *AMPK* and the reduced level of effectiveness compared to the activation via phosphorylation of *AMPK*. In the literature ZMP has been reported not to be as a potent activator as AMP itself (Suter et al., 2006).

Additionally, other *D. melanogaster* models of PD (including *LRRK2* and *PINK1*) have shown metabolic dysfunction as key to tissue (dopaminergic) neurodegeneration, synaptic dysfunction and motor dysfunction (Morais et al., 2009, Vos et al., 2012,

Hindle et al., 2013). Recently in two fly models of PD, *LRRK2* and *parkin*, mutant phenotypes were shown to be alleviated via increased *AMPK* activity using *AMPK* mimetics such as metformin and 5-aminoimidazole-4-carboxamide-1- β -D-ribofuranoside (AICAR). Additionally, Ng and colleagues recently showed *LRRK2*- and *parkin*-dysfunction (including mitochondrial and dopaminergic defects) were rescued with a green tea-derived catechin, epigallocatechin gallate (EGCC) mediating its effects via *AMPK* (Ng et al., 2012). AICAR or its metabolites (ZMP or ZTP) can act on the ATP-sensitive potassium (K_{ATP}) channels. ZTP has shown to exert inhibitory action of K_{ATP} channel at particular concentrations (Malaisse et al., 1994). Another member of the KIR family (Kir2.1) has been recently shown to be inhibited by *AMPK* (Alesutan et al., 2011). *AICAR* toxicity is little to none and has shown promise as an *in vivo* exercise mimetic.

Metformin failed to rescue crawling or RMP defect

Metformin failed to rescue the crawling and RMP in *dparkin* mutant larvae. Metformin was confirmed to robustly activate *AMPK* in a dose dependent manner in *D. melanogaster* via mass spectrometry and western blot analysis (Slack et al., 2012). The efficacy of oral administration of metformin in the fly was measured by quantifying its accumulation in fly tissues. Adult flies were fed increasing concentrations of metformin for a period of 7 days. The fly extracts were prepared after the gut was cleared of ingested food by incubating them for period of 5 hours in the absence of metformin treatment. Western blot analysis of phospho-Thr172-*AMPK* expression was undertaken using the whole-fly protein extracts. After 7 days of metformin treatment at concentrations of 0, 5, 10, 25, 50 and 100 mM, the flies were sampled. A dose-dependent increase in phospho-Thr172-*AMPK* levels was observed compared to actin as a loading control. A high concentration of Metformin (from 10 mM and 100 mM

dose in female or males respectively) was found to be toxic to flies. There was no increased survival observed in males or females with administration of Metformin at concentrations between 1 mM-100 mM (Slack et al., 2012). The concentrations of metformin used in this study were significantly lower than the levels found to be toxic to flies. The lowest level of metformin concentration (1 mM) was detected in the fly in the mass spectrometry experiment (Slack et al., 2012).

The molecular targets of Metformin have not been well understood. In mammals Metformin is known to activate *AMPK* (Zhou et al., 2001), via phosphorylating *LKB1* (Fryer et al., 2002) to exert majority of its effects. Another hypothesis is that Metformin inhibits *AMP* deaminase, thereby reducing ATP concentration thus activating *AMPK* (Ouyang et al., 2011). The effects of metformin is preserved in liver-specific *AMPK* deficient mice, thus suggesting not *AMPK* but complex 1 of the respiratory chain as the primary target of metformin action (El-Mir et al., 2000, Owen et al., 2003). Metformin has been suggested to have lower maximal inhibitory action of complex 1 compared to rotenone (Batandier et al., 2006, Kane et al., 2010). It has also been proposed that in contrast to rotenone, metformin additionally exerts an inhibitory effect on mitochondrial ROS production by selectively blocking the reverse electron flow through the respiratory chain complex 1 (Batandier et al., 2006, Kane et al., 2010).

Resveratrol failed to rescue crawling, overgrowth or RMP defect

200 μ M resveratrol final concentration in instant food administered larval treatment failed to rescue crawling, overgrowth or the RMP defect. Resveratrol treatment of adult flies exposed to manganese (Mn) results in an increase in life span and increase in motor activity. However, when Resveratrol is given after Mn-exposure, resveratrol is unable to ameliorate the motor dysfunction caused by the metal (Bonilla et al., 2012).

0.43 mM concentration was used to feed the adult flies, a much higher dose than the one I used for my experiment (Bonilla et al., 2012). A lower concentration of 200 μ M was used in my experiments as larvae are in the food, whereas adults are on the food.

The uptake of resveratrol into the larvae could be checked via mass spectrometry and *SIRT1* fluorimetric analysis as described by Partridge group (Bass et al., 2007). The activity of resveratrol samples was measured using the *SIRT1* Fluorimetric Drug Discovery Kit. Previous studies have reported that polyphenols may be neuroprotective in *D. melanogaster* acutely treated with oxidative stress inducing agents (Pallàs et al., 2009, Chandrashekara and Shakarad, 2011). Polyphenol exposure is suggested to increase life span and restore motoric defects of *D. melanogaster* chronically exposed to paraquat compared to their controls fed with only paraquat (Ortega-Arellano et al., 2011).

Howitz and colleagues and also other groups have shown resveratrol activated SIRT1 NAD-dependent deacetylase in vitro and then in vivo and in some cases it did so directly (Baur and Sinclair, 2006, Knutson and Leeuwenburgh, 2008). On the other hand, there we reports suggesting resveratrol and sirtuins were not associated thereby claiming the activation of SIRT1 by resveratrol an artefact of the assay used (Baur, 2010). Park and colleagues findings now show that SIRT1 is indeed activated indirectly by down stream signalling cascade involving cyclic AMP, Epac1 (a cAMP effector protein) and AMPK by resveratrol in a response to phosphodiesterase enzyme inhibition, its direct target (Park et al., 2012). The pathway to SIRT1 activation occurs via AMPK, an enzyme that is known to be essential for many of resveratrol's beneficial metabolic effects (Park et al., 2012). These observations support previous reports that AMPK lies upstream of SIRT1 activity upon resveratrol exposure, as AMPK activation is still persistent in cells lacking SIRT1 (Dasgupta and Milbrandt, 2007). The

concentration used to achieve these beneficial effects *in vitro* exceed the those achieved *in vivo*, raising concerns about its specificity. Although, rolipram a phosphodiesterase enzyme inhibitor mimics the effects of resveratrol such as the prevention of diet induced obesity in mice (Park et al., 2012), all the beneficial effects are brought about via the downstream action of *AMPK* activity and thus could be mediated through alternative mechanisms of resveratrol treatment *in vivo*. Resveratrol treatment has been shown to enhance nitric oxide production (Wallerath et al., 2002) and in another study it was found to stimulate adenylate cyclase (El-Mowafy and Alkhalaf, 2003) either of these could result in phosphodiesterase inhibition. The impact of *SIRT1* activation on *AMPK* has not been addressed *in vivo*. A range of more potent *SIRT1* activators than resveratrol have now been developed that show promise with therapeutic potential (Milne et al., 2007), some of which are being tested in phase 1 and phase 2 clinical trials for the treatment of cardiovascular, inflammatory and metabolic disease. The role *SIRT1* plays in regulation of neurodegenerative disorders is an important one (Tang and Chua, 2008). *SIRT1* inhibitors, sirtinol and nicotinamide, have shown to reverse the protective effects of resveratrol in a neuronal culture model of Huntington's Disease (HD) (Tang and Chua, 2008). *SIRT1* cellular substrates include the tumor suppressor p53, transcription factor NF-kappaB, the forkhead box class O (FoxO) family of transcription factors, the peroxisome proliferator-activated receptor (PPAR)-gamma, the PPAR)-gamma co-activator 1-alpha and the endothelial nitric oxide synthase (Michan and Sinclair, 2007).

As cytosolic dopamine and its metabolites are involved in the conjugation of cytosolic protein substrates such as *parkin*, it is likely this is the case in our *dparkin* transheterozygote mutants as they produce very little wild-type *dparkin*. This possibly results in the inactivation of the low levels of *dparkin* and consequently thereby leading to the increase in ROS levels (as *parkin* is involved in both degradation of misfolded

proteins via proteosomal degradation pathway and also autophagy). This could lead to neuronal vulnerability as well as affecting other tissues such as muscles. This is further supported by the fact that *dVMAT* mutant flies show reduced numbers of dopaminergic neurons and the degeneration deteriorates further when these mutants are exposed to oxidative stress inducing agents such as paraquat or rotenone. Lawal and colleagues also show the effects of the *dVMAT* overexpression on *dVAMT* mutant flies, which inhibits the rotenone induced dopaminergic loss (Lawal et al., 2010). This is possibly closely linked to rotenone's action, where it inhibits the mitochondrial respiratory chain component complex I and causes severe loss energy that leading to the failure of the monoamine transporters, such as *dVMAT*, which allow the ATP-dependent reuptake of extracellular amines (Lawal et al., 2010). The reuptake of rotenone into the synaptic vesicles prevents its interaction with mitochondria and further cause oxidative stress. The most plausible explanation is that cytosolic dopamine is limited as it is taken up into synaptic vesicles to prevent the interaction with the cytosolic rotenone to cause oxidative damage (Lawal et al., 2010). This model suggests the interaction of cytosolic dopamine with ROS or sites of ROS (mitochondria) could result in cell damage or death. This also could implicate the dopaminergic cell loss seen in this mutant as a non-cell autonomous effect and caused by the defective signaling of other aminergic cells.

Summary of key findings:

* *dparkin* larvae support 'Braak's hypothesis' and fail to exhibit dopaminergic dysfunction in this early model of PD.

* Metformin and AICAR, the classical *AMPK* activators, fail to show an effect on *parkin* larval phenotypes at their respective concentrations.

* Resveratrol fails to rescue overgrowth, locomotory or neurophysiological defects.

Chapter 6: General Discussion

6.1 Summary of main results of my thesis

The aim of this thesis was to test for early neuronal dysfunction in *dparkin* mutant larvae. These mutant larvae show locomotory defects, neurophysiological dysfunction, and overgrowth at the neuromuscular junction (NMJ). Neuronal loss of *dparkin* is key to the synaptic failure observed in *dparkin* larvae. Oxidative stress induced signaling contributes to the *dparkin* mutant larval phenotypes, as increased expression of *SOD1* or the detoxification enzymes Glutathione-s-transferase (*GST*) or Thioredoxin reductase (*TRX-R2*) rescues the phenotypes. Genetic manipulation of the c-jun-N-terminal kinase (*JNK*) signaling pathway also rescued the *dparkin* phenotype. Additionally, genetically manipulating AMP-activated protein Kinase (*AMPK*), which is involved in the energy homeostasis, rescued the overgrowth and neurophysiological dysfunction but failed to rescue the locomotory defects. Pharmacological manipulation with classical *AMPK* activators (metformin and 5-Aminoimidazole-4-carboxamide ribonucleotide (AICAR)) failed to show a rescue of *dparkin* mutant larval phenotypes. Resveratrol also failed to rescue either overgrowth, neurophysiological or locomotory defects. Dopaminergic manipulations, either pharmacological (L-DOPA) or genetic (*TH*> *dparkin* RNAi) failed to show an effect on overgrowth or locomotory defect.

6.2 Main significance of this thesis

The most significant finding is that it is the neuronal, rather than muscle, loss of *dparkin* that causes locomotory defect in the larva. As noted in chapter 3, previous work had focused on muscle phenotypes; my work is a direct demonstration of a neuronal phenotype at the centre of the *dparkin* defects, and these conclusions were supported by other assays in our lab (Vincent et al., 2012). This makes this larval model of *dparkin*, a particularly useful model of PD. In particular, the demonstration of defects in synaptic

signaling and synaptic overgrowth at a non-dopaminergic (glutamatergic) synapse is important for two reasons. First, it shows that *dparkin* affects not just the dopaminergic system, but other types of neurons, in accord with Braak's hypothesis. Here I note that a larval phenotype was not induced by either *TH > dparkin* RNAi or L-DOPA application. Second, glutamatergic neurons are the most important excitatory neurons in the human brain and the fly neuromuscular junction (NMJ) is proving a significant model of their synapses. This means that the armory of the fly NMJ can, in the future, be deployed to examine the *dparkin* synapse in more detail.

It was also demonstrated here (chapter 4) that oxidative stress was not the cause of neuronal dysfunction, but a secondary consequence. Again, this work was supported by other data presented in Vincent *et al.* (2012), showing metabolic deficits lead to a failure to maintain the normal RMP and synaptic failure, and subsequent oxidative stress.

6.3 Further work investigating the neuronal dysfunction in *dparkin* larvae

One of the key observations in chapter 3, was that *dparkin* expression in nerve or muscle provided rescue both pre- and post-synaptically (of at least some phenotypes). This implied trans-synaptic, non autonomous signaling. It was hypothesized that this trans-synaptic rescue could be mediated by *D. melanogaster* PARKIN itself, by ROS-dependent signals or by a range of growth factors. The fly genetic toolbox provides ways to test these hypotheses. The first hypothesis could be tested by generating a tagged version of *dparkin*, e.g. with a GFP or his/or FLAG tag could be expressed, and immunocytochemistry used to test for its presence in/around the synapse. Secondly, reactive oxygen species (ROS)-signaling could be reduced either pre- or post – synaptically by using *elav*- or *G14*-GAL4 expression of GST, in a manner similar to the ubiquitous expression in chapter 4. This would show if ROS signaling were key.

Equally, a range of growth factor transgenes could be deployed in the *dparkin* background, in a nerve/muscle specific manner.

An exquisitely sensitive approach in this context would be to attempt rescue of *dparkin* in one muscle, while the adjacent muscle was still *dparkin*. The fly offers a suitable tool: the H94-GAL4 line that would drive wild-type UAS-*dparkin* in a mutant background in some of the muscles (not all). This would allow particular muscles to contain wild-type *dparkin* and others to possess a mutant background, all in a single larval (NMJ preparation). The H94 driver will drive specific expression of *dparkin* in few muscles including 6, 13 and moderately in 12 (and very low levels in some motoneurons) whilst others will contain the *dparkin* mutation (Davis et al., 1997). This will measure the RMP and synaptic activity within one preparation, thus limiting variability between preparations. Other drivers also exist such as 5053A-GAL4 line that drives highly in muscle 12 (Ritzenthaler et al., 2000). Similarly, ROS signaling or growth factors could be expressed in this way. Muscles 13 and 13 are innervated by two motoneurons, V and RP5, providing the opportunity for transgenic manipulation of a single motoneuron while using the muscle and other motoneuron as reporters.

The depolarization of the muscle RMP in *dparkin* larvae suggested that the motoneuron may also be depolarized, as the same ATP-dependent system is required to maintain both nerve and muscle RMP. The development of novel, genetically encoded voltage sensors offers the opportunity to record the motoneuron resting membrane potential directly (Jin et al., 2011). The change in mEJP suggested that calcium dynamics may be affected, and the latest genetically modified calcium indicators (G-CAMP) sensors provide tools to investigate this. Again the use of the specific GAL4 lines provides the opportunity to use in preparation controls.

6.4 Larval and adult phenotypes

A key reason for investigating the *dparkin* larva was to assess the early steps in the toxic cascade of PD. It is clear from Fig 6.1 that the physiological rescue by transgenes mostly results in behavioral rescue; whereas if the transgene only rescues the synaptic overgrowth, behavioral rescue is less likely. The larvae can, at this early stage, compensate for the neuronal overgrowth, but not for physiological failure. Third instar larvae are under a maximal metabolic load, as they prepare to pupate (Rechsteiner, 1970a, Rechsteiner, 1970b). Those *dparkin* larvae that do eclose successfully as adults will have a lower metabolic stress, and so may be more responsive to genetic or pharmacological manipulations, for example, with the expression of *GST* or *BSK^{DN}* as observed in chapter 4.

Does loss of *parkin* cause dysfunction in the early juvenile fly?

	Behavioral: Reduced crawling	Anatomical: Overgrown synapses	Physiological: Synaptic dysfunction and resting potential defects
<i>parkin</i>	✓	✓	✓
SOD1	✗	✓	✗
SOD2	✗	✗	✗
CAT	✗	✗	✗
GST	✓	???	✓
TRX-R2	✗	???	✓
JNK ^{DN}	✓	???	✓
JUN ^{DN}	✗	✓	✓
AMPK	✗	✓	✓

Transgenes involved in the rescue of *dparkin* dysfunction?

Figure 6.1 Summary of experiments with genetic expression of transgenes. *dparkin* mutant larvae show locomotory defects, neurophysiological dysfunction, and overgrowth at the neuromuscular junction (NMJ). Neuronal loss of *dparkin* is key to the synaptic failure observed in *dparkin* larvae. Oxidative stress induced signaling contributes to the *dparkin* mutant larval phenotypes, as increased expression of *SOD1* or the detoxification enzymes Glutathione-s-transferase (*GST*) or Thioredoxin reductase (*TRX-R2*) rescues the phenotypes. Genetic manipulation of the c-jun-N-terminal kinase (*JNK*) signaling pathway also rescued the *dparkin* phenotypes. Additionally, genetically manipulating AMP-activated protein Kinase (*AMPK*), which is involved in the energy homeostasis, rescued the overgrowth and neurophysiological dysfunction but failed to rescue the locomotory defects.

6.5 Comparison of pharmacological and genetic approaches

Whereas all the transgenes tested showed at least a partial rescue on either the *dparkin* transheterozygote (chapter 3) or on the *dparkin* homozygote (Vincent et al., 2012), none of the drugs tested showed significant rescue. Although feeding drugs to larvae in this way proved useful for the fly model of *LRRK2*-PD (Afsari et al., 2014), my work suggests that the genetic approach is more powerful than the pharmacologic. In this context, it should be noted that Vos et al. (2012) used bacterial culture of *E. coli* to provide vitamin K₂ in their pharmacologic rescue of *PINK1* or *dparkin* larvae (Vos et al., 2012).

6.6 Implication for Parkinson's Disease therapy

Oxidative stress is commonly seen in a variety of neurodegenerative conditions, including PD. Oxidative stress has been an attractive target for the treatment of PD although it has been a challenge to place this pathogenic factor in the cascade of PD pathogenesis. A large clinical study, known as DATATOP, showed the lack of effect of α -tocopherol (Vitamin E) on the progression of PD (Shoulson, 1998). Coenzyme Q₁₀ is responsible to shuttle electrons via the electron chain. Additionally, ubiquinol (Coenzyme Q₁₀ reduced form) functions as an antioxidant (Ernster and Dallner, 1995). In one pilot study, positive effects were observed in PD patients, such as increased complex I activity, with administration of Coenzyme Q₁₀ (Shults et al., 1998). Another later study showed negative effects in PD patients (Shults et al., 2002), thus showing mixed results from clinical trials. My data suggests that relieving oxidative stress does not affect the primary *dparkin* deficit, and (if this is a faithful model) that such clinical trials need further investigation and more care.

The failure of the trials is not conclusive enough to state that oxidative stress is not

important in PD but may be attributable to the defects in the pharmacological agent used in patients. Small anti-oxidant molecules such as vitamin E seem to be far less effective. I speculate from the effective genetic rescue that a more promising approach could result from focusing our attention on the up-regulation of endogenous anti-oxidant systems such as the thioredoxin and glutathione defence mechanisms. Thus, dysfunctional mitochondria, alterations in mitochondrial dynamics, increased ROS, mtDNA damage, and the loss of energy production are important contributors to the pathophysiology associated with several neurodegenerative diseases including Alzheimer's (AD), PD, and Huntington Disease (HD), and also cancer.

However, the treatment of one or few antioxidants is too simplistic, as reported by the several clinical studies that have shown modest success with antioxidants in the treatment of neurodegenerative diseases (Firuzi et al., 2011). This study showed the importance of energy maintenance to keep up with the demands of neuronal metabolism. A cocktail of drugs with a combination of antioxidant or combination of drugs targeted to other factors of PD such as the metabolic defects, may increase the likelihood of producing significant neuroprotective effect as PD is multi-factorial disease. Current drugs used to target other diseases, for instance metformin used to treat patients with type-2 diabetes could be trailed in PD to target metabolic dysfunction that could result in a neuroprotective effect in PD itself. More effort need to be put into solving energetic failure, as this is the root cause results in secondary effects (i.e. oxidative stress). Creatine/ phosphocreatine system provides an alternative pathway (from glycolysis and oxidative phosphorylation) to promote ATP synthesis. Supporting this, studies with creatine have shown to boost pathways that promote energy synthesis and additional antioxidant actions. Although efforts have begun on this potential neuroprotective agent in PD models (Matthews et al., 1999), there is need for other.

Creatine has been tested and shows signs as a promising agent, but large clinical trials need to be undertaken to validate it as a neuroprotective agent (Ravina et al., 2003).

Abbreviation List

AD	Alzheimer's Disease
ADP	Adenosine Diphosphate
AICAR	5-Aminoimidazole-4-carboxamide 1- β -D-ribofuranoside
AMP	Adenosine Monophosphate
AMPK	AMP-activated Protein Kinase
ANOVA	Analysis of Variance
AP	Action Potential
AP-1	Activator Protein-1
ARJP	Autosomal Recessive Juvenile Parkinsonism
ASK	Apoptosis Signal Regulating Kinase
ATG	Autophagy Related Gene
ATP	Adenosine Triphosphate
Ca ²⁺	Calcium ion
CAT	Catalase
CNS	Central Nervous System
CPG	Central Pattern Generator
CS	Canton-S
Cy3	Cyanine-3 dye

CyO	Curly of Oyster
D-DOPA	3-(3,4-Dihydroxyphenyl)-D-alanine
DA	Dopaminergic Neurons
DDC	DOPA decarboxylase
DN	Dominant Negative
DNA	Deoxyribose Nucleic Acid
DOPAC	Dihydroxyphenyl Acetic Acid
DVMAT	Drosophila Vesicular Aminergic Transporter
EJP	Excitatory Junctional Potential
<i>ELAV</i>	Embryonic Lethal Abnormal Vision
EM	Electron Microscopy
EMS	Ethyl Methane Sulfonate
ER	Endoplasmic reticulum
ETC	Electron Transport Chain
EtOH	Ethanol
FITC	Fluorescein Isothiocyanate
GFP	Green Fluorescent Protein
GST	Glutathione-s-Transferase
H ₂ O	Water

H ₂ O ₂	Hydrogen Peroxide
HL3	Hemolymph-like Buffer solution 3
HRP	Horseradish Peroxidase
JNK	c-jun N-terminal kinase
K ⁺	Potassium ions
L-DOPA	Levodopa
MAO	Monoamine Oxidase
MDA	Malondialdehyde
mDNA	Mitochondrial Deoxyribose Nucleic Acid
mEJP	Minature Excitatory Junctional Potential
minis	Minature Excitatory Junctional Potential
min	Minute
MKKK	Mitogen-Activated Protein Kinase Kinase Kinase
MKRS	Third Chromosome Stubble Marker
mm	Millimeter
mM	Millimolar
MPP ⁺	1-Methyl-4-Phenyl-Pyridinium
MPTP	1-Methyl-4-Phenyl-1,2,3,6-Tetrahydropyridine
mRNA	Messenger RNA

MSA	Muscle Surface Area
mV	Millivolts
Na ⁺	Sodium ion
Na ⁺ /K ⁺ - ATPase	Sodium/ Potassium-ATPase
NMJ	Neuromuscular junction
NO	Nitric Oxide
NOS	Nitric Oxide Synthase
Nrf2	Nuclear factor (erythroid-derived 2)-like 2
O ₂	Oxygen
O ₂ ⁻	Superoxide Anions
OH [·]	Hydroxyl Radical
OH ⁻	Hydroxyl Anion
PBS	Phosphate Buffered Saline
PBS-T	Phosphate Buffered Saline-Triton
PCR	Polymerase Chain Reaction
PD	Parkinson's Disease
PDE	Phosphodiesterase enzyme
PGK	Phosphoglycerate Kinase
RMP	Resting Membrane Potential

RNAi	(Interfering) Ribonucleic Acid
RNS	Reactive Nitrogen Species
ROS	Reactive Oxygen Species
Sec	Second
SN	Segmental Nerve
SOD	Superoxide Dismutase
SPSS	Software for Statistical Analysis
SYT	Synaptotagmin
TH	Tyrosine Hydroxylase
TM6B	Third Chromosome Tubby Marker
TOR	Target of Rapamycin
TORC	Target of Rapamycin complex
Trx	Thioredoxin
Trx-R	Thioredoxin Reductase
UAS	Upstream Activating Sequence
VMAT	Vesicular Aminergic Transporter
ZMP	AICAR Monophosphate
μm	Micrometer
μM	Micromolar

References

1. ABELIOVICH, A., SCHMITZ, Y., FARIÑAS, I., CHOI-LUNDBERG, D., HO, W. H., CASTILLO, P. E., SHINSKY, N., VERDUGO, J. M., ARMANINI, M., RYAN, A., HYNES, M., PHILLIPS, H., SULZER, D. & ROSENTHAL, A. 2000. Mice lacking alpha-synuclein display functional deficits in the nigrostriatal dopamine system. *Neuron*, 25, 239-52.
2. ABERLE, H., HAGHIGHI, A. P., FETTER, R. D., MCCABE, B. D., MAGALHÃES, T. R. & GOODMAN, C. S. 2002. wishful thinking encodes a BMP type II receptor that regulates synaptic growth in *Drosophila*. *Neuron*, 33, 545-58.
3. ABOU-SLEIMAN, P. M., MUQIT, M. M. & WOOD, N. W. 2006. Expanding insights of mitochondrial dysfunction in Parkinson's disease. *Nat Rev Neurosci*, 7, 207-19.
4. ADAMS, M. D., CELNIKER, S. E., HOLT, R. A., EVANS, C. A., GOCAYNE, J. D., AMANATIDES, P. G., SCHERER, S. E., LI, P. W., HOSKINS, R. A., GALLE, R. F., GEORGE, R. A., LEWIS, S. E., RICHARDS, S., ASHBURNER, M., HENDERSON, S. N., SUTTON, G. G., WORTMAN, J. R., YANDELL, M. D., ZHANG, Q., CHEN, L. X., BRANDON, R. C., ROGERS, Y. H., BLAZEJ, R. G., CHAMPE, M., PFEIFFER, B. D., WAN, K. H., DOYLE, C., BAXTER, E. G., HELT, G., NELSON, C. R., GABOR, G. L., ABRIL, J. F., AGBAYANI, A., AN, H. J., ANDREWS-PFANNKOCH, C., BALDWIN, D., BALLEW, R. M., BASU, A., BAXENDALE, J., BAYRAKTAROGLU, L., BEASLEY, E. M., BEESON, K. Y., BENOS, P. V., BERMAN, B. P., BHANDARI, D., BOLSHAKOV, S., BORKOVA, D., BOTCHAN, M. R., BOUCK, J., BROKSTEIN, P., BROTTIER, P., BURTIS, K. C., BUSAM, D. A., BUTLER, H., CADIEU, E., CENTER, A., CHANDRA, I., CHERRY, J. M., CAWLEY, S., DAHLKE, C., DAVENPORT, L. B., DAVIES, P., DE PABLOS, B., DELCHER, A., DENG, Z., MAYS, A. D., DEW, I., DIETZ, S. M., DODSON, K., DOUP, L. E., DOWNES, M., DUGAN-ROCHA, S., DUNKOV, B. C., DUNN, P., DURBIN, K. J., EVANGELISTA, C. C., FERRAZ, C., FERRIERA, S., FLEISCHMANN, W., FOSLER, C.,

- GABRIELIAN, A. E., GARG, N. S., GELBART, W. M., GLASSER, K., GLODEK, A., GONG, F., GORRELL, J. H., GU, Z., GUAN, P., HARRIS, M., HARRIS, N. L., HARVEY, D., HEIMAN, T. J., HERNANDEZ, J. R., HOUCK, J., HOSTIN, D., HOUSTON, K. A., HOWLAND, T. J., WEI, M. H., IBEGWAM, C., et al. 2000. The genome sequence of *Drosophila melanogaster*. *Science*, 287, 2185-95.
5. ADLER, A. I., SHAW, E. J., STOKES, T. & RUIZ, F. 2009. [New drugs for control of blood glucose in type 2 diabetes: summary of the NICE guidelines]. *Praxis (Bern 1994)*, 98, 1161-3.
6. AFSARI, F., CHRISTENSEN, K. V., SMITH, G. P., HENTZER, M., NIPPE, O. M., ELLIOTT, C. J. & WADE, A. R. 2014. Abnormal visual gain control in a Parkinson's disease model. *Hum Mol Genet*, 23, 4465-78.
7. ALESUTAN, I., MUNOZ, C., SOPJANI, M., DËRMAKU-SOPJANI, M., MICHAEL, D., FRASER, S., KEMP, B. E., SEEBOHM, G., FÖLLER, M. & LANG, F. 2011. Inhibition of Kir2.1 (KCNJ2) by the AMP-activated protein kinase. *Biochem Biophys Res Commun*, 408, 505-10.
8. ALLE, H., ROTH, A. & GEIGER, J. R. 2009. Energy-efficient action potentials in hippocampal mossy fibers. *Science*, 325, 1405-8.
9. ANDOH, T., CHIUEH, C. C. & CHOCK, P. B. 2003. Cyclic GMP-dependent protein kinase regulates the expression of thioredoxin and thioredoxin peroxidase-1 during hormesis in response to oxidative stress-induced apoptosis. *J Biol Chem*, 278, 885-90.
10. ANDOH, T., CHOCK, P. B. & CHIUEH, C. C. 2002. The roles of thioredoxin in protection against oxidative stress-induced apoptosis in SH-SY5Y cells. *J Biol Chem*, 277, 9655-60.
11. ANNEPU, J. & RAVINDRANATH, V. 2000. 1-Methyl-4-phenyl-1,2,3,6-tetrahydropyridine-induced complex I inhibition is reversed by disulfide reductant, dithiothreitol in mouse brain. *Neurosci Lett*, 289, 209-12.
12. ANWAR, S., PETERS, O., MILLERSHIP, S., NINKINA, N., DOIG, N.,

- CONNOR-ROBSON, N., THRELFELL, S., KOONER, G., DEACON, R. M., BANNERMAN, D. M., BOLAM, J. P., CHANDRA, S. S., CRAGG, S. J., WADE-MARTINS, R. & BUCHMAN, V. L. 2011. Functional alterations to the nigrostriatal system in mice lacking all three members of the synuclein family. *J Neurosci*, 31, 7264-74.
13. ATTWELL, D. & LAUGHLIN, S. B. 2001. An energy budget for signaling in the grey matter of the brain. *J Cereb Blood Flow Metab*, 21, 1133-45.
 14. ATWOOD, H. L., GOVIND, C. K. & WU, C. F. 1993. Differential ultrastructure of synaptic terminals on ventral longitudinal abdominal muscles in *Drosophila* larvae. *J Neurobiol*, 24, 1008-24.
 15. AULUCK, P. K., CHAN, H. Y., TROJANOWSKI, J. Q., LEE, V. M. & BONINI, N. M. 2002. Chaperone suppression of alpha-synuclein toxicity in a *Drosophila* model for Parkinson's disease. *Science*, 295, 865-8.
 16. AULUCK, P. K., MEULENER, M. C. & BONINI, N. M. 2005. Mechanisms of Suppression of {alpha}-Synuclein Neurotoxicity by Geldanamycin in *Drosophila*. *J Biol Chem*, 280, 2873-8.
 17. BAE, Y. J., PARK, K. S. & KANG, S. J. 2003. Genomic organization and expression of parkin in *Drosophila melanogaster*. *Exp Mol Med*, 35, 393-402.
 18. BARCLAY, J. W., ATWOOD, H. L. & ROBERTSON, R. M. 2002. Impairment of central pattern generation in *Drosophila* cysteine string protein mutants. *J Comp Physiol A Neuroethol Sens Neural Behav Physiol*, 188, 71-8.
 19. BASS, T. M., WEINKOVE, D., HOUTHOOFD, K., GEMS, D. & PARTRIDGE, L. 2007. Effects of resveratrol on lifespan in *Drosophila melanogaster* and *Caenorhabditis elegans*. *Mech Ageing Dev*, 128, 546-52.
 20. BATANDIER, C., GUIGAS, B., DETAILLE, D., EL-MIR, M. Y., FONTAINE, E., RIGOLET, M. & LEVERVE, X. M. 2006. The ROS production induced by a reverse-electron flux at respiratory-chain complex 1 is hampered by metformin. *J Bioenerg Biomembr*, 38, 33-42.
 21. BAUR, J. A. & SINCLAIR, D. A. 2006. Therapeutic potential of

resveratrol: the in vivo evidence. *Nat Rev Drug Discov*, 5, 493-506.

22. BAUR, J. A. 2010. Biochemical effects of SIRT1 activators. *Biochim Biophys Acta*, 1804, 1626-34.
23. BAUR, J. A., PEARSON, K. J., PRICE, N. L., JAMIESON, H. A., LERIN, C., KALRA, A., PRABHU, V. V., ALLARD, J. S., LOPEZ-LLUCH, G., LEWIS, K., PISTELL, P. J., POOSALA, S., BECKER, K. G., BOSS, O., GWINN, D., WANG, M., RAMASWAMY, S., FISHBEIN, K. W., SPENCER, R. G., LAKATTA, E. G., LE COUTEUR, D., SHAW, R. J., NAVAS, P., PUIGSERVER, P., INGRAM, D. K., DE CABO, R. & SINCLAIR, D. A. 2006. Resveratrol improves health and survival of mice on a high-calorie diet. *Nature*, 444, 337-42.
24. BELLEN, H. J. 1999. Ten years of enhancer detection: lessons from the fly. *Plant Cell*, 11, 2271-81.
25. BELLEN, H. J., TONG, C. & TSUDA, H. 2010. 100 years of *Drosophila* research and its impact on vertebrate neuroscience: a history lesson for the future. *Nat Rev Neurosci*, 11, 514-22.
26. BENDER, A., KRISHNAN, K. J., MORRIS, C. M., TAYLOR, G. A., REEVE, A. K., PERRY, R. H., JAROS, E., HERSHESON, J. S., BETTS, J., KLOPSTOCK, T., TAYLOR, R. W. & TURNBULL, D. M. 2006. High levels of mitochondrial DNA deletions in substantia nigra neurons in aging and Parkinson disease. *Nat Genet*, 38, 515-7.
27. BENINGER, R. J. 1983. The role of dopamine in locomotor activity and learning. *Brain Res*, 287, 173-96.
28. BERMAN, S. B. & HASTINGS, T. G. 1999. Dopamine oxidation alters mitochondrial respiration and induces permeability transition in brain mitochondria: implications for Parkinson's disease. *J Neurochem*, 73, 1127-37.
29. BIER, E. 2005. *Drosophila*, the golden bug, emerges as a tool for human genetics. *Nat Rev Genet*, 6, 9-23.
30. BILEN, J. & BONINI, N. M. 2005. *Drosophila* as a model for human

neurodegenerative disease. *Annu Rev Genet*, 39, 153-71.

31. BOGAERTS, V., THEUNS, J. & VAN BROECKHOVEN, C. 2008. Genetic findings in Parkinson's disease and translation into treatment: a leading role for mitochondria? *Genes Brain Behav*, 7, 129-51.
32. BONIFATI, V., RIZZU, P., SQUITIERI, F., KRIEGER, E., VANACORE, N., VAN SWIETEN, J. C., BRICE, A., VAN DUIJN, C. M., OOSTRA, B., MECO, G. & HEUTINK, P. 2003. DJ-1(PARK7), a novel gene for autosomal recessive, early onset parkinsonism. *Neurol Sci*, 24, 159-60.
33. BONILLA, E., CONTRERAS, R., MEDINA-LEENDERTZ, S., MORA, M., VILLALOBOS, V. & BRAVO, Y. 2012. Minocycline increases the life span and motor activity and decreases lipid peroxidation in manganese treated *Drosophila melanogaster*. *Toxicology*, 294, 50-3.
34. BOTELLA, J. A., BAYERSDORFER, F. & SCHNEUWLY, S. 2008. Superoxide dismutase overexpression protects dopaminergic neurons in a *Drosophila* model of Parkinson's disease. *Neurobiol Dis*, 30, 65-73.
35. BOVÉ, J., PROU, D., PERIER, C. & PRZEDBORSKI, S. 2005. Toxin-induced models of Parkinson's disease. *NeuroRx*, 2, 484-94.
36. BRAAK, H. & DEL TREDICI, K. 2008. Invited Article: Nervous system pathology in sporadic Parkinson disease. *Neurology*, 70, 1916-25.
37. BRAAK, H., RÜB, U., GAI, W. P. & DEL TREDICI, K. 2003. Idiopathic Parkinson's disease: possible routes by which vulnerable neuronal types may be subject to neuroinvasion by an unknown pathogen. *J Neural Transm*, 110, 517-36.
38. BRAND, A. H. & PERRIMON, N. 1993. Targeted gene expression as a means of altering cell fates and generating dominant phenotypes. *Development*, 118, 401-15.
39. BRAZIER, M. A. 1979. Challenges from the philosophers to the neuroscientists. *Ciba Found Symp*, 5-43.

40. BROADIE, K. S. & RICHMOND, J. E. 2002. Establishing and sculpting the synapse in *Drosophila* and *C. elegans*. *Curr Opin Neurobiol*, 12, 491-8.
41. BROADIE, K. S. 1995. Genetic dissection of the molecular mechanisms of transmitter vesicle release during synaptic transmission. *J Physiol Paris*, 89, 59-70.
42. BROADIE, K., PROKOP, A., BELLEN, H. J., O'KANE, C. J., SCHULZE, K. L. & SWEENEY, S. T. 1995. Syntaxin and synaptobrevin function downstream of vesicle docking in *Drosophila*. *Neuron*, 15, 663-73.
43. BROIHIER, H. T. & SKEATH, J. B. 2002. *Drosophila* homeodomain protein dHb9 directs neuronal fate via crossrepressive and cell-nonautonomous mechanisms. *Neuron*, 35, 39-50.
44. BUDNIK, V. & WHITE, K. 1988. Catecholamine-containing neurons in *Drosophila melanogaster*: distribution and development. *J Comp Neurol*, 268, 400-13.
45. BUDNIK, V., MARTIN-MORRIS, L. & WHITE, K. 1986. Perturbed pattern of catecholamine-containing neurons in mutant *Drosophila* deficient in the enzyme dopa decarboxylase. *J Neurosci*, 6, 3682-91.
46. BUDNIK, V., ZHONG, Y. & WU, C. F. 1990. Morphological plasticity of motor axons in *Drosophila* mutants with altered excitability. *J Neurosci*, 10, 3754-68.
47. BURKE, R. E., DAUER, W. T. & VONSATTEL, J. P. 2008. A critical evaluation of the Braak staging scheme for Parkinson's disease. *Ann Neurol*, 64, 485-91.
48. CALABRESE, E. J. 2008. Neuroscience and hormesis: overview and general findings. *Crit Rev Toxicol*, 38, 249-52.
49. CARPENTER, J. M. 1950. A new semi-synthetic food medium for *Drosophila*. *Drosophila Information Service*
50. CASTILLO-QUAN, J. I. 2011. Parkin' control: regulation of PGC-1 α

through PARIS in Parkinson's disease. *Dis Model Mech*, 4, 427-9.

51. CATTART, D. & BIRMAN, S. 2001. Blockade of the central generator of locomotor rhythm by noncompetitive NMDA receptor antagonists in *Drosophila* larvae. *J Neurobiol*, 48, 58-73.
52. CAUDLE, W. M., COLEBROOKE, R. E., EMSON, P. C. & MILLER, G. W. 2008. Altered vesicular dopamine storage in Parkinson's disease: a premature demise. *Trends Neurosci*, 31, 303-8.
53. CERTEL, S. J. & THOR, S. 2004. Specification of *Drosophila* motoneuron identity by the combinatorial action of POU and LIM-HD factors. *Development*, 131, 5429-39.
54. CHA, G. H., KIM, S., PARK, J., LEE, E., KIM, M., LEE, S. B., KIM, J. M., CHUNG, J. & CHO, K. S. 2005. Parkin negatively regulates JNK pathway in the dopaminergic neurons of *Drosophila*. *Proc Natl Acad Sci U S A*, 102, 10345-50.
55. CHANDRA, S., FORNAI, F., KWON, H. B., YAZDANI, U., ATASOY, D., LIU, X., HAMMER, R. E., BATTAGLIA, G., GERMAN, D. C., CASTILLO, P. E. & SÜDHOF, T. C. 2004. Double-knockout mice for alpha- and beta-synucleins: effect on synaptic functions. *Proc Natl Acad Sci U S A*, 101, 14966-71.
56. CHANDRASHEKARA, K. T. & SHAKARAD, M. N. 2011. Aloe vera or resveratrol supplementation in larval diet delays adult aging in the fruit fly, *Drosophila melanogaster*. *J Gerontol A Biol Sci Med Sci*, 66, 965-71.
57. CHANG, H. Y., GRYGORUK, A., BROOKS, E. S., ACKERSON, L. C., MAIDMENT, N. T., BAINTON, R. J. & KRANTZ, D. E. 2006. Overexpression of the *Drosophila* vesicular monoamine transporter increases motor activity and courtship but decreases the behavioral response to cocaine. *Mol Psychiatry*, 11, 99-113.
58. CHARTIER-HARLIN, M. C., DACHSEL, J. C., VILARIÑO-GÜELL, C., LINCOLN, S. J., LEPRÊTRE, F., HULIHAN, M. M., KACHERGUS, J.,

- MILNERWOOD, A. J., TAPIA, L., SONG, M. S., LE RHUN, E., MUTEZ, E., LARVOR, L., DUFLOT, A., VANBESIEN-MAILLIOT, C., KREISLER, A., ROSS, O. A., NISHIOKA, K., SOTO-ORTOLAZA, A. I., COBB, S. A., MELROSE, H. L., BEHROUZ, B., KEELING, B. H., BACON, J. A., HENTATI, E., WILLIAMS, L., YANAGIYA, A., SONENBERG, N., LOCKHART, P. J., ZUBAIR, A. C., UTTI, R. J., AASLY, J. O., KRYGOWSKA-WAJS, A., OPALA, G., WSZOLEK, Z. K., FRIGERIO, R., MARAGANORE, D. M., GOSAL, D., LYNCH, T., HUTCHINSON, M., BENTIVOGLIO, A. R., VALENTE, E. M., NICHOLS, W. C., PANKRATZ, N., FOROUD, T., GIBSON, R. A., HENTATI, F., DICKSON, D. W., DESTÉE, A. & FARRER, M. J. 2011. Translation initiator EIF4G1 mutations in familial Parkinson disease. *Am J Hum Genet*, 89, 398-406.
59. CHASE, T. N., HOLDEN, E. M. & BRODY, J. A. 1973. Levodopa-induced dyskinesias. Comparison in Parkinsonism-dementia and amyotrophic lateral sclerosis. *Arch Neurol*, 29, 328-33.
60. CHAUDHRY, F. A., REIMER, R. J., BELLOCCHIO, E. E., DANBOLT, N. C., OSEN, K. K., EDWARDS, R. H. & STORM-MATHISEN, J. 1998. The vesicular GABA transporter, VGAT, localizes to synaptic vesicles in sets of glycinergic as well as GABAergic neurons. *J Neurosci*, 18, 9733-50.
61. CHAUDHURI, K. R. & SCHAPIRA, A. H. 2009. Non-motor symptoms of Parkinson's disease: dopaminergic pathophysiology and treatment. *Lancet Neurol*, 8, 464-74.
62. CHEN, C. Y., JANG, J. H., LI, M. H. & SURH, Y. J. 2005. Resveratrol upregulates heme oxygenase-1 expression via activation of NF-E2-related factor 2 in PC12 cells. *Biochem Biophys Res Commun*, 331, 993-1000.
63. CHINTA, S. J., KUMAR, J. M., ZHANG, H., FORMAN, H. J. & ANDERSEN, J. K. 2006. Up-regulation of gamma-glutamyl transpeptidase activity following glutathione depletion has a compensatory rather than an inhibitory effect on mitochondrial complex I activity: implications for Parkinson's disease. *Free Radic Biol Med*, 40, 1557-63.

64. CHINTAPALLI, V. R., WANG, J. & DOW, J. A. 2007. Using FlyAtlas to identify better *Drosophila melanogaster* models of human disease. *Nat Genet*, 39, 715-20.
65. CHOI, J. C., PARK, D. & GRIFFITH, L. C. 2004. Electrophysiological and morphological characterization of identified motor neurons in the *Drosophila* third instar larva central nervous system. *J Neurophysiol*, 91, 2353-65.
66. CHOI, J. S., PARK, C. & JEONG, J. W. 2010. AMP-activated protein kinase is activated in Parkinson's disease models mediated by 1-methyl-4-phenyl-1,2,3,6-tetrahydropyridine. *Biochem Biophys Res Commun*, 391, 147-51.
67. CHUNG, K. K., DAWSON, V. L. & DAWSON, T. M. 2001. The role of the ubiquitin-proteasomal pathway in Parkinson's disease and other neurodegenerative disorders. *Trends Neurosci*, 24, S7-14.
68. CLARK, I. E., DODSON, M. W., JIANG, C., CAO, J. H., HUH, J. R., SEOL, J. H., YOO, S. J., HAY, B. A. & GUO, M. 2006. *Drosophila pink1* is required for mitochondrial function and interacts genetically with parkin. *Nature*, 441, 1162-6.
69. CLARK, L. N., ROSS, B. M., WANG, Y., MEJIA-SANTANA, H., HARRIS, J., LOUIS, E. D., COTE, L. J., ANDREWS, H., FAHN, S., WATERS, C., FORD, B., FRUCHT, S., OTTMAN, R. & MARDER, K. 2007. Mutations in the glucocerebrosidase gene are associated with early-onset Parkinson disease. *Neurology*, 69, 1270-7.
70. CLAYTON, J. D., CRIPPS, R. M., SPARROW, J. C. & BULLARD, B. 1998. Interaction of troponin-H and glutathione S-transferase-2 in the indirect flight muscles of *Drosophila melanogaster*. *J Muscle Res Cell Motil*, 19, 117-27.
71. COHEN, G. 1984. Oxy-radical toxicity in catecholamine neurons. *Neurotoxicology*, 5, 77-82.
72. COLLINS, C. A. & DIANTONIO, A. 2007. Synaptic development: insights from *Drosophila*. *Curr Opin Neurobiol*, 17, 35-42.
73. CORTI, O., LESAGE, S. & BRICE, A. 2011. What genetics tells us about

the causes and mechanisms of Parkinson's disease. *Physiol Rev*, 91, 1161-218.

74. CORTON, J. M., GILLESPIE, J. G., HAWLEY, S. A. & HARDIE, D. G. 1995. 5-aminoimidazole-4-carboxamide ribonucleoside. A specific method for activating AMP-activated protein kinase in intact cells? *Eur J Biochem*, 229, 558-65.
75. COTZIAS, G. C., PAPAVALIIOU, P. S. & GELLENE, R. 1969. L-dopa in parkinson's syndrome. *N Engl J Med*, 281, 272.
76. COULOM, H. & BIRMAN, S. 2004. Chronic exposure to rotenone models sporadic Parkinson's disease in *Drosophila melanogaster*. *J Neurosci*, 24, 10993-8.
77. CRISP, S., EVERS, J. F., FIALA, A. & BATE, M. 2008. The development of motor coordination in *Drosophila* embryos. *Development*, 135, 3707-17.
78. DAMIER, P., HIRSCH, E. C., AGID, Y. & GRAYBIEL, A. M. 1999. The substantia nigra of the human brain. II. Patterns of loss of dopamine-containing neurons in Parkinson's disease. *Brain*, 122 (Pt 8), 1437-48.
79. DAS, D. K. & MAULIK, N. 2006. Resveratrol in cardioprotection: a therapeutic promise of alternative medicine. *Mol Interv*, 6, 36-47.
80. DASGUPTA, B. & MILBRANDT, J. 2007. Resveratrol stimulates AMP kinase activity in neurons. *Proc Natl Acad Sci U S A*, 104, 7217-22.
81. DAUER, W. & PRZEDBORSKI, S. 2003. Parkinson's disease: mechanisms and models. *Neuron*, 39, 889-909.
82. DAVIS, G. W. 2006. Homeostatic control of neural activity: from phenomenology to molecular design. *Annu Rev Neurosci*, 29, 307-23.
83. DAVIS, G. W., SCHUSTER, C. M. & GOODMAN, C. S. 1997. Genetic analysis of the mechanisms controlling target selection: target-derived Fasciclin II regulates the pattern of synapse formation. *Neuron*, 19, 561-73.
84. DAWSON, T. M., KO, H. S. & DAWSON, V. L. 2010. Genetic animal

models of Parkinson's disease. *Neuron*, 66, 646-61.

85. DENG, H., DODSON, M. W., HUANG, H. & GUO, M. 2008. The Parkinson's disease genes pink1 and parkin promote mitochondrial fission and/or inhibit fusion in *Drosophila*. *Proc Natl Acad Sci U S A*, 105, 14503-8.
86. DEVOS, D., DUJARDIN, K., POIROT, I., MOREAU, C., COTTENCIN, O., THOMAS, P., DESTÉE, A., BORDET, R. & DEFEBVRE, L. 2008. Comparison of desipramine and citalopram treatments for depression in Parkinson's disease: a double-blind, randomized, placebo-controlled study. *Mov Disord*, 23, 850-7.
87. DIANTONIO, A., HAGHIGHI, A. P., PORTMAN, S. L., LEE, J. D., AMARANTO, A. M. & GOODMAN, C. S. 2001. Ubiquitination-dependent mechanisms regulate synaptic growth and function. *Nature*, 412, 449-52.
88. DICKMAN, D. K., LU, Z., MEINERTZHAGEN, I. A. & SCHWARZ, T. L. 2006. Altered synaptic development and active zone spacing in endocytosis mutants. *Curr Biol*, 16, 591-8.
89. DONG, Z., FERGER, B., PATERNA, J. C., VOGEL, D., FURLER, S., OSINDE, M., FELDON, J. & BÜELER, H. 2003. Dopamine-dependent neurodegeneration in rats induced by viral vector-mediated overexpression of the parkin target protein, CDCrel-1. *Proc Natl Acad Sci U S A*, 100, 12438-43.
90. DUDEL, J. & ORKAND, R. K. 1960. Spontaneous potential changes at crayfish neuromuscular junctions. *Nature*, 186, 476-7.
91. DUFFY, J. B. 2002. GAL4 system in *Drosophila*: a fly geneticist's Swiss army knife. *Genesis*, 34, 1-15.
92. EGAN, D. F., SHACKELFORD, D. B., MIHAYLOVA, M. M., GELINO, S., KOHNZ, R. A., MAIR, W., VASQUEZ, D. S., JOSHI, A., GWINN, D. M., TAYLOR, R., ASARA, J. M., FITZPATRICK, J., DILLIN, A., VIOLLET, B., KUNDU, M., HANSEN, M. & SHAW, R. J. 2011. Phosphorylation of ULK1 (hATG1) by AMP-activated protein kinase connects energy sensing to mitophagy. *Science*, 331, 456-61.

93. EIDEN, L. E., SCHÄFER, M. K., WEIHE, E. & SCHÜTZ, B. 2004. The vesicular amine transporter family (SLC18): amine/proton antiporters required for vesicular accumulation and regulated exocytotic secretion of monoamines and acetylcholine. *Pflugers Arch*, 447, 636-40.
94. EKSTRAND, M. I., TERZIOGLU, M., GALTER, D., ZHU, S., HOFSTETTER, C., LINDQVIST, E., THAMS, S., BERGSTRAND, A., HANSSON, F. S., TRIFUNOVIC, A., HOFFER, B., CULLHEIM, S., MOHAMMED, A. H., OLSON, L. & LARSSON, N. G. 2007. Progressive parkinsonism in mice with respiratory-chain-deficient dopamine neurons. *Proc Natl Acad Sci U S A*, 104, 1325-30.
95. EL-MIR, M. Y., NOGUEIRA, V., FONTAINE, E., AVÉRET, N., RIGOULET, M. & LEVERVE, X. 2000. Dimethylbiguanide inhibits cell respiration via an indirect effect targeted on the respiratory chain complex I. *J Biol Chem*, 275, 223-8.
96. EL-MOWAFY, A. M. & ALKHALAF, M. 2003. Resveratrol activates adenylyl-cyclase in human breast cancer cells: a novel, estrogen receptor-independent cytostatic mechanism. *Carcinogenesis*, 24, 869-73.
97. ERESH, S., RIESE, J., JACKSON, D. B., BOHMANN, D. & BIENZ, M. 1997. A CREB-binding site as a target for decapentaplegic signalling during *Drosophila* endoderm induction. *EMBO J*, 16, 2014-22.
98. ERICKSON, J. D. & VAROQUI, H. 2000. Molecular analysis of vesicular amine transporter function and targeting to secretory organelles. *FASEB J*, 14, 2450-8.
99. ERIKSEN, J. L., DAWSON, T. M., DICKSON, D. W. & PETRUCCELLI, L. 2003. Caught in the act: alpha-synuclein is the culprit in Parkinson's disease. *Neuron*, 40, 453-6.
100. ERNSTER, L. & DALLNER, G. 1995. Biochemical, physiological and medical aspects of ubiquinone function. *Biochim Biophys Acta*, 1271, 195-204.
101. EXNER, N., LUTZ, A. K., HAASS, C. & WINKLHOFER, K. F. 2012.

Mitochondrial dysfunction in Parkinson's disease: molecular mechanisms and pathophysiological consequences. *EMBO J*, 31, 3038-62.

102. FAHN, S. & GROUP, P. S. 2005. Does levodopa slow or hasten the rate of progression of Parkinson's disease? *J Neurol*, 252 Suppl 4, IV37-IV42.
103. FAHN, S. 2000. The spectrum of levodopa-induced dyskinesias. *Ann Neurol*, 47, S2-9; discussion S9-11.
104. FARRER, M. J. 2006. Genetics of Parkinson disease: paradigm shifts and future prospects. *Nat Rev Genet*, 7, 306-18.
105. FATT, P. & KATZ, B. 1952. Spontaneous subthreshold activity at motor nerve endings. *J Physiol*, 117, 109-28.
106. FEANY, M. B. & BENDER, W. W. 2000. A *Drosophila* model of Parkinson's disease. *Nature*, 404, 394-8.
107. FEANY, M. B. & PALLANCK, L. J. 2003. Parkin: a multipurpose neuroprotective agent? *Neuron*, 38, 13-6.
108. FEATHERSTONE, D. E. & BROADIE, K. 2000. Surprises from *Drosophila*: genetic mechanisms of synaptic development and plasticity. *Brain Res Bull*, 53, 501-11.
109. FENG, Y., UEDA, A. & WU, C. F. 2004. A modified minimal hemolymph-like solution, HL3.1, for physiological recordings at the neuromuscular junctions of normal and mutant *Drosophila* larvae. *J Neurogenet*, 18, 377-402.
110. FERNAGUT, P. O. & CHESSELET, M. F. 2004. Alpha-synuclein and transgenic mouse models. *Neurobiol Dis*, 17, 123-30.
111. FIRUZI, O., MIRI, R., TAVAKKOLI, M. & SASO, L. 2011. Antioxidant therapy: current status and future prospects. *Curr Med Chem*, 18, 3871-88.
112. FORNO, L. S. 1996. Neuropathology of Parkinson's disease. *J Neuropathol Exp Neurol*, 55, 259-72.
113. FOTOWAT, H., FAYYAZUDDIN, A., BELLEN, H. J. & GABBIANI, F.

2009. A novel neuronal pathway for visually guided escape in *Drosophila melanogaster*. *J Neurophysiol*, 102, 875-85.
114. FOX, L. E., SOLL, D. R. & WU, C. F. 2006. Coordination and modulation of locomotion pattern generators in *Drosophila* larvae: effects of altered biogenic amine levels by the tyramine beta hydroxylase mutation. *J Neurosci*, 26, 1486-98.
115. FRIGGI-GRELIN, F., COULOM, H., MELLER, M., GOMEZ, D., HIRSH, J. & BIRMAN, S. 2003. Targeted gene expression in *Drosophila* dopaminergic cells using regulatory sequences from tyrosine hydroxylase. *J Neurobiol*, 54, 618-27.
116. FRÖJDÖ, S., DURAND, C. & PIROLA, L. 2008. Metabolic effects of resveratrol in mammals--a link between improved insulin action and aging. *Curr Aging Sci*, 1, 145-51.
117. FRYER, L. G., PARBU-PATEL, A. & CARLING, D. 2002. The Anti-diabetic drugs rosiglitazone and metformin stimulate AMP-activated protein kinase through distinct signaling pathways. *J Biol Chem*, 277, 25226-32.
118. FUCHS, J., NILSSON, C., KACHERGUS, J., MUNZ, M., LARSSON, E. M., SCHÜLE, B., LANGSTON, J. W., MIDDLETON, F. A., ROSS, O. A., HULIHAN, M., GASSER, T. & FARRER, M. J. 2007. Phenotypic variation in a large Swedish pedigree due to SNCA duplication and triplication. *Neurology*, 68, 916-22.
119. GIROS, B., JABER, M., JONES, S. R., WIGHTMAN, R. M. & CARON, M. G. 1996. Hyperlocomotion and indifference to cocaine and amphetamine in mice lacking the dopamine transporter. *Nature*, 379, 606-12.
120. GISPERT, S., RICCIARDI, F., KURZ, A., AZIZOV, M., HOEPKEN, H. H., BECKER, D., VOOS, W., LEUNER, K., MÜLLER, W. E., KUDIN, A. P., KUNZ, W. S., ZIMMERMANN, A., ROEPER, J., WENZEL, D., JENDRACH, M., GARCÍA-ARENCÍBIA, M., FERNÁNDEZ-RUIZ, J., HUBER, L., ROHRER, H., BARRERA, M., REICHERT, A. S., RÜB, U., CHEN, A., NUSSBAUM, R. L. & AUBURGER, G. 2009. Parkinson phenotype in aged

PINK1-deficient mice is accompanied by progressive mitochondrial dysfunction in absence of neurodegeneration. *PLoS One*, 4, e5777.

121. GLINKA, Y. Y. & YODIM, M. B. 1995. Inhibition of mitochondrial complexes I and IV by 6-hydroxydopamine. *Eur J Pharmacol*, 292, 329-32.
122. GLUCK, M., EHRHART, J., JAYATILLEKE, E. & ZEEVALK, G. D. 2002. Inhibition of brain mitochondrial respiration by dopamine: involvement of H₂O₂ and hydroxyl radicals but not glutathione-protein-mixed disulfides. *J Neurochem*, 82, 66-74.
123. GOLBE, L. I. 1991. Young-onset Parkinson's disease: a clinical review. *Neurology*, 41, 168-73.
124. GOODMAN, C. & DOE, C. 1993. Embryonic development of the *Drosophila* central nervous system. In: BATE M, M. A. A. (ed.) *The Development of Drosophila melanogaster*. NY: Cold Spring Harbor Laboratory.
125. GORCZYCA, M., AUGART, C. & BUDNIK, V. 1993. Insulin-like receptor and insulin-like peptide are localized at neuromuscular junctions in *Drosophila*. *J Neurosci*, 13, 3692-704.
126. GOSWAMI, S. K. & DAS, D. K. 2009. Resveratrol and chemoprevention. *Cancer Lett*, 284, 1-6.
127. GRANERUS, A. K., JAGENBURG, R. & SVANBORG, A. 1973. Intestinal decarboxylation of L-Dopa in relation to dose requirement in Parkinson's disease. *Naunyn Schmiedebergs Arch Pharmacol*, 280, 429-39.
128. GREENAMYRE, J. T. & HASTINGS, T. G. 2004. Biomedicine. Parkinson's--divergent causes, convergent mechanisms. *Science*, 304, 1120-2.
129. GREENE, J. C., WHITWORTH, A. J., ANDREWS, L. A., PARKER, T. J. & PALLANCK, L. J. 2005. Genetic and genomic studies of *Drosophila* parkin mutants implicate oxidative stress and innate immune responses in pathogenesis. *Hum Mol Genet*, 14, 799-811.
130. GREENE, J. C., WHITWORTH, A. J., KUO, I., ANDREWS, L. A.,

- FEANY, M. B. & PALLANCK, L. J. 2003. Mitochondrial pathology and apoptotic muscle degeneration in *Drosophila parkin* mutants. *Proc Natl Acad Sci U S A*, 100, 4078-83.
131. GREENSPAN, R. J., TONONI, G., CIRELLI, C. & SHAW, P. J. 2001. Sleep and the fruit fly. *Trends Neurosci*, 24, 142-5.
132. GREER, C. L., GRYGORUK, A., PATTON, D. E., LEY, B., ROMERO-CALDERON, R., CHANG, H. Y., HOUSHYAR, R., BAINTON, R. J., DIANTONIO, A. & KRANTZ, D. E. 2005. A splice variant of the *Drosophila* vesicular monoamine transporter contains a conserved trafficking domain and functions in the storage of dopamine, serotonin, and octopamine. *J Neurobiol*, 64, 239-58.
133. GUO, M. 2012. *Drosophila* as a model to study mitochondrial dysfunction in Parkinson's disease. *Cold Spring Harb Perspect Med*, 2.
134. HALL, J. C. 2003. Genetics and molecular biology of rhythms in *Drosophila* and other insects. *Adv Genet*, 48, 1-280.
135. HALLIWELL, B. 1992. Reactive oxygen species and the central nervous system. *J Neurochem*, 59, 1609-23.
136. HARDIE, D. G. 2007. AMP-activated/SNF1 protein kinases: conserved guardians of cellular energy. *Nat Rev Mol Cell Biol*, 8, 774-85.
137. HARDIE, D. G. 2011. AMP-activated protein kinase: an energy sensor that regulates all aspects of cell function. *Genes Dev*, 25, 1895-908.
138. HARDIE, D. G., CARLING, D. & GAMBLIN, S. J. 2011. AMP-activated protein kinase: also regulated by ADP? *Trends Biochem Sci*, 36, 470-7.
139. HARDIE, D. G., SCOTT, J. W., PAN, D. A. & HUDSON, E. R. 2003. Management of cellular energy by the AMP-activated protein kinase system. *FEBS Lett*, 546, 113-20.
140. HARDY, J., LEWIS, P., REVESZ, T., LEES, A. & PAISAN-RUIZ, C. 2009. The genetics of Parkinson's syndromes: a critical review. *Curr Opin Genet*

Dev, 19, 254-65.

141. HARTWELL, L. H., HOOD, L. & GOLDBERG, M. L. 2010. *Genetics: From genes to genomes*, McGraw-Hill
142. HASTINGS, T. G. 1995. Enzymatic oxidation of dopamine: the role of prostaglandin H synthase. *J Neurochem*, 64, 919-24.
143. HECKSCHER, E. S., LOCKERY, S. R. & DOE, C. Q. 2012. Characterization of *Drosophila* larval crawling at the level of organism, segment, and somatic body wall musculature. *J Neurosci*, 32, 12460-71.
144. HENCHCLIFFE, C. & BEAL, M. F. 2008. Mitochondrial biology and oxidative stress in Parkinson disease pathogenesis. *Nat Clin Pract Neurol*, 4, 600-9.
145. HIGASHI, Y., ASANUMA, M., MIYAZAKI, I., HATTORI, N., MIZUNO, Y. & OGAWA, N. 2004. Parkin attenuates manganese-induced dopaminergic cell death. *J Neurochem*, 89, 1490-7.
146. HILL, J. 2008. *The roles of Tyramine and Octopamine in Drosophila melanogaster*. . PhD, University of York.
147. HINDLE, S., AFSARI, F., STARK, M., MIDDLETON, C. A., EVANS, G. J., SWEENEY, S. T. & ELLIOTT, C. J. 2013. Dopaminergic expression of the Parkinsonian gene LRRK2-G2019S leads to non-autonomous visual neurodegeneration, accelerated by increased neural demands for energy. *Hum Mol Genet*, 22, 2129-40.
148. HIRTH, F. 2010. *Drosophila melanogaster* in the study of human neurodegeneration. *CNS Neurol Disord Drug Targets*, 9, 504-23.
149. HOANG, B. & CHIBA, A. 2001. Single-cell analysis of *Drosophila* larval neuromuscular synapses. *Dev Biol*, 229, 55-70.
150. HOANG, B. & CHIBA, A. 2001. Single-cell analysis of *Drosophila* larval neuromuscular synapses. *Dev Biol*, 229, 55-70.

151. HODGKIN, A. L. & HUXLEY, A. F. 1945. Resting and action potentials in single nerve fibres. *J Physiol*, 104, 176-95.
152. HODGKIN, A. L. & HUXLEY, A. F. 1952. Propagation of electrical signals along giant nerve fibers. *Proc R Soc Lond B Biol Sci*, 140, 177-83.
153. HODGKIN, A. L. 1939. The relation between conduction velocity and the electrical resistance outside a nerve fibre. *J Physiol*, 94, 560-70.
154. HOROWITZ, J. M., VERNACE, V. A., MYERS, J., STACHOWIAK, M. K., HANLON, D. W., FRALEY, G. S. & TORRES, G. 2001. Immunodetection of Parkin protein in vertebrate and invertebrate brains: a comparative study using specific antibodies. *J Chem Neuroanat*, 21, 75-93.
155. HOULDEN, H. & SINGLETON, A. B. 2012. The genetics and neuropathology of Parkinson's disease. *Acta Neuropathol*, 124, 325-38.
156. HOWARTH, C., GLEESON, P. & ATTWELL, D. 2012. Updated energy budgets for neural computation in the neocortex and cerebellum. *J Cereb Blood Flow Metab*, 32, 1222-32.
157. HOWITZ, K. T., BITTERMAN, K. J., COHEN, H. Y., LAMMING, D. W., LAVU, S., WOOD, J. G., ZIPKIN, R. E., CHUNG, P., KISIELEWSKI, A., ZHANG, L. L., SCHERER, B. & SINCLAIR, D. A. 2003. Small molecule activators of sirtuins extend *Saccharomyces cerevisiae* lifespan. *Nature*, 425, 191-6.
158. HOYLE, G. 1953. Intracellular recording of 'slow' and 'fast' fibre activity from an insect muscle. *J Physiol*, 121, 32P-33P.
159. HRISTOVA, V. A., BEASLEY, S. A., RYLETT, R. J. & SHAW, G. S. 2009. Identification of a novel Zn²⁺-binding domain in the autosomal recessive juvenile Parkinson-related E3 ligase parkin. *J Biol Chem*, 284, 14978-86.
160. HUGHES, C. L. & THOMAS, J. B. 2007. A sensory feedback circuit coordinates muscle activity in *Drosophila*. *Mol Cell Neurosci*, 35, 383-96.
161. HWANG, S., KIM, D., CHOI, G., AN, S. W., HONG, Y. K., SUH, Y. S.,

- LEE, M. J. & CHO, K. S. 2010. Parkin suppresses c-Jun N-terminal kinase-induced cell death via transcriptional regulation in *Drosophila*. *Mol Cells*, 29, 575-80.
162. ITOH, K., ISHII, T., WAKABAYASHI, N. & YAMAMOTO, M. 1999a. Regulatory mechanisms of cellular response to oxidative stress. *Free Radic Res*, 31, 319-24.
163. ITOH, K., WAKABAYASHI, N., KATOH, Y., ISHII, T., IGARASHI, K., ENGEL, J. D. & YAMAMOTO, M. 1999b. Keap1 represses nuclear activation of antioxidant responsive elements by Nrf2 through binding to the amino-terminal Neh2 domain. *Genes Dev*, 13, 76-86.
164. JÄGER, S., HANDSCHIN, C., ST-PIERRE, J. & SPIEGELMAN, B. M. 2007. AMP-activated protein kinase (AMPK) action in skeletal muscle via direct phosphorylation of PGC-1alpha. *Proc Natl Acad Sci U S A*, 104, 12017-22.
165. JAN, L. Y. & JAN, Y. N. 1976. Properties of the larval neuromuscular junction in *Drosophila melanogaster*. *J Physiol*, 262, 189-214.
166. JAN, Y. N., JAN, L. Y. & DENNIS, M. J. 1977. Two mutations of synaptic transmission in *Drosophila*. *Proc R Soc Lond B Biol Sci*, 198, 87-108.
167. JENNER, P. 2003. Oxidative stress in Parkinson's disease. *Ann Neurol*, 53 Suppl 3, S26-36; discussion S36-8.
168. JEON, B. S., JACKSON-LEWIS, V. & BURKE, R. E. 1995. 6-Hydroxydopamine lesion of the rat substantia nigra: time course and morphology of cell death. *Neurodegeneration*, 4, 131-7.
169. JHA, N., JURMA, O., LALLI, G., LIU, Y., PETTUS, E. H., GREENAMYRE, J. T., LIU, R. M., FORMAN, H. J. & ANDERSEN, J. K. 2000. Glutathione depletion in PC12 results in selective inhibition of mitochondrial complex I activity. Implications for Parkinson's disease. *J Biol Chem*, 275, 26096-101.
170. JIN, L., BAKER, B., MEALER, R., COHEN, L., PIERIBONE, V., PRALLE, A. & HUGHES, T. 2011. Random insertion of split-cans of the

- fluorescent protein venus into Shaker channels yields voltage sensitive probes with improved membrane localization in mammalian cells. *J Neurosci Methods*, 199, 1-9.
171. JOHNSTON, R. M. & LEVINE, R. B. 1996. Crawling motor patterns induced by pilocarpine in isolated larval nerve cords of *Manduca sexta*. *J Neurophysiol*, 76, 3178-95.
172. JOST, W. H. & SCHIMRIGK, K. 1991. Constipation in Parkinson's disease. *Klin Wochenschr*, 69, 906-9.
173. KANE, D. A., ANDERSON, E. J., PRICE, J. W., WOODLIEF, T. L., LIN, C. T., BIKMAN, B. T., CORTRIGHT, R. N. & NEUFER, P. D. 2010. Metformin selectively attenuates mitochondrial H₂O₂ emission without affecting respiratory capacity in skeletal muscle of obese rats. *Free Radic Biol Med*, 49, 1082-7.
174. KANZOK, S. M., FECHNER, A., BAUER, H., ULSCHMID, J. K., MÜLLER, H. M., BOTELLA-MUNOZ, J., SCHNEUWLY, S., SCHIRMER, R. & BECKER, K. 2001. Substitution of the thioredoxin system for glutathione reductase in *Drosophila melanogaster*. *Science*, 291, 643-6.
175. KEENEY, P. M., XIE, J., CAPALDI, R. A. & BENNETT, J. P. 2006. Parkinson's disease brain mitochondrial complex I has oxidatively damaged subunits and is functionally impaired and misassembled. *J Neurosci*, 26, 5256-64.
176. KESHISHIAN, H., BROADIE, K., CHIBA, A. & BATE, M. 1996. The drosophila neuromuscular junction: a model system for studying synaptic development and function. *Annu Rev Neurosci*, 19, 545-75.
177. KIM, J., KUNDU, M., VIOLLET, B. & GUAN, K. L. 2011. AMPK and mTOR regulate autophagy through direct phosphorylation of Ulk1. *Nat Cell Biol*, 13, 132-41.
178. KIM, K., KIM, S. H., KIM, J., KIM, H. & YIM, J. 2012. Glutathione s-transferase omega 1 activity is sufficient to suppress neurodegeneration in a

Drosophila model of Parkinson disease. *J Biol Chem*, 287, 6628-41.

179. KIM, M. D., WEN, Y. & JAN, Y. N. 2009. Patterning and organization of motor neuron dendrites in the *Drosophila* larva. *Dev Biol*, 336, 213-21.
180. KIM, Y., PARK, J., KIM, S., SONG, S., KWON, S. K., LEE, S. H., KITADA, T., KIM, J. M. & CHUNG, J. 2008. PINK1 controls mitochondrial localization of Parkin through direct phosphorylation. *Biochem Biophys Res Commun*, 377, 975-80.
181. KITADA, T., ASAKAWA, S., HATTORI, N., MATSUMINE, H., YAMAMURA, Y., MINOSHIMA, S., YOKOCHI, M., MIZUNO, Y. & SHIMIZU, N. 1998. Mutations in the parkin gene cause autosomal recessive juvenile parkinsonism. *Nature*, 392, 605-8.
182. KITADA, T., TONG, Y., GAUTIER, C. A. & SHEN, J. 2009. Absence of nigral degeneration in aged parkin/DJ-1/PINK1 triple knockout mice. *J Neurochem*, 111, 696-702.
183. KNUTSON, M. D. & LEEUWENBURGH, C. 2008. Resveratrol and novel potent activators of SIRT1: effects on aging and age-related diseases. *Nutr Rev*, 66, 591-6.
184. KO, Y. H., HONG, S. & PEDERSEN, P. L. 1999. Chemical mechanism of ATP synthase. Magnesium plays a pivotal role in formation of the transition state where ATP is synthesized from ADP and inorganic phosphate. *J Biol Chem*, 274, 28853-6.
185. KRANS, J. L., PARFITT, K. D., GAWERA, K. D., RIVLIN, P. K. & HOY, R. R. 2010. The resting membrane potential of *Drosophila melanogaster* larval muscle depends strongly on external calcium concentration. *J Insect Physiol*, 56, 304-13.
186. KRÜGER, R., KUHN, W., MÜLLER, T., WOITALLA, D., GRAEBER, M., KÖSEL, S., PRZUNTEK, H., EPPLEN, J. T., SCHÖLS, L. & RIESS, O. 1998. Ala30Pro mutation in the gene encoding alpha-synuclein in Parkinson's disease. *Nat Genet*, 18, 106-8.

187. KUMAR, S. 2005. Punding in Parkinson's disease related to high-dose levodopa therapy. *Neurol India*, 53, 362.
188. LANDGRAF, M. & THOR, S. 2006a. Development and structure of motoneurons. *Int Rev Neurobiol*, 75, 33-53.
189. LANDGRAF, M. & THOR, S. 2006b. Development of *Drosophila* motoneurons: specification and morphology. *Semin Cell Dev Biol*, 17, 3-11.
190. LANDGRAF, M., BOSSING, T., TECHNAU, G. M. & BATE, M. 1997. The origin, location, and projections of the embryonic abdominal motoneurons of *Drosophila*. *J Neurosci*, 17, 9642-55.
191. LANDGRAF, M., ROY, S., PROKOP, A., VIJAYRAGHAVAN, K. & BATE, M. 1999. even-skipped determines the dorsal growth of motor axons in *Drosophila*. *Neuron*, 22, 43-52.
192. LANGSTON, J. W. & BALLARD, P. A. 1983. Parkinson's disease in a chemist working with 1-methyl-4-phenyl-1,2,5,6-tetrahydropyridine. *N Engl J Med*, 309, 310.
193. LANGSTON, J. W. 2002. Parkinson's disease: current and future challenges. *Neurotoxicology*, 23, 443-50.
194. LAWAL, H. O., CHANG, H. Y., TERRELL, A. N., BROOKS, E. S., PULIDO, D., SIMON, A. F. & KRANTZ, D. E. 2010. The *Drosophila* vesicular monoamine transporter reduces pesticide-induced loss of dopaminergic neurons. *Neurobiol Dis*, 40, 102-12.
195. LECKER, S. H., GOLDBERG, A. L. & MITCH, W. E. 2006. Protein degradation by the ubiquitin-proteasome pathway in normal and disease states. *J Am Soc Nephrol*, 17, 1807-19.
196. LEE, S., LIU, H. P., LIN, W. Y., GUO, H. & LU, B. 2010. LRRK2 kinase regulates synaptic morphology through distinct substrates at the presynaptic and postsynaptic compartments of the *Drosophila* neuromuscular junction. *J Neurosci*, 30, 16959-69.

197. LEES, A. J., HARDY, J. & REVESZ, T. 2009. Parkinson's disease. *Lancet*, 373, 2055-66.
198. LI, H., CHANEY, S., ROBERTS, I. J., FORTE, M. & HIRSH, J. 2000. Ectopic G-protein expression in dopamine and serotonin neurons blocks cocaine sensitization in *Drosophila melanogaster*. *Curr Biol*, 10, 211-4.
199. LI, H., PENG, X. & COOPER, R. L. 2002. Development of *Drosophila* larval neuromuscular junctions: maintaining synaptic strength. *Neuroscience*, 115, 505-13.
200. LI, J. & HOLBROOK, N. J. 2003. Common mechanisms for declines in oxidative stress tolerance and proliferation with aging. *Free Radic Biol Med*, 35, 292-9.
201. LIMA, S. Q. & MIESENBOCK, G. 2005. Remote control of behavior through genetically targeted photostimulation of neurons. *Cell*, 121, 141-52.
202. LINAZASORO, G. 2004. Recent failures of new potential symptomatic treatments for Parkinson's disease: causes and solutions. *Mov Disord*, 19, 743-54.
203. LINGREL, J. B. & KUNTZWEILER, T. 1994. Na⁺,K⁽⁺⁾-ATPase. *J Biol Chem*, 269, 19659-62.
204. LINGREL, J. B., VAN HUYSSSE, J., O'BRIEN, W., JEWELL-MOTZ, E. & SCHULTHEIS, P. 1994b. Na,K-ATPase: structure-function studies. *Ren Physiol Biochem*, 17, 198-200.
205. LINGREL, J. B., VAN HUYSSSE, J., O'BRIEN, W., JEWELL-MOTZ, E., ASKEW, R. & SCHULTHEIS, P. 1994a. Structure-function studies of the Na,K-ATPase. *Kidney Int Suppl*, 44, S32-9.
206. LIU, Y. & EDWARDS, R. H. 1997. The role of vesicular transport proteins in synaptic transmission and neural degeneration. *Annu Rev Neurosci*, 20, 125-56.
207. LIZCANO, J. M., GÖRANSSON, O., TOTH, R., DEAK, M., MORRICE,

- N. A., BOUDEAU, J., HAWLEY, S. A., UDD, L., MÄKELÄ, T. P., HARDIE, D. G. & ALESSI, D. R. 2004. LKB1 is a master kinase that activates 13 kinases of the AMPK subfamily, including MARK/PAR-1. *EMBO J*, 23, 833-43.
208. LNENICKA, G. A. & KESHISHIAN, H. 2000. Identified motor terminals in *Drosophila* larvae show distinct differences in morphology and physiology. *J Neurobiol*, 43, 186-97.
209. LUTHMAN, J., FREDRIKSSON, A., LEWANDER, T., JONSSON, G. & ARCHER, T. 1989. Effects of d-amphetamine and methylphenidate on hyperactivity produced by neonatal 6-hydroxydopamine treatment. *Psychopharmacology (Berl)*, 99, 550-7.
210. MACKLER, J. M., DRUMMOND, J. A., LOEWEN, C. A., ROBINSON, I. M. & REIST, N. E. 2002. The C(2)B Ca(2+)-binding motif of synaptotagmin is required for synaptic transmission in vivo. *Nature*, 418, 340-4.
211. MACLEOD, G. T. & ZINSMAIER, K. E. 2006. Synaptic homeostasis on the fast track. *Neuron*, 52, 569-71.
212. MACLEOD, G. T., CHEN, L., KARUNANITHI, S., PELOQUIN, J. B., ATWOOD, H. L., MCRORY, J. E., ZAMPONI, G. W. & CHARLTON, M. P. 2006. The *Drosophila* cacts2 mutation reduces presynaptic Ca²⁺ entry and defines an important element in Cav2.1 channel inactivation. *Eur J Neurosci*, 23, 3230-44.
213. MAKER, H. S., WEISS, C., WEISSBARTH, S., SILIDES, D. J. & WHETSELL, W. 1981. Regional activities of metabolic enzymes and glutamate decarboxylase in human brain. *Ann Neurol*, 10, 377-83.
214. MALAISSE, W. J., CONGET, I., SENER, A. & RORSMAN, P. 1994. Insulinotropic action of AICA riboside. II. Secretory, metabolic and cationic aspects. *Diabetes Res*, 25, 25-37.
215. MANDEL, S. A., AMIT, T., KALFON, L., REZNICHENKO, L., WEINREB, O. & YAUDIM, M. B. 2008. Cell signaling pathways and iron chelation in the neurorestorative activity of green tea polyphenols: special

- reference to epigallocatechin gallate (EGCG). *J Alzheimers Dis*, 15, 211-22.
216. MANN, V. M., COOPER, J. M., DANIEL, S. E., SRAI, K., JENNER, P., MARSDEN, C. D. & SCHAPIRA, A. H. 1994. Complex I, iron, and ferritin in Parkinson's disease substantia nigra. *Ann Neurol*, 36, 876-81.
217. MAO, Z. & DAVIS, R. L. 2009. Eight different types of dopaminergic neurons innervate the *Drosophila* mushroom body neuropil: anatomical and physiological heterogeneity. *Front Neural Circuits*, 3, 5.
218. MARDER, E. & BUCHER, D. 2001. Central pattern generators and the control of rhythmic movements. *Curr Biol*, 11, R986-96.
219. MARKHAM, C. H. 1971. The choreoathetoid movement disorder induced by levodopa. *Clin Pharmacol Ther*, 12, 340-3.
220. MARQUÉS, G. 2005. Morphogens and synaptogenesis in *Drosophila*. *J Neurobiol*, 64, 417-34.
221. MARRUS, S. B., PORTMAN, S. L., ALLEN, M. J., MOFFAT, K. G. & DIANTONIO, A. 2004. Differential localization of glutamate receptor subunits at the *Drosophila* neuromuscular junction. *J Neurosci*, 24, 1406-15.
222. MARTIN, I., DAWSON, V. L. & DAWSON, T. M. 2011. Recent advances in the genetics of Parkinson's disease. *Annu Rev Genomics Hum Genet*, 12, 301-25.
223. MATTHEWS, R. T., FERRANTE, R. J., KLIVENYI, P., YANG, L., KLEIN, A. M., MUELLER, G., KADDURAH-DAOUK, R. & BEAL, M. F. 1999. Creatine and cyclocreatine attenuate MPTP neurotoxicity. *Exp Neurol*, 157, 142-9.
224. MATTSON, M. P. & MAGNUS, T. 2006. Ageing and neuronal vulnerability. *Nat Rev Neurosci*, 7, 278-94.
225. MATTSON, M. P. 2006. Neuronal life-and-death signaling, apoptosis, and neurodegenerative disorders. *Antioxid Redox Signal*, 8, 1997-2006.

226. MCNAUGHT, K. S., BELIZAIER, R., ISACSON, O., JENNER, P. & OLANOW, C. W. 2003. Altered proteasomal function in sporadic Parkinson's disease. *Exp Neurol*, 179, 38-46.
227. MEISSNER, W. G., FRASIER, M., GASSER, T., GOETZ, C. G., LOZANO, A., PICCINI, P., OBESO, J. A., RASCOL, O., SCHAPIRA, A., VOON, V., WEINER, D. M., TISON, F. & BEZARD, E. 2011. Priorities in Parkinson's disease research. *Nat Rev Drug Discov*, 10, 377-93.
228. MERSHIN, A., PAVLOPOULOS, E., FITCH, O., BRADEN, B. C., NANOPOULOS, D. V. & SKOULAKIS, E. M. 2004. Learning and memory deficits upon TAU accumulation in *Drosophila* mushroom body neurons. *Learn Mem*, 11, 277-87.
229. MICHAN, S. & SINCLAIR, D. 2007. Sirtuins in mammals: insights into their biological function. *Biochem J*, 404, 1-13.
230. MIDDLETON, C. A., NONGTHOMBA, U., PARRY, K., SWEENEY, S. T., SPARROW, J. C. & ELLIOTT, C. J. 2006. Neuromuscular organization and aminergic modulation of contractions in the *Drosophila* ovary. *BMC Biol*, 4, 17.
231. MILLER, D. W., HAGUE, S. M., CLARIMON, J., BAPTISTA, M., GWINN-HARDY, K., COOKSON, M. R. & SINGLETON, A. B. 2004. Alpha-synuclein in blood and brain from familial Parkinson disease with SNCA locus triplication. *Neurology*, 62, 1835-8.
232. MILLER, G. W., GAINETDINOV, R. R., LEVEY, A. I. & CARON, M. G. 1999. Dopamine transporters and neuronal injury. *Trends Pharmacol Sci*. England.
233. MILNE, J. C., LAMBERT, P. D., SCHENK, S., CARNEY, D. P., SMITH, J. J., GAGNE, D. J., JIN, L., BOSS, O., PERNI, R. B., VU, C. B., BEMIS, J. E., XIE, R., DISCH, J. S., NG, P. Y., NUNES, J. J., LYNCH, A. V., YANG, H., GALONEK, H., ISRAELIAN, K., CHOY, W., IFFLAND, A., LAVU, S., MEDVEDIK, O., SINCLAIR, D. A., OLEFSKY, J. M., JIROUSEK, M. R., ELLIOTT, P. J. & WESTPHAL, C. H. 2007. Small molecule activators of SIRT1 as therapeutics for the treatment of type 2 diabetes. *Nature*, 450, 712-6.

234. MILTON, V. J., JARRETT, H. E., GOWERS, K., CHALAK, S., BRIGGS, L., ROBINSON, I. M. & SWEENEY, S. T. 2011. Oxidative stress induces overgrowth of the *Drosophila* neuromuscular junction. *Proc Natl Acad Sci U S A*, 108, 17521-6.
235. MIROUSE, V., SWICK, L. L., KAZGAN, N., ST JOHNSTON, D. & BRENMAN, J. E. 2007. LKB1 and AMPK maintain epithelial cell polarity under energetic stress. *J Cell Biol*, 177, 387-92.
236. MISSIRLIS, F., PHILLIPS, J. P. & JÄCKLE, H. 2001. Cooperative action of antioxidant defense systems in *Drosophila*. *Curr Biol*, 11, 1272-7.
237. MIZUNO, Y., OHTA, S., TANAKA, M., TAKAMIYA, S., SUZUKI, K., SATO, T., OYA, H., OZAWA, T. & KAGAWA, Y. 1989. Deficiencies in complex I subunits of the respiratory chain in Parkinson's disease. *Biochem Biophys Res Commun*, 163, 1450-5.
238. MORAIS, V. A., VERSTREKEN, P., ROETHIG, A., SMET, J., SNELLINX, A., VANBRABANT, M., HADDAD, D., FREZZA, C., MANDEMAKERS, W., VOGT-WEISENHORN, D., VAN COSTER, R., WURST, W., SCORRANO, L. & DE STROOPER, B. 2009. Parkinson's disease mutations in PINK1 result in decreased Complex I activity and deficient synaptic function. *EMBO Mol Med*, 1, 99-111.
239. MORTIBOYS, H., THOMAS, K. J., KOOPMAN, W. J., KLAFFKE, S., ABOU-SLEIMAN, P., OLPIN, S., WOOD, N. W., WILLEMS, P. H., SMEITINK, J. A., COOKSON, M. R. & BANDMANN, O. 2008. Mitochondrial function and morphology are impaired in parkin-mutant fibroblasts. *Ann Neurol*, 64, 555-65.
240. MOSHAROV, E. V., LARSEN, K. E., KANTER, E., PHILLIPS, K. A., WILSON, K., SCHMITZ, Y., KRANTZ, D. E., KOBAYASHI, K., EDWARDS, R. H. & SULZER, D. 2009. Interplay between cytosolic dopamine, calcium, and alpha-synuclein causes selective death of substantia nigra neurons. *Neuron*, 62, 218-29.
241. MÜFTÜOĞLU, M., ELIBOL, B., DALMIZRAK, O., ERCAN, A.,

- KULAKSIZ, G., OGÜS, H., DALKARA, T. & OZER, N. 2004. Mitochondrial complex I and IV activities in leukocytes from patients with parkin mutations. *Mov Disord*, 19, 544-8.
242. NAOI, M., YI, H., MARUYAMA, W., INABA, K., SHAMOTO-NAGAI, M., AKAO, Y., GERLACH, M. & RIEDERER, P. 2009. Glutathione redox status in mitochondria and cytoplasm differentially and sequentially activates apoptosis cascade in dopamine-melanin-treated SH-SY5Y cells. *Neurosci Lett*, 465, 118-22.
243. NARENDRA, D., TANAKA, A., SUEN, D. F. & YOULE, R. J. 2008. Parkin is recruited selectively to impaired mitochondria and promotes their autophagy. *J Cell Biol*, 183, 795-803.
244. NARENDRA, D., TANAKA, A., SUEN, D. F. & YOULE, R. J. 2009. Parkin-induced mitophagy in the pathogenesis of Parkinson disease. *Autophagy*, 5, 706-8.
245. NASS, R. & BLAKELY, R. D. 2003. The *Caenorhabditis elegans* dopaminergic system: opportunities for insights into dopamine transport and neurodegeneration. *Annu Rev Pharmacol Toxicol*, 43, 521-44.
246. NÄSSEL, D. R. & ELEKES, K. 1992. Aminergic neurons in the brain of blowflies and *Drosophila*: dopamine- and tyrosine hydroxylase-immunoreactive neurons and their relationship with putative histaminergic neurons. *Cell Tissue Res*, 267, 147-67.
247. NATHAN, D. M., BUSE, J. B., DAVIDSON, M. B., FERRANNINI, E., HOLMAN, R. R., SHERWIN, R., ZINMAN, B., ASSOCIATION, A. D. & DIABETES, E. A. F. S. O. 2009. Medical management of hyperglycemia in type 2 diabetes: a consensus algorithm for the initiation and adjustment of therapy: a consensus statement of the American Diabetes Association and the European Association for the Study of Diabetes. *Diabetes Care*, 32, 193-203.
248. NG, C. H., GUAN, M. S., KOH, C., OUYANG, X., YU, F., TAN, E. K., O'NEILL, S. P., ZHANG, X., CHUNG, J. & LIM, K. L. 2012. AMP kinase activation mitigates dopaminergic dysfunction and mitochondrial abnormalities

- in *Drosophila* models of Parkinson's disease. *J Neurosci*, 32, 14311-7.
249. NGUYEN, T., SHERRATT, P. J. & PICKETT, C. B. 2003. Regulatory mechanisms controlling gene expression mediated by the antioxidant response element. *Annu Rev Pharmacol Toxicol*, 43, 233-60.
250. NICKLAS, W. J., VYAS, I. & HEIKKILA, R. E. 1985. Inhibition of NADH-linked oxidation in brain mitochondria by 1-methyl-4-phenyl-pyridine, a metabolite of the neurotoxin, 1-methyl-4-phenyl-1,2,5,6-tetrahydropyridine. *Life Sci*, 36, 2503-8.
251. NIVEN, J. E. & LAUGHLIN, S. B. 2008. Energy limitation as a selective pressure on the evolution of sensory systems. *J Exp Biol*, 211, 1792-804.
252. OBESO, J. A., RODRIGUEZ-OROZ, M. C., GOETZ, C. G., MARIN, C., KORDOWER, J. H., RODRIGUEZ, M., HIRSCH, E. C., FARRER, M., SCHAPIRA, A. H. & HALLIDAY, G. 2010. Missing pieces in the Parkinson's disease puzzle. *Nat Med*, 16, 653-61.
253. OBESO, J. A., RODRÍGUEZ-OROZ, M. C., RODRÍGUEZ, M., ARBIZU, J. & GIMÉNEZ-AMAYA, J. M. 2002. The basal ganglia and disorders of movement: pathophysiological mechanisms. *News Physiol Sci*, 17, 51-5.
254. OLIVERAS-SALVÁ, M., VAN DER PERREN, A., CASADEI, N., STROOBANTS, S., NUBER, S., D'HOOGE, R., VAN DEN HAUTE, C. & BAEKELANDT, V. 2013. rAAV2/7 vector-mediated overexpression of alpha-synuclein in mouse substantia nigra induces protein aggregation and progressive dose-dependent neurodegeneration. *Mol Neurodegener*, 8, 44.
255. ORR, W. C. & SOHAL, R. S. 1994. Extension of life-span by overexpression of superoxide dismutase and catalase in *Drosophila melanogaster*. *Science*, 263, 1128-30.
256. ORTEGA-ARELLANO, H. F., JIMENEZ-DEL-RIO, M. & VELEZ-PARDO, C. 2011. Life span and locomotor activity modification by glucose and polyphenols in *Drosophila melanogaster* chronically exposed to oxidative stress-stimuli: implications in Parkinson's disease. *Neurochem Res*, 36, 1073-86.

257. OTTONE, C., GALASSO, A., GEMEI, M., PISA, V., GIGLIOTTI, S., PICCIONI, F., GRAZIANI, F. & VERROTTI DI PIANELLA, A. 2011. Diminution of eIF4E activity suppresses parkin mutant phenotypes. *Gene*, 470, 12-9.
258. OUYANG, J., PARAKHIA, R. A. & OCHS, R. S. 2011. Metformin activates AMP kinase through inhibition of AMP deaminase. *J Biol Chem*, 286, 1-11.
259. OWEN, K. R., DONOHOE, M., ELLARD, S. & HATTERSLEY, A. T. 2003. Response to treatment with rosiglitazone in familial partial lipodystrophy due to a mutation in the LMNA gene. *Diabet Med*, 20, 823-7.
260. PACHOLEC, M., BLEASDALE, J. E., CHRUNYK, B., CUNNINGHAM, D., FLYNN, D., GAROFALO, R. S., GRIFFITH, D., GRIFFOR, M., LOULAKIS, P., PABST, B., QIU, X., STOCKMAN, B., THANABAL, V., VARGHESE, A., WARD, J., WITHKA, J. & AHN, K. 2010. SRT1720, SRT2183, SRT1460, and resveratrol are not direct activators of SIRT1. *J Biol Chem*, 285, 8340-51.
261. PAISÁN-RUÍZ, C., JAIN, S., EVANS, E. W., GILKS, W. P., SIMÓN, J., VAN DER BRUG, M., LÓPEZ DE MUNAIN, A., APARICIO, S., GIL, A. M., KHAN, N., JOHNSON, J., MARTINEZ, J. R., NICHOLL, D., CARRERA, I. M., PENA, A. S., DE SILVA, R., LEES, A., MARTÍ-MASSÓ, J. F., PÉREZ-TUR, J., WOOD, N. W. & SINGLETON, A. B. 2004. Cloning of the gene containing mutations that cause PARK8-linked Parkinson's disease. *Neuron*, 44, 595-600.
262. PALACINO, J. J., SAGI, D., GOLDBERG, M. S., KRAUSS, S., MOTZ, C., WACKER, M., KLOSE, J. & SHEN, J. 2004. Mitochondrial dysfunction and oxidative damage in parkin-deficient mice. *J Biol Chem*, 279, 18614-22.
263. PALACINO, J. J., SAGI, D., GOLDBERG, M. S., KRAUSS, S., MOTZ, C., WACKER, M., KLOSE, J. & SHEN, J. 2004. Mitochondrial dysfunction and oxidative damage in parkin-deficient mice. *J Biol Chem*, 279, 18614-22.
264. PALLÀS, M., CASADESÚS, G., SMITH, M. A., COTO-MONTES, A.,

- PELEGRI, C., VILAPLANA, J. & CAMINS, A. 2009. Resveratrol and neurodegenerative diseases: activation of SIRT1 as the potential pathway towards neuroprotection. *Curr Neurovasc Res*, 6, 70-81.
265. PARK, J., LEE, G. & CHUNG, J. 2009. The PINK1-Parkin pathway is involved in the regulation of mitochondrial remodeling process. *Biochem Biophys Res Commun*, 378, 518-23.
266. PARK, J., LEE, S. B., LEE, S., KIM, Y., SONG, S., KIM, S., BAE, E., KIM, J., SHONG, M., KIM, J. M. & CHUNG, J. 2006. Mitochondrial dysfunction in *Drosophila* PINK1 mutants is complemented by parkin. *Nature*, 441, 1157-61.
267. PARK, S. J., AHMAD, F., PHILP, A., BAAR, K., WILLIAMS, T., LUO, H., KE, H., REHMANN, H., TAUSSIG, R., BROWN, A. L., KIM, M. K., BEAVEN, M. A., BURGIN, A. B., MANGANIELLO, V. & CHUNG, J. H. 2012. Resveratrol ameliorates aging-related metabolic phenotypes by inhibiting cAMP phosphodiesterases. *Cell*, 148, 421-33.
268. PARK, S. S. & LEE, D. 2006. Selective loss of dopaminergic neurons and formation of Lewy body-like aggregations in alpha-synuclein transgenic fly neuronal cultures. *Eur J Neurosci*, 23, 2908-14.
269. PEERAULLY, T. & TAN, E. K. 2012. Genetic variants in sporadic Parkinson's disease: East vs West. *Parkinsonism Relat Disord*, 18 Suppl 1, S63-5.
270. PENDLETON, R. G., RASHEED, A., SARDINA, T., TULLY, T. & HILLMAN, R. 2002. Effects of tyrosine hydroxylase mutants on locomotor activity in *Drosophila*: a study in functional genomics. *Behav Genet*, 32, 89-94.
271. PENG, Y., RIDEOUT, D. A., RAKITA, S. S., GOWER, W. R., YOU, M. & MURR, M. M. 2010. Does LKB1 mediate activation of hepatic AMP-protein kinase (AMPK) and sirtuin1 (SIRT1) after Roux-en-Y gastric bypass in obese rats? *J Gastrointest Surg*, 14, 221-8.
272. PESAH, Y., PHAM, T., BURGESS, H., MIDDLEBROOKS, B.,

- VERSTREKEN, P., ZHOU, Y., HARDING, M., BELLEN, H. & MARDON, G. 2004. *Drosophila parkin* mutants have decreased mass and cell size and increased sensitivity to oxygen radical stress. *Development*, 131, 2183-94.
273. PICKART, C. M. 2001. Mechanisms underlying ubiquitination. *Annu Rev Biochem*, 70, 503-33.
274. POLYMEROPOULOS, M. H., LAVEDAN, C., LEROY, E., IDE, S. E., DEHEJIA, A., DUTRA, A., PIKE, B., ROOT, H., RUBENSTEIN, J., BOYER, R., STENROOS, E. S., CHANDRASEKHARAPPA, S., ATHANASSIADOU, A., PAPAPETROPOULOS, T., JOHNSON, W. G., LAZZARINI, A. M., DUVOISIN, R. C., DI IORIO, G., GOLBE, L. I. & NUSSBAUM, R. L. 1997. Mutation in the alpha-synuclein gene identified in families with Parkinson's disease. *Science*, 276, 2045-7.
275. POOLE, A. C., THOMAS, R. E., ANDREWS, L. A., MCBRIDE, H. M., WHITWORTH, A. J. & PALLANCK, L. J. 2008. The PINK1/Parkin pathway regulates mitochondrial morphology. *Proc Natl Acad Sci U S A*, 105, 1638-43.
276. PORRAS, G., LI, Q. & BEZARD, E. 2012. Modeling Parkinson's disease in primates: The MPTP model. *Cold Spring Harb Perspect Med*, 2, a009308.
277. PRZEDBORSKI, S. & GOLDMAN, J. 2004. Pathogenic role of glial cells in Parkinson's disease, In: *Non-neuronal cells of the nervous system: function and dysfunction* (Hertz L, ed), pp.967–982, Elsevier, New York, NY, USA.
278. PRZEDBORSKI, S. & ISCHIROPOULOS, H. 2005. Reactive oxygen and nitrogen species: weapons of neuronal destruction in models of Parkinson's disease. *Antioxid Redox Signal*, 7, 685-93.
279. PRZEDBORSKI, S., TIEU, K., PERIER, C. & VILA, M. 2004. MPTP as a mitochondrial neurotoxic model of Parkinson's disease. *J Bioenerg Biomembr*, 36, 375-9.
280. PULVER, S. R. & GRIFFITH, L. C. 2010. Spike integration and cellular memory in a rhythmic network from Na⁺/K⁺ pump current dynamics. *Nat Neurosci*, 13, 53-9.

281. RAMIREZ, A., HEIMBACH, A., GRÜNDEMANN, J., STILLER, B., HAMPSHIRE, D., CID, L. P., GOEBEL, I., MUBAIDIN, A. F., WRIEKAT, A. L., ROEPER, J., AL-DIN, A., HILLMER, A. M., KARSAK, M., LISS, B., WOODS, C. G., BEHRENS, M. I. & KUBISCH, C. 2006. Hereditary parkinsonism with dementia is caused by mutations in ATP13A2, encoding a lysosomal type 5 P-type ATPase. *Nat Genet*, 38, 1184-91.
282. RAMONET, D., DAHER, J. P., LIN, B. M., STAFA, K., KIM, J., BANERJEE, R., WESTERLUND, M., PLETNIKOVA, O., GLAUSER, L., YANG, L., LIU, Y., SWING, D. A., BEAL, M. F., TRONCOSO, J. C., MCCAFFERY, J. M., JENKINS, N. A., COPELAND, N. G., GALTER, D., THOMAS, B., LEE, M. K., DAWSON, T. M., DAWSON, V. L. & MOORE, D. J. 2011. Dopaminergic neuronal loss, reduced neurite complexity and autophagic abnormalities in transgenic mice expressing G2019S mutant LRRK2. *PLoS One*, 6, e18568.
283. RAVIKUMAR, B., VACHER, C., BERGER, Z., DAVIES, J. E., LUO, S., OROZ, L. G., SCARAVILLI, F., EASTON, D. F., DUDEN, R., O'KANE, C. J. & RUBINSZTEIN, D. C. 2004. Inhibition of mTOR induces autophagy and reduces toxicity of polyglutamine expansions in fly and mouse models of Huntington disease. *Nat Genet*, 36, 585-95.
284. RAVINA, B. M., FAGAN, S. C., HART, R. G., HOVINGA, C. A., MURPHY, D. D., DAWSON, T. M. & MARLER, J. R. 2003. Neuroprotective agents for clinical trials in Parkinson's disease: a systematic assessment. *Neurology*, 60, 1234-40.
285. RAVINA, B., MARDER, K., FERNANDEZ, H. H., FRIEDMAN, J. H., MCDONALD, W., MURPHY, D., AARSLAND, D., BABCOCK, D., CUMMINGS, J., ENDICOTT, J., FACTOR, S., GALPERN, W., LEES, A., MARSH, L., STACY, M., GWINN-HARDY, K., VOON, V. & GOETZ, C. 2007. Diagnostic criteria for psychosis in Parkinson's disease: report of an NINDS, NIMH work group. *Mov Disord*, 22, 1061-8.
286. RECHSTEINER, M. C. 1970a. *Drosophila* lactate dehydrogenase and alpha-glycerolphosphate dehydrogenase: distribution and change in activity

- during development. *J Insect Physiol*, 16, 1179-92.
287. RECHSTEINER, M. C. 1970b. *Drosophila* lactate dehydrogenase: partial purification and characterization. *J Insect Physiol*, 16, 957-77.
288. REICHMANN, H. & JANETZKY, B. 2000. Mitochondrial dysfunction--a pathogenetic factor in Parkinson's disease. *J Neurol*, 247 Suppl 2, II63-8.
289. REITER, L. T., POTOCKI, L., CHIEN, S., GRIBSKOV, M. & BIER, E. 2001. A systematic analysis of human disease-associated gene sequences in *Drosophila melanogaster*. *Genome Res*, 11, 1114-25.
290. REMY, P., DODER, M., LEES, A., TURJANSKI, N. & BROOKS, D. 2005. Depression in Parkinson's disease: loss of dopamine and noradrenaline innervation in the limbic system. *Brain*, 128, 1314-22.
291. REN, J., FAN, C., CHEN, N., HUANG, J. & YANG, Q. 2011. Resveratrol pretreatment attenuates cerebral ischemic injury by upregulating expression of transcription factor Nrf2 and HO-1 in rats. *Neurochem Res*, 36, 2352-62.
292. REN, Y., ZHAO, J. & FENG, J. 2003. Parkin binds to alpha/beta tubulin and increases their ubiquitination and degradation. *J Neurosci*, 23, 3316-24.
293. RICHMOND, J. E. & BROADIE, K. S. 2002. The synaptic vesicle cycle: exocytosis and endocytosis in *Drosophila* and *C. elegans*. *Curr Opin Neurobiol*, 12, 499-507.
294. RIEMENSPERGER, T., ISABEL, G., COULOM, H., NEUSER, K., SEUGNET, L., KUME, K., ICHÉ-TORRES, M., CASSAR, M., STRAUSS, R., PREAT, T., HIRSH, J. & BIRMAN, S. 2011. Behavioral consequences of dopamine deficiency in the *Drosophila* central nervous system. *Proc Natl Acad Sci U S A*, 108, 834-9.
295. RITZ, B. R., MANTHRIPRAGADA, A. D., COSTELLO, S., LINCOLN, S. J., FARRER, M. J., COCKBURN, M. & BRONSTEIN, J. 2009. Dopamine transporter genetic variants and pesticides in Parkinson's disease. *Environ Health Perspect*, 117, 964-9.

296. RITZENTHALER, S., SUZUKI, E. & CHIBA, A. 2000. Postsynaptic filopodia in muscle cells interact with innervating motoneuron axons. *Nat Neurosci*, 3, 1012-7.
297. ROTH, J. A. 2014. Correlation between the biochemical pathways altered by mutated parkinson-related genes and chronic exposure to manganese. *Neurotoxicology*, 44, 314-25.
298. ROTH, J. A., GANAPATHY, B. & GHIO, A. J. 2012. Manganese-induced toxicity in normal and human B lymphocyte cell lines containing a homozygous mutation in parkin. *Toxicol In Vitro*, 26, 1143-9.
299. RUBIN, G. M. 2000. Biological annotation of the *Drosophila* genome sequence. *Novartis Found Symp*, 229, 79-82; discussion 82-3.
300. RUIZ-CAÑADA, C. & BUDNIK, V. 2006. Introduction on the use of the *Drosophila* embryonic/larval neuromuscular junction as a model system to study synapse development and function, and a brief summary of pathfinding and target recognition. *Int Rev Neurobiol*, 75, 1-31.
301. SABINA, R. L., PATTERSON, D. & HOLMES, E. W. 1985. 5-Amino-4-imidazolecarboxamide riboside (Z-riboside) metabolism in eukaryotic cells. *J Biol Chem*, 260, 6107-14.
302. SAINI, N., GEORGIEV, O. & SCHAFFNER, W. 2011. The parkin mutant phenotype in the fly is largely rescued by metal-responsive transcription factor (MTF-1). *Mol Cell Biol*, 31, 2151-61.
303. SAINI, N., OELHAFEN, S., HUA, H., GEORGIEV, O., SCHAFFNER, W. & BÜELER, H. 2010. Extended lifespan of *Drosophila* parkin mutants through sequestration of redox-active metals and enhancement of anti-oxidative pathways. *Neurobiol Dis*, 40, 82-92.
304. SAITO, M., MATSUMINE, H., TANAKA, H., ISHIKAWA, A., SHIMODA-MATSUBAYASHI, S., SCHÄFFER, A. A., MIZUNO, Y. & TSUJI, S. 1998. Refinement of the gene locus for autosomal recessive juvenile parkinsonism (AR-JP) on chromosome 6q25.2-27 and identification of markers

exhibiting linkage disequilibrium. *J Hum Genet*, 43, 22-31.

305. SAITOH, M., NISHITOH, H., FUJII, M., TAKEDA, K., TOBIUME, K., SAWADA, Y., KAWABATA, M., MIYAZONO, K. & ICHIJO, H. 1998. Mammalian thioredoxin is a direct inhibitor of apoptosis signal-regulating kinase (ASK) 1. *EMBO J*, 17, 2596-606.
306. SAKAKIBARA, R., HATTORI, T., UCHIYAMA, T. & YAMANISHI, T. 2001. Videourodynamic and sphincter motor unit potential analyses in Parkinson's disease and multiple system atrophy. *J Neurol Neurosurg Psychiatry*, 71, 600-6.
307. SANG, T. K., CHANG, H. Y., LAWLESS, G. M., RATNAPARKHI, A., MEE, L., ACKERSON, L. C., MAIDMENT, N. T., KRANTZ, D. E. & JACKSON, G. R. 2007. A *Drosophila* model of mutant human parkin-induced toxicity demonstrates selective loss of dopaminergic neurons and dependence on cellular dopamine. *J Neurosci*, 27, 981-92.
308. SANG, T. K., CHANG, H. Y., LAWLESS, G. M., RATNAPARKHI, A., MEE, L., ACKERSON, L. C., MAIDMENT, N. T., KRANTZ, D. E. & JACKSON, G. R. 2007. A *Drosophila* model of mutant human parkin-induced toxicity demonstrates selective loss of dopaminergic neurons and dependence on cellular dopamine. *J Neurosci*, 27, 981-92.
309. SANYAL, S., SANDSTROM, D. J., HOEFFER, C. A. & RAMASWAMI, M. 2002. AP-1 functions upstream of CREB to control synaptic plasticity in *Drosophila*. *Nature*, 416, 870-4.
310. SAVITT, J. M., DAWSON, V. L. & DAWSON, T. M. 2006. Diagnosis and treatment of Parkinson disease: molecules to medicine. *J Clin Invest*, 116, 1744-54.
311. SCHAEFER, J. E., WORRELL, J. W. & LEVINE, R. B. 2010. Role of intrinsic properties in *Drosophila* motoneuron recruitment during fictive crawling. *J Neurophysiol*, 104, 1257-66.
312. SCHAPIRA, A. H. 2008. Mitochondria in the aetiology and pathogenesis of

- Parkinson's disease. *Lancet Neurol*, 7, 97-109.
313. SCHAPIRA, A. H., COOPER, J. M., DEXTER, D., CLARK, J. B., JENNER, P. & MARSDEN, C. D. 1990. Mitochondrial complex I deficiency in Parkinson's disease. *J Neurochem*, 54, 823-7.
314. SCHMID, A., CHIBA, A. & DOE, C. Q. 1999. Clonal analysis of *Drosophila* embryonic neuroblasts: neural cell types, axon projections and muscle targets. *Development*, 126, 4653-89.
315. SCHNEIDER, C. A., RASBAND, W. S. & ELICEIRI, K. W. 2012. NIH Image to ImageJ: 25 years of image analysis. *Nat Methods*, 9, 671-5.
316. SCHROETER, H., BAHIA, P., SPENCER, J. P., SHEPPARD, O., RATTRAY, M., CADENAS, E., RICE-EVANS, C. & WILLIAMS, R. J. 2007. (-)Epicatechin stimulates ERK-dependent cyclic AMP response element activity and up-regulates GluR2 in cortical neurons. *J Neurochem*, 101, 1596-606.
317. SCHROETER, H., SPENCER, J. P., RICE-EVANS, C. & WILLIAMS, R. J. 2001. Flavonoids protect neurons from oxidized low-density-lipoprotein-induced apoptosis involving c-Jun N-terminal kinase (JNK), c-Jun and caspase-3. *Biochem J*, 358, 547-57.
318. SCHULZE, K. L., BROADIE, K., PERIN, M. S. & BELLEN, H. J. 1995. Genetic and electrophysiological studies of *Drosophila* syntaxin-1A demonstrate its role in nonneuronal secretion and neurotransmission. *Cell*, 80, 311-20.
319. SCHUSTER, C. M., DAVIS, G. W., FETTER, R. D. & GOODMAN, C. S. 1996. Genetic dissection of structural and functional components of synaptic plasticity. II. Fasciclin II controls presynaptic structural plasticity. *Neuron*, 17, 655-67.
320. SELCHO, M., PAULS, D., EL JUNDI, B., STOCKER, R. F. & THUM, A. S. 2012. The role of octopamine and tyramine in *Drosophila* larval locomotion. *J Comp Neurol*, 520, 3764-85.
321. SHAW, R. J., KOSMATKA, M., BARDEESY, N., HURLEY, R. L., WITTERS, L. A., DEPINHO, R. A. & CANTLEY, L. C. 2004. The tumor

- suppressor LKB1 kinase directly activates AMP-activated kinase and regulates apoptosis in response to energy stress. *Proc Natl Acad Sci U S A*, 101, 3329-35.
322. SHEN, W. & GANETZKY, B. 2009. Autophagy promotes synapse development in *Drosophila*. *J Cell Biol*, 187, 71-9.
323. SHERER, T. B., BETARBET, R., TESTA, C. M., SEO, B. B., RICHARDSON, J. R., KIM, J. H., MILLER, G. W., YAGI, T., MATSUNO-YAGI, A. & GREENAMYRE, J. T. 2003. Mechanism of toxicity in rotenone models of Parkinson's disease. *J Neurosci*, 23, 10756-64.
324. SHIMURA, H., HATTORI, N., KUBO, S., MIZUNO, Y., ASAKAWA, S., MINOSHIMA, S., SHIMIZU, N., IWAI, K., CHIBA, T., TANAKA, K. & SUZUKI, T. 2000. Familial Parkinson disease gene product, parkin, is a ubiquitin-protein ligase. *Nat Genet*, 25, 302-5.
325. SHIMURA, H., SCHLOSSMACHER, M. G., HATTORI, N., FROSCHE, M. P., TROCKENBACHER, A., SCHNEIDER, R., MIZUNO, Y., KOSIK, K. S. & SELKOE, D. J. 2001. Ubiquitination of a new form of alpha-synuclein by parkin from human brain: implications for Parkinson's disease. *Science*, 293, 263-9.
326. SHIN, J. H., KO, H. S., KANG, H., LEE, Y., LEE, Y. I., PLETINKOVA, O., TROCONSO, J. C., DAWSON, V. L. & DAWSON, T. M. 2011. PARIS (ZNF746) repression of PGC-1 α contributes to neurodegeneration in Parkinson's disease. *Cell*, 144, 689-702.
327. SHISHIDO, E., TAKEICHI, M. & NOSE, A. 1998. *Drosophila* synapse formation: regulation by transmembrane protein with Leu-rich repeats, CAPRICIOUS. *Science*, 280, 2118-21.
328. SHOULSON, I. 1998. DATATOP: a decade of neuroprotective inquiry. Parkinson Study Group. Deprenyl And. *Ann Neurol*, 44, S160-6.
329. SHULMAN, J. M., DE JAGER, P. L. & FEANY, M. B. 2011. Parkinson's disease: genetics and pathogenesis. *Annu Rev Pathol*, 6, 193-222.
330. SHULTS, C. W., BEAL, M. F., FONTAINE, D., NAKANO, K. & HAAS, R. H. 1998. Absorption, tolerability, and effects on mitochondrial activity of oral

coenzyme Q10 in parkinsonian patients. *Neurology*, 50, 793-5.

331. SHULTS, C. W., OAKES, D., KIEBURTZ, K., BEAL, M. F., HAAS, R., PLUMB, S., JUNCOS, J. L., NUTT, J., SHOULSON, I., CARTER, J., KOMPOLITI, K., PERLMUTTER, J. S., REICH, S., STERN, M., WATTS, R. L., KURLAN, R., MOLHO, E., HARRISON, M., LEW, M. & GROUP, P. S. 2002. Effects of coenzyme Q10 in early Parkinson disease: evidence of slowing of the functional decline. *Arch Neurol*, 59, 1541-50.
332. SIMUNI, T. & SETHI, K. 2008. Nonmotor manifestations of Parkinson's disease. *Ann Neurol*, 64 Suppl 2, S65-80.
333. SINGLETON, A. B., FARRER, M., JOHNSON, J., SINGLETON, A., HAGUE, S., KACHERGUS, J., HULIHAN, M., PEURALINNA, T., DUTRA, A., NUSSBAUM, R., LINCOLN, S., CRAWLEY, A., HANSON, M., MARAGANORE, D., ADLER, C., COOKSON, M. R., MUENTER, M., BAPTISTA, M., MILLER, D., BLANCATO, J., HARDY, J. & GWINN-HARDY, K. 2003. alpha-Synuclein locus triplication causes Parkinson's disease. *Science*, 302, 841.
334. SLACK, C., FOLEY, A. & PARTRIDGE, L. 2012. Activation of AMPK by the putative dietary restriction mimetic metformin is insufficient to extend lifespan in *Drosophila*. *PLoS One*, 7, e47699.
335. SOONG, N. W., HINTON, D. R., CORTOPASSI, G. & ARNHEIM, N. 1992. Mosaicism for a specific somatic mitochondrial DNA mutation in adult human brain. *Nat Genet*, 2, 318-23.
336. SPILLANTINI, M. G., SCHMIDT, M. L., LEE, V. M., TROJANOWSKI, J. Q., JAKES, R. & GOEDERT, M. 1997. Alpha-synuclein in Lewy bodies. *Nature*, 388, 839-40.
337. SPRATT, D. E., MARTINEZ-TORRES, R. J., NOH, Y. J., MERCIER, P., MANCZYK, N., BARBER, K. R., AGUIRRE, J. D., BURCHELL, L., PURKISS, A., WALDEN, H. & SHAW, G. S. 2013. A molecular explanation for the recessive nature of parkin-linked Parkinson's disease. *Nat Commun*, 4, 1983.

338. SQUIRE, L. R., BLOOM, F. E., MCCONNELL, S. K., ROBERTS, J. L., SPITZER, N. C. & ZIGMOND, M. J. 2003. Membrane potentials and action potentials. *Fundamental Neuroscience*. Second Edition ed. USA: Academic Press.
339. SRIRAM, K., SHANKAR, S. K., BOYD, M. R. & RAVINDRANATH, V. 1998. Thiol oxidation and loss of mitochondrial complex I precede excitatory amino acid-mediated neurodegeneration. *J Neurosci*, 18, 10287-96.
340. STAAL, R. G., MOSHAROV, E. V. & SULZER, D. 2004. Dopamine neurons release transmitter via a flickering fusion pore. *Nat Neurosci*, 7, 341-6.
341. STAROPOLI, J. F., MCDERMOTT, C., MARTINAT, C., SCHULMAN, B., DEMIREVA, E. & ABELIOVICH, A. 2003. Parkin is a component of an SCF-like ubiquitin ligase complex and protects postmitotic neurons from kainate excitotoxicity. *Neuron*, 37, 735-49.
342. STEINBERG, G. R. & KEMP, B. E. 2009. AMPK in Health and Disease. *Physiol Rev*, 89, 1025-78.
343. STEINERT, J. R., CAMPESAN, S., RICHARDS, P., KYRIACOU, C. P., FORSYTHE, I. D. & GIORGINI, F. 2012. Rab11 rescues synaptic dysfunction and behavioural deficits in a *Drosophila* model of Huntington's disease. *Hum Mol Genet*, 21, 2912-22.
344. STEWART, B. A., ATWOOD, H. L., RENGER, J. J., WANG, J. & WU, C. F. 1994. Improved stability of *Drosophila* larval neuromuscular preparations in haemolymph-like physiological solutions. *J Comp Physiol A*, 175, 179-91.
345. STOKES, A. H., HASTINGS, T. G. & VRANA, K. E. 1999. Cytotoxic and genotoxic potential of dopamine. *J Neurosci Res*, 55, 659-65.
346. STRAUSS, K. M., MARTINS, L. M., PLUN-FAVREAU, H., MARX, F. P., KAUTZMANN, S., BERG, D., GASSER, T., WSZOLEK, Z., MÜLLER, T., BORNEMANN, A., WOLBURG, H., DOWNWARD, J., RIESS, O., SCHULZ, J. B. & KRÜGER, R. 2005. Loss of function mutations in the gene encoding Omi/HtrA2 in Parkinson's disease. *Hum Mol Genet*, 14, 2099-111.

347. SULZER, D. & ZECCA, L. 2000. Intraneuronal dopamine-quinone synthesis: a review. *Neurotox Res*, 1, 181-95.
348. SULZER, D. 2007. Multiple hit hypotheses for dopamine neuron loss in Parkinson's disease. *Trends Neurosci*, 30, 244-50.
349. SUN, B. & SALVATERRA, P. M. 1995. Two *Drosophila* nervous system antigens, Nervana 1 and 2, are homologous to the beta subunit of Na⁺,K⁽⁺⁾-ATPase. *Proc Natl Acad Sci U S A*, 92, 5396-400.
350. SUN, J., MOLITOR, J. & TOWER, J. 2004. Effects of simultaneous over-expression of Cu/ZnSOD and MnSOD on *Drosophila melanogaster* life span. *Mech Ageing Dev*, 125, 341-9.
351. SUTER, M., RIEK, U., TUERK, R., SCHLATTNER, U., WALLIMANN, T. & NEUMANN, D. 2006. Dissecting the role of 5'-AMP for allosteric stimulation, activation, and deactivation of AMP-activated protein kinase. *J Biol Chem*, 281, 32207-16.
352. SUZUKI, K., MIZUNO, Y., YAMAUCHI, Y., NAGATSU, T. & MITSUO, Y. 1992. Selective inhibition of complex I by N-methylisoquinolinium ion and N-methyl-1,2,3,4-tetrahydroisoquinoline in isolated mitochondria prepared from mouse brain. *J Neurol Sci*, 109, 219-23.
353. SVENSSON, M. J. & LARSSON, J. 2007. Thioredoxin-2 affects lifespan and oxidative stress in *Drosophila*. *Hereditas*, 144, 25-32.
354. SWEENEY, S. T. & DAVIS, G. W. 2002. Unrestricted synaptic growth in spinster-a late endosomal protein implicated in TGF-beta-mediated synaptic growth regulation. *Neuron*, 36, 403-16.
355. SWICK, L. L., KAZGAN, N., ONYENWOKE, R. U. & BRENMAN, J. E. 2013. Isolation of AMP-activated protein kinase (AMPK) alleles required for neuronal maintenance in *Drosophila melanogaster*. *Biol Open*, 2, 1321-3.
356. TAIN, L. S., MORTIBOYS, H., TAO, R. N., ZIVIANI, E., BANDMANN, O. & WHITWORTH, A. J. 2009. Rapamycin activation of 4E-BP prevents parkinsonian dopaminergic neuron loss. *Nat Neurosci*, 12, 1129-35.

357. TAKEUCHI, A. & TAKEUCHI, N. 1963. Glutamate-induced depolarization in crustacean muscle. *Nature*, 198, 490-1.
358. TANAKA, N. K., TANIMOTO, H. & ITO, K. 2008. Neuronal assemblies of the *Drosophila* mushroom body. *J Comp Neurol*, 508, 711-55.
359. TANG, B. L. & CHUA, C. E. 2008. SIRT1 and neuronal diseases. *Mol Aspects Med*, 29, 187-200.
360. THOR, S. & THOMAS, J. B. 2002. Motor neuron specification in worms, flies and mice: conserved and 'lost' mechanisms. *Curr Opin Genet Dev*, 12, 558-64.
361. THOR, S., ANDERSSON, S. G., TOMLINSON, A. & THOMAS, J. B. 1999. A LIM-homeodomain combinatorial code for motor-neuron pathway selection. *Nature*, 397, 76-80.
362. TOM, T. & CUMMINGS, J. L. 1998. Depression in Parkinson's disease. Pharmacological characteristics and treatment. *Drugs Aging*, 12, 55-74.
363. TORROJA, L., PACKARD, M., GORCZYCA, M., WHITE, K. & BUDNIK, V. 1999. The *Drosophila* beta-amyloid precursor protein homolog promotes synapse differentiation at the neuromuscular junction. *J Neurosci*, 19, 7793-803.
364. TRINH, K., MOORE, K., WES, P. D., MUCHOWSKI, P. J., DEY, J., ANDREWS, L. & PALLANCK, L. J. 2008. Induction of the phase II detoxification pathway suppresses neuron loss in *Drosophila* models of Parkinson's disease. *J Neurosci*, 28, 465-72.
365. TSUDA, M., OOTAKA, R., OHKURA, C., KISHITA, Y., SEONG, K. H., MATSUO, T. & AIGAKI, T. 2010. Loss of Trx-2 enhances oxidative stress-dependent phenotypes in *Drosophila*. *FEBS Lett*, 584, 3398-401.
366. UMEDA-KAMEYAMA, Y., TSUDA, M., OHKURA, C., MATSUO, T., NAMBA, Y., OHUCHI, Y. & AIGAKI, T. 2007. Thioredoxin suppresses Parkin-associated endothelin receptor-like receptor-induced neurotoxicity and extends longevity in *Drosophila*. *J Biol Chem*, 282, 11180-7.

367. UNDERWOOD, B. R., IMARISIO, S., FLEMING, A., ROSE, C., KRISHNA, G., HEARD, P., QUICK, M., KOROLCHUK, V. I., RENNA, M., SARKAR, S., GARCÍA-ARENCEBIA, M., O'KANE, C. J., MURPHY, M. P. & RUBINSZTEIN, D. C. 2010. Antioxidants can inhibit basal autophagy and enhance neurodegeneration in models of polyglutamine disease. *Hum Mol Genet*, 19, 3413-29.
368. USHERWOOD, P. N. 1963. Spontaneous miniature potentials from insect muscle fibres. *J Physiol*, 169, 149-60.
369. VALENTE, E. M., ABOU-SLEIMAN, P. M., CAPUTO, V., MUQIT, M. M., HARVEY, K., GISPERT, S., ALI, Z., DEL TURCO, D., BENTIVOGLIO, A. R., HEALY, D. G., ALBANESE, A., NUSSBAUM, R., GONZÁLEZ-MALDONADO, R., DELLER, T., SALVI, S., CORTELLI, P., GILKS, W. P., LATCHMAN, D. S., HARVEY, R. J., DALLAPICCOLA, B., AUBURGER, G. & WOOD, N. W. 2004a. Hereditary early-onset Parkinson's disease caused by mutations in PINK1. *Science*, 304, 1158-60.
370. VALENTE, E. M., SALVI, S., IALONGO, T., MARONGIU, R., ELIA, A. E., CAPUTO, V., ROMITO, L., ALBANESE, A., DALLAPICCOLA, B. & BENTIVOGLIO, A. R. 2004b. PINK1 mutations are associated with sporadic early-onset parkinsonism. *Ann Neurol*, 56, 336-41.
371. VALENZANO, D. R. & CELLERINO, A. 2006. Resveratrol and the pharmacology of aging: a new vertebrate model to validate an old molecule. *Cell Cycle*, 5, 1027-32.
372. VAUZOUR, D. 2012. Dietary polyphenols as modulators of brain functions: biological actions and molecular mechanisms underpinning their beneficial effects. *Oxid Med Cell Longev*, 2012, 914273.
373. VAUZOUR, D., VAFEIADOU, K., RICE-EVANS, C., WILLIAMS, R. J. & SPENCER, J. P. 2007. Activation of pro-survival Akt and ERK1/2 signalling pathways underlie the anti-apoptotic effects of flavanones in cortical neurons. *J Neurochem*, 103, 1355-67.
374. VEAL, E. A., DAY, A. M. & MORGAN, B. A. 2007. Hydrogen peroxide

sensing and signaling. *Mol Cell*, 26, 1-14.

375. VENKEN, K. J., SIMPSON, J. H. & BELLEN, H. J. 2011. Genetic manipulation of genes and cells in the nervous system of the fruit fly. *Neuron*. United States: 2011 Elsevier Inc.
376. VILARIÑO-GÜELL, C., WIDER, C., ROSS, O. A., DACHSEL, J. C., KACHERGUS, J. M., LINCOLN, S. J., SOTO-ORTOLAZA, A. I., COBB, S. A., WILHOITE, G. J., BACON, J. A., BEHROUZ, B., MELROSE, H. L., HENTATI, E., PUSCHMANN, A., EVANS, D. M., CONIBEAR, E., WASSERMAN, W. W., AASLY, J. O., BURKHARD, P. R., DJALDETTI, R., GHIKA, J., HENTATI, F., KRYGOWSKA-WAJS, A., LYNCH, T., MELAMED, E., RAJPUT, A., RAJPUT, A. H., SOLIDA, A., WU, R. M., UITTI, R. J., WSZOLEK, Z. K., VINGERHOETS, F. & FARRER, M. J. 2011. VPS35 mutations in Parkinson disease. *Am J Hum Genet*, 89, 162-7.
377. VINCENT, A., BRIGGS, L., CHATWIN, G. F., EMERY, E., TOMLINS, R., OSWALD, M., MIDDLETON, C. A., EVANS, G. J., SWEENEY, S. T. & ELLIOTT, C. J. 2012. parkin-induced defects in neurophysiology and locomotion are generated by metabolic dysfunction and not oxidative stress. *Hum Mol Genet*, 21, 1760-9.
378. VON COELLN, R., THOMAS, B., SAVITT, J. M., LIM, K. L., SASAKI, M., HESS, E. J., DAWSON, V. L. & DAWSON, T. M. 2004. Loss of locus coeruleus neurons and reduced startle in parkin null mice. *Proc Natl Acad Sci U S A*, 101, 10744-9.
379. VOON, V., FERNAGUT, P. O., WICKENS, J., BAUNEZ, C., RODRIGUEZ, M., PAVON, N., JUNCOS, J. L., OBESO, J. A. & BEZARD, E. 2009. Chronic dopaminergic stimulation in Parkinson's disease: from dyskinesias to impulse control disorders. *Lancet Neurol*, 8, 1140-9.
380. VOS, M., ESPOSITO, G., EDIRISINGHE, J. N., VILAIN, S., HADDAD, D. M., SLABBAERT, J. R., VAN MEENSEL, S., SCHAAP, O., DE STROOPER, B., MEGANATHAN, R., MORAIS, V. A. & VERSTREKEN, P. 2012. Vitamin K2 is a mitochondrial electron carrier that rescues pink1

deficiency. *Science*, 336, 1306-10.

381. WALLERATH, T., DECKERT, G., TERNES, T., ANDERSON, H., LI, H., WITTE, K. & FÖRSTERMANN, U. 2002. Resveratrol, a polyphenolic phytoalexin present in red wine, enhances expression and activity of endothelial nitric oxide synthase. *Circulation*, 106, 1652-8.
382. WAN, H. I., DIANTONIO, A., FETTER, R. D., BERGSTROM, K., STRAUSS, R. & GOODMAN, C. S. 2000. Highwire regulates synaptic growth in *Drosophila*. *Neuron*, 26, 313-29.
383. WANG, C., LU, R., OUYANG, X., HO, M. W., CHIA, W., YU, F. & LIM, K. L. 2007. *Drosophila* overexpressing parkin R275W mutant exhibits dopaminergic neuron degeneration and mitochondrial abnormalities. *J Neurosci*, 27, 8563-70.
384. WANG, D., QIAN, L., XIONG, H., LIU, J., NECKAMEYER, W. S., OLDHAM, S., XIA, K., WANG, J., BODMER, R. & ZHANG, Z. 2006. Antioxidants protect PINK1-dependent dopaminergic neurons in *Drosophila*. *Proc Natl Acad Sci U S A*, 103, 13520-5.
385. WANG, J. W., WONG, A. M., FLORES, J., VOSSHALL, L. B. & AXEL, R. 2003. Two-photon calcium imaging reveals an odor-evoked map of activity in the fly brain. *Cell*, 112, 271-82.
386. WANG, P., SARASWATI, S., GUAN, Z., WATKINS, C. J., WURTMAN, R. J. & LITTLETON, J. T. 2004. A *Drosophila* temperature-sensitive seizure mutant in phosphoglycerate kinase disrupts ATP generation and alters synaptic function. *J Neurosci*, 24, 4518-29.
387. WATERSTON, R. H., LINDBLAD-TOH, K., BIRNEY, E., ROGERS, J., ABRIL, J. F., AGARWAL, P., AGARWALA, R., AINSCOUGH, R., ALEXANDERSSON, M., AN, P., ANTONARAKIS, S. E., ATTWOOD, J., BAERTSCH, R., BAILEY, J., BARLOW, K., BECK, S., BERRY, E., BIRREN, B., BLOOM, T., BORK, P., BOTCHERBY, M., BRAY, N., BRENT, M. R., BROWN, D. G., BROWN, S. D., BULT, C., BURTON, J., BUTLER, J., CAMPBELL, R. D., CARNINCI, P., CAWLEY, S., CHIAROMONTE, F.,

CHINWALLA, A. T., CHURCH, D. M., CLAMP, M., CLEE, C., COLLINS, F. S., COOK, L. L., COPLEY, R. R., COULSON, A., COURONNE, O., CUFF, J., CURWEN, V., CUTTS, T., DALY, M., DAVID, R., DAVIES, J., DELEHAUNTY, K. D., DERI, J., DERMITZAKIS, E. T., DEWEY, C., DICKENS, N. J., DIEKHANS, M., DODGE, S., DUBCHAK, I., DUNN, D. M., EDDY, S. R., ELNITSKI, L., EMES, R. D., ESWARA, P., EYRAS, E., FELSENFELD, A., FEWELL, G. A., FLICEK, P., FOLEY, K., FRANKEL, W. N., FULTON, L. A., FULTON, R. S., FUREY, T. S., GAGE, D., GIBBS, R. A., GLUSMAN, G., GNERRE, S., GOLDMAN, N., GOODSTADT, L., GRAFHAM, D., GRAVES, T. A., GREEN, E. D., GREGORY, S., GUIGO, R., GUYER, M., HARDISON, R. C., HAUSSLER, D., HAYASHIZAKI, Y., HILLIER, L. W., HINRICHS, A., HLAVINA, W., HOLZER, T., HSU, F., HUA, A., HUBBARD, T., HUNT, A., JACKSON, I., JAFFE, D. B., JOHNSON, L. S., JONES, M., JONES, T. A., JOY, A., KAMAL, M., KARLSSON, E. K., et al. 2002. Initial sequencing and comparative analysis of the mouse genome. *Nature*. England.

388. WEBER, U., PARICIO, N. & MLODZIK, M. 2000. Jun mediates Frizzled-induced R3/R4 cell fate distinction and planar polarity determination in the *Drosophila* eye. *Development*, 127, 3619-29.
389. WHITWORTH, A. J., THEODORE, D. A., GREENE, J. C., BENES, H., WES, P. D. & PALLANCK, L. J. 2005. Increased glutathione S-transferase activity rescues dopaminergic neuron loss in a *Drosophila* model of Parkinson's disease. *Proc Natl Acad Sci U S A*, 102, 8024-9.
390. WOLTERS, E. C. H. 2009. Non-motor extranigral signs and symptoms in Parkinson's disease. *Parkinsonism Relat Disord*, 15 Suppl 3, S6-12.
391. XIONG, H., WANG, D., CHEN, L., CHOO, Y. S., MA, H., TANG, C., XIA, K., JIANG, W., RONAI, Z., ZHUANG, X. & ZHANG, Z. 2009. Parkin, PINK1, and DJ-1 form a ubiquitin E3 ligase complex promoting unfolded protein degradation. *J Clin Invest*, 119, 650-60.
392. YANG, Y., GEHRKE, S., IMAI, Y., HUANG, Z., OUYANG, Y., WANG, J. W., YANG, L., BEAL, M. F., VOGEL, H. & LU, B. 2006. Mitochondrial

- pathology and muscle and dopaminergic neuron degeneration caused by inactivation of *Drosophila* Pink1 is rescued by Parkin. *Proc Natl Acad Sci U S A*, 103, 10793-8.
393. YANG, Y., NISHIMURA, I., IMAI, Y., TAKAHASHI, R. & LU, B. 2003. Parkin suppresses dopaminergic neuron-selective neurotoxicity induced by Pael-R in *Drosophila*. *Neuron*, 37, 911-24.
394. YANG, Y., OUYANG, Y., YANG, L., BEAL, M. F., MCQUIBBAN, A., VOGEL, H. & LU, B. 2008. Pink1 regulates mitochondrial dynamics through interaction with the fission/fusion machinery. *Proc Natl Acad Sci U S A*, 105, 7070-5.
395. YELLMAN, C., TAO, H., HE, B. & HIRSH, J. 1997. Conserved and sexually dimorphic behavioral responses to biogenic amines in decapitated *Drosophila*. *Proc Natl Acad Sci U S A*, 94, 4131-6.
396. ZHANG, J., PERRY, G., SMITH, M. A., ROBERTSON, D., OLSON, S. J., GRAHAM, D. G. & MONTINE, T. J. 1999. Parkinson's disease is associated with oxidative damage to cytoplasmic DNA and RNA in substantia nigra neurons. *Am J Pathol*, 154, 1423-9.
397. ZHOU, G., MYERS, R., LI, Y., CHEN, Y., SHEN, X., FENYK-MELODY, J., WU, M., VENTRE, J., DOEBBER, T., FUJII, N., MUSI, N., HIRSHMAN, M. F., GOODYEAR, L. J. & MOLLER, D. E. 2001. Role of AMP-activated protein kinase in mechanism of metformin action. *J Clin Invest*, 108, 1167-74.
398. ZIMPRICH, A., BENET-PAGÈS, A., STRUHAL, W., GRAF, E., ECK, S. H., OFFMAN, M. N., HAUBENBERGER, D., SPIELBERGER, S., SCHULTE, E. C., LICHTNER, P., ROSSLE, S. C., KLOPP, N., WOLF, E., SEPPI, K., PIRKER, W., PRESSLAUER, S., MOLLENHAUER, B., KATZENSCHLAGER, R., FOKI, T., HOTZY, C., REINTHALER, E., HARUTYUNYAN, A., KRALOVICS, R., PETERS, A., ZIMPRICH, F., BRÜCKE, T., POEWE, W., AUFF, E., TRENKWALDER, C., ROST, B., RANSMAYR, G., WINKELMANN, J., MEITINGER, T. & STROM, T. M. 2011. A mutation in VPS35, encoding a subunit of the retromer complex, causes

late-onset Parkinson disease. *Am J Hum Genet*, 89, 168-75.

399. ZIMPRICH, A., BISKUP, S., LEITNER, P., LICHTNER, P., FARRER, M., LINCOLN, S., KACHERGUS, J., HULIHAN, M., UTTI, R. J., CALNE, D. B., STOESSL, A. J., PFEIFFER, R. F., PATENGE, N., CARBAJAL, I. C., VIEREGGE, P., ASMUS, F., MÜLLER-MYHSOK, B., DICKSON, D. W., MEITINGER, T., STROM, T. M., WSZOLEK, Z. K. & GASSER, T. 2004. Mutations in LRRK2 cause autosomal-dominant parkinsonism with pleomorphic pathology. *Neuron*, 44, 601-7.
400. ZITO, K., PARNAS, D., FETTER, R. D., ISACOFF, E. Y. & GOODMAN, C. S. 1999. Watching a synapse grow: noninvasive confocal imaging of synaptic growth in *Drosophila*. *Neuron*, 22, 719-29.
401. ZUKER, C. S., MISMER, D., HARDY, R. & RUBIN, G. M. 1988. Ectopic expression of a minor *Drosophila* opsin in the major photoreceptor cell class: distinguishing the role of primary receptor and cellular context. *Cell*, 53, 475-82.